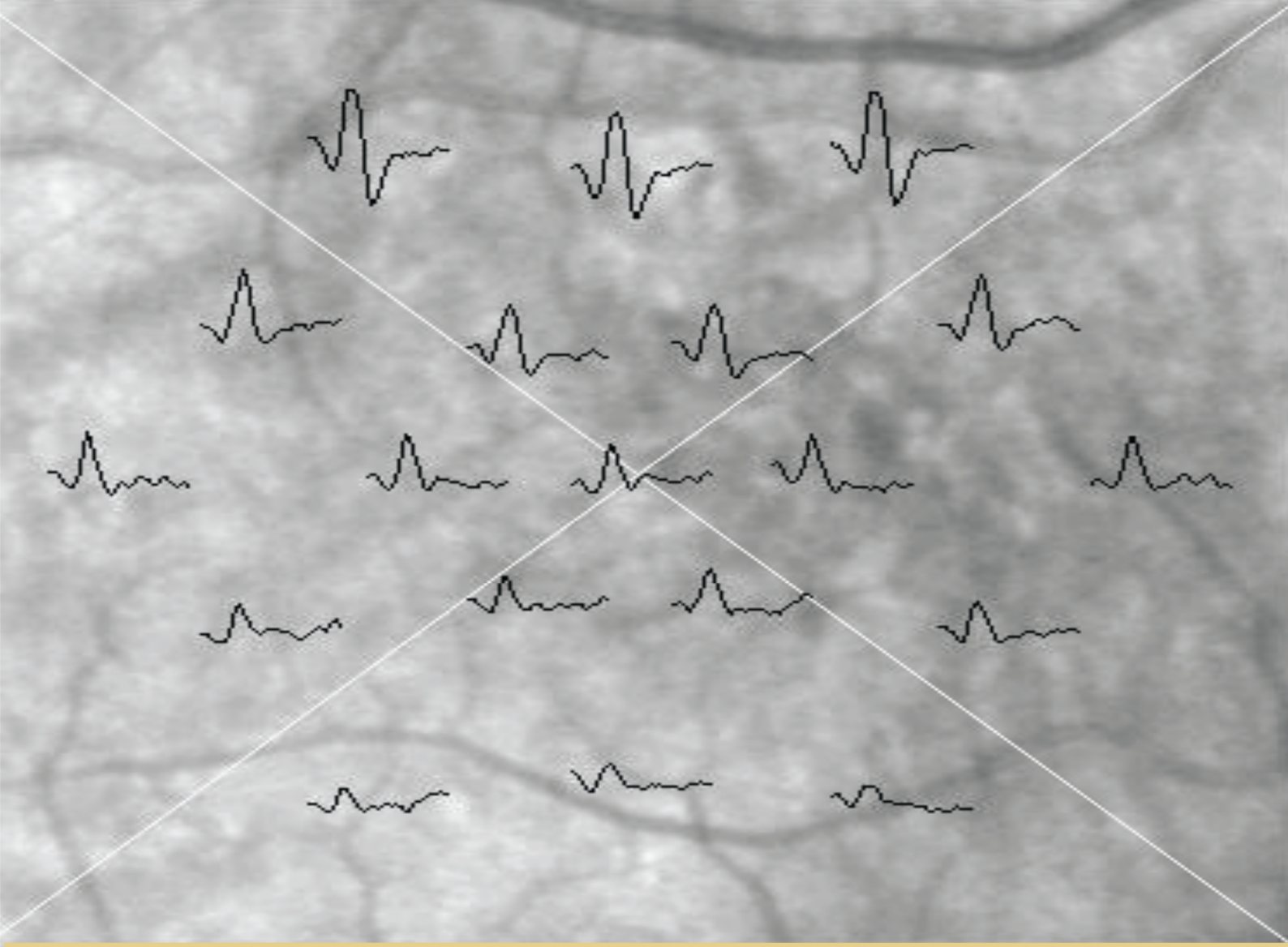

ALDINA SUSANA ARAGONÊS DA CONCEIÇÃO PIRES REIS

GANGLION CELL AND OPTIC NERVE PHYSIOLOGY IN HEALTH AND DISEASE

THE ROLE OF NOVEL PSYCHOPHYSICAL AND ELECTROPHYSIOLOGICAL TECHNIQUES

♦

Fisiologia das Células Ganglionares e do Nervo Óptico na Saúde e na Doença

O Papel das Novas Metodologias Psicofísicas e Electrofisiológicas

2012

· U C ·

UNIVERSIDADE DE COIMBRA

GANGLION CELL AND OPTIC NERVE PHYSIOLOGY IN HEALTH AND DISEASE

THE ROLE OF NOVEL PSYCHOPHYSICAL AND ELECTROPHYSIOLOGICAL TECHNIQUES

♦

Fisiologia das Células Ganglionares e do Nervo Óptico na Saúde e na Doença

O Papel das Novas Metodologias Psicofísicas e Electrofisiológicas

ALDINA SUSANA ARAGONÊS DA CONCEIÇÃO PIRES REIS

GANGLION CELL AND OPTIC NERVE PHYSIOLOGY IN HEALTH AND DISEASE

THE ROLE OF NOVEL PSYCHOPHYSICAL AND ELECTROPHYSIOLOGICAL TECHNIQUES

♦

Fisiologia das Células Ganglionares e do Nervo Óptico na Saúde e na Doença

O Papel das Novas Metodologias Psicofísicas e Electrofisiológicas

2012

· U C ·

UNIVERSIDADE DE COIMBRA

Dissertação de Doutoramento apresentada à
Faculdade de Medicina da Universidade de Coimbra,
para prestação de provas de Doutoramento em Ciências da Saúde

Trabalho realizado em:

· Laboratório de Neurociências da Visão
Instituto Biomédico de Investigação da Luz e Imagem
Faculdade de Medicina da Universidade de Coimbra
(Prof. Doutor Miguel Castelo-Branco)

· Associação para Investigação Biomédica e Inovação em Luz e Imagem
Coimbra
(Prof. Doutor José Cunha-Vaz)

· Serviço de Oftalmologia dos Hospitais da Universidade de Coimbra
Centro Hospitalar e Universitário de Coimbra
(Prof. Doutor Joaquim Neto Murta)

A todos os que guardo no meu coração

Ao Prof. Doutor José Cunha-Vaz,
que me incentivou a ir sempre mais longe

Ao Prof. Doutor Miguel Castelo-Branco,
mestre e amigo

PREFÁCIO

Em Dezembro de 2004, logo após a conclusão do Mestrado em Ciências da Visão (Faculdade de Medicina - Universidade de Coimbra), iniciei o meu percurso doutoral em Espanha, como aluna da Universidade de Valladolid.

Passados pouco mais de dois anos, com a criação de um novo ramo no Doutoramento em Ciências da Saúde, foi-me lançado o desafio, pelo Prof. Doutor José Cunha-Vaz, para ser a primeira doutorada em Tecnologias da Saúde pela Faculdade de Medicina da Universidade de Coimbra, que aceitei, terminando, deste modo, esta importante etapa da minha vida na cidade que me viu nascer.

Inserida, desde 2002, na equipa de investigação do Laboratório de Neurociências da Visão, do Instituto Biomédico de Investigação da Luz e Imagem (IBILI), sob coordenação do Prof. Doutor Miguel Castelo-Branco, a minha actividade hospitalar e de investigação tinha vindo a desenvolver-se principalmente na avaliação da função visual nas vertentes electrofisiológica e psicofísica, em doenças adquiridas e hereditárias da retina e do nervo óptico.

Tendo as doenças da retina, nomeadamente as doenças maculares, sido objecto de investigação por parte de outros alunos de mestrado e de doutoramento do referido grupo (nos quais também participei), existia uma área por investigar, estando em aberto algumas questões científicas relacionadas com as Neuropatias Ópticas, cujos casos são frequentes nos doentes que acedem ao nosso laboratório, provenientes quer do Serviço de Oftalmologia quer do Serviço de Neurologia dos Hospitais da Universidade de Coimbra.

Dado ainda o destaque que a Retinopatia Diabética sempre teve no Centro de Oftalmologia do IBILI, mas situando-se, predominantemente, no estudo das alterações vasculares relacionadas com alterações da barreira hemato-retiniana, outras questões científicas se colocavam, nomeadamente na sequência de achados observados pelo grupo dedicado à investigação animal (liderado pelo Doutor Francisco Ambrósio), em que foram evidentes alterações neuronais prévias ao desenvolvimento de patologia vascular em ratos diabéticos, e que consubstanciam o debate científico actual entre as teorias vascular e neuronal na retinopatia diabética.

Estavam, assim, reunidos os pressupostos para o início dos meus trabalhos de investigação com vista a esta Dissertação, tendo como ponto comum o estudo da fisiologia das células ganglionares em patologias do nervo óptico e na retinopatia diabética, desenvolvida, especificamente, nas neuropatias ópticas adquiridas e

hereditárias (nomeadamente relacionadas com a esclerose múltipla, e nas atrofias ópticas autossómicas dominantes e neuropatia óptica de Leber) e ainda na "neuro-retinopatia diabética".

Alguns dos resultados aqui apresentados foram já divulgados em eventos científicos internacionais, encontrando-se, nesta fase, parcialmente publicados em revistas científicas da área.

A todos os que colaboraram de forma significativa nesta etapa, expresso a minha gratidão, em especial aos meus colegas Dr. Pedro Melo, Dr. Mário Soares, Drª Ana Rita Santos, Téc. Graciete Abreu e, muito em particular, à Drª Catarina Mateus, que foi o meu braço direito na recolha de dados e análise dos mesmos. Para o Engº João Castelhano vai também o meu "obrigada".

Ao Prof. Doutor José Cunha-Vaz e ao Prof. Doutor Miguel Castelo-Branco aqui deixo o meu sincero agradecimento por todo o contributo científico e disponibilidade permanentes, e pela amizade com que me acompanharam ao longo do trabalho destes anos.

Aos médicos que participaram na avaliação clínica dos pacientes, de um modo especial ao Prof. Doutor José Rui Faria de Abreu, ao Prof. Doutor Eduardo Silva, à Dra. Maria Luísa Ribeiro, ao Dr. João Figueira e à Dra. Maria do Carmo Macário, aqui deixo o meu reconhecimento por toda a disponibilidade manifestada.

À Prof. Doutora Manuela Grazina, assim como ao Prof. Doutor Arthur Bergen e Prof. Doutor Ralph Florijn (Amsterdão), agradeço a contribuição para a caracterização genética das neuropatias ópticas hereditárias.

Fica também a minha gratidão à Dra. Cristina Ramos, pelo apoio bibliográfico.

Às secretárias, em especial Sandra Pardal (pela ajuda disponibilizada nos contactos com os doentes) e Alda Gonçalves (sempre disponível nas mais variadas tarefas), vai o meu 'muito obrigada'.

Por fim, uma palavra de agradecimento à minha família, em particular aos meus pais, pela forma com que sempre me apoiaram, com carinho, ao longo da vida; às minhas irmãs, pela boa disposição; aos meus filhos, pela compreensão que sempre demonstraram na conciliação das múltiplas tarefas de sua mãe; e ao João, pela dedicação aos nossos filhos, nos momentos em que não pude estar presente.

INDEX

ABBREVIATION LIST

ADOA – Autosomal dominant optic atrophy
AFC – Alternative forced choice
ALH – Anterior left hemisphere
ARH – Anterior right hemisphere
ASP – Automated static perimetry
BCVA – Best-corrected visual acuity
BRB – Blood-retinal barrier
CCT – Cambridge Colour Test
cm – Centimetre
cpd – Cycles per degree
CRT – Catodic ray tube
CS – Contrast sensitivity
dB – Decibels
deg^2 – Square degree
DNA – deoxyribonucleic acid
DR – Diabetic retinopathy
EDSS – Expanded disability status scale
EOG – Electro-oculogram
ERG – Electroretinogram
ETDRS – Early Treatment of Diabetic Retinopathy Study
FA – Fluorescein angiography
FDT – Frequency doubling technology
GC – Ganglion cell
GLM – General linear models
HRA – Heidelberg retina angiograph
Hz – Hertz
IOP – Intraocular pressure
IR – Infra-red
IT– Implicit time
LGN – Lateral geniculate nucleus

LHON – Leber's hereditary optic neuropathy
LV – Loss variance
M – Magnocellular
MD – Mean defect
MfERG – Multifocal electroretinogram
MfVEP – Multifocal visual evoked potentials
mm – Millimetre
MRI - Magnetic resonance imaging
MS – Multiple sclerosis
MS' – Mean sensitivity
ms – Miliseconds
MtDNA – Mitochondrial DNA
NI – Nasal inferior
NPDR – Nonproliferative diabetic retinopathy
nV – Nanovolts
OCT – Optical coherence tomography
ON – Optic neuritis
ONy – Optic neuropathy/ies
OP – Oscillatory potentials
OZ – Midline occipital location
P – Parvocellular
PDR – Proliferative diabetic retinopathy
PERG – Pattern electroretinogram
PHONy - Primary hereditary optic neuropathy
PLH – Posterior left hemisphere
PR – Penetration ratio
PRH – Posterior right hemisphere
PSD – Pattern standard deviation
PVEP – Pattern visual evoked potentials
RNFL – Retinal nervous fibre layer
RPE – Retinal pigment epithelium
RT – Retinal thickness
RTA – Retinal thickness analyzer
s – Seconds
SD – Standard deviation
SEM – Standard error of the mean

SLO – Scanning laser ophthalmoscope

SN – Superior nasal

SPSS – Statistical package for the social sciences

ST – Superior temporal

TI – Temporal inferior

SWAP – Short-wavelenght automated perimetry

VA – Visual acuity

VEP – Visual evoked potentials

VF – Vitreous fluorometry

µV – Microvolt

RESUMO

Introdução e Objectivos

As células ganglionares (CG) têm um papel preponderante no processamento da Visão, dadas as suas características estruturais e funcionais. As diferenças anatómicas destas células imprimem uma variedade de mosaicos e circuitos neuronais que estão na base de diferentes vias visuais. Esta especificidade começa na retina e estende-se até ao córtex visual através de vias retinocorticais paralelas, de acordo com as propriedades funcionais intrínsecas dos seus neurónios. As células do sistema parvocelular são pequenas (originando campos receptores pequenos) e especializadas no processamento da informação cromática (eixo vermelho-verde), apresentando alta resolução espacial e baixa resolução temporal, contrariamente às do sistema magnocelular, que são maiores (com campos receptores igualmente de maiores dimensões). A via magnocelular apresenta elevada sensibilidade ao contraste para estímulos dinâmicos de baixa frequência espacial. O sistema coniocelular é constituído por células biestratificadas, com propriedades espaciais e temporais intermédias comparativamente às das outras vias retinocorticais, sendo sensível ao contraste cromático no eixo azul-amarelo.

Diferentes mecanismos de doença, intrinsecamente relacionados com patologias da retina e do nervo óptico, podem causar lesões ao nível da camada das CG, com impacto nas vias retinocorticais. Este trabalho teve como objectivo global investigar o impacto dos mecanismos de doença nas CG e no nervo óptico, nomeadamente em patologias que afectam tipicamente estas estruturas, sejam hereditárias (Atrofia Óptica Autossómica Dominante e Neuropatia Óptica Hereditária de Leber) ou adquiridas (Neuropatia Óptica Inflamatória-Desmielinizante / relacionada com Esclerose Múltipla), não só ao nível das CG, como também ao nível de via aferentes e eferentes (pré e pós-ganglionares, neste caso através de diferentes canais funcionais). Pretendeu-se, ainda, pesquisar a presença de disfunção neuronal retiniana "pura", independente da ruptura da barreira hemato-retiniana e vasculopatia, em doentes diabéticos do tipo 1, sem retinopatia diabética (RD) ou com RD incial, em termos das vias paralelas retinocorticais. Por último, o objectivo final deste trabalho foi investigar o papel das novas metodologias psicofísicas e electrofisiológicas na caracterização funcional de doenças que afectam a retina interna.

Métodos

Foram escolhidos métodos que incluíram estímulos preferencialmente selectivos para as vias parvo, conio e magnocelulares, de forma a possibilitar a comparação de mecanismos patofisiológicos, em diferentes populações, divididas em quatro linhas de investigação, de acordo com os objectivos globais do projecto:

- Estudo 1: Amostra de 44 indivíduos com Esclerose Múltipla (EM), com (n=14) e sem (n=30) episódio prévio de Nevrite Óptica (NO) – modelo de neuropatia óptica adquirida.

- Estudo 2: Amostra de 22 indivíduos de 13 famílias com Atrofia Óptica Autossómica Dominante (AOAD); mutação *OPA1* – modelo de neuropatia óptica hereditária.

- Estudo 3: Amostra de 17 indivíduos portadores assintomáticos de Neuropatia Óptica Hereditária de Leber (NOHL) associada à mutação DNAmt 11778G>A, provenientes do mesmo "pedigree" – modelo de neuropatia óptica hereditária, assintomática.

- Estudo 4: Amostra de 42 indivíduos diabéticos do tipo 1 com acuidade visual preservada, sem retinopatia diabética (RD) – n=26, ou RD inicial (n=16) – modelo de lesão neuronal funcional da retina interna (não excluindo afecção da retina externa).

Estes dados foram comparados com os dados obtidos em diferentes grupos de controlo, ajustados (em número e à idade) às características da amostra de doentes para cada linha de estudo.

Os métodos psicofísicos englobaram a avaliação da sensibilidade ao contraste cromático parametrizado ao longo de diferentes eixos de cor (Cambridge Colour Test - vias parvo e coniocelulares) e da sensibilidade ao contraste acromático (para várias frequências espaciais - Metropsis Contrast Sensitivity Function Test, ou avaliação perimétrica da via magnocelular - Perimetria de Frequência Dupla). A Perimetria Estática Computorizada foi também utilizada nos estudos em que foi necessário obter uma comparação perimétrica "golden standard".

Foram também utilizados vários métodos electrofisiológicos, de acordo com os diferentes objectivos neurofisiológicos: as medidas relativas da função pré-ganglionar e ganglionar foram obtidas através do Electroretinograma Multifocal e do Electroretinograma Pattern, respectivamente. Os Potenciais Evocados Visuais, globais e

multifocais, foram medidos para registo do processamento retinocortical, para caracterização da lesão funcional ao nível pós-CG. Foram também registados potenciais evocados visuais de alta densidade, nas neuropatias ópticas hereditárias, com vista a investigar as diferenças entre as respostas corticais induzidas por estímulos preferencialmente selectivos para o desempenho dos sistemas parvo e magnocelulares, com o objectivo de separar os mecanismos patofisiológicos da visão central versus paracentral/periférica, baseados na hipótese de diferentes susceptibilidades lesionais.

Para além dos métodos mencionados, foram ainda utilizados métodos de imagem, para caracterização funcional e para análise de correlação estrutura-função: Fotografia do Fundo Ocular, Angiografia Flurescéinica, avaliação da camada de fibras nervosas / espessura da retina (Tomógrafo de Coerência Óptica ou Analisador da Espessura da Retina). Estes foram aplicados diferentemente em cada grupo, de acordo com os objectivos específicos de cada estudo. Para o estudo da Diabetes, foi ainda utilizada a Fluorometria do Vítreo, para quantificação da barreira hemato-retiniana, crucial para a detecção de alterações vasculares subclínicas.

Resultados e Discussão

Sumariamente, na EM encontrámos evidência de lesão independente nas diferentes vias retinocorticais, mas apenas em doentes sem NO (grupo pré-neuropatia). O dano axonal encontrado neste grupo (através dos PEVs) deu consistência à corrente emergente que sugere existir dano axonal mesmo nos estadios pré-clínicos de NO, no processo fisiopatológico da EM. Ainda no mesmo grupo foi observada uma correlação significativa das medidas visuais funcionais com o estadio da EM, sugerindo que ocorrem diferentes mecanismos de lesão antes e após um episódio de NO.

Nas neuropatias ópticas hereditárias, verificámos que as alterações estruturais e funcionais reflectem-se também ao nível pré-ganglionar.

No caso da AOAD, estas alterações sugerem a existência de um mecanismo de lesão retrógrado, com impacto significativo na função visual, principalmente no desempenho do sistema parvocelular.

Relativamente à NOHL (assintomática), as alterações pré-ganglionares não podem ser interpretadas como resultantes de um processo retrógado (dado que não foi encontrada evidência de disfunção das CG), mas sim derivadas de um mecanismo lesional independente.

Nos diabéticos do tipo 1, encontrámos alterações retinianas neuronais, nas vias gangionares magno, conio e parvocelulares, mesmo antes de evidência de ruptura da barreira hemato-retiniana ou início do processo vasculopático. Alterações neurofisiológicas evidenciadas pelos métodos electrofisiológicos sugerem ainda que estas alterações neuronais ocorrem também ao nível pré-CG.

Os métodos psicofísicos e electrofisiológicos podem, assim, assumir um papel preponderante na detecção de alterações subclínicas e/ou pré-clínicas em doenças que afectam as vias paralelas ganglionares retinocorticais, e ainda na identificação de padrões patofisiológicos distintos, em diferentes mecanismos de doença, nas patologias da retina e do nervo óptico.

Este trabalho deixa, ainda, em aberto um caminho para investigação e desenvolvimento em biomarcadores para a caracterização precoce e quantitativa do dano retrógrado ou anterógrado, em doenças que afectam, directa ou indirectamente, as CG e o nervo óptico.

ABSTRACT

Background and Goals

Ganglion Cells (GC) are key players in vision processing due to their structural and functional characteristics. There are different structural types of GC, defining distinct mosaics and circuits organized to subserve different functional roles. This specificity starts at retinal level and continues up to the visual cortex across parallel retinocortical pathways, related to the functional tuning properties of their respective neurons. Cells within the parvocellular pathway are small (with small receptive fields) and specialized in colour processing (red-green axis), having high spatial resolution and low temporal resolution, while the cells of the magnocellular pathway are larger (with correspondingly large receptive fields). This pathway is highly sensitive to contrast of low spatial frequency dynamic stimuli. The koniocellular system has bistratified cells with intermediate spatial and temporal tuning properties as compared to the other retinocortical pathways, and is sensitive to contrast along the blue-yellow colour axis.

GC damage can be caused by several intrinsic disease mechanisms related with retinal and/or optic nerve pathologies, with consequent impact on the retinocortical pathways. The global aim of this work was to investigate the impact of disease mechanisms in GC and optic nerve, namely in pathologies that typically affect these structures, namely inherited conditions (Autosomal Dominant Optic Atrophy and Leber Hereditary Optic Neuropathy) and acquired optic neuropaties (Inflammatory-Demyelinating Optic Neuropathy / Multiple Sclerosis-related), not only at the GC level, but also at post- and even pre-GC levels, across distinct functional channels. In addition, we also aimed to probe retinal neuronal dysfunction independently of breakdown of the blood-retinal barrier and vasculopathy in type 1 diabetic patients, with minimal or no diabetic retinopathy, across parallel retinocortical pathways. Finally, the last goal of this work was to investigate the role of novel psychophysical and electrophysiological methods in the functional characterization of diseases affecting the inner retina.

Methods

We used functional methods that assess parvo-, konio- and magnocellular pathways in order to compare pathophysiological mechanisms of damage in different populations, divided into four research lines, according to the global aims of the project:

- Study 1: Sample of 44 subjects with Multiple Sclerosis (MS), with (n=14) and without (n=30) a previous episode of Optic Neuritis (ON) (acquired optic neuropathy model).

- Study 2: Sample of 22 subjects from 13 families with Autosomal Dominant Optic Atrophy (ADOA); *OPA1* mutation (inherited optic neuropathy model).

- Study 3: Sample of 17 asymptomatic carriers of Leber's hereditary optic neuropathy (LHON) associated to mtDNA 11778G>A mutation, from the same pedigree (asymptomatic inherited optic neuropathy model).

- Study 4: Sample of 42 type 1 diabetic patients with preserved visual acuity, with no diabetic retinopathy (DR) – n=26, and with mild nonproliferative DR (n=16) (a model for neural impairment including the inner retina).

These data were compared with those obtained in different control groups adjusted (in number and age) to the characteristics of the patients' sample of each study line.

The psychophysical methods included chromatic contrast sensitivity across different chromatic axes (Cambridge Colour Test - parvo/konio pathways) and achromatic contrast sensitivity testing (across multiple spatial frequencies - Metropsis Contrast Sensitivity Function Test, or perimetric evaluation for the magnocellular pathway - Frequency Doubling Technology). Automated Static Perimetry was also used in some of these studies in order to provide a golden standard perimetric comparison.

Different electrophysiological methods were used according to distinct neurophysiological purposes: preganglionic and GC measures were assessed with Multifocal Electroretinogram (mfERG) and Pattern Electroretinogram (PERG), respectively. Global Pattern and Multifocal VEP (visual evoked potentials) were used to assess retinocortical processing, in order to characterize impairment at the post-GC level. High density visual evoked potentials were also recorded in hereditary optic neuropathies, in order to investigate the differences between cortical responses induced by parvo- and magnocellular biased stimuli, to identify separate pathophysiological mechanisms of impaired central versus paracentral/peripheral vision, based on the hypothesis of different susceptibility to damage.

Besides the above mentioned functional tools, we also used imaging methods, for structural characterization and establishment of structure-function correlation. These included Fundus Fotography, Fluorescein Angiography, retinal nerve fibre layer / global retinal thickness evaluation (Optical Coherence Tomography or Retinal Thickness Analyzer) which were applied differently in each group, according to the specific goals of each study. For the study of Diabetes we also used Vitreous Fluorometry for quantifying the blood-retinal barrier permeability, which is critical to define pre-vascular changes.

Results and Discussion

In sum, in MS we found evidence for independent damage of all retinocortical pathways only in patients with MS without ON (pre-neuropathy group). Axonal damage found in this group (evidenced by VEP) supported the emerging notion of axonal damage even in preclinical stages of ON/MS physiopathology. Again, only in the same group, significant correlation of functional measures with disease stage was observed, suggesting that distinct pathophysiological milestones are present before and after ON has occurred.

In both hereditary optic neuropathies, we verify that structural changes and physiological impairment also occur at a pre-ganglionic level.

These changes in ADOA patients suggest a retrograde damage mechanism with significant clinical impact on visual function, mainly in parvocellular-related tasks.

In LHON carriers, we cannot conclude about the referred retrograde mechanism, since GC function is preserved. This suggests that independent changes may occur at the retinal outer layers in the absence of overt ganglion cell damage.

In type 1 diabetic patients, we found evidence for retinal neuronal changes, in magno-, konio- and parvocellular GC pathways even before breakdown of the blood-retinal barrier or onset of vasculopathy. Neurophysiological changes as shown by electrophysiological measures suggest that neuronal changes also occur at pre-GC level.

Psychophysical and electrophysiological methods can thus play an important role in detecting sub and/or pre clinical changes in diseases affecting GC parallel retino-cortical pathways, and in identifying distinct pathophysiological patterns according to the retinal or optic nerve disease mechanisms.

This work also suggests a path for biomarker research and development in the characterization of quantitatively early and retrograde/anterograde impairment in diseases directly or indirectly affecting the GC and the optic nerve.

PUBLICATION LIST

1. Castelo-Branco M, Mendes M, Sebastião AR, Reis A, Soares M, Saraiva J, Bernardes R, Flores R, Pérez-Jurado L, Silva E. Visual phenotype 1n Williams-Beuren syndrome challenges magnocellular theories explaining human neurodevelopmental visual cortical disorders. J Clin Invest. 2007; 117(12):3720-3729.

2. Maia-Lopes S, Silva ED, Silva MF, Reis A, Faria P, Castelo-Branco M. Evidence of widespread retinal dysfunction in patients with Stargardt disease and morphologically unaffected carrier relatives. Invest Ophthalmol Vis Sci. 2008; 49(3):1191-1199.

3. Maia-Lopes S, Silva ED, Reis A, Silva MF, Mateus C, Castelo-Branco M. Retinal function in Best Macular Dystrophy: relationship between electrophysiological, psychophysical and structural measures of damage. Invest Ophthalmol Vis Sci. 2008; 49(12): 5553-5560.

4. Silva MF, Mateus C, Reis A, Nunes S, Fonseca P, Castelo-Branco M. Asymmetry of visual sensory mechanisms: electrophysiological, structural and psychophysical evidences. J Vis. 2010; 10(6):26, 1-11.

5. Reis A, Mateus C, Macário MC, de Abreu JR, Castelo-Branco M. Independent patterns of damage to retinocortical pathways in multiple sclerosis without a previous episode of optic neuritis. J Neurol. 2011; 258: 1695-1704.

6. Reis A, Mateus C, Viegas T, Florijn R, Bergen A, Silva ED, Castelo-Branco M. Physiological evidence for impairment in autosomal dominant optic atrophy at the pre-ganglion level Graefe's Arch Clin Exp Ophthalmol. 2012 [Epub ahead of print].

7. Reis A, Mateus C, Silva ED, Grazina M, Castelo-Branco M. Evidence for early changes in outer retinal circuits in asymptomatic carriers of Leber hereditary optic neuropathy of the same pedigree. Invest Ophthalmol Vis Sci. *(Submited)*

8. Mateus C, Reis A, Silva MF, Maia-Lopes S, Silva R, Castelo-Branco M. Psychophysics in age-related macular degeneration: a study on potential predictors of conversion of the atrophic to the exudative form. Graefe's Arch Clin Exp Ophthalmol. *(Submitted)*

9. Mateus C, Lemos R, Silva MF, Reis A, Fonseca P, Oliveiros B, Castelo-Branco M. Aging of low and high level vision: from chromatic and achromatic contrast sensitivity to local and 3D object motion perception. PLoS One *(Submitted)*

10. Reis A, Castelhano J, Mateus C, Silva ED, Castelo-Branco M. Central and paracentral visual cortical responses across multiple spatiotemporal channels in autosomal dominant optic atrophy: patterns of impairment and reorganization. *(Under submission)*

11. Reis A, Mateus C, Melo P, Figueira J, Cunha-Vaz JG, Castelo-Branco M. Retinal neuronal dysfunction in type 1 diabetic patients without breakdown of the blood-retinal barrier and absent vasculopathy. *(Under submission)*

.

CHAPTER I

GENERAL INTRODUCTION

CHAPTER I

GENERAL INTRODUCTION

1. BIOLOGY OF THE RETINA AND THE OPTIC NERVE

1.1. BIOLOGY OF THE RETINA - OVERVIEW

The first anatomic descriptions of the cell type of the retina and how they are organized in neural layers in a number of vertebrate species were made by Ramón y Cajal in 1892. He introduced the idea of the vertical pathways (stating that bipolar cells were involved in rod or cone channels of information) and horizontal interactions in which horizontal and amacrine cells contribute (Kolb, 1994).

After this first work, seminal work by Polyak (in primate retina) and Golgi (Kolb, 1992), many others have provided detailed knowledge of the detailed architecture of the retina including the stratified arrangement of the neuron's dendrites and axons, in which the electron microscopy was important (Stell, 1967), allowing for early elucidation of the general organization of this highly complex and layered structure containing millions of closely packed nerve cells that is the retina.

The neural architecture of this tissue can be simply classified in layers of cells and respective synapses, as follows (Fig. 1):

1. Inner limiting membrane (glial cell fibres separating the retina from the vitreous body);
2. Layer of optic nerve fibres (axons of the third neuron – ganglion cell);
3. Layer of ganglion cells (cell nuclei of the multipolar ganglion cells of the third neuron; "data acquisition system" in the sense that these cell convey action potential base information to the rest of the brain);
4. Inner plexiform layer (synapses between the axons of the second neuron – bipolar cell – and dendrites of the third neuron);
5. Inner nuclear layer (cell nuclei of the bipolar cells – second neuron – and horizontal and amacrine cells);

6. Outer plexiform layer (synapses between the axons of the first neuron and dendrites of the second neuron);
7. Outer nuclear layer (cell nuclei of the rods and cones; first neuron);
8. Outer limiting membrane (sieve-like plate of processes of glial cells through which rods and cones project);
9. Layer of rods and cones (the photoreceptors);
10. Retinal pigment epithelium (a single cubic layer of heavily pigmented epithelial cells).

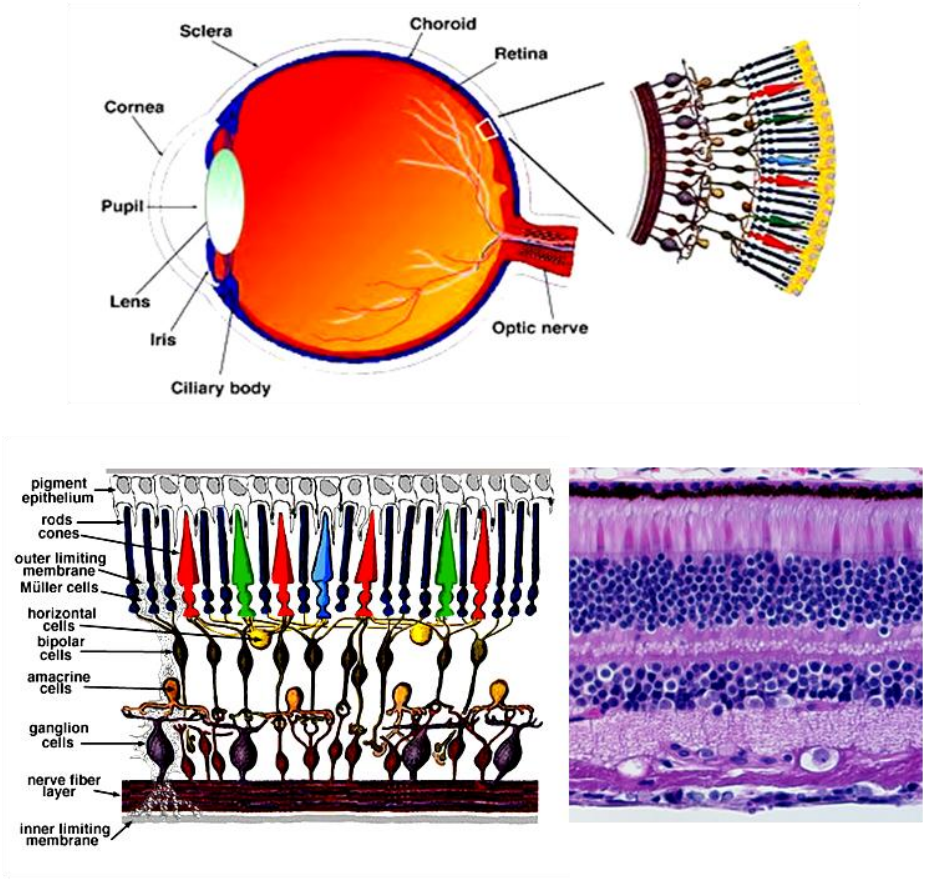

Fig. 1 – Layers of the human retina and their relationships with other structures of the eye (scheme and histological image).
(Sources: humaneresearch.org.uk and pathology.wustl.edu)

Besides this laminar organization of cell layers, neurons do not have a homogenous distribution across the retina, namely considering different eccentricity zones relatively to the centre (Pirenne, 1945).

The central region (macula) differs thus anatomically and functionally from the surrounding retina. In the centre of the fovea (fovea centralis) rods do not exist but only cones, which are different in shape (much more thinner and longer, measuring 70 μm in

length and 1.5 µm in thickness) from those in the surrounding retina, in order to absorber the photons of light in a more efficient way, contributing for a maximal performance in visual acuity. This rod-free area covers a region about 0.3 mm in diameter (corresponding to a visual angle of about one degree), which is the region of the highest density of cones.

Out of the foveola (central 20' of arc), the first rods emerge (at about 0.13 mm from the centre), being thinner than cones in this area. The number of cones per area of retinal surface decreases rapidly from the centre, falling to a low value in the periphery, rising again slightly at the ora serrata. Outside the rod-free area the number of rods increases rapidly, reaching its maximum in a region 5 to 6 mm from the centre. In more peripheral regions the number of rods decreases, but still remaining higher than the number of cones.

Figure 2 shows the distribution of cones and rods in the retina, with millimetres converted in visual angle, in degrees (Osterberg, 1935).

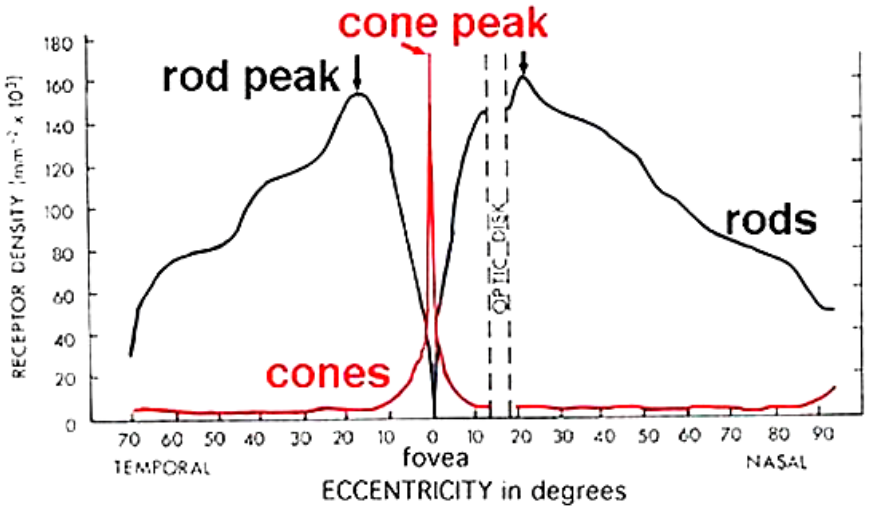

Fig. 2 – Distribution of the rods and cones in the human retina.

(Source: webvision.umh.es)

Polyak (1941) has divided the retina further into seven regions:

Region I – corresponding to the central fovea (also called foveola – Fig. 3) characterized by a small depression caused by the bending away of all the layers of the retina other than the photoreceptors and the outer nuclear and plexiform layers (the latter two are actually thickened, measuring around 1,500 µm from edge to edge,

corresponding to a visual angle of about 5 degrees. The floor of the pit is about 400 µm across.

The area of the fovea contains only cones and is a little larger than the pit, measuring about 500-600 µm across and containing about 34,000 cones.

In the whole region of the fovea (about 1,500 µm) there are about 115,000 cones.

Region II – parafoveal region, measuring about 2,500 µm.

Region III – perifoveal region, measuring about 5,500 µm. In this region, the density of cones diminishes (about 12 cones per 100 µm) and the number of rods increases (approximately two rods interposed between each pair of cones).

Regions IV to VII – lie outside the previously mentioned central regions and extend out to the ora serrata.

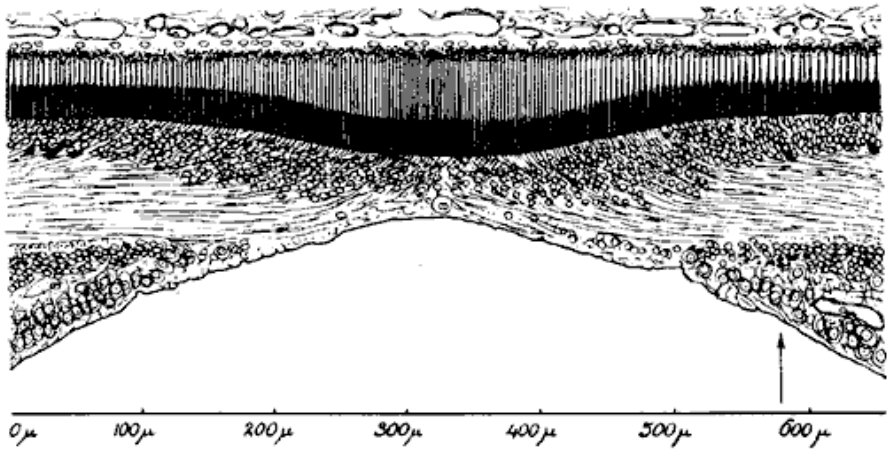

Fig. 3 – Central fovea in the adult eye.
(Source: Adler, 1959; From Polyak, 1941)

Curcio et al. (1987) investigated the density of cones in human retina considering the eccentricity relatively to the fovea, and observed a uniform distribution around the centre that is lost in the most peripheral areas.

This distribution is represented by isodensity maps of cone densities – Fig. 4.

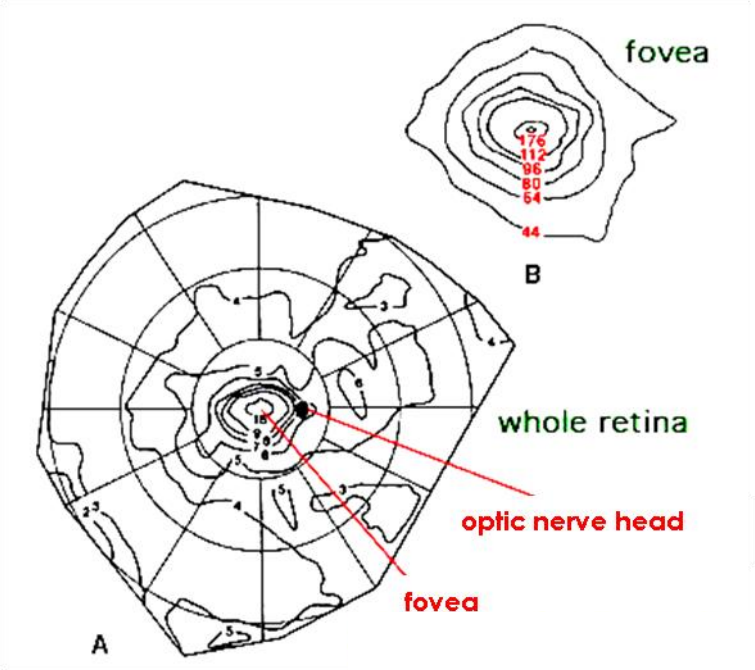

Fig. 4 – Isodensity maps of cone densities (x1000) in the human retina, considering the whole retina (A) and the fovea (B).
(Source: ncbi.nlm.nih.gov)

Having all this structure in mind, the retina cannot be seen as a simple sensory receptive structure, but a very complex nervous tissue composed by many different types of cells and fibres. Light rays firstly pass through the whole thickness reaching the cones and rods, producing there bioelectrical signals that have to pass through the most internal cells. The output message to the brain represents information already processed at two prior levels (photoreceptor and bipolar cell levels), and exits the retina from the most superficial cell layer containing the ganglion cells.

1. 2. THE GANGLION CELLS

Since the early studies from Golgi, followed by Polyak's (1941), it is known that there are different structural types of ganglion cells (GC), involved in several circuits organized according to different functional roles. These cells collect vertical information from the bipolar cells and, concomitantly, different amacrine cells interact in additional lateral modulating netwoks to influence and integrate the GC signals. Lateral conduction is also mediated by the horizontal cells, previously, when synapse with the bipolar cells.

Basically, there are two types of ganglion cells – midget and diffuse (parasol) – Fig. 5.

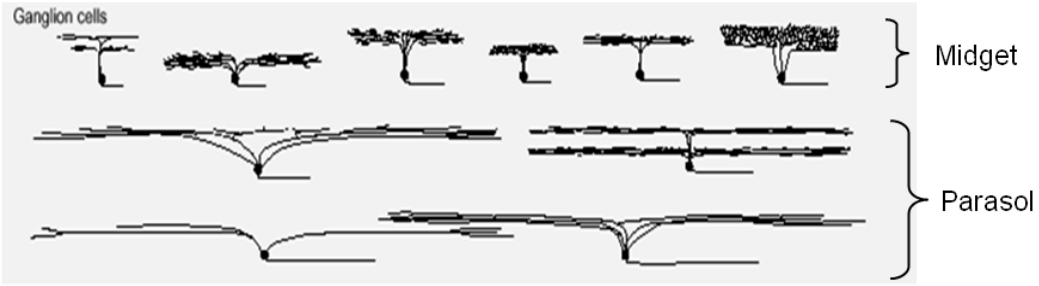

Fig. 5 – Two types of ganglion cells recognized in the retina.
(Source: Masland, 2001).

Midget cell has small size, in particular in which concerns the dendritic tree. In foveal area, midget cell effects a synaptic contact with a single individual or cone bipolar cell and is related therefore to a single cone. The diffuse GCs have relatively long and numerous dendrites, with considerable reciprocal overlapping of the adjacent cells receptive field area. The corresponding axons have larger diameter and faster conduction timing.

Subjacent to the anatomical features of the ganglion cells, there are also two types of concentrically organized receptive fields, depending on cell type: one with a small, linearly summing receptive field centre (P-cells, of the parvocellular system) and another with a large, non-linear responsive area (M-cells, of the magnocellular system).

M-cells respond transiently to the presentation of visual stimuli, while P-cells respond in a sustained fashion.

P-ganglion cells can transmit information about colour, differently from the M-cells. This is due to the fact that receptive field centres and surrounds of P-cells are driven by different class of cones (responding with greatest sensitivity to short-, medium- or long-wavelength light), being chromatically opponent, as shown in Fig. 6. Although M-cells also receive inputs from cones, the centre and surround of each receptive field is driven by all cone types, processing no specific information about colour, given such mixing.

Distinct functional connectivity properties of the two populations suggest that M cells participate in motion analysis, while P-cells are related with the analysis of form, texture, besides colour (Kaplan, 2001).

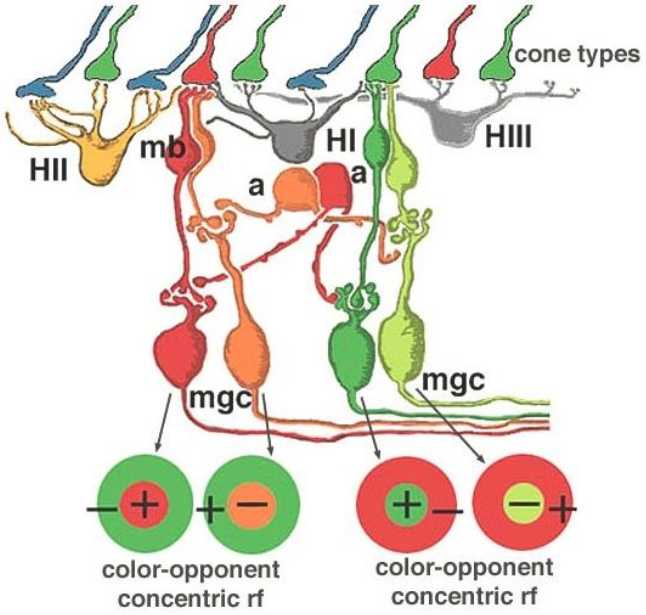

Fig. 6 – The receptive fields of the ganglion cells on colour processing
(midget pathways with centre and surround wiring)
(Source: webvision.uhm.es)

Other types of GCs can be identified in the retina, like biestratified neurons (e.g.: blue-ON cell, of the koniocellular system, and ON-OFF direction-selective cell), ON-type direction-selective cell (projecting to the accessory optic system, related with the optokinetic nystagmus), neurons that project to the suprachiasmatic nucleus, etc.

The ganglion cell axons converge and define nerve fibres, having a characteristic arching arrangement around the fovea, temporally to the optic disc, dividing retina into two altitudinal halves, forming a horizontal meridian. The fibres which come from GCs in the nasal half of the retina run directly into the optic disc in a straight line from each origin point. The fibres from the macula go directly into the temporal portion of the optic disc (papillomacular bundle).

Ganglion cell axons thus exit the retina through the optic disk, where they bundle together to form the optic nerve. This region of the retina contains no photoreceptors and, being insensitive to the light, produces the perceptual blind spot.

1.3. THE OPTIC NERVE AND THE VISUAL PATHWAYS

The optic nerve, although is a part of a tract of the central nervous system (since retina has developed, in the embryo, from the optic vesicle from the original neural tube), does not have the same origin as the fibres of ordinary sensory nerves (growing into the cerebrospinal axis from structures outside the primitive neural tube) (Adler, 1959).

The optic nerve contains approximately 1.2 million axons, each originating from a single retinal GC. Optic nerve fibres are initially unmyelinated (according to the optical needs of the retina) becoming myelinated behind the ocular globe, in order to provide a rapid and efficient propagation of visual impulses to the lateral geniculate nucleus (LGN).

Special structural features are needed to protect the optic nerve from different mechanisms that induced mechanical stress (such as changes in intraocular pressure [IOP] and eye movements). These include the *lamina cribrosa* and the associated astrocytes within the prelaminar and laminar optic nerve head, which provide structural and metabolic support for potentially vulnerable axons. Multiple sources of blood supply to the optic nerve, ensuring steady and reliable perfusion, are also probably related with these anatomic complex features – Fig. 7.

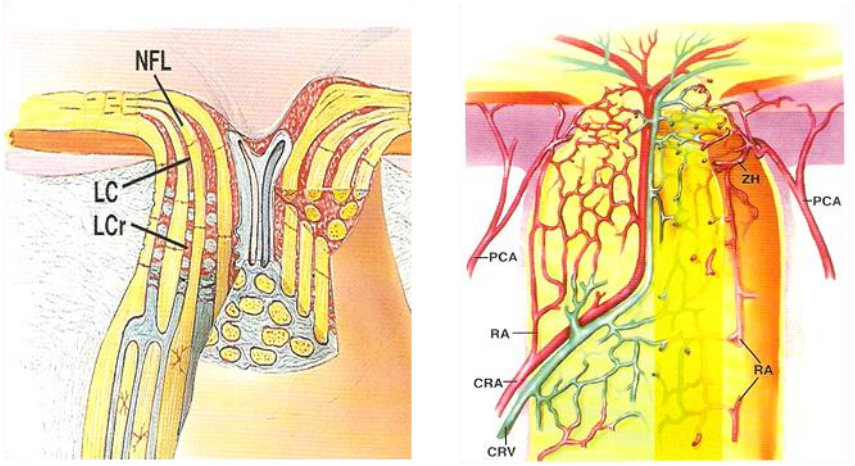

Fig. 7 – The three major portions of optic disc (left) and vasculature (right).
NFL-Nerve fibre layer; LC-Lamina choroidalis; Cr-Lamina cribosa;
PCA-Short posterior ciliary arteries, supplying centripetal capillary beds of anterior optic nerve head;
CRA-Central retinal artery, restricted to nervo fibre layer capillaries and those of anterior intraorbital into central retinal vein (CRV); ZH-intrascleral circle of Zinn-Haller;
RA-recurrent posterior ciliary artery to pial plexus.

(Source: Morrison 2007, pp 4,14)

The optic nerve receives the axons of the GCs in an ordered way: all nerve fibres arising from the temporal half remain on the same side of the pathway in the course through the optic nerve, chiasm, optic tract and radiations up to the occipital cortex. By opposition, all the fibres arising from the nasal side of the retina remains nasally in the optic nerve, cross in the chiasm to enter the optic tract in the opposite side, remaining on this location of the pathway up to the visual cortex (Fig. 8). These crossing fibres are in a larger number (60-75%) compared with the non crossing ones (Adler, 1959).

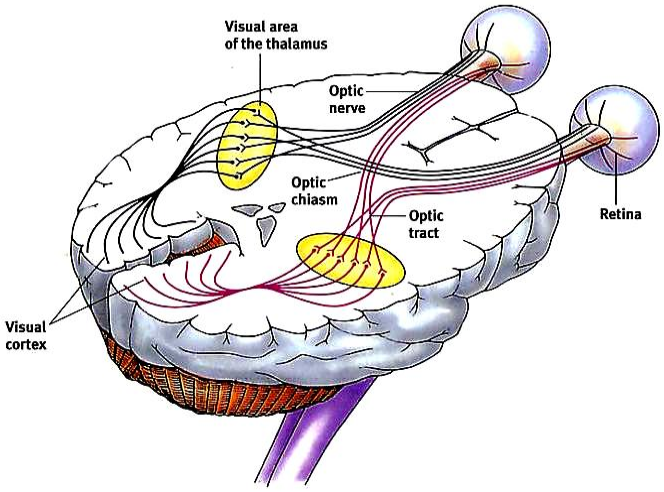

Fig. 8 – The visual pathways: from retina to primary visual cortex.
(Source: lynnwei.com)

In its pathway, optic nerve can be divided into four segments (Fig. 9): intraocular (1 mm), intraorbital (30 mm), intracanicular (6-9 mm) and intracranial (10 mm).

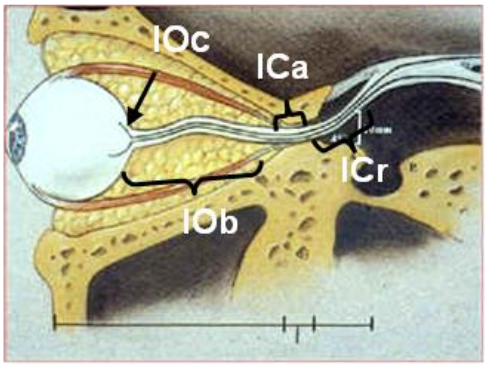

Fig. 9 – Optic nerve and its four portions: IOc – intraocular; IOb – intraorbital;
ICa – intracanicular; ICr – intracranial.
(Source: ipj.quintessenz.de)

Nevertheless, it is important to state that the information concerning the distinct attributes of the visual stimulus remains segregated in parallel functional channels, namely composed by the inputs of the cells of the magno-, parvo- and koniocellular systems. In fact, P-ganglion cells project to the parvocellular layers of the LGN, being highly specialized in colour vision processing and spectrally opponent (in the red-green axis). M-cells project to the magnocellular layers of that structure and are not spectrally opponent, although showing a broad spectral sensitivity created by additive input from L and M cones. K-cells (blue-ON) providing inputs for the blue-yellow axis of colour vision, project to thin layers intercalated between the M and P layers of the LGN (Fig. 10).

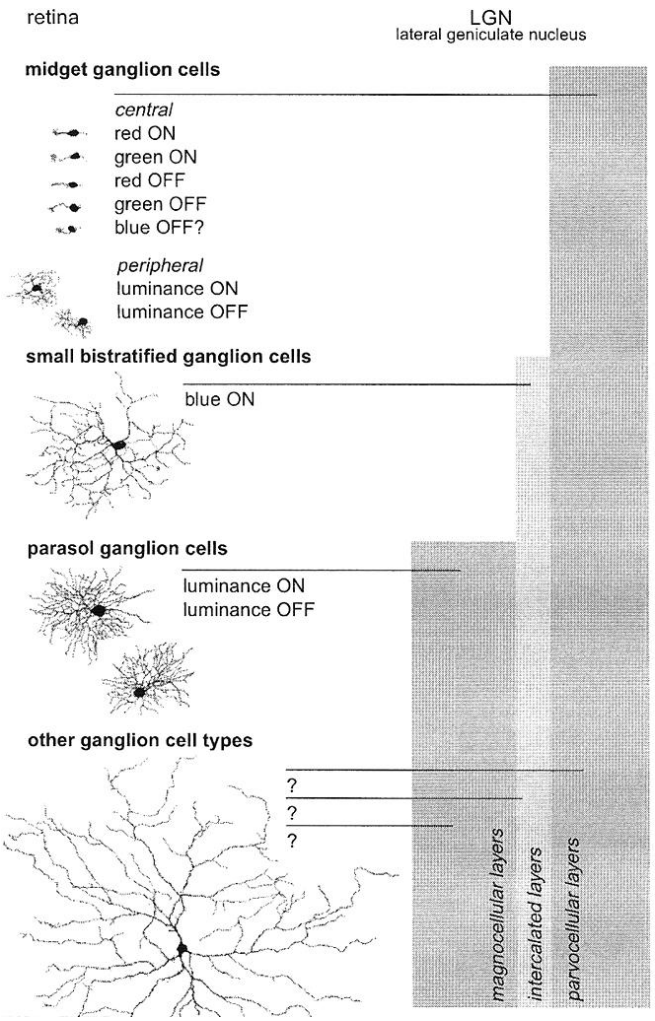

Fig. 10 – The retinal projections of the different ganglion cell types to the layers of the lateral geniculate nucleus.
(Source: Dacey, 2000, p. 748)

Multiple aspects of visual information are encoded in different types of neurons with distinct selectivity to physical stimulus properties (luminance, orientation, motion, texture…). This information remains partially segregated in primary visual cortex and the parallel processing continues in upstream cortical pathways that extend beyond it, including visual areas in the occipital, parietal and temporal lobes (Fig. 11).

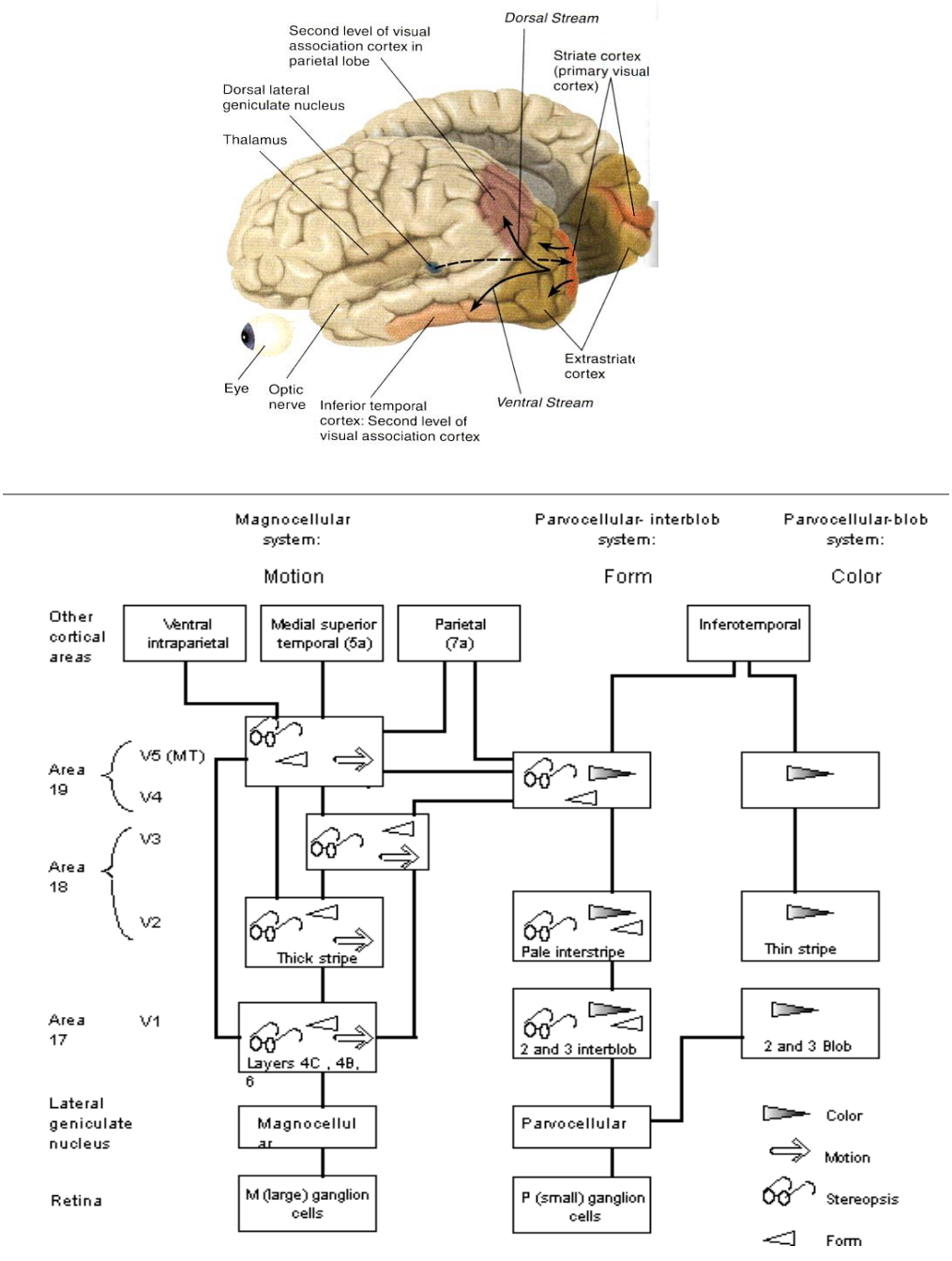

Fig. 11 – Cortical areas and visual pathways beyond primary visual cortex (top) and their suggested functions (down)
(Sources: philosophy.hku.hk; cs.cmu.edu, from Kendel, 1991)

2. OPTIC NEUROPATHIES

2.1. INTRODUCTION

The clinical entity of Optic Neuropathy (ONy) is related with mechanisms of axonal damage in the optic nerve manifested by changes in optic nerve appearance associated with characteristic features as decreased visual acuity, visual field defect, decreased brightness sensation, altered colour vision and relative afferent pupillary defect (if the ONy is unilateral) (Newman, 1996; Biousse 2005).

Combining information about these changes in visual function with clinical and demographic data such as subject's age, ocular and medical history, and concomitant diseases, the clinician may establish the etiological diagnosis of ONy. In some cases, electrophysiology, namely the visual evoked potential, is of utmost importance, since it records objectively the optic nerve function by measuring visual impulse transmission to the primary visual cortex. In other clinical situations, pattern electroretinography is also useful for measuring the integrity of the inner retinal layers, including the GCs, providing evidence of optic nerve dysfunction related with the involvement of inner retinal fibre projections (see chapter III for more details on electrophysiological methods).

Current imaging methods, such as computerized tomography and magnetic resonance imaging can provide detailed information about disease processes within the central nervous system, including the findings in the optic nerve. Ultrasonography and Colour Doppler imaging can also provide supplementary information for the diagnosis and follow-up of the ONy.

The most common categories of ONy are inflammatory, ischemic, compressive, toxic/nutritional, hereditary and neoplastic. The treatment options are many times inefficient mainly due to the fact that the molecular mechanisms of axonal loss are yet not completely understood, leading to an inevitable optic atrophy at an end stage (Lagrèze, 2009).

Other forms of optic nerve diseases can also be observed, namely traumatic or associated with a systemic disease (such as diabetes mellitus) or a therapeutic modality (e.g., radiation therapy) or may be of unknown cause (e.g., papillophlebitis).

In this chapter, special emphasis will be place on the discussion of pathophysiology of Demyelinating and the Hereditary Optic Neuropathies, given the purpose of this thesis.

2.2. INFLAMMATORY-DEMYELINATING OPTIC NEUROPATHY

Idiopathic demyelinating diseases (such as Multiple Sclerosis, Devic's disease or Schilder's disease) lead frequently to primary inflammation of the optic nerve (optic neuritis - ON), being multiple sclerosis (MS) by far the most common known cause of this condition. Neverthless, ON can occur isolated (Plant, 2008), namely in children (Alper and Wang, 2009) in whom it is usually post- or para-infectious.

ON may be symptomatic (being the most common cause of acute visual loss from optic nerve disease in young and middle-aged adults) or asymptomatic. In the first case, a triad of symptoms is characteristic: acute visual loss (variable from minimal reduction in Snellen acuity to no light perception), ipsilateral eye pain, deficits in colour vision (often more severe than visual acuity). Other symptoms can also be present as movement phosphenes, sound-induced phosphenes, visual obscurations in bright light, difficulty with depth perception and Uhthoff's symptom. Other clinical signs of ON are those of an optic nerve disease, including: impaired constrast sensitivity, reduced stereo-acuity, visual field defects (generalized depression, particularly pronounced centrally), afferent papillary defect and optic disc features (hyperemia and acute swelling). However, subclinical cases may occur, even in the absence of visual symptoms (Wray, 1994). For the diagnosis of the asymptomatic ON, besides the mild presence of dyschromatopsia, electrophysiology can be very useful, revealing prolongation of P100-wave latency, not necessarily correlated with visual acuity (Engell et al., 1987).

Although irreversible optic nerve damage occurs in 85% of patients with ON (Fleishman et al., 1987), prognosis concerning the recovery of visual acuity is good, with 65-80% of cases reaching 20/30 or better (Celesia et al., 1990).

The guidelines for treatment of optic neuritis (based on corticotherapy) are presented by the Optic Neuritis Treatment Trial, and the effects of the treatment are continuously studied by the Optic Neuritis Study Group (2008).

2.2.1. MULTIPLE SCLEROSIS AND OPTIC NEURITIS

The first pathological characteristics of Multiple Sclerosis (MS), also known as disseminated sclerosis or encephalomyelitis disseminata, were described in 1838 by Carswell and then Cruveilhier, while Charcot referred it as distinct nosological entity, after his clinico-pathological studies in 1868 (Compston, 1988). Initially considered to be a rare condition, this concept changed in the first half of the 20th century, with the increase of the necessary skills for the neurologists to make the correct diagnosis in patients of MS, whose had been misdiagnosed with other diseases (Pearce, 2005;

Talley, 2005). Today, it is considered to be a frequent acquired disease of the central nervous system (the most common in young adults), but the prevalence varies considerably in the world (Weinshenker et al., 1994). The diagnosis based on established clinical and, if necessary, laboratory criteria (Poser et al., 1983). Although human and animal research studies have suggested that MS could also have an infectious or viral cause (Gilden, 2002 and 2005) based on a previous hypothesis generated in the 1970s (Koprowski, 1976), or be associated with environmental factors (Kurtzke et al., 1987) it is widely accepted to be an autoimmune disease, characterized by progressive demyelination of white matter connections of the central nervous system – brain and spinal cord. Instead of twins-based studies showing a non-inheritable correlation with MS (Sadovnick et al., 1993; Willer et al., 2003) genes are likely to play a role in determining the risk of developing MS, as well as how the disease progresses and how it responds to therapy. However, this role seems to be complex (Sawcer et al., 1996; Marrosu et al., 1998; Barcellos et al., 2006; Hauser and Oksenberg, 2006).

Overall 15-20% of cases of definite MS present ON, and an additional 35-40% develop this condition during the time course of the disease (Ebers, 1986).

On the other hand, ON is a risk factor for developing MS and this risk is highly dependent on the number of lesions present on brain magnetic resonance imaging (MRI) (Ghezzi et al., 2000; Optic Neuritis Study Group, 1997). Several studies show that a significant number of patients having the first acute episode of ON have been subsequently diagnosed with MS, incidence varying with the number of years of follow-up (Bradley and Whitty, 1968; Rizzo and Lessel, 1988; Rodriguez et al., 1995; Ghezzi et al., 2000).

Nevertheless, the common conclusion of these studies is that at least half of those who develop MS will show clinical signs within three years of an optic neuritis attack, and thereafter 2%-5% per year will continue to develop demyelination.

2.3. HEREDITARY OPTIC NEUROPATHIES

The hereditary forms of optic neuropathies consist of a group of disorders in which optic nerve dysfunction occurs as a solely symptomatic deficit related with loss of retinal GCs (primary hereditary optic neuropathies - PHONy), with a prevalence between 1:10 000 to 1:50 000, or may be related with other defects of the central nervous system, in which direct inheritance is clinically or genetically proven.

The most common PHONy are Autosomal Dominant Optic Atrophy (ADOA) and maternally-inherited Leber's Hereditary Optic Neuropathy (LHON), to which special attention will be given in this thesis, but other forms exist (autosomal recessive and X-linked recessive optic atrophy).

The conventional classification of the hereditary optic neuropathies is based on the typical clinical features and classical patterns of familial transmission. When patients do not present a family history, it is important to exclude an acquired cause and to examine related family members, who may be subclinically affected (Votruba et al., 2003). However, sporadic cases may occur.

Presently, genetics analysis can contribute for the diagnosis of some of these disorders in the absence of a family history or in cases of unusual clinical presentation (Newman, 2004).

In general, all inherited ONy have symmetric and bilateral vision loss (except LHON). As the papillomacular nerve fibre bundle is usually affected, central or cecocentral scotomas appear in the visual field, with concomitant optic nerve damage (manifested by a typical optic disc pallor) that is permanent or progressive, according to the type of disorder. However, it is important to exclude primary retinal degenerations (such as cone dystrophies) in which optic nerve pallor may be an early finding and may masquerade the primary ONy (Newman, 2005). Electrophysiological findings include delayed and reduced cortical evoked responses (related with a conduction deficit), abnormal pattern electroretinogram (with reduction of N95 component, consistent with typical GC axonal dysfunction) and normal flash electroretinography (Holder, 1991; Votruba et al., 2003).

Other inherited neurologic and systemic diseases will often manifest optic neuropathy, namely congenital deafness (dominant inheritance), ataxia/deafness (dominant inheritance), diabetes mellitus/deafness (recessive inheritance), DIDMOAD (diabetes insipidus, diabetes mellitus, optic atrophy, deafness) or Wolfram syndrome (recessive inheritance), Behr's syndrome (pyramidal tract signs, mental retardation, ataxia, pes cavus - recessive inheritance), Freidreich's and Marie's hereditary ataxia

(dominant or recessive inheritance), and X-linked Charcot-Marie-Tooth disease (progressive muscular weakness, pes cavus, hammertoes) (Miller, 1982).

Metabolic diseases can also be associated with ONy. In this case, there is a "storage" resulting from a deficiency of a lisosomal hydrolytic enzyme, causing a metabolic block in the catabolism of one or more macromolecules that normally require the missing enzyme for degradating.

The most frequent lysosomal storage diseases affecting the optic nerve include the Mucopolysaccharidoses and Lipidoses which are summarized in the following table, indicating the respective responsible enzymes.

Nevertheless, besides this variety of inherited disorders, a selective vulnerability of the optic nerve to perturbations in mitochondrial function may underlie a final common pathway among them (Newman, 2005).

Disease	**Enzyme Deficiency**
MUCOPOLYSACCHARIDOSES	
Hurler (I-H)	α-L-iduronidase
Scheie (I-S)	α-L-iduronidase (partial)
Hunter A (IIA) (severe phenotype)	Iduronate sulfatase
Hunter B (IIB) (mild phenotype)	Iduronate sulfatase
Sanfillippo A (IIIA)	Heparan sulphate sulfatase
Sanfillippo B (IIIB)	N-acetyl-glucosaminidase
Morquio (IV)	N-acetyl-galactosamine sulfatase
Maroteaux-Lamy A (VIA) (severe phenotype)	Acrylsulfatase B
LIPIDOSES	
Generalyzed gangliosidosis (GM_1_I)	β-galactosidase A,B,C
Juvenile gangliosidosis (GM_1_II)	β-galactosidase B,C
Tay-Sachs (GM_2_I)	Hexosaminodase A
Sandhoff (GM_2_II)	Hexosaminodase A
Juvenile gangliosidosis (GM_2_III) (partial)	Hexosaminidase A
Niemann-Pick A(infantile)	Sphingomyelinase
Krabbe (globoid cell leukodystrophy)	Galactocerebroside β-galactosidase
Metachromatic leukodystrophy (infantile)	Acrysulfatase A
Metachromatic leukodystrophy (juvenile and adult)	Acrysulfatase A
Sulfatidosis, Austin variant (mucosulfatidosis)	Acrysulfatase A,B,C

Table 1 – Inborn metabolic disorders with optic atrophy.
(Source: Kline et al., 2007, p. 171)

2.3.1. AUTOSOMAL DOMINANT OPTIC ATROPHY

Autosomal dominant optic atrophy (ADOA) is the most common autosomally inherited optic neuropathy, although often misdiagnosed, affecting between 1:12.000 to 1:50.000 people (Kjer et al., 1996). First clinically described by Batten in 1896, it was named Kjer's optic neuropathy in 1959, after Poul Kjer's studies in 19 families affected with this disease (Kjer, 1959). It is also known as autosomal dominant optic atrophy - Kjer type, Kjer optic atrophy and Kjer's autosomal dominant optic atrophy.

Patients present bilateral mild to severe reduced visual acuity, usually symmetrical (stationary or slightly progressive), beginning with an insidious onset in childhood typically between 4 and 6 years of age (Newman, 2005; Votruba et al., 2003). In general, severity of symptoms by adolescence reflects the level of visual function to be expected throughout most of the patient's adult life (Elliot et al., 1993; Votruba et al., 1998). However, ADOA may remain subclinical until early adulthood in some cases (Hoyt, 1980). Characteristic clinical features are associated with the vision loss (Votruba et al., 1998; Hoyt, 1980): the optic nerve pallor, varying from a subtle diffuse pallor to a typical wedge-shapped temporal pallor, or to a total atrophy; visual field defect is classically a cecocentral scotoma, although could be central or paracentral; impairment in colour vision was initially reported as a blue-yellow deffect or tritanopia (Kline and Glaser, 1979), and more rarely a red-green deffect (Kok-van-Alphen, 1970). However, recent studies have demonstrated that a generalized nonspecific dyschromatopsia is the most common (81%) type of colour vision deficit (Votruba et al., 1998). This high variability on clinical expression correlates with the degree of atrophy (Carelli et al., 2002).

This neuropathy is often caused by mutations in the *OPA1* gene on cromosome 3q28-q29 (Eiberg et al., 1994; Bonneau et al., 1995). However, other loci for optic atrophy have been found and mapped (from *OPA2* to *OPA7* genes) – Ref. OMIM #165500. A high variability of mutations of *OPA1* (over two hundred) have been reported (Yu-Wai-Man et al., 2010; Ferré et al., 2005), probably related with the considerable intra and interfamiliar phenotyping. Some of them are related with hearing loss (Ke et al., 2006; Li et al., 2005) or mental retardation (Newman and Biousse, 2004). *OPA1* gene encodes a mitochondrial protein with 960 amino acids with similarity to dynamin-related GTPases, being a component of the mitochondrial network (Alexander et al., 2000; Delettre et al., 2000), anchored to the mitochondrial inner membrene facing the inter-membrane space (Olichon et al., 2002). The consequent mitochondrial dysfunction leads to the death of optic nerve fibres, by degeneration of

the retinal GCs, in particular the smallest and less myelinated neurons of the papillo-macular bundle and their axons, since these cells have high energy demand, as well as the unmyelinated part of the axons anterior to the *lamina cribosa* (Carelli et al., 2002, 2004; Pech et al., 2004), resulting thus in a clinical appearance of optic atrophy. These structural lesions can be confirmed histologically (Johnston et al., 1979; Kjer, 1982) and functionally by electrophysiological testing. A reduced N95 component of the pattern electroretinogram (also with a reduced P50 component, but rarely extinguished, even in more severely affected eyes), an absent or of reduced amplitude pattern visual evoked potentials with delay and a normal full-field electroretinogram are electrophysiological characteristics of DOA (Holder, 1987; Holder et al., 1999).

2.3.2. LEBER'S HEREDITARY OPTIC NEUROPATHY

Leber Hereditary Optic Neuropathy (LHON, Ref. OMIM #535000) has been firstly clinically described by Leber in 1871 but only in the late 1980s it is known to be a maternally inherited neuropathy associated with a mutation in mitochondrial DNA (mtDNA) causing dysfunction (Wallace et al., 1988). The respiratory deficit may lead to axoplasmic stasis and swelling, with intramitochondrial calcification (Kerrison et al., 1995), which can be reversible in some ganglion cells, if apoptosis is not yet activated. After this activation GCs will be permanently loss.

LHON affects predominantly young males (80-90%), being 3.22:100 000 the minimal estimated prevalence of resulting visual failure (Man et al., 2003), although a higher prevalence (11.82:100 000) was also described (Mackey DA, 1994).

The first symptoms are unilateral painless acute central vision loss and colour vision desaturation; the second eye is usually sequentially affected weeks to months later (Newman, 2005), although it can be rarely affected simultaneously (Harding et al., 1995). This central visual loss, related with the preferential and earlier involvement of the vulnerable small diameter nerve fibres (Sadun et al., 2000), occurs most frequently between the ages of 15 and 35 years (although younger or older individuals have been reported) with a range of 2-80 years, stabilizing after months of visual function deterioration down to acuities worse than 20/200 (Newman, 2005). This is consistent with the observed visual field defect, initially characterized by a central scotoma that rapidly becomes centrocecal. OCT, by measuring the retinal layer fibre thickness, also confirms the early involvement of the papillomacular bundle (Barboni et al. 2010), as well as the predominant parvocellular (red-green) impairment in colour vision testing even in asymptomatic carriers (Ventura et al., 2007).

Some fundoscopic findings are characteristic during the acute stage, consisting of a triad of signs (Smith et al., 1973): circumpapillary telangiectatic microangiopahy, swelling of the nerve fibre layer around the optic disc (pseudoedema) with microvascular anomalies, and absence of leakage from the papillary region on fluorescein angiography (differently from truly edematous discs). Nevertheless, these signs can also be observed in presymptomatic eyes or in even asymptomatic maternal relatives' eyes (Nikoskelainen et al., 1996), which can be very helpful in these cases.

Besides this triad is believed to be pathognomonic for LHON, its absence in the acute stage or in presymptomatic eyes does not exclude this diagnosis. In this case, pattern-reversal visual evoked responses can play an important role (Livingstone et al., 1980).

As the disease progresses, the telangiectatic vessels disappear and the pseudoedema of the disc resolves, and optic atrophy develops with loss of the nerve

fibre layer (Newman, 2005; Votruba et al, 2003). In most patients with LHON visual dysfunction remains very poor and permanent, although some individuals can recover up to an excellent performance level, which is probably related with the genetic backgroung.

Three point mutations in the mtDNA ("primary" LHON mutations) are responsible for at least 90% of cases of LHON worldwide (Newman 2005; Man et al., 2002), and are located at positions 11778 (69%), 3460 (13%) and 14484 (14%). Mutations at G11778A and G3460A appear to be associated with a similar visual outcome (1/60 to 3/60), while mutation at nucleotide position (np) 11778 is particularly severe in one-third of female patients (Riordan-Eva and Harding, 1995) even with a later age of onset (Harding et al., 1995). Patients with the T14484C mutations are considerably better than those with the other two mentioned mutations, having some recovery of vision in 50% of the cases, with a better visual outcome if the onset of visual loss is before the age of 20 years, reaching 6/24 or better in 71% of cases (Johns et al., 1993).

Besides these three mutations (found almost exclusively in multiple LHON families and alter evolutionarily conserved amino acids) there are other rarer primary mutations, such as T14596A, C14498T, G13730A, G14459A, C14482G and A14495G. Secondary mutations may also be related with the pathogenesis of LHON, but they are also present in control populations at a lower prevalence, probably representing polymorphisms. These are associated with a primary mutation or other secondary mutations, usually causing the mutation of a less highly conserved amino acid. Np G13708A, G15812A, A4917G, T4216C, G9804A and G15257A are examples of secondary LHON mutations.

In most of the patients with LHON visual dysfunction is the only manifestation of the disease. However, some pedigrees have members with associated cardiac conduction or minor neurological changes (Leber Plus phenotype), although more severe neurological abnormalities can be found in multiple maternal members of some pedigrees (Newman, 2005).

Association between LHON and Multiple Sclerosis may occur, with LHON mutation causing a worse prognosis of optic neuritis in patients with MS (Bhatti and Newman, 1999).

3. DIABETIC RETINOPATHY. VASCULAR AND NEURAL APPROACHES

3.1. PRESENTATION AND CLASSIFICATION OF DIABETIC RETINOPATHY

Diabetic Retinopathy (DR) is a complication of diabetes and is characterized by a group of retinal lesions, generally found after several years from the beginning of the disease. According to Cunha-Vaz (2011), the retinal involvement in diabetes may be divided into different stages: preclinical stage, nonproliferative retinopathy and complications of diabetic retinopathy (diabetic macular edema, and preproliferative and proliferative retinopathy), with increased levels of severity.

Preclinical stage is characterized by the absence of visual lesions on ophthalmoscopic examination. However, some subclinical changes may occur, evidenced by some sensitive functional methods (Klein et al., 2008; Lopes de Faria et al., 2001; Di Leo et al., 1990). Biochemical, pharmacological and histological studies do corroborate this concept (Barber, 2003; Santiago et al., 2006a; Santiago et al., 2006b; Leal et al., 2005).

In nonproliferative DR some ocular fundus alterations can be detected by ophthalmoscopy: microaneurysms (usually the first ophthalmoscopic signs of DR), intra-retinal hemorrhages, hard exsudates and some degree of retinal edema.

Diabetic macular edema is often the first retinal alteration that causes vision loss and does not fit necessarily into the regular course of diabetic retinopathy progression, since it may be present at any stage of DR, nonproliferative, moderate or severe (or even at the more advanced stages) (Klein and Klein, 2003).

Preproliferative DR is an intermediate stage between background retinopathy and proliferative retinopathy, presenting signs of increasing retinal ischemia. These include soft exudates, venous beading and loops, intraretinal microvascular abnormalities (IRMA) and widespread areas of capillary nonperfusion (Benson et al, 1988).

In proliferative retinopathy new vessels arise from the optic disc or from the peripheral retina. Complications associated with retinal neovascularization include vitreous hemorrhage, growing of fibrous tissue, with consequent fibrovascular tissue contraction and cellular proliferation with risk of localized of generalized detachment.

DR is highly prevalent in the western world and is a major cause of vision loss. There are several risk factors for the DR development, but the disease duration is probably the most consensual parameter (Cunha-Vaz, 2011; Williams et al., 2004; Henricsson et al., 2003; Likitmascul et al., 2006). Another important factor concerning likelihood of developing DR is the metabolic control. Correlation studies with these two variables show that patients with higher glycated hemoglobin (HbA1c) percentages have higher risk for DR development when compared with patients with lower levels of HbA1c (Henricsson et al., 2033; Kullberg et al., 2002). Nevertheless, a fraction of patients presenting good metabolic control (about 10%) do develop DR and still another proportion of patients with poor metabolic control do not develop it (Zhang et al., 2001).

The prevalence of type 2 DR is much higher than type 1 DR (~9:1) due to the larger number of diabetic 2 patients in the human population (Eden and Klein, 2007). However, due to the earlier age of onset of type 1 diabetes (leading to longer time duration of disease in a lifetime), the prevalence of DR in type 1 diabetic patients is very high (~90% after 15 years of duration disease) as shown by long-term epidemiological studies (Klein et al., 2008).

3.2. DIAGNOSTIC METHODOLOGIES

There are several methodologies for the diagnosis and follow-up of DR, ones focusing on vascular study others allowing a functional (neuronal) characterization.

Retinography and fluorescein angiography are the current clinical tools for detecting the presence or absence of vascular lesions, allowing the grading of DR. However, these techniques do not provide information on quantification of blood-retinal barrier (BRB) permeability, which was firstly provided by vitreous fluorometry. In 1975, Cunha-Vaz and col. published new and important results enhancing the clinical importance of this method, evidencing alterations of the BRB in diabetic eyes with apparently normal ocular fundi. After several years, a more detailed characterization on the permeability of the BRB became possible, with the Retinal Leakage Analyzer (Lobo et al., 1999). This method, based on a modified confocal scanning laser ophthalmoscope allows a localized quantification of the BRB over a region of interest, extracted from the ocular image fundus.

Retinal thickness is another important parameter to evaluate, since diabetic macular edema is often the first retinal alteration causing vision loss. The most common methods for imaging and measure retinal thickness are Retinal Thickness Analyzer (Sahidi et al., 1991) and Optical Coherence Tomography (OCT) (Hee at al., 1995) – for

details see Chapters III and VII. Spectral-domain OCT have been substituting time-domain OCT, providing high resolution images, with greater detail in a shorter period of time, with consequent decrease in motion artefact and a larger area to be scanned (Kiernan et al., 2010).

Retinal neural impairment evaluation can be important to probe the consequences of vascular damage in visual function. Moreover, it is still an open question whether primary neural damage occurs early in the natural history of diabetic retinopathy (thus in pre-clinical stage of DR). This is actually one of the major goals of our work.

Psychophysical and electrophysiological methods could play an important role in this evaluation. Some important psychophysical methods in this early stage include chromatic contrast sensitivity with sensitive computerized assessment and perimetric techniques selective for particular functional pathways (Castelo-Branco, 2011), such as short-wavelength automated perimetry (SWAP - assessing the koniocellular system performance) and the frequency doubling technology (FDT), a perimetric achromatic contrast sensitivity test for magnocellular performance evaluation.

Electrophysiological assessment in the pre-clinical stage allows us to evaluate neurophysiological changes from different points of view:

Oscillatory potentials (OP) record the bioelectrical activity of the inner layer of retina (including amacrine cells). Thus, as retinal capillaries within the inner nuclear layer (close to cell bodies of amacrine and bipolar cells) seem to be affected in quite early stages of DR (Chakrabarti et al., 2000; Ciulla et al., 2003) OP are a relatively useful biomarker in detecting early neuronal dysfunction.

The results of pattern ERG (PERG) are not coincident among the authors. Some studies report clinical relevance of PERG (Arden et al., 1986) while others found no difference between diabetic and controls' responses in early DR (Jenkins and Cartwright, 1990; Wanger and Persson, 1985).

Multifocal ERG (mfERG) is a relative recent technique that allows to record topographic responses within central vision (Sutter and Tran, 1992). While previous studies on DR report no changes in global ERG (Jenkins and Cartwright, 1990; Wanger and Persson, 1985), mfERG proved to be very useful in detecting localized changes in amplitude and implicit time in diabetes, showing an increase delay in implicit time with the increasing stage of DR (Fortune et al., 1999). Thus, this technique proved to be clinically important in regular evaluation of neuronal impairment, even in pre-clinical DR stages.

4. ASSESSEMENT OF RETINA AND OPTIC NERVE FUNCTION BY PSYCHOPHYSICS AND ELECTROPHYSIOLOGY

4.1. PSYCHOPHYSICS – BASIC PRINCIPLES

Psychophysics (*psycho* = perception; *physics* = physical nature of the stimulus) was founded by the German psychologist Gustav Fechner (1801-1887), with his work "Elemente der Psychophysik" (1860). The most famous outcome of his inquiries is the *Weber–Fechner law*: "In order that the intensity of a sensation may increase in arithmetical progression, the stimulus must increase in geometrical progression", implying that sensation is a logarithmic function of physical intensity.

Psychophysics is, thus, the scientific study of the relationship between stimuli (specified in physical terms) and the sensations and perceptions evoked by these stimuli. The term *psychophysics* is used to denote both the substantive study of stimulus-response relationships and the methodologies used for this study, and is a very important concept in Vision Science.

For psychophysical measurements, different methods can be used in order to determine the threshold for different parameters of the visual stimulus, namely colour and contrast, including visual field analysis. For a perfect observer, threshold is either the point where the stimulus can just be detected or either the point from which it cannot be detected, simultaneously. As not a perfect observer, thresholds for the human eye are often defined in probabilistic terms: half the points presented would be detected and half would not. Thus, in some psychophysical techniques, threshold can be considered the point where 50% of the stimuli are detected, depending on the neural noise of cellular activity.

According to the differences between a perfect (physical) and human observer there are two parallel sets of units for measuring light: one is based on its detection by physical radiometric devices (radiometric units) and the other is based on the psychophysical impact of the light on a human observer (photometric units), respectively (interconvertible by means of the spectral luminous efficiency function).

Measurement of visual response can be achieved through several psychophysical methods, namely Method of Adjustment, Method of Limits, Staircase (modified Method of Limits) and Method of Constant Stimuli. Adaptative strategies can also be used.

Method of Adjustment – In this case, subject has to adjust the stimulus properties to a given pattern. The classical example is the method subjacent to the Anomaloscopy, in which the subject is asked to adjust the colour presented in an area to the colour of the pattern (Fig. 12).

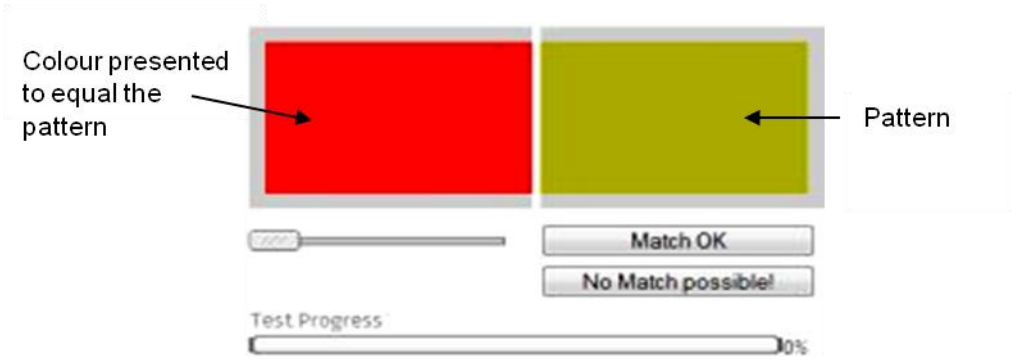

Fig. 12 – Method of adjustment. Principle of Anomaloscopy.
(Source: colblindor.com)

Method of Limits – Stimulus is presented well above threshold and its intensity decreases in small steps until the subject cannot detect the stimulus (threshold obtained by descending limits), or the stimulus is first presented well below threshold and its intensity is increased to reach threshold (ascending limits). Some errors of habituation (after repeated responses) and anticipation (due to premature response before the threshold has been reached) can occur.
Combined ascending and descendent limits can be presented for quickly determining threshold (Fig. 13).

Stimulus Intensity	A	D	A	D	A	D	A	D
9		Y						
8		Y				Y		Y
7		Y		Y		Y		Y
6		Y		Y		Y		Y
5		Y		Y		Y		Y
4	Y	Y		Y		Y		Y
3	N	Y	Y	Y	Y	Y		Y
2	N	N	N	Y	N	N	Y	Y
1	N	N	N	N	N		N	N
0	N		N		N		N	
-1	N		N		N		N	
-2	N		N		N		N	
-3	N		N		N		N	
-4	N		N		N		N	
-5	N		N				N	
-6	N						N	
Transition Points	3.5	2.5	2.5	1.5	2.5	2.5	1.5	1.5

Mean Threshold = 2.25

Fig. 13 – Threshold obtained by the method of combined ascending (A) and descending (D) limits (Y = Yes, the stimulus is seen; N = No, the stimulus cannot be seen).
(Source: Kalloniatis and Luu, 2007)

Method of Staircase – This method is a variation of the method of limits, involving both the ascending and descending limits in a same trial. Stimulus intensity is progressively increased (ascending limits) until the subject reports seeing the stimulus. At this point, the intensity value is recorded and the stimulus intensity is then progressively reduced (descending limits), until the subject reports not seeing the stimulus. Again, intensity increases and decreases when subject stops seeing the stimulus. This series repeats until final threshold is obtained, considering the average of several of these reversal points (Fig. 14).

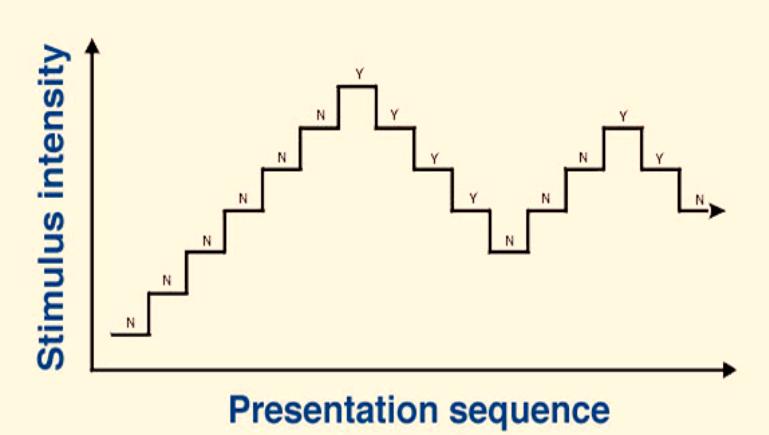

Fig. 14 – Staircase method (Y = the stimulus is seen; N = the stimulus cannot be seen).
(Source: Kalloniatis and Luu, 2007)

Method of Constant Stimuli – A certain number of stimuli is repeatedly presented with different intensities in a randomly way. Subject is asked to respond when seeing a stimulus, and the percentage of detection is determined as a function of its intensity. Some stimuli with higher intensity values will always be detected while other of low intensity will never be detected. The value where 50% of the stimuli are detected lies somewhere within this intensity range, corresponding to the obtained threshold.

Figure 15 shows a graphic with the percentage of detection versus the stimulus intensity. In this example, threshold corresponds to a value of 23.5 of intensity. This function – the *psychometric function* – has a characteristic feature of a S-shaped curve (ogive).

In this method, different procedures can be applied. In this particular case, the YES-NO PROCEDURE involves the subject judgement about the presence or absence of the signal (a stimulus is presented during which the subject has to decide between a "yes" and a "no" response). Correct response can range from 0% to 100% as shown again in figure 15.

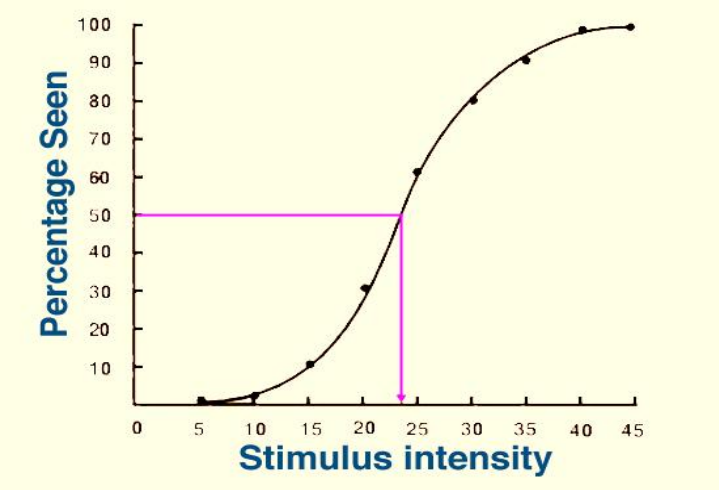

Fig. 15 – Psychometric function obtained from a YES-NO paradigm.
(Source: Kalloniatis and Luu, 2007)

In the FORCED CHOICE PROCEDURE subject is forced to choose from alternative choices, one of which contains the stimulus. With a two-alternative forced choice (2AFC) subject has to choose between two alternatives. Choosing from four or six alternatives we have a 4AFC and a 6AFC, respectively.

The number of alternative answers leads to different points of origin in the psychometric function. Thus, as there is already a 50% chance of a correct response in a 2AFC procedure, the origin point starts at the level of 50% of stimuli seen, being the threshold the middle point between 50% and 100% (75%) – see Fig. 16.

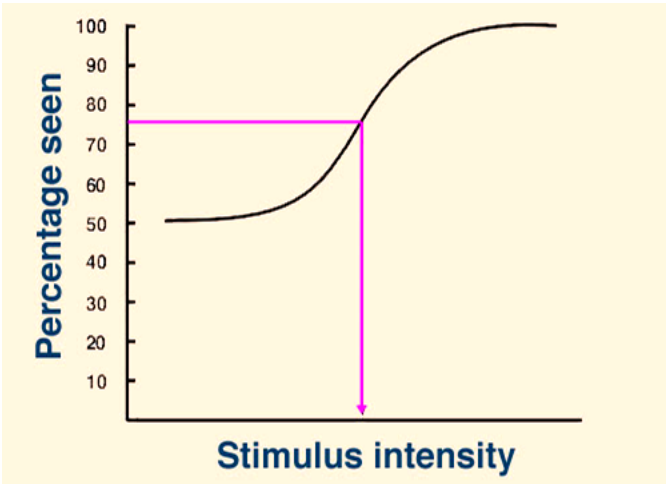

Fig. 16 – Psychometric function for a two-alternative forced choice (2AFC) strategy.
(Source: Kalloniatis and Luu, 2007)

For a 4AFC, threshold is considered to be at the 62.5% seen level, as this is the middle point between 25% (corresponding to the origin of the ogive, since there is already a 25% chance of a correct response) and 100%, and so on.

Adaptive Psychophysical Methods - In a psychophysical test, stimuli can be presented according to the performance of the subjects' previous response. Thus, when subjects correctly respond, stimulus intensity is decreased by one step. A wrong response leads to one step increase in stimulus intensity. The session ends when a narrow range of stimuli level is reached, threshold being considered the average of the intensity level within the period of stable tracking.

Step size is an important factor to take into account. If steps are too small, the subject may not be able to discern differences in intensity and the test will be also too long. On the other hand, large steps may miss the real threshold, because final reversals can be located a little above or below it.

Some techniques use a parameter estimation by sequential testing, with large steps in the beginning and smaller steps (half intensity) in the subsequent series (after a reversal point), as shown in figure 17.

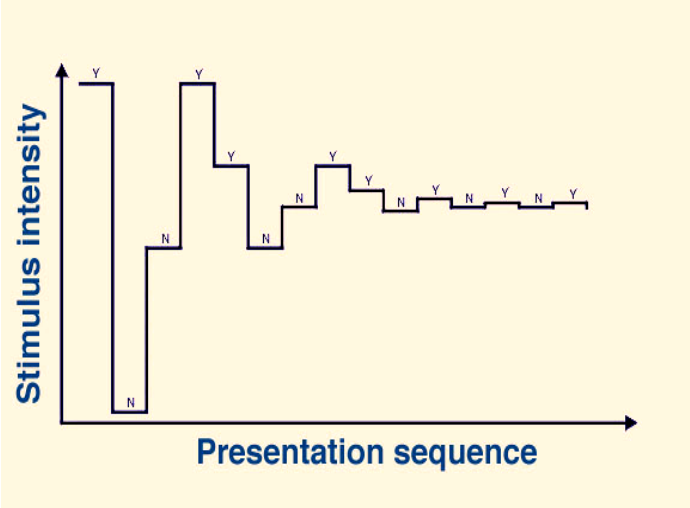

Fig. 17 – Obtaining a threshold using an adaptive psychophysical method, based on parameter estimation by sequential testing.
(Source: Kalloniatis and Luu, 2007)

4.2. PSYCHOPHYSICAL EVALUATION

Psychophysics is a useful tool for visual function evaluation, since it is the only way to understand how the subject percepts different attributes of the visual stimulus. It is also important for characterizing the vision, as a whole, since visual acuity can only tell us about "quantity of vision", and the visual function much more than this.

Thus, vision is a complex perception about all components of the visual stimulus, processed by different parallel functional channels (already mentioned in the previous chapter), acting at the same time for the same purpose, contributing not only for the "quantity of vision" but also for the "quality of vision".

Psychophysical methods can be applied in Colour Vision or Contrast Sensitivity evaluation.

Besides these, psychophysics is also subjacent in different perimetric techniques for detecting visual fields defects in retinal and optic nerve diseases, namely in standard approaches (white-on-white perimetry) or in selective testing for a specific functional channel, such as short-wavelength automated perimetry (SWAP) or frequency doubling technology (FDT) – for details of some of these methods, see Chapter III.

4.3. ELECTROPHYSIOLOGY – BASIC PRINCIPLES

Electrophysiological methodologies provide an objective evaluation of neuronal function, by recording bioelectrical responses to different types of stimulation. These stimuli (and the electrodes) are adjusted to the aimed neuronal population to be studied, according to its structural and functional properties.

Thus, electrophysiological responses can have a retinal or cortical origin and different electrophysiological methods can separate the responses of different cell populations, as can be shown in figure 18.

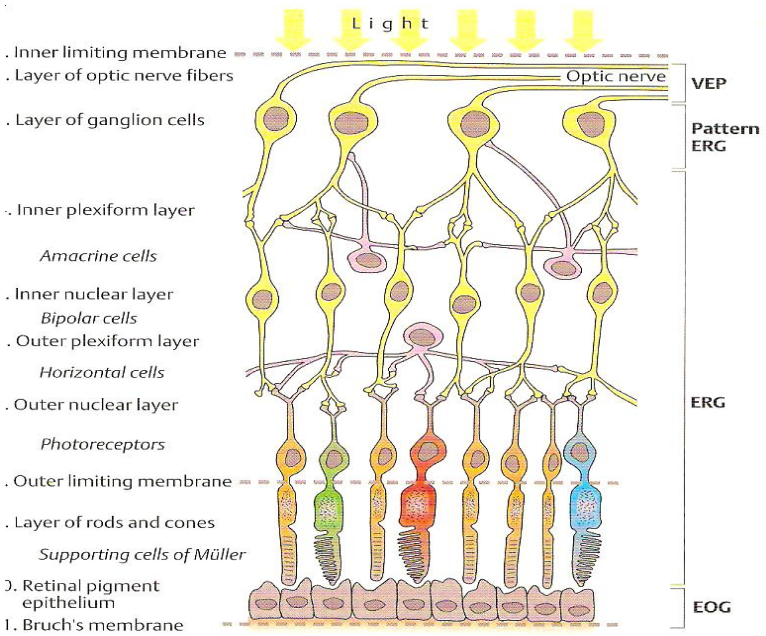

Fig. 18 - Layers of the retina and electrophysiological methods to record the bioelectrical activity in the respective layers
(Source: Lang, 2000, p. 301)

Electro-oculogram (EOG) tests the function of the outer retina and retinal pigment epithelium (RPE) in which changes in electrical potential across the RPE are recorded during successive periods of dark and light adaptation (Marmor et al., 2010). The results are expressed by the Arden ratio, which is the ratio between the light peak and the dark trough of the physiologic EOG recording. Normal values are established by each laboratory, but as a reference, Arden ratios lower than 1.5 are generally reported as abnormally low, while those higher than 2.0 are generally reported as normal; ratios between 1.5 and 2.0 may be reported as borderline (Marmor et al., 2010).

Figure 19 shows a normal EOG recording.

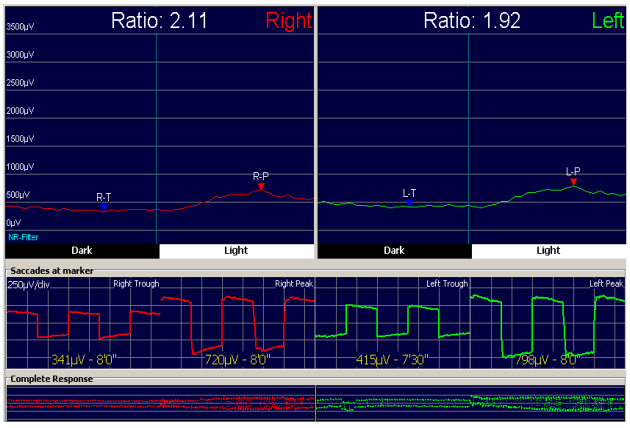

Fig. 19 – EOG recordings obtained in both eyes of a control.
(Source: data - IBILI; image - the author)

The full-field electroretinogram (ERG) records the global retinal response under different conditions of stimulation (flashes presented in a full-field dome stimulator), allowing concomitantly different types of responses: (1) Dark-adapted 0.01 ERG (rod response); (2) Dark-adapted 3.0 ERG (combined rod-cone response); (3) Dark-adapted 3.0 oscillatory potentials; (4) Light-adapted 3.0 ERG (cone response); (5) Light-adapted 3.0 flicker (30 Hz flicker) (Marmor et al., 2009).

Figure 20 presents the data obtained in a healthy subject.

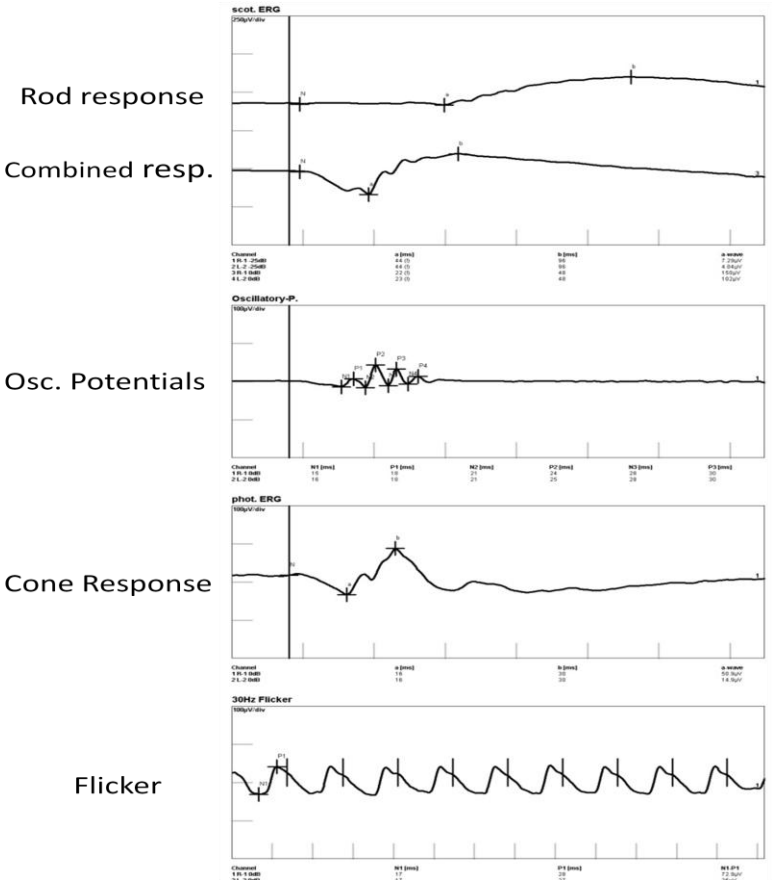

Fig. 20 – ERG recordings obtained in a healthy eye.
(Source: data - IBILI; image - the author)

The pattern electroretinogram (PERG) is a retinal response evoked by a reversal pattern, usually a black and white checkerboard. This response provides information about GC and macular function (since the stimulus is viewed with central fixation). Furthermore, PERG recording is useful in cases of abnormal VEP, since gives information about the retinal response to the same type of stimulus (Holder et al., 2007; Holder, 2001), allowing a conclusion about the impairment source/origin.

A normal PERG recording can be seen in Figure 21.

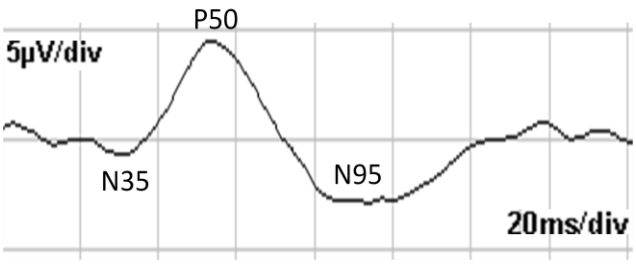

Fig. 21 – Pattern ERG recorded in a healthy eye.
(Source: data - IBILI; image - the author)

Visual evoked potentials (VEP) are visually evoked electrophysiological signals extracted from the electroencephalographic activity in the primary visual cortex, recorded from the overlying scalp, by means of a single recording channel with a midline occipital active electrode. Additional lateral active electrodes can also be placed in order to search for inter-hemispheric asymmetries.

As visual cortex is activated primarily by the central visual field, VEPs depend on functional integrity of central vision at any level of the visual pathway including the eye, retina, the optic nerve, optic radiations, and occipital cortex (Odom et al., 2010).

Different recordings can be obtained by this technique:

1. Pattern-reversal VEPs elicited by checkerboard stimuli with large 1° (60 min of arc) and small 0.25° (15 min) checks.
2. Pattern onset/offset VEPs elicited by checkerboard stimuli with large 1° (60 min) and small 0.25° (15 min) checks.
3. Flash VEP elicited by a brief luminance increment, a flash, which subtends a visual field of at least 20°.

Pattern reversal is the preferred stimulus for most clinical purposes. Pattern-reversal VEPs are less variable in waveform and timing than the VEPs elicited by other stimuli. However, the pattern onset/offset stimulus is best suited for the detection of malingering and in cases of nystagmus. Flash VEPs are useful in low vision, poor cooperation and media opacities.

Figure 22 presents pattern-reversal VEP recordings, elicited by 60’ and 15´ arc, obtained in a control subject.

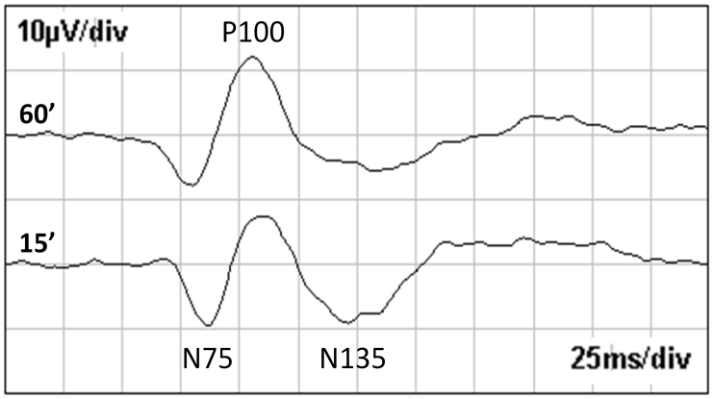

Fig. 22 – Pattern-reversal VEP recorded in a healthy subject.
(Source: data - IBILI; image - the author)

4.4. MULTIFOCAL ELECTROPHYSIOLOGY

Multifocal electrophysiological recordings provide detailed / localized information about retina or retinocortical performance (mfERG and mfVEP, respectively). These techniques use a strategy based on m-sequence stimulation and, by reversal correlation approach, it is possible to obtain a map of topographic central responses (Hood et al., 2012).

The clinical multifocal electroretinogram (mfERG) is an electrophysiological test of local retinal function in which many local ERG responses (typically 61 or 103) are recorded from the central cone-driven retina under light-adapted conditions.

This technique is of particular interest when a macular lesion is present (and thus cannot be detected by full-field ERG, which records the response of the whole retina) allowing a full characterization in multiple localizations. Other important applications of this method include all the clinical entities that affect the peripheral retina massively (e.g. retinitis pigmentosa); when full-field ERG is isoelectric sometimes it is possible to record residual central responses with mfERG, no visible by other electrophysiological methods.

Figure 23 shows m-sequence stimulation and mfERG recordings obtained in a control.

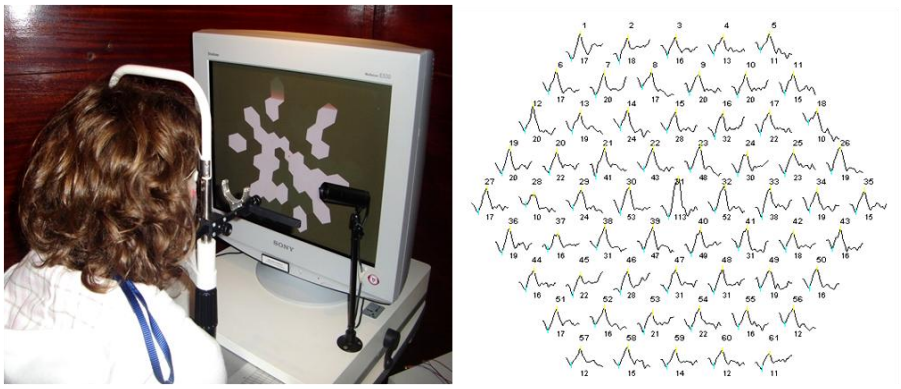

Fig. 23 – Multifocal ERG recorded in a healthy eye.
(Source: data - IBILI; image - the author)

Multifocal VEP provides objective perimetric information of the visual field, showing several topographic responses generated in the primary visual cortex, evoked by stimuli presented peuso-randomly. Thus, a limited retinal area is stimulated at a time and separate responses from different parts of the visual field can be obtained (Baseler et al., 1994). This technique has been used in glaucoma an optic neuropathies studies (Klistorner and Graham, 2000; Fraser et al., 2006).

Figure 24 presents m-sequence stimulation and mfVEP recordings obtained in a control.

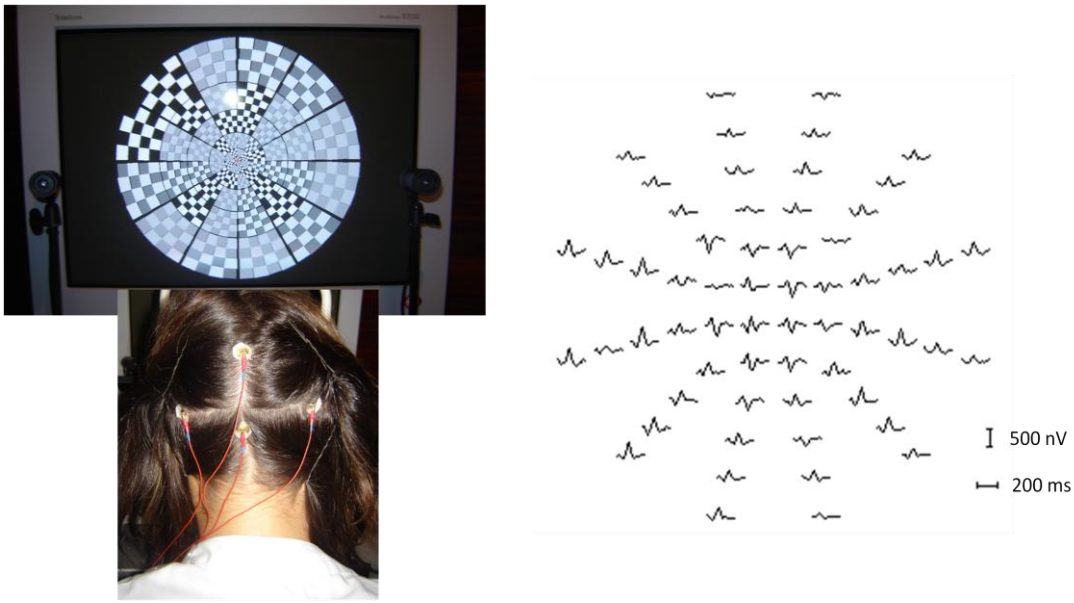

Fig. 24 – Multifocal VEP recorded in a healthy subject
(Source: data - IBILI; image - the author)

CHAPTER II

MAIN GOALS

CHAPTER II

MAIN GOALS

The main goals of this work were:

- To probe the functional impact of disease mechanisms in GC and optic nerve, namely in pathologies that typically affect these structures, such as in two inherited hereditary optic neuropathies (ADOA and LHON) and one acquired optic neuropathy (inflammatory-demyelinating / MS-related).

- To probe the impact of disease mechanisms of Diabetic Retinopathy in retinal neuronal dysfunction independently of breakdown of the blood-retinal barrier and vasculopathy in type 1 diabetic patients.

- To investigate the role of novel psychophysical and electrophysiological methods in the assessment of GC and optic nerve function.

Additional specific goals were also established:

- To characterize the neuronal impairment across parallel functional channels, namely by means of new psychophysical and/or electrophysiological methods biased for parvo-, konio- and magnocellular pathways.

- To investigate the possible effect of GC damage at pre- and post-GC levels and to obtain new insights on pathophysiological mechanisms of damage in the previously mentioned diseases.

- To gather evidence concerning the potential value of these methods as early neuronal biomarkers.

Disease specific investigation goals concerning MS, ADOA, LHON and DR are further defined in chapters IV-VII.

CHAPTER III

METHODS

CHAPTER III

PATIENTS AND METHODS

1. CHARACTERIZATION OF THE STUDY GROUPS

According to the goals of this work (for details, see Chapter II), we have studied different patients' populations, distributed into four study lines:

1. Forty-four subjects with **Multiple Sclerosis** (MS), with (n=14) and without (n=30) previous history of optic neuritis (ON), with at least 12 months having elapsed from the acute period of the episode.
The diagnosis of ON was verified by clinical examination and standard visual function testing comprising BCVA, contrast sensitivity with the Vistech Test, colour vision screening with the Ishihara pseudo-isochromatic plates, automated white-on-white static perimetry and visual evoked potentials. An aged-matched group (n=28) was also considered, for comparison data.
Pseudophakic and aphakic eyes, media opacities, retinal diseases, high ammetropy (sphere > ± 4D; cylinder > ± 2D) and reduced visual acuity due to ambliopy were the exclusion criteria for both patients and controls. All subjects were also checked for the presence of (other) neuro-ophthalmologic pathology and were excluded if so.
Table 2 summarizes the general characterization of the subgroups.

Parameters		Controls	MS with no previous ON	MS with previous ON
Age (years)	Mean ± SD	39.10 ± 12.87	42.37 ± 10.79	41.79 ± 11.32
	Range	[23;58]	[21;62]	[22;62]
Gender	Male	n = 12	n = 10	n = 2
	Female	n = 16	n = 20	n = 12
Visual Acuity (decimal scale)	Mean ± SD	1.09 ± 0.13	1.07 ± 0.21	0.85 ± 0.33
	Range	[1.0; 1.3]	[0.1;1.3]	[0.05;1.2]
Disease duration (yrs)	Mean ± SD		9.11 ± 6.08	14 ± 11.11
	Range		[1;24]	[2;38]
EDSS	Mean ± SD		3.09 ± 2.17	2.29 ± 1.55
	Range		[0;7]	[1;6.5]
Time from the ON episode	Mean ± SD			6.71 ± 7.78
	Range			[1;30]

Table 2 – Characterization of the 3 study groups in MS study.

2. Twenty-two subjects from 13 families with **ADOA** submitted to *OPA1* mutation analysis. Mean age of the patient group was 31.86 ± 16.43, ranging from 11 to 73 years (controls: 33.29 ± 14.22 years; n=21). Visual acuity ranged from 0.05 to 0.8 (decimal scale; mean ± SD = 0.29 ± 0.16). Exclusion criteria included pseudophakic and aphakic eyes, media opacities, retinal diseases, amblyopia and high ammetropies (sphere> ± 4D; cylinder> ± 2D). Patients and controls were explicitly checked for the presence of other neuro–ophthalmologic pathology (besides ADOA) and were excluded if so.

Table 3 summarizes the demographic data, visual acuities and clinical findings in the patients enrolled in the study.

Patient	Family	Age (years)	Gender	Eye	VA	Optic Disc Atrophy
1	A	36	F	RE LE	0.4 0.4	Temporal
2	A	15	M	RE LE	0.3 0.3	Temporal
3	A	38	F	RE LE	0.12 0.1	Temporal
4	A	14	F	RE LE	0.5 0.5	Temporal
5	B	73	F	RE LE	0.2 0.1	Temporal
6	B	44	F	RE LE	0.66 0.5	Temporal
7	C	46	M	RE LE	0.2 0.4	Temporal
8	C	15	M	RE LE	0.5 0.4	Temporal
9	D	53	F	RE LE	0.1 0.1	Temporal
10	E	11	M	RE LE	0.2 0.2	Temporal
11	F	37	F	RE LE	0.6 0.4	Temporal
12	F	35	M	RE LE	0.05 0.1	Total
13	G	24	F	RE LE	0.1 0.05	Total
14	G	44	F	RE LE	0.05 <0.05	Total
15	H	11	F	RE LE	0.28 0.2	Temporal
16	I	29	F	RE LE	0.16 0.16	Temporal
17	J	56	F	RE LE	0.3 0.3	Temporal
18	K	17	F	RE LE	0.3 0.2	Temporal
19	L	34	F	RE LE	0.3 0.3	Temporal
20	L	17	F	RE LE	0.8 0.4	Temporal
21	L	29	M	RE LE	0.3 0.2	Temporal
22	M	23	M	RE LE	0.25 0.3	Temporal

Table 3 – Demographic and clinical data of ADOA patients.

3. Seventeen asymptomatic carriers of **LHON** associated to mtDNA 11778G>A mutation, from the same pedigree, with mean age ± SD = 27.94 ± 12.97 years and mean VA ± SD = 1.25 ± 0.11 (decimal scale). The data was compared with data obtained in an age-matched control group (n=18; mean age ± SD = 31.28 ± 13.48 years; mean visual acuity ± SD = 1.09 ± 0.17). Exclusion criteria included pseudophakic and aphakic eyes, media opacities, retinal and clinical neuro-ophtahlomological diseases, amblyopia and high ammetropies (sphere > ± 4D; cylinder > ± 2D).

4. Forty-two **type 1 diabetic patients** with preserved VA, with no diabetic retinopathy (DR) – n=26, and with mild nonproliferative DR (n=16). The control group for this study line included 25 subjects with mean age ± SD = 27.4 ± 5.8 years. Exclusion criteria included media opacities, neurophthalmological and retinal diseases (besides DR), amblyopia and high ammetropies (sphere > ± 4D; cylinder > ± 2D). Special attention was given to the subgroup of patients without DR, which was characterized into more detail (see Table 4).

Patient	Gender	VA	Duration disease(yrs)	PR (BRB)
1	M	1.3	12	1.88
3	M	1.3	15	1.72
5	M	1.0	12	1.53
6	F	1.0	7	2.81
7	M	1.0	13	4.69 *
8	M	1.0	17	3.41 *
9	M	1.3	24	1.82
11	M	1.3	15	2.20
14	M	1.3	14	1.08
15	M	1.0	18	1.60
17	M	1.0	12	2.22
18	M	1.0	12	2.64
21	F	1.0	24	1.91
23	M	1.0	10	2.63
25	M	1.0	19	1.70
27	F	1.0	13	2.55
28	M	1.0	14	3.42 *
29	F	1.0	15	3.30 *
30	F	1.0	12	3.28 *
32	M	1.0	13	3.68 *
33	F	1.0	25	3.40 *
34	M	1.0	19	2.45
38	F	1.3	29	2.12
39	M	0.9	17	2.58
40	F	1.0	13	2.46
42	M	1.0	20	3.21 *

Table 4 – Characterization of the diabetic group with no DR (* indicates abnormal PR).

2. METHODS

The studies of this work followed the tenets of the Declaration of Helsinki and were approved by our Ethics Committee. Prior to the inclusion in the study, informed consent was obtained from all subjects after a full given explanation.

Besides the general ophthalmological examination, the psychophysical and electrophysiological methods that were commonly used in the study lines of the global work are described below. The most relevant imaging methods that were used for structure-function correlation are also referred.

Other few methodological procedures adjusted to the specific goals of each study line are described in chapters IV-VII.

2.1. OPHTHALMOLOGICAL EXAMINATION

All participants were submitted to a complete ophthalmological examination including the best-corrected visual acuity (BCVA), slit lamp examination of anterior chamber, IOP measurement (Goldmann applanation tonometer), angle and fundus examination (non-contact lens) and the assessment of subjective visual complaints.

2.2. FUNCTIONAL ASSESSMENT

2.2.1. PSYCHOPHYSICS

2.2.1.1. CHROMATIC CONTRAST SENSITIVITY

An adapted version of the psychophysical method developed by Regan et al. (1994), taken from the Cambridge Colour Test (CRS-Cambridge Research Systems, Rochester, UK) was used, in order to study the chromatic contrast sensitivity along three parallel, randomly interleaved staircases, corresponding to the simultaneous assessment of the three cone confusion axes, modulated in the CIE 1976 u'v' colour space, using the Trivector strategy of the setup. The stimulus consists of a Landolt-like C-shaped ring, having a gap size of 1.6º, and outer and inner diameters of 7.6º and 3.81, respectively, and appears over a pattern of grey circles of different sizes and luminances (from 8 to 18 cd/m^2) providing background noise (in size and luminance) ensuring thus

that only stimulus chromaticity can be used to identify the location of the gap – see Figure 25.

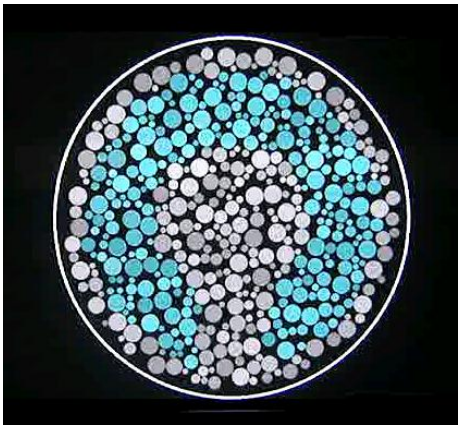

Fig. 25 – Cambridge Colour Test chromatic stimulus, over a background noise, in size and luminance. (Source: the author)

Responses were inserted into a four-button box, corresponding to the same locations of the ring aperture - top, down, left, right.

Stimuli were presented monocularly on a 21-inch gamma corrected monitor (GDM-F520; Sony, Tokyo, Japan; refresh rate: 100 Hz), at a viewing distance of 1.8 metres, in a completely dark room. Calibration was checked by means of a Colorcal colorimeter (Minolta, Osaka, Japan) as well as calibration software and hardware (implemented through a VSG 2/5 graphics card [CRS, UK]).

Far vision refractive correction was worn by participants and tinted contact or spectacle lenses were replaced by trial lenses in a trial frame, when applicable.

Psychophysical thresholds were thus obtained by using a four-alternative spatial forced choice. The test ended after 11 reversals of each of the three individual adaptive staircases, and the mean of the last 7 reversals was obtained as the threshold estimate for a given confusion chromatic line. A small number of trials, randomly intermixed with the test trials, were used in order to detect false negative or positive responses. Quantitative thresholds were expressed in confusion vector length for each protan, deutan and tritan axes, in CIE 1976 u'v' colour space units. Minimum and maximum excursions were 0.002 and 0.11 units, respectively (Castelo-Branco et al., 2004; Reis et al., 2011).

2.2.1.2. ACHROMATIC CONTRAST SENSITIVITY

2.2.1.2.1. CONTRAST SENSITIVITY FUNCTION

In this case, achromatic contrast sensitivity was assessed using Contrast Sensitivity Function test system (Metropsis - Cambridge Research Systems, Rochester, UK), testing six spatial frequencies (0.2, 1, 2.1, 3.3, 5.2 and 9.1 cycles/degree), by means of Gabor stimuli with one degree of standard deviation size, oriented at 90 degrees with spatial phase of 180 degrees, that were presented monocularly during 200 ms, at 2 degrees from the central fixation target, either at left or right locations (two-alternative spatial forced choice strategy), at a viewing distance of one metre.

Stimuli were generated at the same 21 inch monitor used to assess chromatic contrast sensitivity (GDM-F520; Sony, Tokyo, Japan), at a mean luminance of 71 cd/m^2 in a complete dark room, ensuring a reproducible luminance. The procedures for luminance calibration were the same as for the colour test (see above).

Contrast of the stimuli was modulated according to Michelson luminance contrast (%) = $(L_{max} - L_{min}) / (L_{max} + L_{min}) * 100$ and contrast sensitivity thresholds were obtained by an adaptive logarithmic staircase strategy (starting from 50% initial contrast). The initial step size was 2 dB until the first reversal occurred and the following step sizes were 0.1 dB and 0.5 dB, for positive and negative answers, respectively, while staircases were running for a total of four reversals, with the contrast at the final two reversals being averaged to estimate the contrast threshold for each spatial frequency. A small number of catch trials were randomly intermixed with the test trials, in order to detect false negative or positive responses.

Participants were far vision corrected and tinted contact or spectacle lenses were replaced by trial lenses in a trial frame, when applicable.

The threshold results were expressed as a percentage of contrast.

2.2.1.2.2. FREQUENCY DOUBLING PERIMETRY (FDT)

Achromatic contrast sensitivity within the magnocellular pathway was probed using a perimetric test based on frequency doubling technology (White, 2002; Kelly, 1966). Vertically oriented sinusoidal grating stimuli were presented monocularly, with a spatial frequency of 0.25 cpd modulated at 25 Hz, at different contrast levels, by means of Humphrey Matrix Visual Field Instrument (Carl Zeiss Meditec Inc., USA).

An N-30-F (nasal 30º) threshold testing strategy was chosen. This procedure consisted of a modified binary search using a four-reversal rule to determine the

threshold level at each of the 19 tested locations. The range of possible raw data is between 0 dB (maximum contrast / lowest patient sensitivity) and 56 dB. The formula to calculate sensitivity in dB units was $\log_{10}$ x (2048 / *c*) x 10 x *H*, where *c* ranges from 1 to 2048 (scaled minimum and maximum contrast, respectively), and *H* (Humphrey scaling factor) is approximately 2.

Analysis was performed considering both global parameters (MD – mean defect and PSD – pattern standard deviation) and contrast sensitivity pooled from five regions: the 5º central area (C) and the four visual field quadrants (ST- superior temporal, SN- superior nasal, IN- inferior nasal and IT- inferior temporal).

2.2.1.3. AUTOMATED STATIC PERIMETRY

Automated static perimetry was performed with the Octopus 311 version (Haag-Streit AG, Germany), using the Program 32 (General Threshold Examination), including 76 locations up to 30º, spaced in an equidistant grid pattern with 6º resolution.

Individual local thresholds (luminance perceived with a probability of 50%) were obtained in an optimized way, taking into account every answer at a particular point in the adjustment of the neighbouring locations (TOP strategy algorithm) (Morales et al., 2000).

Mean sensitivity (MS), mean defect (MD) and loss variance (LV), as global parameters, were analyzed, as well as the mean threshold value of each quadrant (ST- superior temporal, SN- superior nasal, IN- inferior nasal and IT- inferior temporal), expressed in decibels.

2.2.2. ELECTROPHYSIOLOGY

2.2.2.1. CORTICAL VISUAL EVOKED POTENTIALS

2.2.2.1.1. PATTERN VEP - GLOBAL MEASURES

We have analyzed conventional Visual Evoked Potentials (Pattern VEPs) in terms of timing and amplitude to measure the functional integrity of retino-cortical visual pathways. A RETIport32 (Roland Consult, Germany) device was used for

stimulation and electrophysiological recordings, with a pattern reversal checkerboard stimulus, at a contrast level of 97 %, on a 20 inch monitor at a viewing distance of one metre. Two spatial frequencies (60' and 15') were monocularly presented at 1.5 reversals/sec, at a frame rate of 60 Hz, with participant´s far vision refractive correction, if applicable. Voltage range was +/-100 μV and the signal was 1-50 Hz banded-pass filtered. The artefact rejection level was set at 5% below the range mentioned above. An hundred trial P100 average waveform was thus obtained, and its amplitude (in μV) and peak time (in ms) were taken for analysis.

2.2.2.1.2. MULTIFOCAL VEP - LOCAL MEASURES

We have recorded multifocal visual cortical evoked potentials (mf VEP) using the RETIscan system (Roland Consult, Germany), with four gold-cup electrodes for recording action potentials originated from the striate cortex, in four different inion-oriented locations: 3 cm above and 1 cm below (upper and lower midline electrodes) and 4 cm for each lateral position from the inion (horizontally), as proposed by Hood et al. (2002) – for details see Fig. 24 (Chapter I).

A neutral electrode was placed in the frontal region. All 5 electrodes were connected into a VEP-Box (Roland Consult), allowing different combinations of the electrode connections, thus yielding four bipolar channels – vertical (channel 1), horizontal (channel 2), left oblique (channel 3) and right oblique (channel 4), allowing for a multiple channel recording. A fifth virtual channel was obtained by posthoc analysis, which is the "best response channel", an array of the "best responses" (Klistorner and Graham, 2000).

Stimuli consisted in a 60-sector, pattern-reversing display (checkerboard / dartboard configuration) arranged in concentric rings cortically scaled with eccentricity, up to 30º of the visual field (see also Fig. 24), presented monocularly in a 20-inch CRT monitor at a viewing distance of 33 cm, temporally modulated according to a pseudorandom binary m-sequence (frame rate: 60 Hz). Participant´s far vision refractive correction was compensated, according to the adjustment scale for this purpose, and near refractive correction was added if necessary.

Patients were instructed to fixate the central target (with non-dilated pupils) that was continuously checked by means of real-time video-monitoring. In cases of poor visual acuity, an eccentric target was used as reference for the patient to ensure centring the position of the pupil with the help of real-time eye monitoring. Eight blocks were considered per eye for averaging each mfVEP measurement. Each 140 second-block was separated by brief resting periods of time, in order to avoid fatigue induced by continuous fixation. Biosignals had an active voltage range of +/-100 μV, being

amplified and band-pass filtered at 5–300 Hz, and sampled at 1024 Hz. Recordings were obtained at an artefact rejection level of 10% (see the range above).

Analyses were performed using the first-order kernels. For each hexagon, the peak amplitude (defined as the difference between N1 and P1 waves, in nV/deg^2) was calculated and the implicit time (ms) of P1 determined.

2.2.2.2. RETINAL RESPONSES

2.2.2.2.1. PATTERN ELECTRORETINOGRAM

Pattern electroretinogram (PERG) was assessed with RETIport32 (Roland Consult, Germany), using DTL-Plus electrodes, to record population GC responses.

The stimulus consisted in a pattern reversal checkerboard, with element sizes of 48' at 4.3 reversals/sec, at a contrast level of 97 %, presented binocularly at a viewing distance of one metre on a 20-inch monitor, at 60 Hz refresh rate.

Participant´s far vision refractive correction was worn, when applicable.

The active voltage range of bioelectrical signal was +/-100 μV using a band-pass filter of 5-50 Hz, and amplification with a gain of 100,000. A two hundred trial average waveform was obtained twice, at an artefact rejection level of 5%, and the average of amplitudes (μV) and peak time values (ms) for each of P-50 and N-95 components were obtained and subsequently analyzed.

2.2.2.2.2. MULTIFOCAL ELECTRORETINOGRAM

Topographic retinal responses were recorded using RETIscan system (Roland Consult, Germany), using DTL-Plus electrodes, to objectively record activity within photoreceptor/bipolar cell circuitry.

The stimulus consisted in a hexagonal pattern, with 61 elements, adjusted for the magnification factor within the 30º central visual field, pseudo-randomly presented binocularly according the standard m-sequence, at a viewing distance of 33 cm on a 20 inch CRT monitor, at a frame rate of 60 Hz (for details, see Fig. 23) . Participants' far vision refractive correction was compensated, when applicable, according to the adjustment scale for this purpose and near refractive correction was added if necessary.

As for the MfVEP, patients were instructed to fixate the central target, which was continuously checked by means of real-time video-monitoring. In cases of very poor visual acuity, an eccentric target was used as reference for the patient to ensure centring the position of the pupil with the help of real-time eye monitoring.

The active voltage range of the bioelectrical signal was +/-200 μV using a band-pass filter of 5-100 Hz, and amplification at a gain of 100,000. Eight cycles of 47 seconds each were obtained for averaging, at an artefact rejection level of 10%.

Analyses were performed using the first-order kernels. For each hexagon, the peak amplitude, defined as the difference between N1 and P1 waves, was calculated and the implicit time of P1 determined, in amplitude per area (nV/deg²) and in milliseconds (ms), respectively.

2.3. IMAGING

2.3.1. COLOUR FUNDUS PHOTOGRAPHY

Colour fundus photographies (35º) of both eyes (centred to the macula and to the optic nerve) were taken in order to document the features of these structures, with a Topcon TRC-50 IA Retinal Ophthalmic Camera, including a Sony DXC 950 P digital camera, with a resolution of 0.5 MPixels / 768x576.

Specifically for the Diabetes study, seven standard fields of the retina were taken according ETDRS procedures (Early Treatment Diabetic Retinopathy Study Research Group, 1991a).

These photos were always obtained after psychophysical and electrophysiological assessment to prevent artifactual changes in retinal adaptation.

2.3.2. OPTICAL COHERENCE TOMOGRAPHY

Optical Coherence Tomography (OCT) provides a cross-sectional tomography of retinal tissue in real time, based on optical interferometry, using infra-red (843 nm), low coherence light, with high longitudinal resolution (Hee et al., 1995; Zeimer et al., 1996) of at least 10 μm - see also Kiernan et al. (2010). Because it is a quantitative non-invasive method, OCT is useful in the assessment of diseases of the macula and the optic nerve (Henderson et al., 2008).

For the studies of this thesis, we have used Stratus OCT3 (Humphrey, Carl Zeiss Meditec, Dublin, CA, USA) to obtain thickness measurements of various layers of the

retina, including the retinal nerve fibre layer (RNFL) obtained from the macula and from the peripapillary area. Using the "Fast Macular Protocol", six-radial 6-mm in length line scans, 30º apart and of 128 A-scans each, were obtained to extrapolate retinal thickness centred in the fovea. Other two acquisitions were also performed centred in optic disc, using the Fast Optic Disc and RFNL protocols.

Cross-sectional images of retinal anatomy were thus obtained, with an axial resolution of ≤ 10 µm, a transversal resolution of 20 µm and 2 mm of longitudinal scan range. Retinal thickness is presented as a 9 region bidimensional interpolated thickness map, with 1-mm diameter central circle and two outer circles of 3 and 6 mm diameters.

2.4. STATISTICAL ANALYSIS

Statistical analyses were performed using standard statistical packages (SPSS 15 – SPSS, Inc., Chicago, IL, and StatView – SAS, Cary, NC), using parametric (ANOVA, including Person correlation analysis) or nonparametric procedures (Mann-Whitney testing, including Spearman correlation analysis), depending on normality and homogeneity checks.

Cut-off levels of statistical significance were set at 0.05 and we have used a 95% confidence interval as cut-off for the different measurements of all tests.

As previously mentioned, other few methodological procedures were also performed, adjusted to the specific goals of each study. These are described in chapters IV-VII.

CHAPTER IV

INDEPENDENT PATTERNS OF DAMAGE TO RETINOCORTICAL PATHWAYS IN MULTIPLE SCLEROSIS WITHOUT A PREVIOUS EPISODE OF OPTIC NEURITIS

CHAPTER IV

INDEPENDENT PATTERNS OF DAMAGE TO RETINOCORTICAL PATHWAYS IN MULTIPLE SCLEROSIS WITHOUT A PREVIOUS EPISODE OF OPTIC NEURITIS

1. ABSTRACT

Asymptomatic visual loss is a feature of Multiple Sclerosis (MS) but its relative impact on distinct retinocortical pathways is still unclear. The goal of this work was to investigate patterns of subclinical visual impairment in patients with MS with and without clinically associated previous Optic Neuritis (ON).

We have used functional methods that assess parvo, konio and magnocellular pathways in order to compare pathophysiological mechanisms of damage in a population of 44 subjects with MS (87 eyes), with and without a previous episode of ON. These methods included chromatic contrast sensitivity across multiple chromatic axes (Cambridge Colour Test – parvo/konio pathways), perimetric achromatic contrast sensitivity for the magno pathway (Frequency Doubling Technique – FDT) and pattern visual evoked potentials (VEP). These measures were correlated with field sensitivity measures obtained using conventional Automated Static Perimetry (ASP) and were also compared with conventional clinical chromatic/achromatic contrast sensitivity chart-based measures.

We have found evidence for uncorrelated damage of all retinocortical pathways only in patients with MS without ON. VEP evidence for axonal damage was found in this group supporting the emerging notion of axonal damage even in sub-clinical stages of ON/MS pathophysiology. Only in this group was significant correlation of functional measures with disease stage observed, suggesting that distinct pathophysiological milestones are present before and after ON has occurred.

2. INTRODUCTION

Parvo-, magno- and koniocellular systems, the three main retinocortical pathways of the visual system, process visual information according to the functional tuning properties of their respective neurons (Shapley and Hawken, 1999). Cells within the parvocellular pathway are small (with small receptive fields) and specialized in the

colour processing (red-green axis), having high spatial resolution and low temporal resolution, while the cells of the magnocellular pathway are larger (with correspondingly large receptive fields). This pathway is highly sensitive to contrast of low spatial frequency dynamic stimuli. The koniocellular system has cells with intermediate spatial and temporal tuning properties as compared to the other retinocortical pathways, and is sensitive to contrast along the blue-yellow colour axis.

Earlier studies addressing visual function in ON have emphasized colour vision deficits (Harrison et al., 1987; Travis and Thompson, 1989; Porciatti and Sartucci, 1996; Caruana et al., 2000) and suggested that the parvocellular stream is preferentially impaired in ON, as compared to the magnocellular stream. However, these studies (Harrison et al., 1987; Travis and Thompson, 1989; Porciatti and Sartucci, 1996) focused on foveal vision, equated the magnocellular pathway with a pure luminance stream, and used a relatively low number of patients, with heterogeneous clinical status (some chronic, some subacute). In an additional study (Caruana et al., 2000), the relative isolation of parvocellular versus magnocellular (luminance) pathways was not optimized, given that temporal and spatial frequencies were neither explicitly manipulated nor optimized for functional separation.

Optic neuritis (ON) is often one of the first clinical manifestations of MS (Optic Neuritis Study Group, 1997; Ghezzi et al., 2000), but it likely just the clinical tip of the iceberg. Despite recognition of anterior visual pathway structural changes in the absence of overt clinical phenomena in MS patients (Parisi et al., 1999), potential effects on functionally independent retinocortical pathways have not previously been fully characterised. It is thus relevant to explore specific patterns of visual loss prior to clinical onset of the disease given the large amount of retinocortical pathways that are devoted to vision and likely to be affected by demyelination. Furthermore, the fact that retinocortical visual impairment is often undetectable during the recovery period using conventional assessment methods (Korsholm et al., 2007) raises the question whether more sensitive psychophysiological methods can uncover subtle parallel damage in retinocortical pathways, which may be potentially useful as possible outcomes for research and/or clinical practice.

In sum, the goal of this work was to evaluate and quantify subtle visual dysfunction in MS across magno-, parvo- and koniocellular pathways with or without associated ON and to correlate quantitative electrophysiological and psychophysical measures with classical clinical staging parameters. With this multimodal strategy we searched for new insights into the pathophysiology of the disease, in particular in terms of subclinical visual impairment.

3. METHODS

This study followed the tenets of the Declaration of Helsinki and written informed consent was obtained from all subjects after a full given explanation, following the procedure approved by our Institutional Ethics Committee**.**

3.1. PATIENT SELECTION

We have studied a group of 44 subjects with MS, with or without previous history of ON, studied in our University Hospital based setting, with at least 12 months having elapsed from the acute period of the single episode.

The diagnosis of ON was verified by clinical examination and standard visual function testing comprising best-corrected visual acuity (BCVA), contrast sensitivity with the Vistech Test, colour vision screening with the Ishihara pseudo-isochromatic plates, automated white-on-white static perimetry and visual evoked potentials. Careful assessment of peripheral visual function was thus considered as important in the clinical work-up to ensure proper diagnosis of ON (and minimization of potential false negatives).

All cases of MS were diagnosed on the basis of standard clinical criteria and a battery of tests, including multisensory evoked potentials, magnetic resonance imaging and cerebrospinal fluid analysis. All MS patients fulfilled the revised McDonald criteria (Polman et al., 2005).

Pseudophakic and aphakic eyes, media opacities, retinal diseases, high ammetropy (sphere > ± 4D; cylinder > ± 2D) and reduced VA due to amblyopia were the exclusion criteria for both patients and controls. All subjects were also checked for the presence of (other) neuro-ophthalmologic pathologies and were excluded if so.

3.2. STANDARD CLINICAL PROCEDURES

Patients were submitted to a standard neurological examination which included clinical staging as assessed by the Expanded Disability Status Scale (EDSS) (Kurtzke, 1983). Complete ophthalmological examination was also performed, including BCVA obtained by Snellen Chart, and pupil afferent defect testing; a fundus photography was also taken, in order to document optic disc and blood vessel features. In a second visit (within a week), participants were assessed by specific testing (see below) according to the goal of this study.

3.3. EVALUATION OF VISUAL FUNCTION – PSYCHOPHYSICS AND ELECTROPHYSIOLOGY

3.3.1. CHROMATIC CONTRAST SENSITIVITY TO ASSESS PARVO AND KONIOCELLULAR PATHWAYS

We have studied chromatic contrast sensitivity using three parallel, randomly interleaved staircases, corresponding to the simultaneous assessment of the three cone confusion axes, modulated in the CIE 1976 u'v' colour space – Cambridge Colour Test (for details see Chapter III - 2.2.1.1).

Patients were nevertheless previously submitted to routine clinical testing procedures, namely Ishihara pseudo-isochromatic plates (Roth and Lanthony, 1999a), for a comparison with standard evaluation approaches. Anomaloscopy data (relying on subjective equality) were also collected in a subgroup of 14 patients using the All-Colour-Anomaloscope IF-2 (Roland Consult, Germany), exploring both red-green and blue-green ranges, by metamerical equations of Rayleigh (Rayleigh, 1881) and Moreland (Moreland and Kerr, 1978). The following measures were then extracted: central mean point (CMP), setting range (SR) and the abnormality quotient (AQ).

3.3.2. ACHROMATIC CONTRAST SENSITIVITY TO ASSESS THE MAGNOCELLULAR PATHWAY

Achromatic contrast sensitivity within the magnocellular pathway was tested using Frequency Doubling Technology (FDT) – for details, see Chapter III (2.2.1.2.2).

To compare the above mentioned method with more widely used semi-quantitative clinical methods, central achromatic contrast sensitivity was also assessed using a Vistech screen (Vistech Consultants, Inc., USA), whereby five distinct spatial frequencies (1.5, 3, 6, 12 and 18 cpd) were presented monocularly to the participants at eight contrast levels plus blank, under normal room lighting conditions (30-60 ft-L) (Roth and Lanthony, 1999b).

3.3.3. AUTOMATED STATIC PERIMETRY

Participants were evaluated with Automated Static Perimetry (ASP) - central 30º, with the Octopus 311 version (Haag-Streit AG, Germany) – for details, see Chapter III (2.2.1.3).

3.3.4. VISUAL EVOKED POTENTIALS

We have measured Visual Evoked Potentials (VEPs) using a pattern reversal stimulus – for description of Pattern VEP see Chapter III (2.2.2.1.1).

3.3.5. STATISTICAL ANALYSIS

Statistical analyses were performed using standard statistical packages (SPSS 15 – SPSS, Inc., Chicago, IL and StatView – SAS, Cary, NC), using parametric (ANOVA) or nonparametric procedures (including Spearman correlation analysis) depending on normality and homogeneity checks. Cut-off levels of statistical significance were set at 0.05 and we have used a 95% confidence interval as cut-off for the different measurements of all tests.

To prevent biases caused by violations of independence we took the conservative measure of averaging measures from both eyes in case a significant interocular correlation was found (this was surprisingly only present for the control group).

Given the equivalence of regression and ANOVA (now increasingly jointly referred to as General Linear Models, or GLM, implying coding of categorical predictors/groups and testing whether there is a mean difference between two or more groups) we have used this methodology when their respective assumptions held true, groups representing indicator variables. Alternative statistical non-parametric approaches were used when applicable.

4. RESULTS

Clinical and Demographic Characterization of the Study Groups

We have studied a group of 44 subjects (87 eyes – one eye was excluded due to amblyopia) with MS, with or without previous history of ON, that were compared with our age-matched control group (age comparisons, Mann-Whitney test, *ns*).

The course of the disease was majorly relapsing-remitting (n=30; 68.18% of the patients), secondary-progressive with relapses (n=20; 22.72%), secondary-progressive (n=3; 6.82%) and just one case of primary-progressive MS (2.28%) was observed. Treatment consisted mainly on immunomodulatory (in 36 patients – 81.82%) and

immunosuppressive therapy (n=4; 9.09%) and combined treatment was considered for 4 patients (9.09%). Mean time (in years) from the ON episode was 4.33 ± 3.16 (SD).

The clinical and demographic data of each study group, namely age, gender, VA, disease duration, EDSS and time from the ON episode (when applicable) are summarized in Table 5.

Parameters		Controls	MS with no previous ON	MS with previous ON
Age (years)	Mean ± SD	39.10 ± 12.87	42.37 ± 10.79	41.79 ± 11.32
	Range	[23;58]	[21;62]	[22;62]
Gender	Male	n = 12	n = 10	n = 2
	Female	n = 16	n = 20	n = 12
Visual Acuity (decimal scale)	Mean ± SD	1.09 ± 0.13	1.07 ± 0.21	0.85 ± 0.33
	Range	[1.0; 1.3]	[0.1;1.3]	[0.05;1.2]
Disease duration (yrs)	Mean ± SD		9.11 ± 6.08	14 ± 11.11
	Range		[1;24]	[2;38]
EDSS	Mean ± SD		3.09 ± 2.17	2.29 ± 1.55
	Range		[0;7]	[1;6.5]
Time from the ON episode	Mean ± SD			6.71 ± 7.78
	Range			[1;30]

Table 5 – Clinical and demographic data of the 3 study groups.

Chromatic Contrast Sensitivity to probe Parvocellular/Koniocellular Pathways: Evidence for early damage in MS

Our computerized quantitative approach reveals impairment of all cone pathways in MS, even in the absence of ON, for all colour axes ($p<0.0001$, Kruskal-Wallis test; Fig. 26). The finding that a significant deterioration of chromatic function may occur even in MS without previous ON is noteworthy because it was obtained using a nonparametric analysis that is insensitive to outliers.

Conventional clinical colour vision testing (see Methods of this chapter and Table 6) showed very little sensitivity (even in the group with previous ON). Even anomaloscopy, which was performed in a subgroup of patients (n = 14, 8 and 19 eyes from patients with and without previous episode of ON, respectively), showed a relatively high variability. Accordingly, no statistical difference was found between

both patients groups, as well as between controls and patients with a previous episode of ON, for both Rayleigh and Moreland equations. Nevertheless, a difference was found in Central Mid Point (p=0.0434) and Setting Range (p=0.0078) between controls and MS patients without ON, just for the red-green axis.

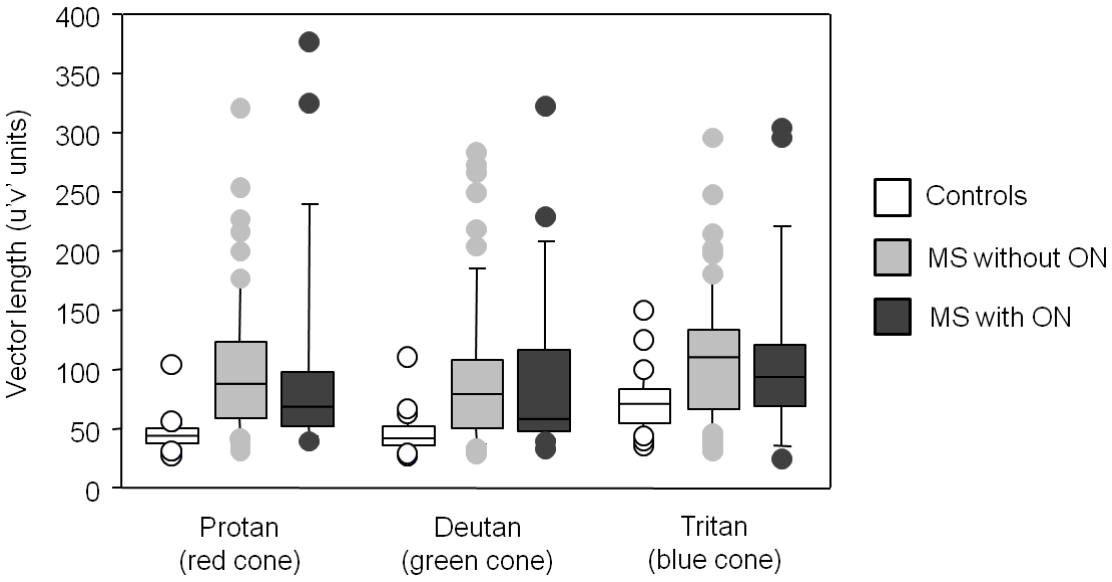

Fig. 26 – Chromatic performance along the three chromatic axes (Protan, Deutan and Tritan, tested with Cambridge Colour Test) is impaired both in MS with and without ON.
Y axis: performance in terms of colour space u'v'units (mean ± SEM).

Classical Methods		Group 2 MS – no ON (mean ± SEM)	Group 3 MS – ON (mean ± SEM)
Ishihara	Number of errors	3.25 ± 0.50	6.32 ± 1.46
Anomaloscope Rayleigh equation	Central Mid Point	49 ± 1.40	50.86 ± 2.64
	Setting Range	5.37 ± 1.93	12.25 ± 4.37
Anomaloscope Moreland equation	Central Mid Point	46.26 ± 2.04	44.75 ± 2.33
	Setting Range	11.74 ± 2.47	24.50 ± 11.81
A. Static Perimetry	Mean Defect (dB)	3.70 ± 0.54	4.19 ± 0.82

Table 6 – Visual function results obtained with classical methods.

Achromatic Contrast Sensitivity to probe the Magnocellular Pathway

MD (mean deviation), a global parameter of magnocellular performance (FDT test procedure, see Methods), showed yielded significant differences (main GLM effect $p<0.0001$) between controls and each group of patients ($p=0.0001$, Fisher's PLSD), but no significant effect could be detected between patient groups (Fig. 27). Concerning PSD (field heterogeneity measure) strong differences were again only found between controls and patient groups ($p<0.0001$, for the comparison with the MS group without previous ON and $p=0.0028$ for the other group).

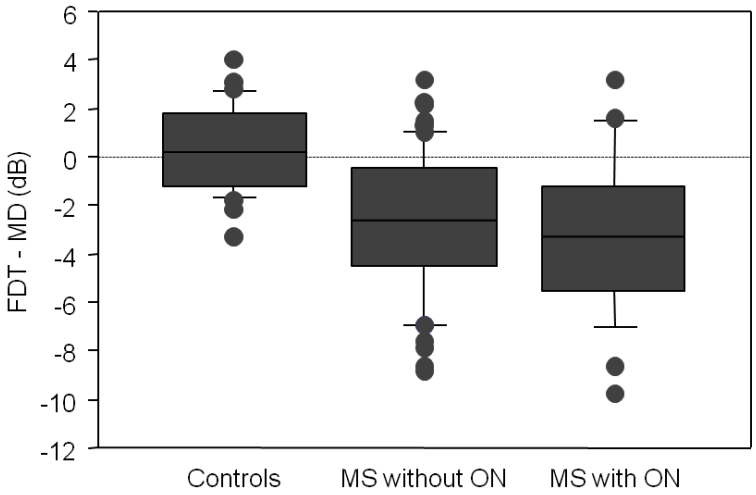

Fig. 27 – Magnocellular contrast sensitivity in terms whole field deviation measure (MD: mean defect) in the three groups.

To probe whether regional differences were underlying these effects, we then analysed magnocellular achromatic contrast sensitivity in distinct regions (central and quadrantic fields – GLM and posthoc Fisher's PLSD) – see Table 7. Significant differences were found in all five locations, between controls and both patient groups: all main effects are significant with $p << 0.001$ and all posthoc effects with $p \leq 0.001$ for comparisons between controls and each of MS groups. Comparisons between both patient groups were non significant.

Conventional clinical achromatic contrast sensitivity assessment tools (Vistech), did not detect subclinical visual dysfunction in the group with MS without previous ON (all comparisons, *ns*).

Areas / Groups	Central (dB)	ST (dB)	SN (dB)	IN (dB)	IT (dB)
Group 1 (Controls)	31.82 ± 0.54	29.38 ± 0.46	31.05 ± 0.45	30.56 ± 0.55	30.39 ± 0.45
Group 2 (MS-no ON)	27.53 ± 0.92	25.36 ± 0.76	25.88 ± 0.75	25.98 ± 0.77	26.53 ± 0.73
Group 3 (MS - ON)	26.56 ± 1.12	24.24 ± 1.16	24.82 ± 1.01	25.73 ± 1.11	26.30 ± 0.97

Table 7 – Magnocellular performance in the central and quadrantic visual fields (ST – superior temporal; SN – superior nasal; IN – inferior nasal; IT – inferior temporal) - mean ± SEM.

Assessment of visual function across the visual field with Automated Static Perimetry

Although automated static perimetry (ASP) does not evaluate specific visual pathways it provides a valuable gold standard. According to our normative database, we found 28 normal visual fields (32.18 % from the total sample of patients eyes): in the group with no history of ON, 19 eyes out of 59 eyes (32.20 %) and on the group with previous ON, 9 eyes out of 28 eyes **(**32.14 %), corresponding to a non-significant chi-square p-value. Further statistical comparison between both patient groups did not yield significant differences in global – MD and LV – and regional parameters.

Objective analysis of axonal damage and conduction deficits using Visual Evoked Potentials

We have analyzed P100 waveform amplitudes as markers of axonal damage (with two spatial frequencies, 15’ and 60’ stimuli, assessing small/large fibres respectively) and latencies (implicit times) as markers of the demyelination process.

Peak time of the P100-wave revealed underlying pathology in both clinical groups (significantly delayed comparing with controls – $p<0.0001$, Mann-Whitney test), but did not differentiate between them, either for the 60’ or for the 15’ stimuli (ns, Mann-Whitney test) – see Table 8 for details.

Amplitude values of P100 were also significantly impaired concerning both MS groups, being clearly distinct from the control group ($p<0.0001$ for 60´ and 15’ stimuli;

Mann-Whitney test), providing a signature of significant axonal impairment even if ON was not previously present – see also Table 8.

Since these particular comparisons were evaluated using non-parametric statistics, all significant differences (between control and patient groups) remained so when corrected for the number of multiple comparisons ($p < 0.001$).

Parameters / Groups	60' Peak Time (ms)	15' Peak Time (ms)	60'Amplitude (μV)	15'Amplitude (μV)
Group 1 (Controls)	104.29 ± 0.84	110.50 ± 1.11	17.50 ± 1.10	18.39 ± 1.19
Group 2 (MS-no ON)	118.35 ± 1.88	125.83 ± 2.51	7.35 ± 0.59	7.97 ± 0.76
Group 3 (MS - ON)	121.91 ± 3.06	128.93 ± 3.05	8.44 ± 1.12	8.08 ± 1.12

Table 8 – Statistical summary of Peak Times (in milliseconds) and Amplitudes (in microvolts) of the P100 waveforms, obtained at two fundamental spatial frequencies (half-periods: 60' and 15'), for the three groups (controls, and patients with and without previous ON) - mean ± SEM.

Quantitative chromatic measures show that it is possible to detect early physiological impairment even when visual acuity is relatively preserved

Colour vision testing with CCT showed that even relatively normal VA could be associated with dramatic increases (deterioration) in chromatic discrimination thresholds (see Fig. 28, where patients with a VA=0.9 or 1.0 already show decreased chromatic sensitivity).

Our patient groups showed overall preserved VA (decimal scale - 1.07 ± 0.21 in patients with no history of ON and 0.85 ± 0.33 in the group of previous ON) which enabled us to study subtle functional impairment in the presence of preserved foveal vision. Nevertheless, a significant difference in VA in both patient groups can still be detected ($p<0.001$, Mann-Whitney test).

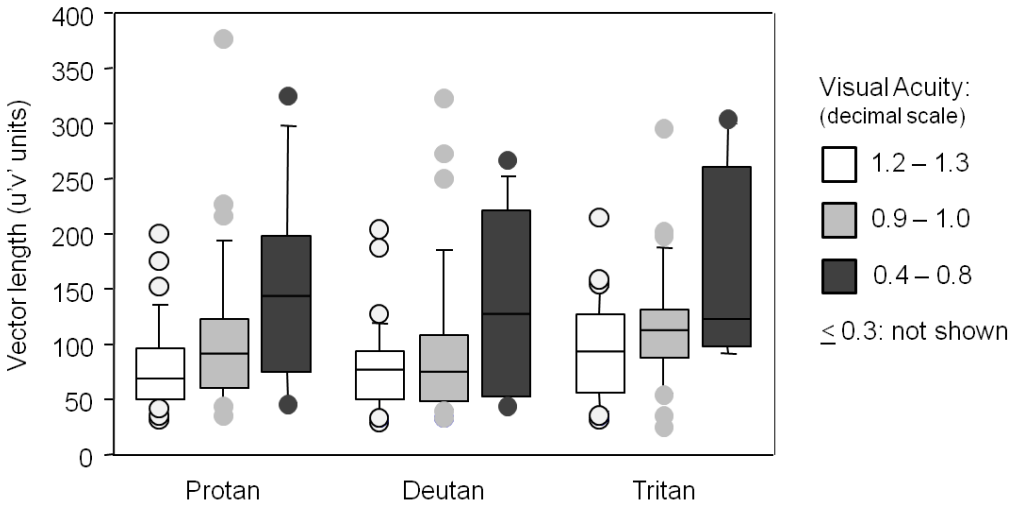

Fig. 28 – Colour vision discrimination is impaired even if visual acuity (converted decimal scale) is relatively preserved (e.g, 0.9–1).

Correlation Analysis

Correlation with clinical stage (EDSS) is only present prior to ON

Correlation patterns showed a very distinct profile across patient groups (Spearman correlation) specifically for EDSS measures and not for disease duration. Visual dysfunction in the MS group without previous ON correlated significantly with EDSS namely for konio-, parvo- and magnocellular measures ($p<0.001$ with $|r|>0.35$ in all cases – see Figure 29a for more details).

This specific pattern generalized to the standard perimetric (ASP) and VEP measures (Fig. 29b).

Surprisingly, no significant correlation was present for comparisons in the MS group with previous ON.

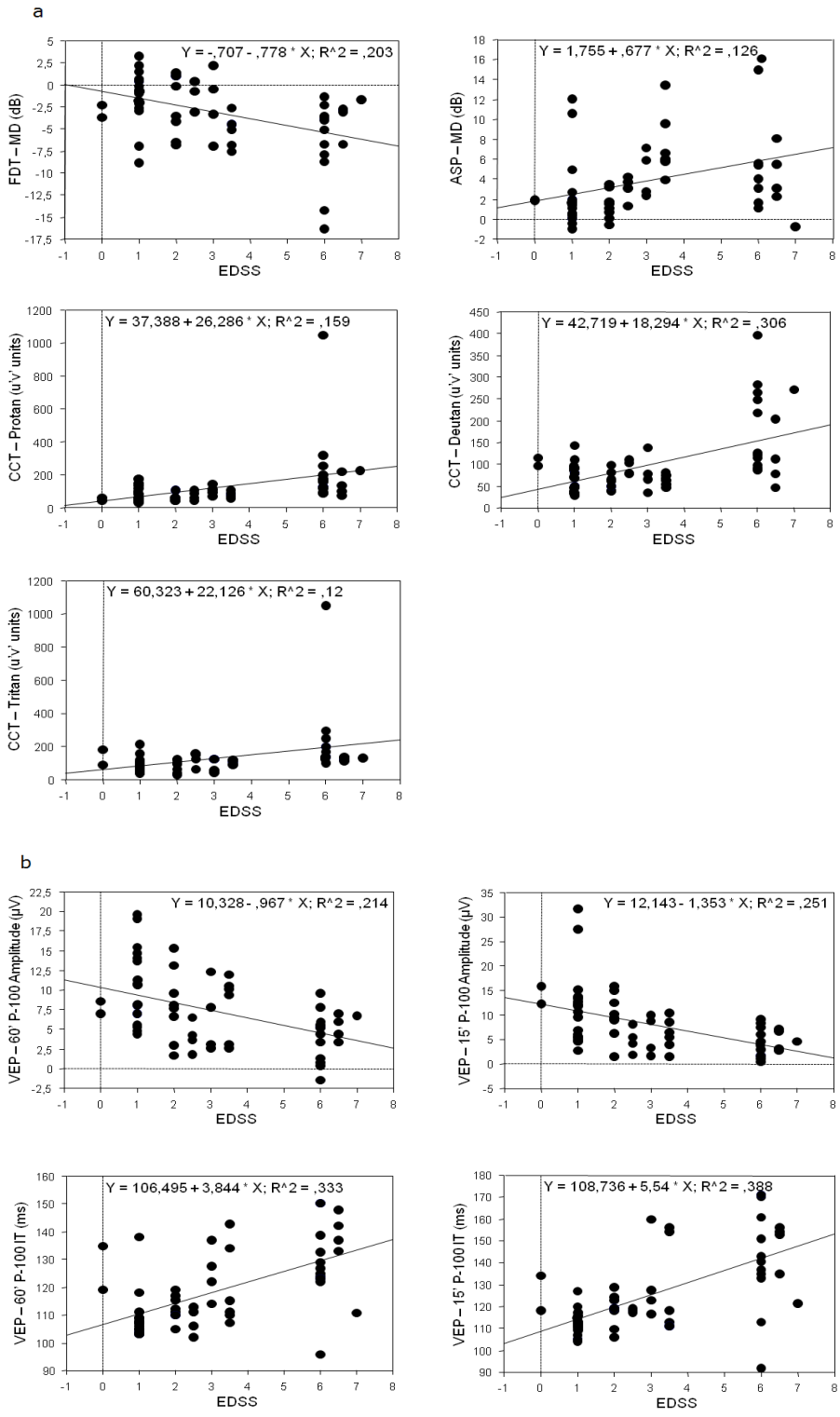

Fig. 29 – Correlation between EDSS and visual function parameters in the MS without optic neuritis group. These correlations are absent in the MS with previous optic neuritis group.
(**a**) Psychophysical measures – FDT-MD: mean defect of magnocellular perimetry; ASP-MD: mean defect of standard perimetry; CCT Protan / Deutan / Tritan: colour vision impairment, for the 3 colour axes). (**b**) Electrophysiological measures - VEP 60' P-100 Amplitude / IT: VEP response for low spatial frequency stimulus (amplitude and implicit time, respectively);
VEP 15' P-100 Amplitude / IT: VEP response for high spatial frequency stimulus (amplitude and implicit time, respectively).

In MS without previous ON, damage in retinocortical pathways is independent across visual pathways, unlike in MS with previous ON

We have found independent (uncorrelated) patterns of impairment only for the MS group without ON. An opposite pattern is observed in the group of patients with previous ON (significant correlations between chromatic/ achromatic measures and chromatic/standard perimetric measures – CCT / ASP: |r| above 0.5, with p<<0.01) – see Tables 9 and 10.

CCT	FDT	MS with ON	MS without ON
Protan	MD	r=-0.577; p=0.002	ns
	PSD	ns	ns
	Central	r=-0.680; p=0.0001	ns
	TS	r=-0.523; p=0.0065	r=-0.273; p=0.0359
	NS	r=-0,531; p=0.0055	ns
	NI	r=-0,599; p=0.0012	ns
	TI	r=-0,581; p=0.0018	ns
Deutan	MD	r=-0.616; p=0.0007	r=-0.330; p=0.0103
	PSD	ns	ns
	Central	r=-0.708; p<0.0001	r=-0.358; p=0.0051
	TS	r=-0.548; p=0.0039	r=-0.433; p=0.0005
	NS	r=-0.573; p=0.0022	r=-0.288; p=0.0265
	NI	r=-0.628; p=0.0005	r=-0.425; p=0.0007
	TI	r=-0.630; p=0.0005	r=-0.371; p=0.0036
Tritan	MD	r=-0.617; p=0.0007	ns
	PSD	ns	ns
	Central	r=-0.678; p=0.0001	ns
	TS	r=-0.576; p=0.0021	ns
	NS	r=-0.585; p=0.0017	ns
	NI	r=-0.632; p=0.0005	ns
	TI	r=-0.641; p=0.0004	ns

Table 9 – Correlation analysis of magnocellular (FDT), konio- and parvocellular (CCT) performance measures.

CCT	ASP	MS with ON	MS without ON
Protan	MD	r=0.439; p=0.0272	ns
	LV	r=0.575; p=0.0021	ns
	TS	*r=-0.369;p=0.0696*	ns
	NS	r=-0.447; p=0.0241	ns
	NI	r=-0.395; p=0.0500	ns
	TI	r=-0,556; p=0.0033	ns
	Central	r=-0,498; p=0.0103	ns
Deutan	MD	r=0.454; p=0.0216	ns
	LV	r=0.539; p=0.0047	ns
	TS	*r=-0.388;p=0.0551*	ns
	NS	r=-0.468; p=0.0173	ns
	NI	r=-0.398; p=0.0479	ns
	TI	r=-0,573; p=0.0022	ns
	Central	r=-0,532; p=0.0054	ns
Tritan	MD	r=0.473; p=0.0159	ns
	LV	r=0.606; p=0.0010	ns
	TS	r=-0.423; p=0.0341	ns
	NS	r=-0.486; p=0.0127	ns
	NI	r=-0.420; p=0.0358	ns
	TI	r=-0,589; p=0.0015	ns
	Central	r=-0,495; p=0.0109	r=-0,287; p=0.0370

Table 10 – Correlation analysis between colour discrimination (CCT) and standard perimetric measures (ASP)

Correlation between psychophysical and electrophysiological measures confirms distinct pathophysiological patterns and mechanisms in MS with and without previous ON

Correlation analysis between psychophysical and electrophysiological measures (chromatic measures and VEP) showed significant relationships between the three colour contrast sensitivity axes and amplitudes (reflecting axonal loss) of P100 waveforms, even in patients without previous ON ($|r| \sim 0.3$ in this case, with $p \leq 0.05$

and |r| > 0.47 with p ≤ 0.02 in the other group – for details see Table 11). Correlations with latencies (which probe demyelination) were only observed in MS with previous ON (|r| > 0.4 with p ≤ 0.035; ns for the group without previous MS).

CCT	VEP	MS with ON	MS without ON
Protan	60’ Amp.	r=-0.443; p=0.0254	r=-0.300; p=0.0206
	60’ IT	r=0.637; p=0.0004	ns
	15’ Amp.	r=-0.521; p=0.0067	r=-0.333; p=0.0095
	15’ IT	r=0.463; p=0.0188	ns
Deutan	60’ Amp.	r=-0.467; p=0.0176	r=-0.389; p=0.0021
	60’ IT	r=0.656; p=0.0002	ns
	15’ Amp.	r=-0.554; p=0.0034	r=-0.354; p=0.0056
	15’ IT	r=0.463; p=0.0188	r=0.317; p=0.0142
Tritan	60’ Amp.	r=-0.467; p=0.0175	ns
	60’ IT	r=0.611; p=0.0009	ns
	15’ Amp.	r=-0.567; p=0.0026	r=-0.255;p=0.0514
	15’ IT	r=0.421; p=0.0355	ns

Table 11 – Correlation analysis between colour discrimination (CCT) and electrophysiological measures (VEP; Amp –Amplitude, IT – implicit time).

Correlation analysis of specific magnocellular and VEP measures (Table 12) corroborated the same dissociation: in patients with previous ON, there was a strong correlation only with latency (implicit time) measures, in particular for low spatial frequency stimuli (r=-0.547; p=0.004 for the mean deviation parameter). In contrast, patients without previous ON showed correlation mainly with amplitude measures (r=-0.319; p=0.0133 for low frequencies, and r=-0.356; p=0.0053, for local defect measures at high spatial frequencies).

Comparison of standard visual fields and VEP measures replicated the same pattern (Table 13).

FDT	VEP	MS with ON	MS without ON
MD	60’ Amp.	ns	ns
	60’ IT	r=-0.547; p=0.0040	ns
	15’ Amp.	ns	ns
	15’ IT	ns	ns
PSD	60’ Amp.	ns	r=-0.319; p=0.0133
	60’ IT	ns	ns
	15’ Amp.	ns	r=-0.356; p=0.0053
	15’ IT	ns	ns
Central Area	60’ Amp.	ns	*r=0.249; p=0.0570*
	60’ IT	r=-0.707; p<0.0001	ns
	15’ Amp.	ns	r=0.291; p=0.0249
	15’ IT	r=-0.454; p=0.0216	ns
TS Quadrant	60’ Amp.	ns	ns
	60’ IT	r=-0.426; p=0.0329	ns
	15’ Amp.	ns	*r=0241; p=0.0661*
	15’ IT	ns	ns
NS Quadrant	60’ Amp.	ns	ns
	60’ IT	r=-0.416; p=0.0378	r=-0.267; p=0.0409
	15’ Amp.	ns	ns
	15’ IT	ns	ns
NI Quadrant	60’ Amp.	ns	ns
	60’ IT	r=-0.551; p=0.0037	ns
	15’ Amp.	ns	ns
	15’ IT	ns	ns
TI Quadrant	60’ Amp.	ns	ns
	60’ IT	r=-0.415; p=0.0381	ns
	15’ Amp.	ns	ns
	15’ IT	ns	r=-0.257; p=0.0493

Table 12 – Correlation analysis between magnocellular performance (FDT) and the effect of demyelination on visual inputs conduction (VEP amplitude and implicit times).

ASP	VEP	MS with ON	MS without ON
MD	60’ Amp.	ns	r=-0.291; p=0.0307
	60’ IT	ns	ns
	15’ Amp.	ns	r=-0.361; p=0.0065
	15’ IT	ns	ns
LV	60’ Amp.	ns	r=-0.274; p=0.0426
	60’ IT	ns	ns
	15’ Amp.	ns	r=-0.324; p=0.0153
	15’ IT	ns	ns
TS Quadrant	60’ Amp.	ns	ns
	60’ IT	ns	ns
	15’ Amp.	ns	r=0.291; p=0.0339
	15’ IT	ns	ns
NS Quadrant	60’ Amp.	ns	r=0.276; p=0.0455
	60’ IT	ns	ns
	15’ Amp.	ns	r=0.316; p=0.0207
	15’ IT	ns	ns
NI Quadrant	60’ Amp.	ns	ns
	60’ IT	ns	ns
	15’ Amp.	ns	r=0.331; p=0.0149
	15’ IT	ns	ns
TI Quadrant	60’ Amp.	ns	ns
	60’ IT	ns	ns
	15’ Amp.	ns	ns
	15’ IT	ns	ns
Central (mean of 4 central points)	60’ Amp.	ns	ns
	60’ IT	r=-0.575; p=0.0022	ns
	15’ Amp.	ns	ns
	15’ IT	ns	ns

Table 13 – Correlations between standard perimetry (ASP) and electrophysiological measures (VEP).

5. DISCUSSION

We were able to show that patterns of long term retinocortical damage in MS depend on the occurrence of previous ON. Independent (uncorrelated) deficits of retinocortical pathways were found only for MS without previous ON with a significant correlation with disease stage. Such dependence on disease stage is no longer present after an optic neuritis episode, suggesting distinct disease mechanisms. Given that the majority of all cases of ON are caused by demyelination, in particular the ones that are MS-related, it is interesting that this pathophysiological dichotomy is observed.

These distinct patterns of pathophysiological impairment of the optic nerve with/without previous ON are in agreement with previous studies (Brusa et al., 2001; Brusa et al., 1999) that suggested that a balance between demyelination and/or axonal degeneration (also occurring in the fellow optic nerve) has to be considered. Interestingly, visual function across eyes was found to be uncorrelated in both clinical groups, unlike the control group, suggesting that natural history and trajectories of visual impairment become independent between fellow optic nerves.

The fact that damage is independent in distinct retinocortical pathways only in MS without previous ON is consistent with the hypothesis that axonal integrity is affected in parallel across multiple visual streams prior to an episode of acute inflammation. This renders detection of subtle initial damage an important goal.

In this regard, computerized psychophysical colour testing proved to be very sensitive in the detection of magno-, parvo- and koniocellular impairment, revealing clear-cut damage of these visual parallel pathways in MS, even in the absence of a previous episode of ON. On the other hand, conventional clinical colour vision testing showed very little sensitivity even in the group with previous ON, which is not surprising given that such methods are at most semiquantitative and usually considered just as screening procedures (Silva et al., 2008). In fact, it is known that the quantitative colour assessment approach performs far better than more conventional colour vision testing methods (Silva et al., 2005). A recent study (just focusing on chromatic function) (Moura et al., 2008) is in agreement with this view, although it did not include other methods to verify and provide a correlational profile of visual impairment.

In sum, conventional colour vision testing does not show enough sensitivity to detect early damage in chromatic pathways.

A previous study has also suggested that the parvocellular pathway is significantly impaired in patients of MS with previous ON, as measured by retinal and cortical evoked responses to chromatic contrast stimuli (Porciatti and Sartucci, 1996). However, the magnocellular pathway was just equated with the luminance (achromatic)

pathway which may have reduced sensitivity to detect damage in that study. Nevertheless, comparing our data with those of previous studies, it is important to point that the pathophysiological measures are strongly dependent on the stimuli characteristics. Thus, the relative sensitivity of chromatic and achromatic systems is directly related with their anatomical differences (size of receptive fields / foveal and peripheral vision) and may depend on the spatial and temporal characteristics of the stimulus (Mullen and Plant, 1986). Moreover, as pathways are connected (Evangelou et al., 2001), some cells multiplex chromatic/luminance information which further challenges the design of psychophysical and electrophysiological tasks.

Studies in patients with previous ON do suggest that contrast sensitivity measures are useful in this context (Noval et al., 2006; Fisher et al., 2006) and we extend this notion by proving that a specific magnocellular contrast detection perimetric method can be very useful in detecting subtle functional damage. Interestingly, in our study we replicated also in the patient groups the previously reported lower physiological magnocellular contrast sensitivity in the superior temporal region in normal subjects (Silva et al., 2008).

Electrophysiological measures revealed, as expected, nerve conduction delays even in cases of MS with no history of ON (Brusa et al., 2001; Brusa et al., 1999; Frederiksen and Petrera, 1999; Sater et al., 1999). Amplitude analysis suggested significant axonal damage, which in turn may lead to retinal damage, by retrograde degeneration, as suggested by measures of retinal nervous fibre layer thickness and macular volume, by OCT (Henderson et al., 2008). This may explain the pattern of colour vision deficits we have observed.

The correlation obtained between VEP amplitude and other functional measurements (perimetric methods – FDT / ASP) confirms the evidence that amplitude changes dominate in MS prior to ON, suggesting an important role for axonal changes. Future studies should address comparison with morphological measures obtained with optical coherence tomography.

We also found evidence of psychophysical damage even when visual acuity was largely preserved, confirming that subclinical manifestations may occur, even in the absence of overt visual symptoms (Wray, 1994). Striking doubling in chromatic threshold measures were observed even for differences of about 0.1 in visual acuity. These findings are consistent with a recent study showing that a substantial proportion of patients show suggestive symptoms even prior to consulting for a putative "first" demyelinating event (Gout et al., 2010; Noble et al., 2006).

In sum, we have found evidence for independent damage of retinocortical parallel pathways in patients with MS without previous ON, in distinction to the post-ON group. Patterns of performance were correlated with disease stage only in pre-ON group and signatures of axonal damage were also present.

We conclude that visual impairment relates in a dichotomic way to distinct pathophysiological entities before and after ON has occurred, which may have strong implications in terms of clinical management.

CHAPTER V

AUTOSOMAL DOMINANT OPTIC ATROPHY

CHAPTER V

AUTOSOMAL DOMINANT OPTIC ATROPHY

– Part I –

PHYSIOLOGICAL EVIDENCE FOR IMPAIRMENT AT THE PRE-GANGLION LEVEL

1. ABSTRACT

Functional studies in patients with Autosomal Dominant Optic Atrophy (ADOA) are usually confined to analysis of physiological and clinical impact at the ganglion cell (GG) and post-GC levels. Here we aimed to investigate the impact of the disease at a pre-GC level and its correlation with GC/post-GC related measures.

Visual function was assessed in a population of 22 subjects (44 eyes) from 13 families with ADOA submitted to *OPA1* mutation analysis. Quantitative psychophysical methods were used to assess konio and parvocellular chromatic pathways (Cambridge Colour Test) and distinct achromatic spatial frequency channels (Metropsis Contrast Sensitivity Test). Preganglionic and GC measures were assessed with the Multifocal Electroretinogram (mfERG) and Pattern Electroretinogram (PERG), respectively. Global Pattern and Multifocal VEP (visual evoked potentials) were used to assess retinocortical processing, in order to characterize impaired processing at the post-GC level. Perimetric sensitivity, retinal and ganglion cell nerve fibre layer (RNFL) thickness measurements were also obtained.

Chromatic thresholds were significantly increased for protan, deutan and tritan axes ($p<<0.001$ for all comparisons) and achromatic contrast sensitivity (CS) was reduced for all studied six spatial frequency channels ($p<<0.001$). We observed significant decreases in peripapillary ($p\leq0.0008$) and macular (ring 2: $p=0.02$; ring 3: $p<0.0001$) RNFL and overall retinal thickness ($p<0.0001$ in all regions, except the central one). Interestingly, we found significant decreases in pre-ganglionic multifocal ERG response amplitudes (P1-wave: $p\leq0.005$) that were correlated with retinal thickness (ring 2: $r=0.512$; $p=0.026$ / ring 3: $r=0.583$; $p=0.011$) and visual acuity ($r=0.458$; $p=0.03$, central ring 1). Reductions in GC and optic nerve responses amplitude (PERG: $p<0.0001$ – P50 and N95 components; Pattern VEP: $p<0.0001$ –

P100) were accompanied by abnormalities of the MfVEP primarily in central locations (ring 1: p=0.0007; ring 2: p=0.012).

In the ADOA model of ganglion cell damage, parvo-, konio- and magnocellular pathways are concomitantly affected. Structural changes and physiological impairment also occurs at a preganglionic level suggesting a retrograde damage mechanism with a significant clinical impact on visual function, as shown by correlation analysis. Cortical impairment is only moderately explained by the retinal phenotype, suggesting additional damage mechanisms at the cortical level.

2. INTRODUCTION

ADOA is the most common autosomally inherited optic neuropathy (Kjer et al., 1996) and is mainly caused by mutations in the *OPA1* gene on chromosome 3q28-q29 (Eiberg et al., 1994; Bonneau et al., 1995). However, other loci for optic atrophy have been found and mapped (from *OPA2* to *OPA7* genes) – Ref. OMIM #165500. The *OPA1* gene encodes for a mitochondrial protein with 960 amino acids with similarity to dynamin-related GTPases (Alexander et al., 2000; Delettre et al., 2000). The consequent mitochondrial dysfunction leads to degeneration of retinal GC and loss of optic nerve fibres (Yu-Wai-Man et al., 2009).

ADOA is thus characterized by bilateral mild to severe reduced visual acuity (VA), which is tipically symmetrical. Typically, the disease is slightly progressive, beginning with an insidious onset in childhood, typically between 4 and 6 years of age (Newman, 2005; Votruba et al., 2003; Elliot et al., 1993; Votruba et al., 1998). Clinical features include optic nerve pallor (varying from subtle diffuse pallor to typical wedge-shaped temporal pallor or to total atrophy), a characteristic cecocentral scotoma visual field defect and a reported early blue-yellow defect or tritanopia (Kline and Glaser, 1979), which was supposed to be more frequent than the rarely reported red-green defect (Kok-van-Alphen, 1970), until Votruba and coll. challenged this concept (Votruba et al., 1998).

Typical electrophysiological characteristics of ADOA are already described in the literature (Holder, 1987; Holder et al., 1999), but usually focusing either on global GC activity or on retinocortical processing. In spite of normal full-field ERG (mainly revealing contributions from pre-GC neurons - photoreceptors and bipolar cells), it remains, however possible that small/localized ERG signals (evidenced by multifocal techniques) can still reveal retrograde damage.

In this study we have asked the question whether damage at the GC level can lead to hitherto unidentified functional damage in afferent layers of the retina, by

recording multifocal ERG signals. We have also correlated putative physiological changes with structural measures obtained by means of optical coherence tomography (OCT), which measured the joint integrity of the several retinal layers as well the retinal nerve fibre layer (RNFL). Although it is often difficult to obtain a precise spatial match between these measures, which reduces statistical power, we were able to detect significant correlations. We predicted that if preganglionic damage occurs the multifocal ERG should be changed. Finally, we also probed whether cortical damage has an independent component in relation to retinal damage, using multifocal VEP.

In sum, this study attempted to identify structure-function correlations at different levels of visual processing in ADOA, from the photoreceptor to the cortical level, by separating pathophysiological mechanisms of impairment at the retinal pre, post and GC level.

3. METHODS

3.1. PATIENT SELECTION, DEMOGRAPHIC CHARACTERISTICS AND OPHTHALMOLOGICAL EXAMINATION

The study followed the tenets of the Declaration of Helsinki and was approved by our Ethics Committee. Prior to the inclusion in the study, informed consent was obtained from all subjects after a full given explanation.

We have tested 22 affected individuals (44 eyes) from 13 families with ADOA. This diagnosis was primarily based on classical clinical criteria, including the pedigree (for genetic characterization see below). Mean age of the patient group was 31.86 ± 16.43, ranging from 11 to 73 years (controls: 33.29 ± 14.22 years; n=21).

Participants were submitted to a complete ophthalmological examination, including the best-corrected visual acuity (BCVA), slit lamp examination of anterior chamber, IOP measurement (Goldmann applanation tonometer), angle and fundus examination (non-contact lens), cataract grading by the Lens Opacities Classification System II (LOCS) and the assessment of subjective visual complaints. No cases of high intraocular pressure or cataract were found. Exclusion criteria included pseudophakic and aphakic eyes, media opacities, retinal diseases and high ammetropies (sphere > ± 4D; cylinder > ± 2D). Patients and controls (matched for the demographic characteristics, see above) were explicitly checked for the presence of other neuro–ophthalmologic pathology (besides ADOA) and were excluded if so.

3.2. *OPA1* MUTATION ANALYSIS

To confirm the *OPA1* diagnosis, mutation analysis was carried out in our study population. DNA was extracted from peripheral blood using an automated DNA extractor (BioRobot EZI, Qiagen, Hilden, Germany).

PCR amplification of the *OPA1* exons and exon-intro boundaries was essentially carried out as described, using amplicon specific primers and a universal common poly-nucleotide tail (Booij et al., 2011 - primer sequences available on request) followed by Sanger sequencing.

3.3. IMAGING

3.3.1. COLOUR FUNDUS PHOTOGRAPHY

A fundus photography centred to the optic nerve was taken and an additional fundus image was also taken from the macula of each eye (for details see Chapter III - 2.3.1). These photos were always obtained after psychophysical and electrophysiological assessment to prevent artifactual changes in retinal adaptation.

3.3.2. OPTICAL COHERENCE TOMOGRAPHY

Besides fundus photography, structural characteristics of the optic disc were assessed using an optical coherence tomography device (Stratus OCT3).

This was also used to measure central retina and retinal nerve fibre layer (centrally and peripapillary) thickness which enabled the correlation with mfERG and PERG responses (related to preganglionic and GC activity, respectively).

For details about this method, see Chapter III – 2.3.2.

3.4. FUNCTIONAL ASSESSMENT

We have applied the following psychophysical and electrophysiological methods (in all patients and controls):

- Computerized chromatic contrast sensitivity – Cambridge Colour Test;
- Computerized achromatic contrast sensitivity – Metropsis (Cambridge Research Systems);
- Automated static perimetry (central 30º);
- Pattern ERG;
- Multifocal ERG;
- Pattern VEP;
- Multifocal VEP.

For details, see Chapter III- 2.2.

3.5. STATISTICAL ANALYSIS

To prevent issues related to violations of independence, in our statistical analysis we used the mean of both eyes values of each participant, since all variables (except latencies of multifocal electrophysiological measures of patients) were statistically correlated (Spearman correlation). Given the observed violation of ANOVA assumptions, non-parametric analyses at a significance level of $p \leq 0.05$ were performed, using StatView (SAS, Cary, NC, USA).

4. RESULTS

Patient Demographic Characteristics and Ophthalmological Examination

Table 14 summarizes the demographic data, visual acuities (decimal scale) and clinical findings in the patients enrolled in the study.

Note the visual acuity ranges from 0.05 to 0.8 (mean ± SD = 0.29 ± 0.16).

Patient	Family	Age (years)	Gender	Eye	VA	Optic Disc Atrophy
1	A	36	F	RE LE	0.4 0.4	Temporal
2	A	15	M	RE LE	0.3 0.3	Temporal
3	A	38	F	RE LE	0.12 0.1	Temporal
4	A	14	F	RE LE	0.5 0.5	Temporal
5	B	73	F	RE LE	0.2 0.1	Temporal
6	B	44	F	RE LE	0.66 0.5	Temporal
7	C	46	M	RE LE	0.2 0.4	Temporal
8	C	15	M	RE LE	0.5 0.4	Temporal
9	D	53	F	RE LE	0.1 0.1	Temporal
10	E	11	M	RE LE	0.2 0.2	Temporal
11	F	37	F	RE LE	0.6 0.4	Temporal
12	F	35	M	RE LE	0.05 0.1	Total
13	G	24	F	RE LE	0.1 0.05	Total
14	G	44	F	RE LE	0.05 <0.05	Total
15	H	11	F	RE LE	0.28 0.2	Temporal
16	I	29	F	RE LE	0.16 0.16	Temporal
17	J	56	F	RE LE	0.3 0.3	Temporal
18	K	17	F	RE LE	0.3 0.2	Temporal
19	L	34	F	RE LE	0.3 0.3	Temporal
20	L	17	F	RE LE	0.8 0.4	Temporal
21	L	29	M	RE LE	0.3 0.2	Temporal
22	M	23	M	RE LE	0.25 0.3	Temporal

Table 14 – Demographic and clinical data of ADOA patients.

OPA1 Mutation Analysis

Four types of mutations including deletions and missense mutations were identified in 11 patients of 5 families (50%), detection rate which is consistent with the literature (Yu-Wai-Man et al., 2011a) – see Table 15 for details.

Given that patients with and without *OPA1* mutations had no significant phenotypic differences (confirmed statistically in data obtained by each method), results were pooled.

Family	Number of individuals	Mutation at coding DNA level	Mutation at protein level	Reference
A	4	c.869G>A	p.Arg290Gln het	Alexander et al., 2000
B	2	c.2708_2711del	p.Val903Glyfs*3	Delettre et al., 2000
C	2	c.2131C>T	p.Arg711* het	Delettre et al. 2001
D	1	c.2708_2711del	p.Val903Glyfs*3	Delettre et al., 2000
E	1	c.190 -194del het	p.Ser64Aspfs*7	*Not previously reported. Pathogenic?*
F-M	11	*No mutation identified*		

Table 15 – *OPA1* mutations analysis (reference sequence: NM_015560.2).

Psychophysics

Evidence for damage of both parvocellular and koniocellular pathways

As illustrated in Figure 30 (A) chromatic contrast sensitivity measures were significantly different between controls and patients across all three cone axes (p-values for all comparisons < < 0.001 – Mann-Whitney).

Impairment on achromatic contrast sensitivity in all measured spatial frequency channels suggests that a broad range of fibre types is affected in ADOA

We have observed significantly elevated achromatic contrast sensitivity (CS) thresholds for all spatial frequencies in ADOA ($p<<0.001$ for all comparisons, Mann-Whitney tests). Note the distinct peak for the maximum CS, corresponding to a spatial

frequency of 1 cpd in patients (controls: 3.3 cpd) showing a shift toward preferred lower frequencies (see Fig. 30 – B).

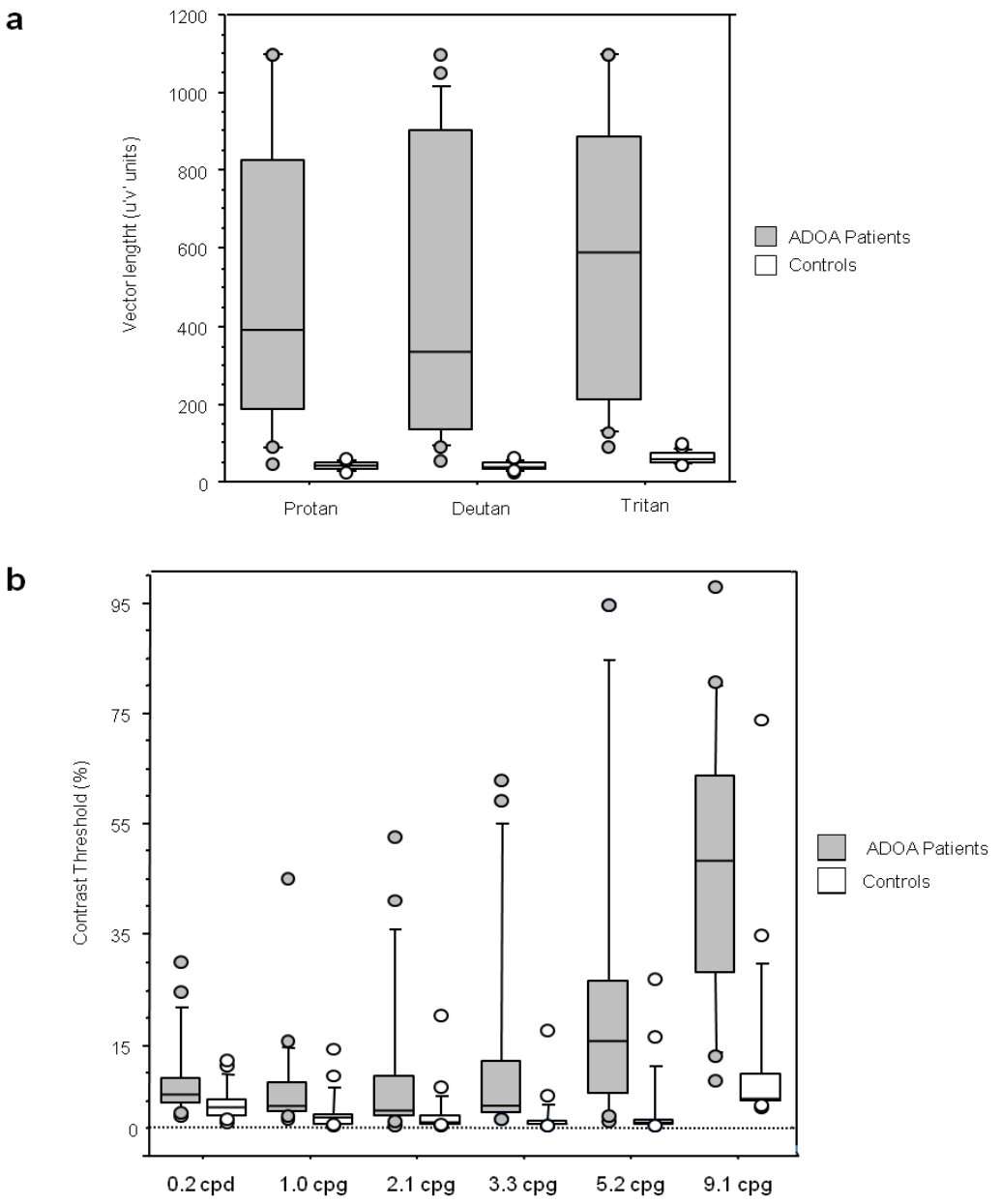

Fig. 30 - Chromatic (**a**) and achromatic (**b**) contrast thresholds (CS) in patients and in controls. Severe impairment is observed for the three chromatic axes and across the six tested spatial frequencies.

Visual field loss and patterns of scotomas in our patient sample

Automated static perimetry (ASP) allowed us to confirm the typical of patterns of scotomatous changes observed in this condition, varying from cecocentral, paracentral and central defects (50%, 46% and 4% of total cases in our study, respectively). Mean field sensitivity (MS'), Mean defect (MD) and mean loss variance (LV) were very abnormal in the patient group (mean ± SD values = MS': 21.34 ± 5.91 dB; MD: 7.77 ± 6.12 dB; LV: 20.99 ± 15.82 dB. These values differ by more than 2 SDs from the normative database.

When thresholds are analyzed by quadrants (mean ± SD values) the superior temporal quadrant shows more significantly decreased values: ST: 19.77 ± 6.54 dB; SN: 21.24 ± 6.82 dB; IN: 20.54 ± 5.80 dB; IT: 20.13 ± 6.46 dB. Accordingly, the posthoc difference between the ST and the SN quadrants reached statistical significance (p=0.013).

These subjective perimetric data showed significant correlations with objective perimetry (mfVEP) (see below).

Neurophysiology

Cortical pattern visual evoked potentials reveal global field differences between ADOA patients and controls

A significant decrease of the amplitude of the P-100 wave is evident ($p<0.0001$), for both 60' and 15' stimuli (mean ± SD 60' values: patients = 6.01 ± 4.04 μV; controls = 17.35 ± 5.11 μV; mean ± SD 15' values: patients = 3.15 ± 2.39 μV; controls = 17.92 ± 5.12 μV), while implicit time is concomitantly increased (mean ± SD values for 60'stimuli: patients = 114.19 ± 14.60 ms; controls = 104.23 ± 3.93 ms / p=0.006; mean ± SD values for 15': patients = 129.10 ± 20.74 ms; controls = 110.70 ± 5.12 ms / p=0.004).

Two patients of different families (#12 and #14) showed undetectable VEPs for both spatial frequency stimuli.

All other patients presented a P100 wave with normal morphology in spite of the low amplitude – see Figure 31 showing representative data.

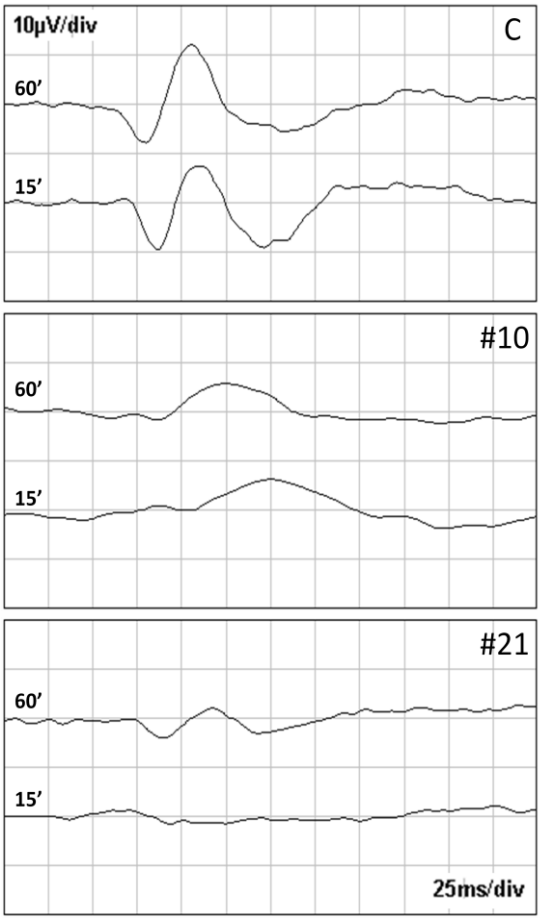

Fig. 31 – VEP plots of control (C) and two representative cases of ADOA patients.
Patient 10 presents relative amplitude loss and peak time delay for both spatial frequency stimuli, while patient 21 shows a more severe pattern, with undetectable response for the stimulus with dominant higher spatial frequency.

Multifocal visual evoked potentials – Evidence for preferential damage of central cortical mechanisms

To further investigate the contribution of central versus peripheral mechanisms between ADOA patients and controls, we performed multifocal VEP cortical recordings (see Fig. 32 for representative cases).

Significant amplitude differences were found mainly in most central rings, 1 ($p=0.0007$) and 2 ($p=0.012$) – see Fig. 33.

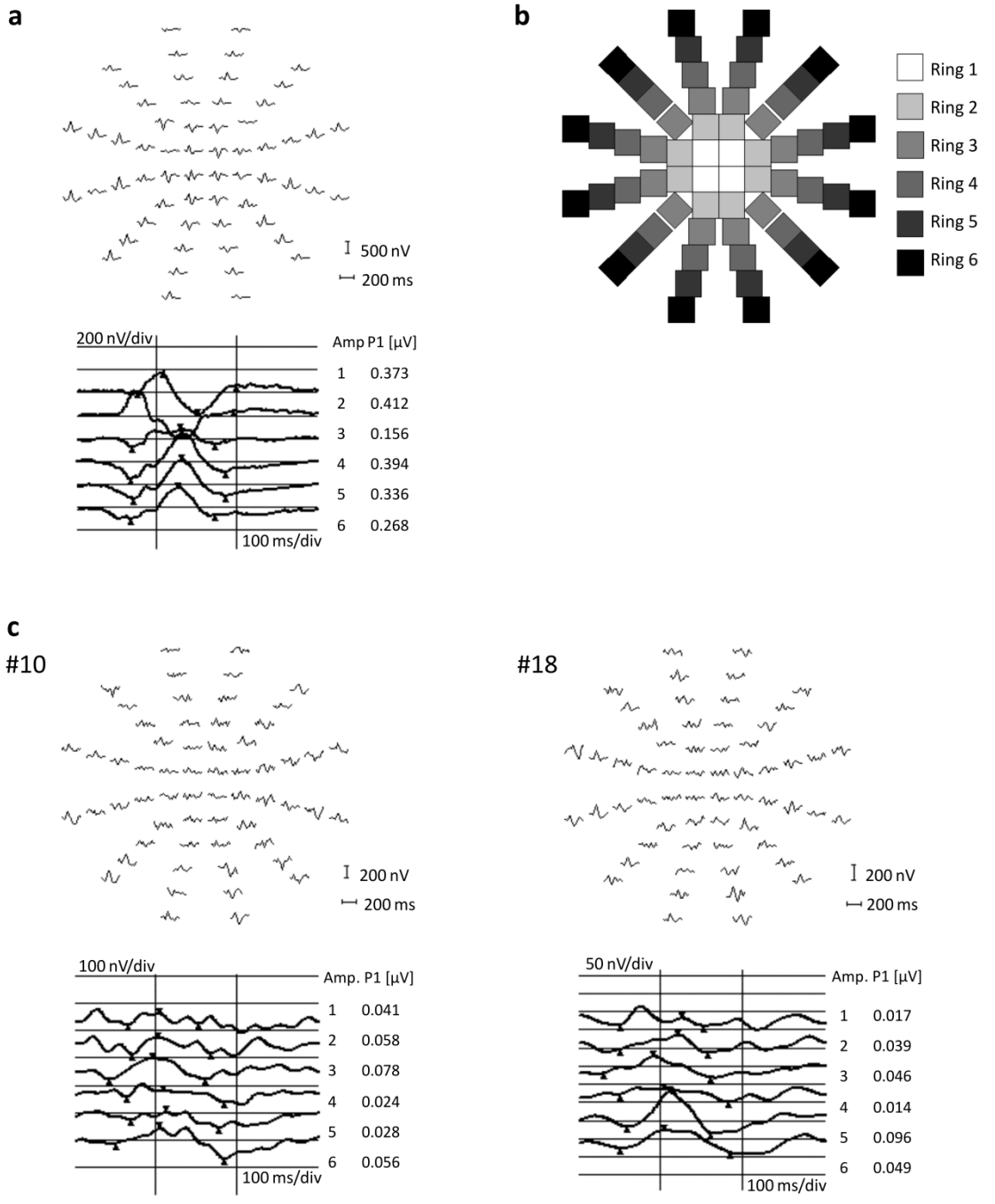

Fig. 32 – Multifocal VEP plots:
Control (**a**), schematic representation of analysis by concentric rings (**b**) and two representative cases of ADOA patients (**c**) – both cases showing low response amplitudes (note the difference in scale when compared with the control), with central recordings at the noise level, but with relative pericentral preservation, more evident in patient 18.

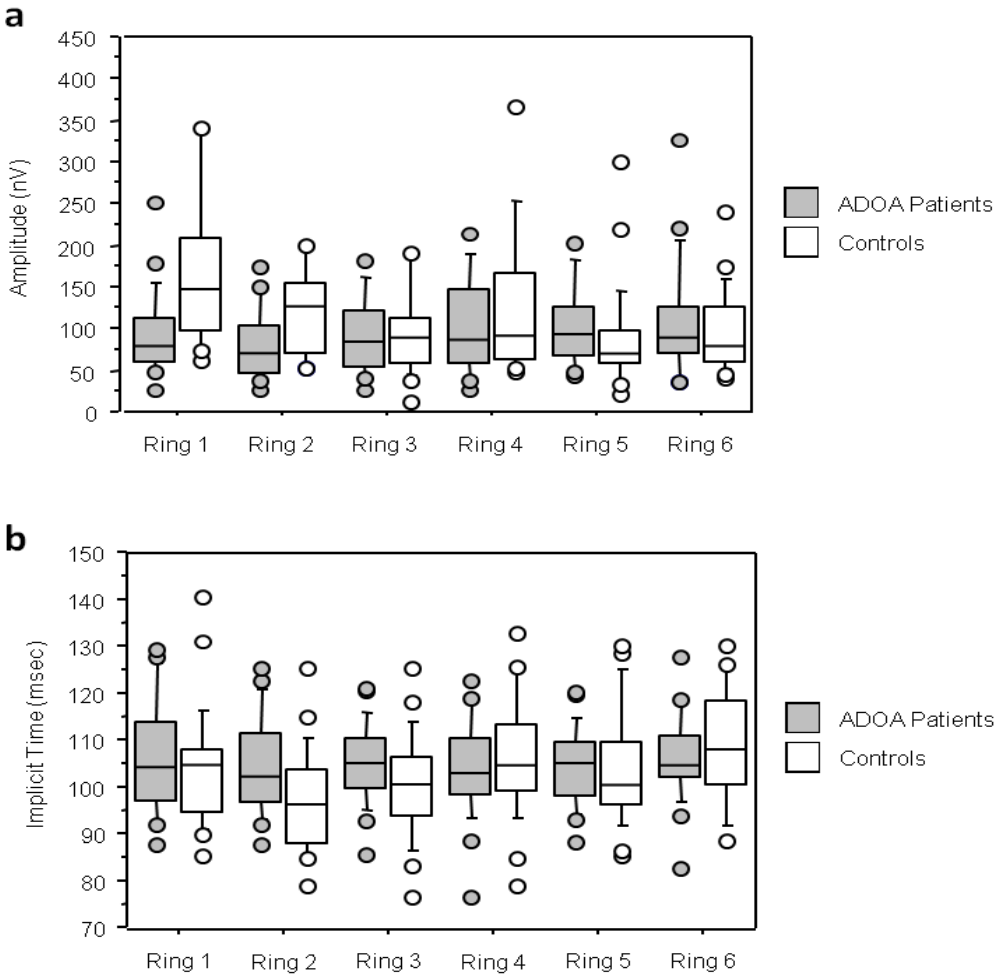

Fig. 33 – Amplitude (**a**) and Implicit Times (**b**) of P100-waves of the cortical mfVEP, across eccentricity rings, in patients and in controls. Note the predominant and significant reduction of amplitude and increase in latencies in the most central rings, in the patient group.

Pattern electroretinogram shows impairment at both waveform components

We found a decrease both in the amplitude of P-50 and N-95 waves ($p<0.0001$), while the implicit times of components were in the normal range. A decrease of N-95 / P-50 ratio was concomitantly observed ($p=0.0002$) – Fig. 34.

Some representative examples of PERG responses are shown in Fig. 35.

Ganglion cell damage was thus demonstrated by the pattern of decrease in the PERG response and it is consistent with the cortical Pattern (global) VEP results as well as those concerning the more central locations of the mfVEP.

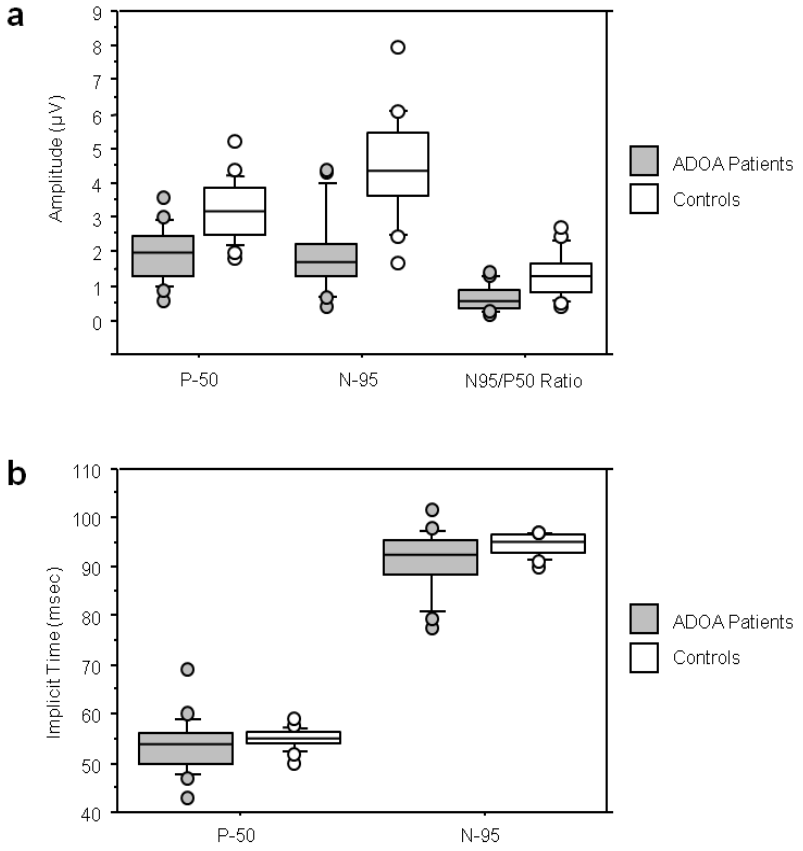

Fig. 34 – Amplitude (**a**) and implicit times (**b**) of P-50 and N-95 components of pattern ERG, in patients and in controls. Note the decrease in the N-95/P-50 ratio in the ADOA group, in keeping with ganglion cell dysfunction.

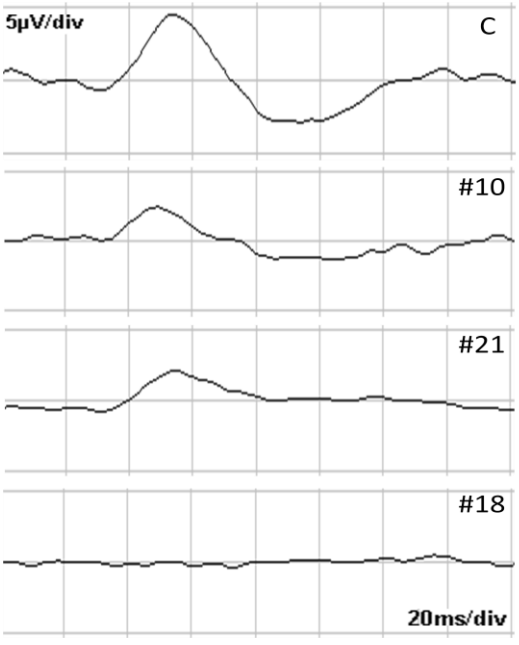

Fig. 35 – Control (C) and three representative cases of PERG recorded in ADOA patients. Patient 10 presents a normal N95/P50 ratio (with a subtle P-50 peak time shortening), differently from the patient 21 (with a severe reduction of N-95 component). Patient 18 revealing undetectable PERG response.

Multifocal Electroretinogram – Evidence for preganglion functional impairment in central and peripheral visual representations

The MfERG showed a significant decrease in amplitude in all concentric rings when compared with control subjects (P1 wave – R1: $p<0.0001$; R2: $p=0.0013$; R3: $p=0.0005$; R4: $p=0.005$; R5: $p=0.004$ – see also Fig. 36 A), suggesting a pre-CG lesion, since it reflects the activity of the cone/bipolar cell systems. Accordingly, a significant effect was also found concerning the N1 component across all rings, except R1 (R2: $p=0.0003$; R3: $p=0.0001$; R4: $p=0.005$; R5: $p=0.004$) – Fig. 36 B.

In comparison with cortical measures, all locations (central and paracentral) were therefore affected (see Fig. 37 for representative clinical examples).

Furthermore, analysis of implicit times showed significant increases between groups but only in Ring 1 of P1 ($p=0.033$) and Ring 5 of N1 component ($p=0.031$).

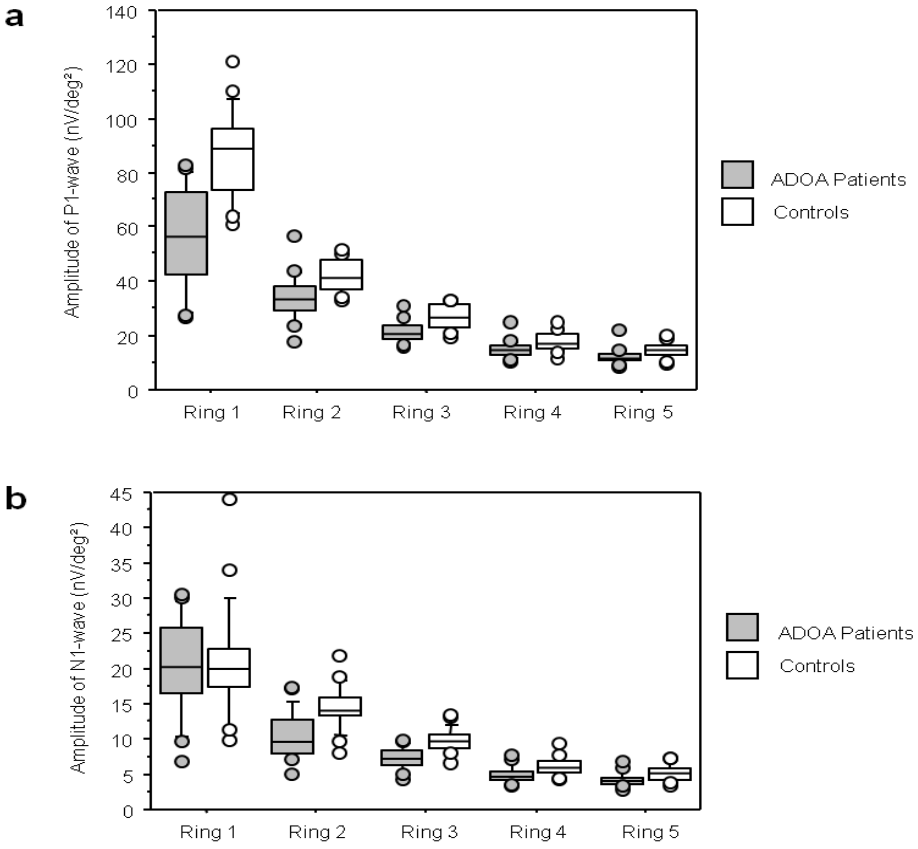

Fig. 36 – P1-wave (**a**) and N1-wave (**b**) amplitudes of mfERG, across concentric rings. Impairment is not exclusive to central representations and also includes pericentral regions.

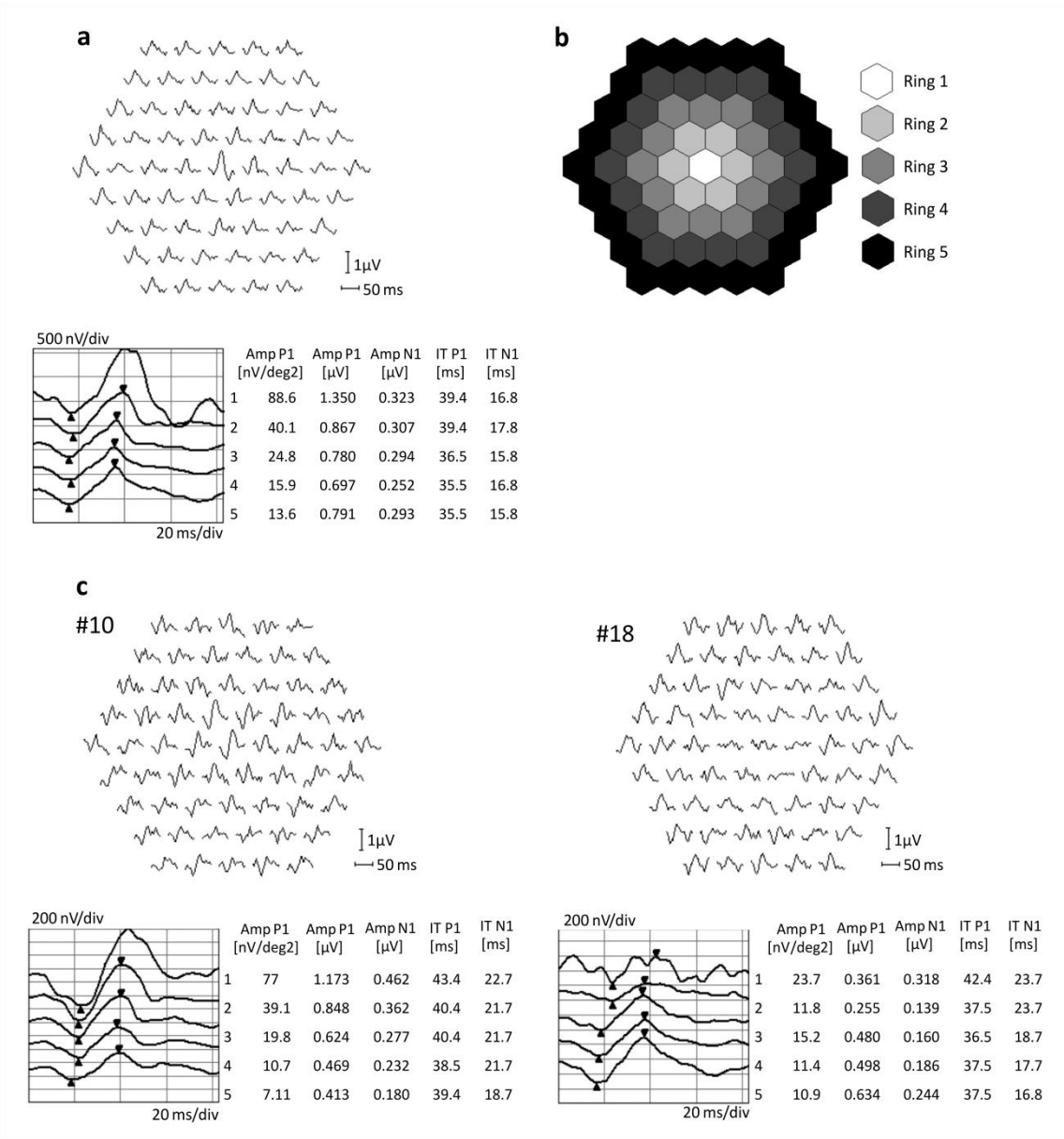

Fig. 37 – Multifocal ERG recordings:
Control (**a**), schematic representation of average waveforms by concentric rings (**b**) and two representative cases of waveforms in ADOA patients (**c**). Patient 10 shows normal amplitudes, with increase of peak times, differently from patient 18, in whom a central amplitude reduction is observed (consistent with PERG recording – see also fig. 35), with normal implicit times.

Optical coherence tomography provides evidence for damage that is not exclusive to the nerve fibre layer

Decreased values of global retinal thickness in all 9 measured regions were seen in ADOA group, with p<0.0001 for all regions, except for the central one (ns). Analysis by rings confirms these differences – Table 16.

RINGS	CONTROLS	PATIENTS	Group Comparisons
1 (1 mm)	200.4 ± 11.9	193.2 ± 30.1	p = 0.1861
2 (1-3 mm)	272.3 ± 13.9	226.2 ± 24.9	p < 0.0001
3 (3-6 mm)	240.1 ± 18.8	203.4 ± 18.4	p < 0.0001

Table 16 – Retinal thickness (mean ± SD µm) across rings within the 6 mm of central retina. Posthoc analyses.

Peripapillary RNFL thickness measures are decreased in both analyzed rings (Table 17). By refining the analysis by quadrants (average value), when comparing the nasal versus temporal RNFL thicknesses, one can see a preferential involvement of the temporal fibres – see also Table 17 for details.

		CONTROLS	PATIENTS	Group Comparisons
RINGS	**Inner**	97.5 ± 10.8	63.8 ± 13.8	p < 0.0001
	Outer	68.6 ± 8.2	50.4 ± 8.5	p < 0.0001
QUADRANTS	**Superior**	101.5 ± 11.3	72.3 ± 13.1	p < 0.0001
	Inferior	100.9 ± 12.8	64.3 ± 18.4	p < 0.0001
	Nasal	66.0 ± 13.8	51.0 ± 10.2	p =0.0008
	Temporal	64.0 ± 10.8	40.8 ± 10.4	p < 0.0001

Table 17 – Peripapillary RNFL thickness (mean ± SD µm) and analysis by rings / quadrants. All quadrants show severe loss of fibres, the nasal being the most spared.

In addition to these peripapillary differences, RNFL measures showed a significant decrease also in the macula (ring 2 - mean ± SD values: patients = 31.39 ± 4.77 µm; controls = 34.59 ± 4.16 µm / p=0.024; ring 3: patients = 34.14 ± 6.81 µm; controls = 51.16 ± 7.79 µm / p<0.0001). Note that central measures (ring 1) cannot be used given the almost absence of GC/fibres in the central part of the retina.

When subtracting macular RNFL from the total retinal thickness, one can still demonstrate a decrease in retinal thickness (post hoc analyses: ring 2: p<0.0001; ring 3: p=0.004) – see Fig. 38 for details.

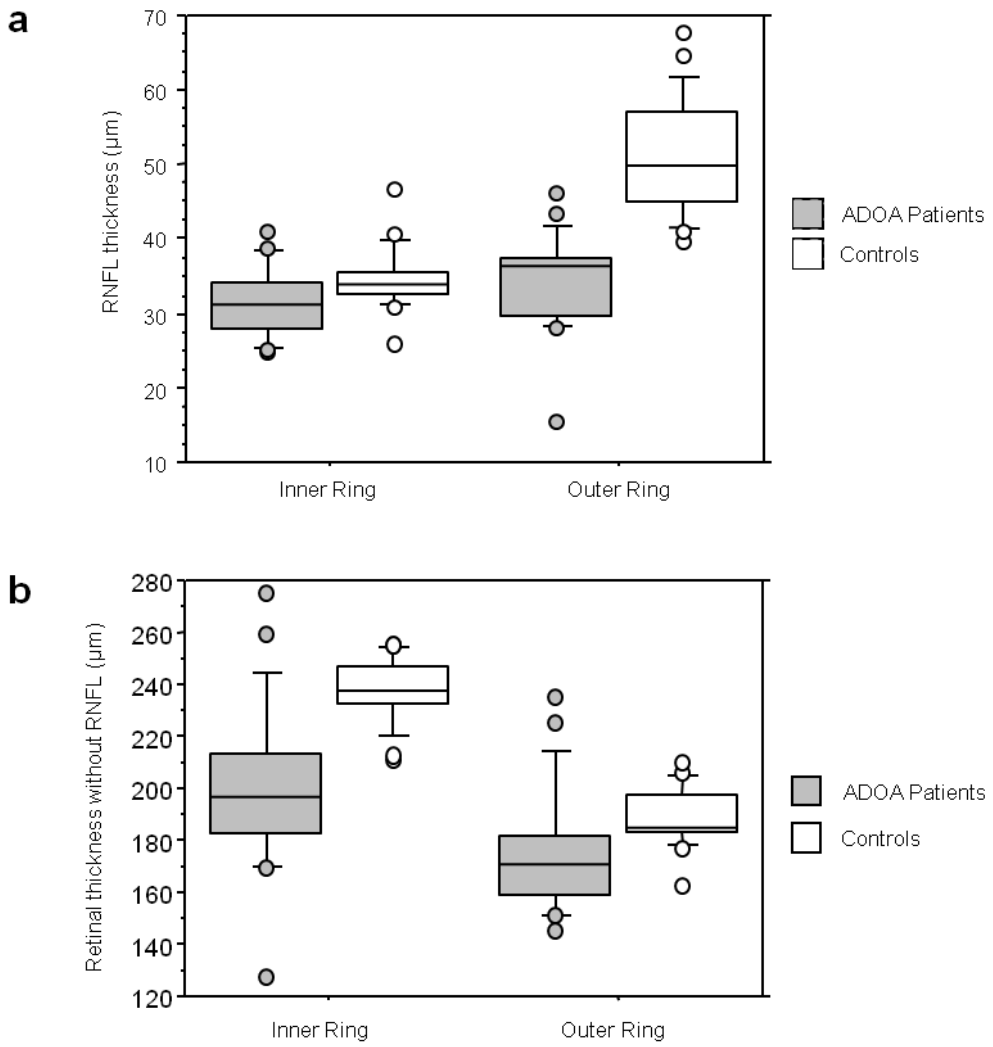

Fig. 38 – Macular RNFL thickness (**a**) and pre-ganglion macular thickness (**b**) - global thickness subtracted from RNFL, showing a significant decrease in both measures.

Structure function correlations

The locally decreased values on mfERG amplitudes (P1-wave) were significantly correlated with neural retinal thickness, except for the central area (ring 1) – Table 18.

RINGS	Amplitude – Group Comparisons	Imp. Time – Group Comparisons
1	r= 0.349; p = 0.13 (ns)	ns
2	r= 0.512; p = 0.026	ns
3	r= 0.583; p = 0.011	ns

Table 18 – Correlation between retinal thickness and electrophysiological measures (amplitude and implicit time of mfERG – P1-wave)

We have also found a significant correlation between the pre-RNFL layer (which was obtained by subtracting the RNFL thickness from the total retinal thickness, as mentioned above) and mfERG amplitude (P1 but not N1) of Ring 3 (r=0.536; p=0.019), corresponding to the outer ring measured by OCT.

No correlation was found (as expected from the distinct neural sources) between mfERG and RNFL, for the same topographic regions. However, correlations between macular RNFL thickness (inner and outer rings) with PERG (P-50 and N-95 amplitude / timing) were also not significant.

As a cautionary note, one should bear in mind the possibility of reduced statistical power due to the lack of precision in spatial match of such measures.

Cortical impact of retinal damage

Although some care should be taken with correlation analyses due to waveform shape distortions, we found a significant negative correlation between N-95 (PERG) implicit time and P-100 (VEP) amplitude evoked by high frequency spatial stimuli (r=-0.63; p=0.006).

No other significant correlations were found, namely when comparing P-50 (PERG) implicit times and amplitudes, with P-100 parameters.

Correlation patterns in the control group

Unlike the patient group, correlations between PERG (N95) and mfVEP were not significant in controls.

Correlations with visual acuity

Mean visual acuity (VA) in the patient group was correlated with the amplitude of the mfERG, at central Ring 1 of mfERG (r=0.458; p=0.03), as well as with the amplitude of VEP P100-wave for both spatial frequencies (60': r=0.44; p=0.049; 60': r=0.52; p=0.02).

Comparing the VA with the data obtained by the other methods of this study, we also found significant correlations between this parameter and contrast level (%) at threshold for all spatial frequencies of achromatic contrast sensitivity testing (0.2 cpg: r=-0.44; p=0.048 / 1 cpg: r=-0.56; p=0.012 / 2.1 cpg: r=-0.51; p=0.024 / 3.3 cpg: r=-0.46; p=0.039 / 5.2 cpg: r=-0.54; p=0.016 / 9.1 cpg: r=-0.44; p=0.049).

A stronger correlation was found between VA and mean sensitivity of automated static perimetry (r=0.73; p=0.001).

5. DISCUSSION

In this study, we have found evidence for functional damage in afferent layers of the retina to the ganglion cell layer, as probed by multifocal ERG recordings, which was correlated with patterns of visual loss.

Multifocal ERG was abnormal, and correlated with both functional psychophysical loss (suggesting that some of the dysfunction is not confined to an optic nerve origin) and structural changes as indexed by retinal thickness measures.

Reduction in cortical multifocal responses was in general independent from changes in retinal measures.

Damage of small fibres relates to central visual loss within multiple retinal parallel pathways

We identified damage of both parvocellular and koniocellular pathways, as demonstrated by chromatic contrast sensitivity testing, and likely additional loss of

magnocellular function (responsible for the highest contrast gain) related to the decreased achromatic contrast function and a shift of the corresponding peak sensitivity (1 cpd for patients and 3.3 cpd for controls).

These findings imply that small fibre damage in this condition (Carelli et al., 2002; Pesch et al., 2004; Carelli et al., 2004) is not restricted to any specific pathway. Indeed, the "small fibre" bias observed in histological studies (Johnston et al., 1979; Kjer et al., 1983) is therefore related to central fibres being smaller, and not to predominant damage of the parvocellular ("small neuron") pathway. These results are also consistent with the data of Votruba et al. (1998).

Further evidence to this claim lies on our finding of impairment in CS across multiple spatial frequency channels suggesting that a broad range of fibre types is affected in ADOA. Accordingly, the peripapillay RNFL shows more sparing of the nasal fibres, which is consistent with the OCT literature referring a preferential involvement of the temporal papillomacular bundle (Yu-Wai-Man et al., 2011b).

Our results are also consistent with those of Barboni et al. (2011), reporting an additional involvement of the inferior sector, since we found a fibre loss percentage of ~ 36 % for both temporal and inferior quadrants.

Patterns of amplitude changes found using multifocal cortical evoked responses confirm that the differences identified in Pattern VEP are mainly due to damage to central fibres independently of the underlying pathway (as further corroborated by the correlation patterns of VA and other structural and functional measures).

Interestingly we found VEP delays in the absence of the waveform shape distortion that can be observed in early stages (Holder, 2001, 2004; Holder et al., 2009).

The most eccentric retinal deficit is compensated at the cortical level, in contrast to the central pattern of deficit

We found a central bias in the impairment of visual representations that was amplified from the retina to the cortex, unlike the most eccentric deficit within central vision.

At the cortical level, only central vision mechanisms were impaired, with preservation of most eccentric cortical physiological responses, which contrasts with the pattern observed in the multifocal ERG, where all regions showed significant changes.

In this respect, it is interesting to note that we have identified a particular vulnerability in the Superior Temporal quadrant, which corroborates previous findings in glaucoma (Wescott et al., 1999) as well as in multiple sclerosis (Reis et al., 2011) and

in line with a previously documented physiological weakness in this quadrant (Silva et al., 2008).

Evidence for impairment at the pre-ganglionic level

As expected, dysfunction at the ganglion cell level was corroborated by the findings of decreased retinal nerve fibre layer thickness, and abnormal pattern ERG recordings.

Evidence for physiological dysfunction in preganglion components is clear from the analysis of the early components of the mfERG (N1 and P1 components), and is also consistent with the structural data (in particular after subtraction of RNFL measures). Importantly, visual acuity did correlate with these focal central objective responses, further suggesting that retrograde damage to preganglionic pathways has relevant clinical impact.

The evidence of overall structural damage with concomitant physiological impairment not confined to the ganglion cell layer is in agreement of a previous study that concluded that *OPA1* is expressed not only in the GC layer and in the myelinated region of the optic nerve, but also in the inner plexiform, inner nuclear and outer plexiform layers of the retina of the adult human eye (Aijaz et al., 2004). Accordingly, two previous studies found a significant decrease in macular volume in ADOA (Ito et al., 2007; Milea et al., 2010).

In conclusion, Autosomal Dominant Optic Atrophy involves preganglion (retrograde) physiological impairment of central visual representations (including central and more eccentric locations) and anterograde impairment that dominates in the more central representations. Moreover, konio- parvo- and magnocellular pathways seem to be concomitantly affected in this condition.

The clinical impact of retrograde functional damage, as suggested by correlation with measures of visual function, suggests that its measures are clinically relevant to study disease severity and progression.

Finally, functional cortical compensation mechanisms seem to vary across pathways in central and pericentric vision, suggesting that future studies should address the cortical phenotype and its clinical relevance.

– Part II –

CENTRAL AND PARACENTRAL VISUAL CORTICAL RESPONSES ACROSS MULTIPLE SPATIOTEMPORAL CHANNELS IN ADOA: PATTERNS OF IMPAIRMENT AND REORGANIZATION

1. ABSTRACT

The goal of this study was to characterize neurophysiologic responses across multiple spatiotemporal channels in Autosomal Dominant Optic Atrophy (ADOA) patients, in order to investigate the impact of this optic neuropathy across multiple cortical locations, in central and peripheral vision.

We have recorded high density visual evoked potentials, monocular and binocularly, according to the international 10-20 system, with a SynAmps 2 system (Compumedics NeuroScan, Texas, USA) in 22 subjects (44 eyes) from 13 families with ADOA submitted to *OPA1* mutation analysis (mean age ± SD = 31.86 ± 16.43 years; mean visual acuity ± SD = 0.29 ± 0.16). A cap with 64 electrodes was used to collect biosignals evoked by stimuli with distinct relative biases for the activation of magno- or parvocellular pathways, namely gratings with low spatial frequency (0.25 cpd) with an associated temporal frequency of 10 Hz, and static gratings of 4 cpd, respectively, presented in full-field or only in the paracentral visual locations. Full-field checkerboard (reversal presentation) with two spatial frequencies (0.25 and 4 cpg) was also applied, similarly to the conventional visual evoked potentials (VEP). According to the distribution of data, parametric statistical analysis was performed using ANOVA. Paired t-Tests were used for within group analyses and Pearson coefficient for data correlation. Significance level was set at $p \leq 0.05$.

In the primary visual cortex (midline occipital electrode/OZ) evoked responses are considerably reduced for all types of stimulation in patients as compared with controls ($p \leq 0.02$), in particular for parvocellular responses. Interestingly, some binocular compensation (significant summation as compared to monocular stimuli) could be found for paracentral parvo-biased stimuli in patients. Unlike in controls, response amplitudes remained relatively stable across posterior-anterior cortical regions suggesting increasing cortical propagation.

Our results show cortical impairment of distinct spatiotemporal channels with distinct biases for parvo and magno driven responses with a distinct pattern of cortical propagation in patients. Dominant impairment of parvo representations was partially

compensated by binocular peripheral representations. Together, these findings suggest cortical reorganization of stimulus driven responses induced by visual impairment.

2. INTRODUCTION

(For a general overview of clinical and genetic characterization of ADOA, see Introduction of Part I of this Chapter)

Neurophysiological studies in ADOA patients have usually been confined to the application of standard electrophysiological methods, namely pattern electroretinogram (PERG) and pattern visual evoked potential (PVEP).

PERG is reported to present reduced amplitude of the N95 (optic nerve) and P50 (with a ganglion cell contribution) components and a consequent reduction of the N95/P50 ratio. Substantial decrease of the amplitude of pattern visual evoked potential (PVEP) with concomitant timing delay and a normal full-field ERG are also typical electrophysiological characteristics of ADOA (Holder, 1987; Holder et al., 1999).

Our previous work (provided in Part I of Chapter V of this thesis) has advanced the notion of a retrograde functional damage (Reis et al., 2012). This was shown by multifocal ERG data (with main contributions from the photoreceptor and bipolar layers), and corroborated by structural data obtained by optical coherence tomography. It is nevertheless also important to test high level mechanisms in ADOA and in particular how cortical responses reorganize to impaired retinocortical input.

In the present study we investigated the differences between the cortical responses evoked by stimuli with distinct spatiotemporal properties, differently biased for parvo- and magnocellular activation. We tested such responses under full-field (central/paracentral) and paracentral vision configurations, to investigate the relative contribution of the latter to global responses. Data were collected with a high density array of 64 electrodes cap, which also allowed us to study response propagation patterns of the above mentioned visual spatiotemporal channels (Tobimatsu et al., 1995; Souza et al., 2008).

3. METHODS

3.1. PATIENT SELECTION, DEMOGRAPHIC CHARACTERISTICS, *OPA1* MUTATION ANALYSIS AND OPHTHALMOLOGICAL EXAMINATION

See Part I of this Chapter (same study population).

Besides the previously mentioned clinical evaluation (mentioned above – Part I), neuropysiological function was assessed with high density electrode recording of visual evoked potentials, evoked by different types of stimuli biased for parvo- and magnocellular systems (for details, see below), in order to separate the respective responses and to evaluate the relative damage across those pathways as well as the contribution of the central versus paracentral vision.

3.2. HIGH DENSITY VISUAL EVOKED POTENTIALS

We record multiple visual evoked potentials, with a SynAmps 2 system (Compumedics NeuroScan, Texas, USA - 4.3.1 version).

We measured evoked responses in different cortical locations, generated by different types of stimuli. A cap with 64 electrodes (with labels according to the international 10-20 system) was used to collect induced biosignals generated by stimuli of different characteristics with relative biases for magno- and parvocellular pathways. Vertical gratings of low spatial frequency (0.25 cpd) with an associated temporal frequency of 10 Hz and stationary vertical gratings of 4 cpd (reversal interval: 1000 ms) were presented mono- and binocularly, on a CRT monitor (15'' / resolution: 1280x1024 / refresh rate: 60 Hz), at a distance of 114 cm, with participant´s far vision refractive correction (when applicable**).**

In order to identify the most peripheral contributions to overall full-field responses, all stimulus types were either presented in an area from 7.5 to 15 degrees, or in a full-field mode (up to 15 degrees). Participants were instructed to fixate the target on the centre of the monitor during recordings. Checkerboard stimuli with two spatial frequencies (0.25 and 4 cpd) were also applied in order to obtain similar data with those obtained with conventional VEP.

Bioelectrical signals were recorded with a sampling rate of 2 kHz and an online low-pass filter of 500 Hz. Data was band-pass filtered offline (1-30Hz) and segmented into epochs locked to stimulus onset (-100 ms to 500 ms). Epochs with artefacts that exceed 100 µV were rejected and the remaining sweeps were averaged. Peak times (in ms) and amplitudes (in µV) were extracted for every subject and condition for statistical comparisons.

For analysis, we considered the obtained data grouped by four clusters of responses: two of them in each cerebral hemisphere (anterior and posterior), excluding the midline and anterior-posterior line locations – see Fig. 39 for details. OZ activity was also analyzed, since that is corresponds to the striate cortex region recorded in the conventional VEPs, in order to have a standard comparison.

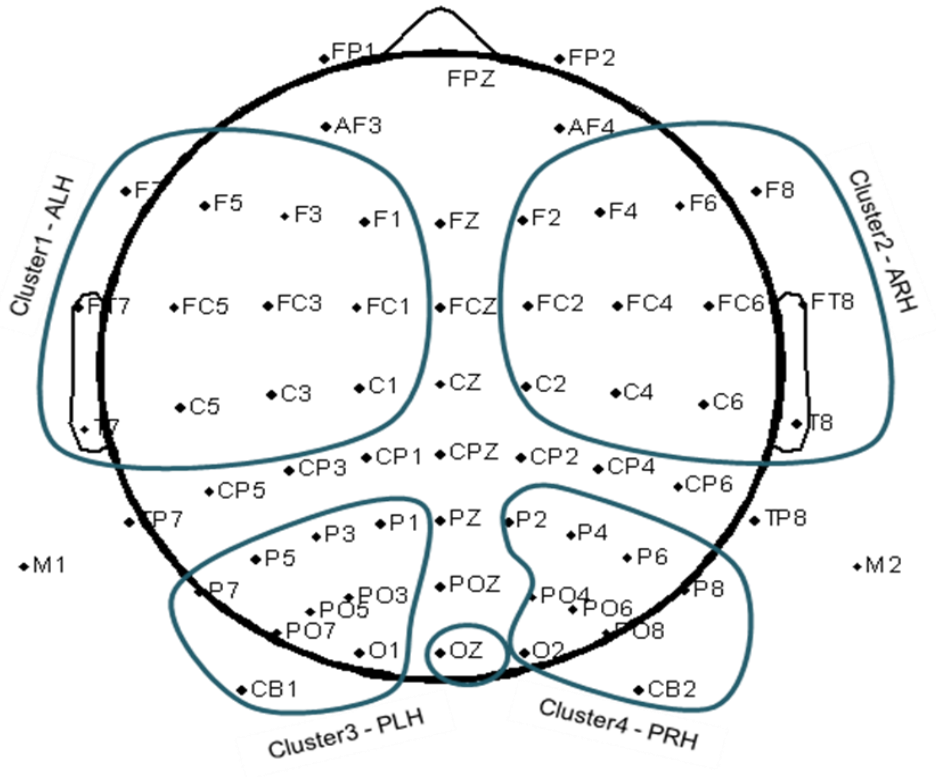

Fig. 39 – Definition of Clusters for data analysis (Cluster 1 – ALH: anterior left hemisphere; Cluster 2 – ARH: anterior right hemisphere; Cluster 3 – PLH: posterior left hemisphere; Cluster 4 – PRH: posterior right hemisphere; OZ – occipital midline).

3.3. STATISTICAL ANALYSIS

To prevent issues related to violations of independence, in our statistical analysis we used the mean of monocular cortical responses of each participant, since all variables were statistically correlated (Pearson coefficient).

According to the distribution of data, parametric statistical analysis was performed using ANOVA and t-tests, with StatView (SAS, Cary, NC, USA). Paired t-Tests were used for within group analyses. Significance level was set at $p \leq 0.05$.

4. RESULTS

Patient Demographic Characterization, *OPA1* Analysis and Ophthalmological Evaluation

See these results in Part I of this Chapter.

High Density Visual Evoked Responses

Average recordings obtained for each type of acquisition and in each study group are globally presented in figures 40, 41 and 42, and the respective analyses will be detailed in the following subsections. The statistical results are summarized in tables.

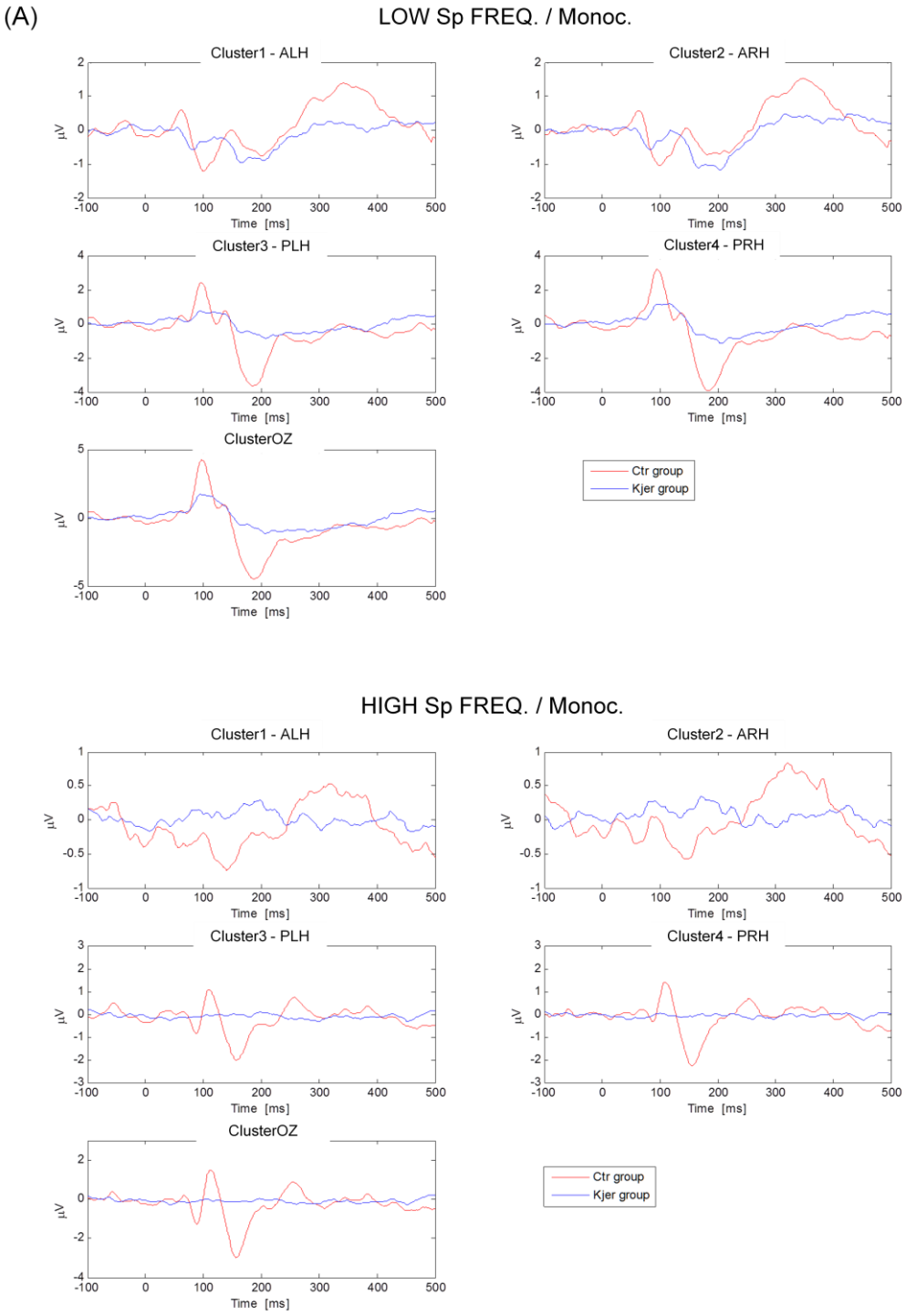

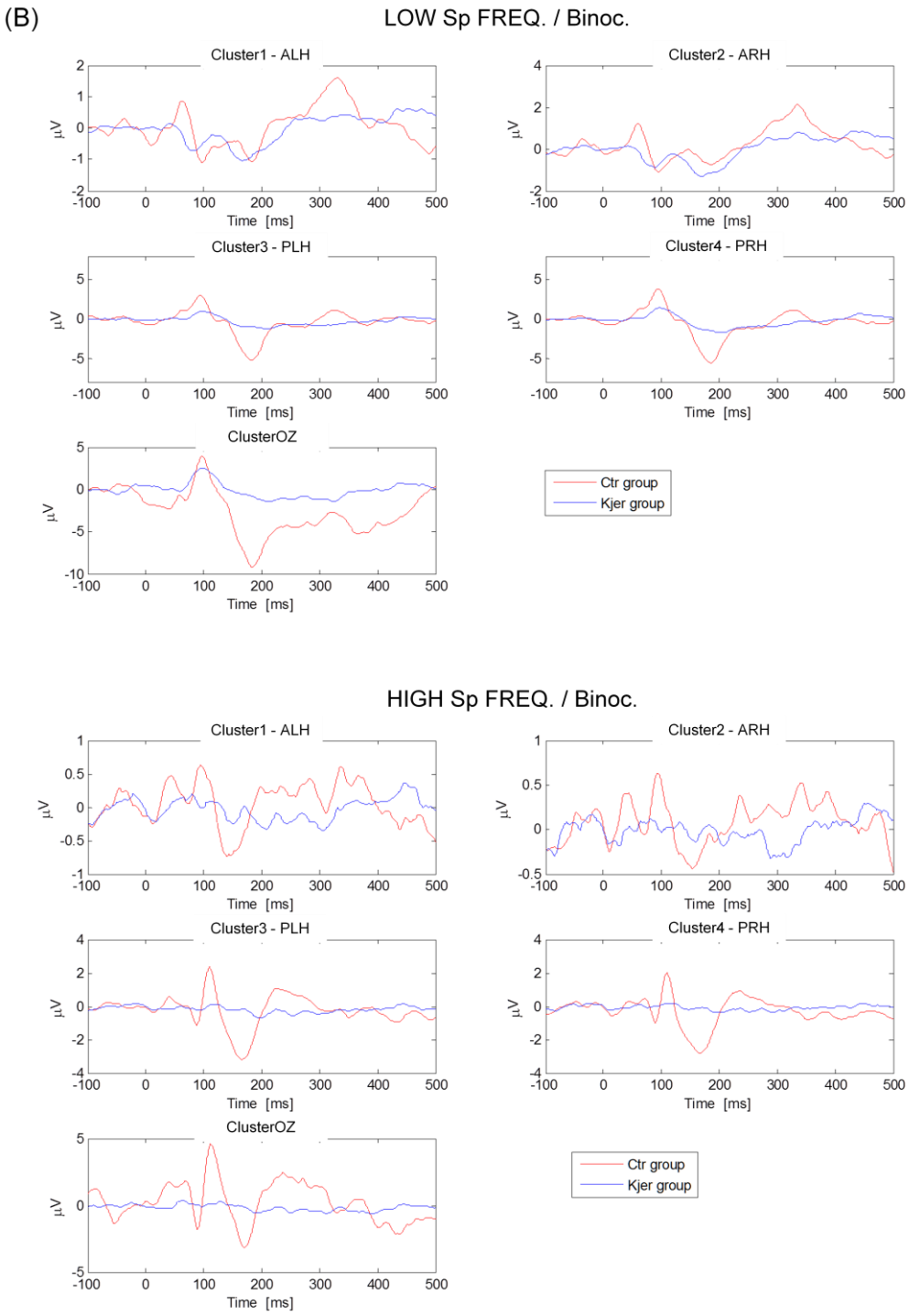

Fig. 40 – Average group responses to *low* and *high spatial frequency* CHECKERBOARD stimuli (full-field), presented mono- (A) and binocularly (B), across cortical clusters.
Comparisons between patients and controls. Differences are present in the early P100 component (and absent in patients - ensuing extrastriate N190 component, which is out of the scope of this thesis). High frequency responses for this stimulus type are virtually absent in patients, even under binocular conditions.

(A)

FULL-FIELD / Monoc.

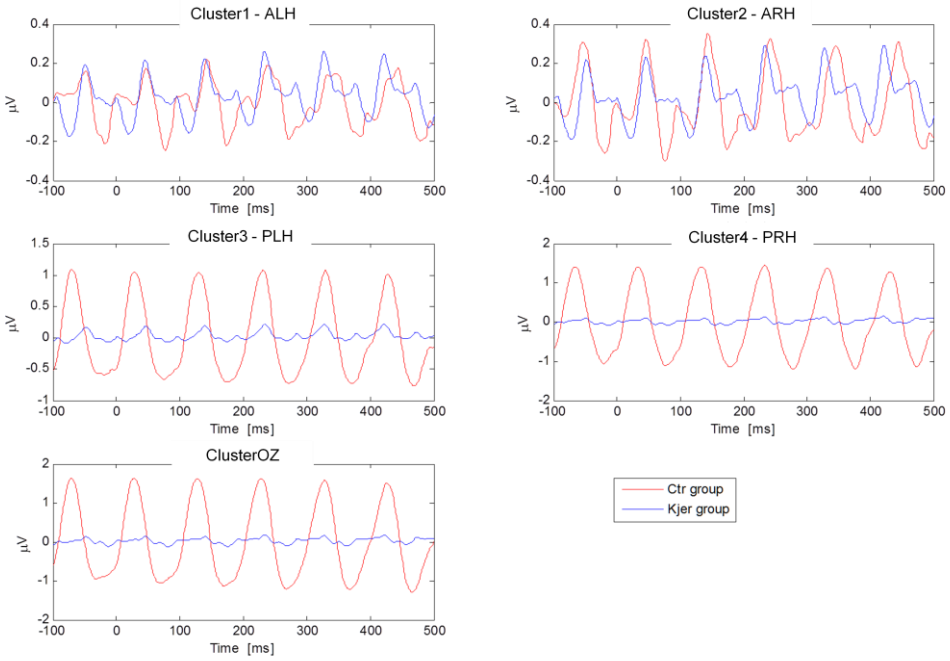

PERIPHERY / Monoc.

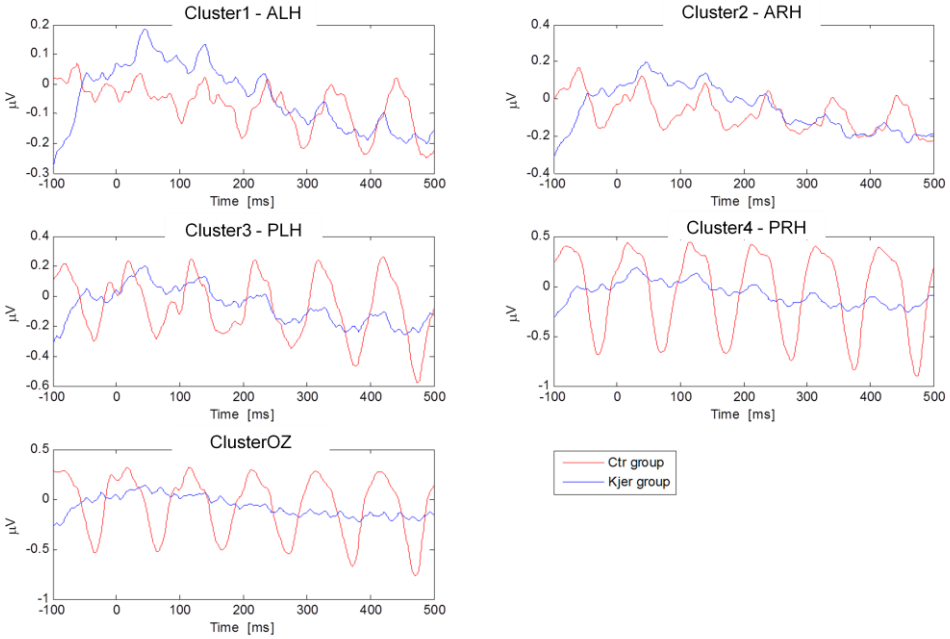

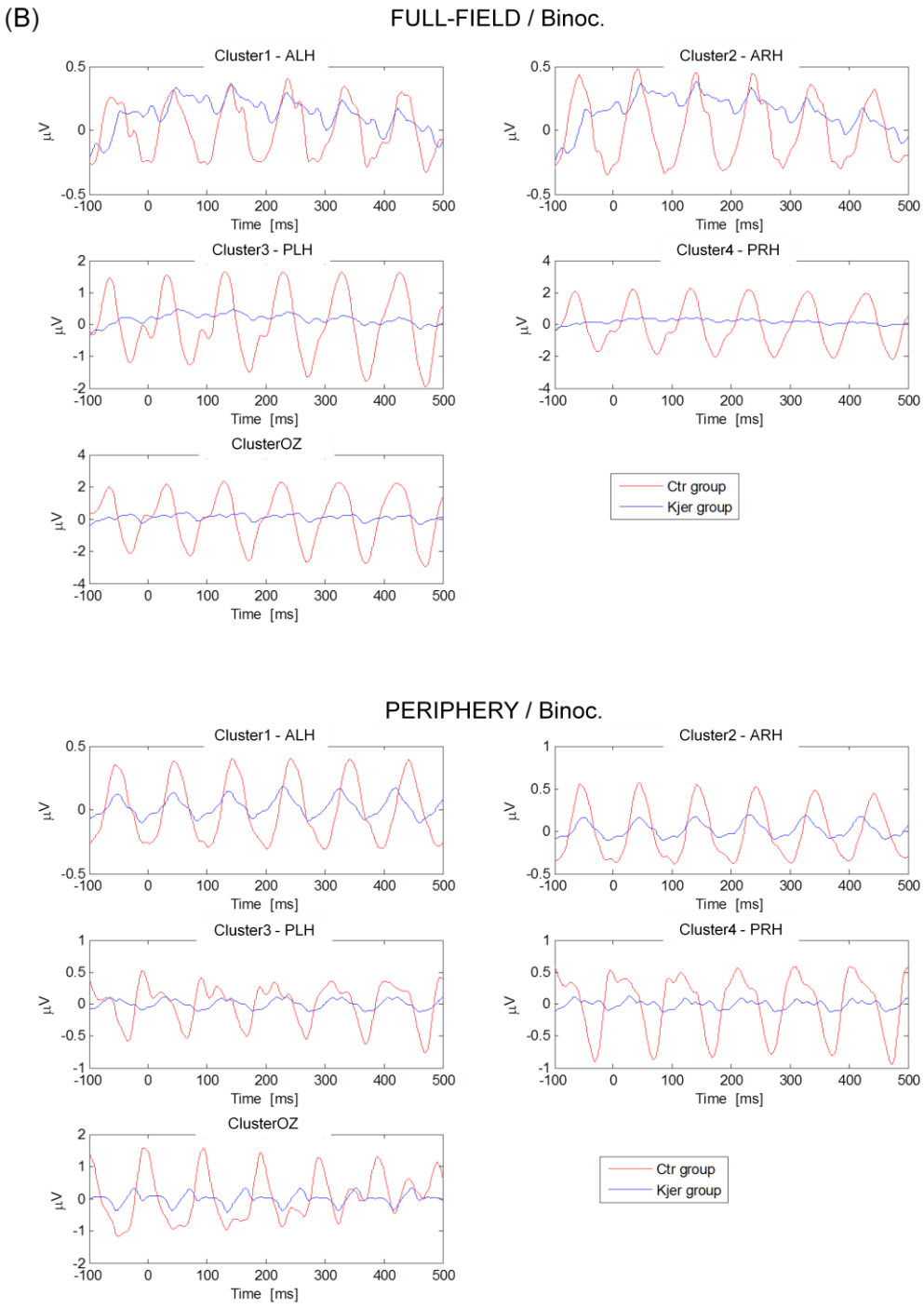

Fig. 41 – Average group responses obtained with FLICKERING LOW SPATIAL FREQUENCY GRATINGS presented either in *full-field* or in *peripheral* visual field, mono- (A) and binocularly (B) across cortical clusters. Only in controls a small asymmetry can be found (higher amplitude in the right hemisphere). One can also observe a specific binocular "recovery" in patients of peripheral flickering responses.

(A)

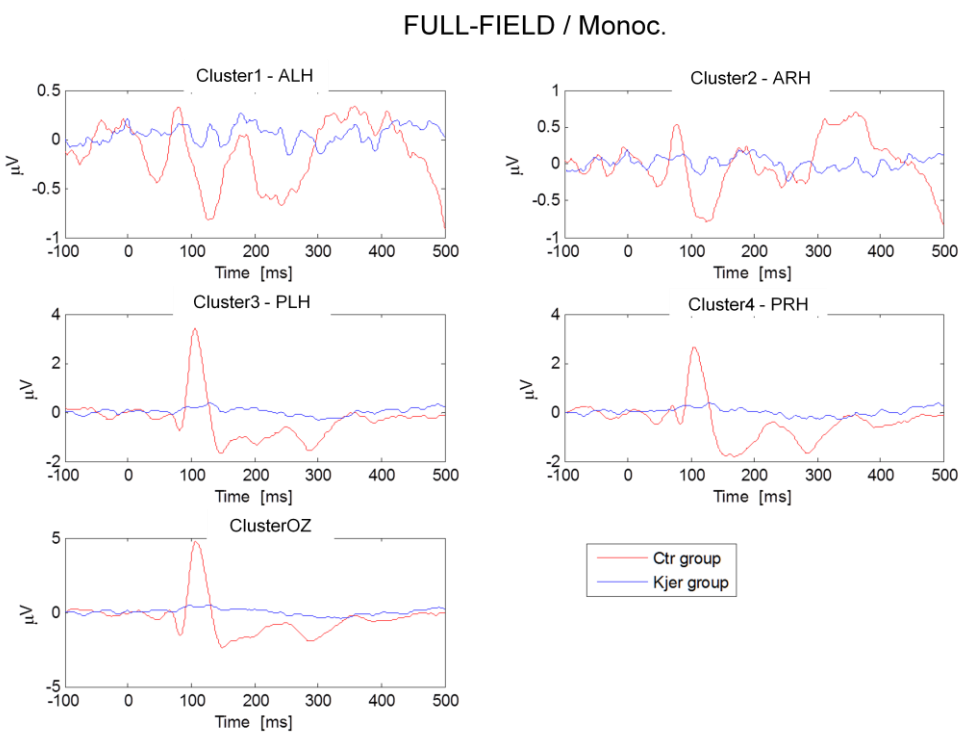
FULL-FIELD / Monoc.
Cluster1 - ALH
Cluster2 - ARH
Cluster3 - PLH
Cluster4 - PRH
ClusterOZ
µV
Time [ms]
Ctr group
Kjer group

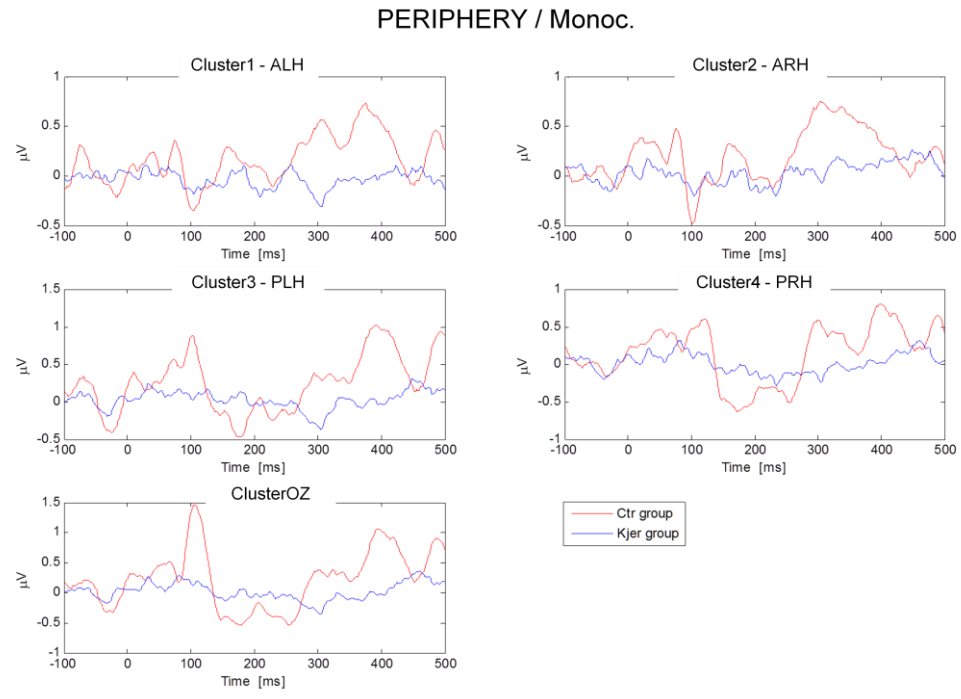
PERIPHERY / Monoc.
Cluster1 - ALH
Cluster2 - ARH
Cluster3 - PLH
Cluster4 - PRH
ClusterOZ
µV
Time [ms]
Ctr group
Kjer group

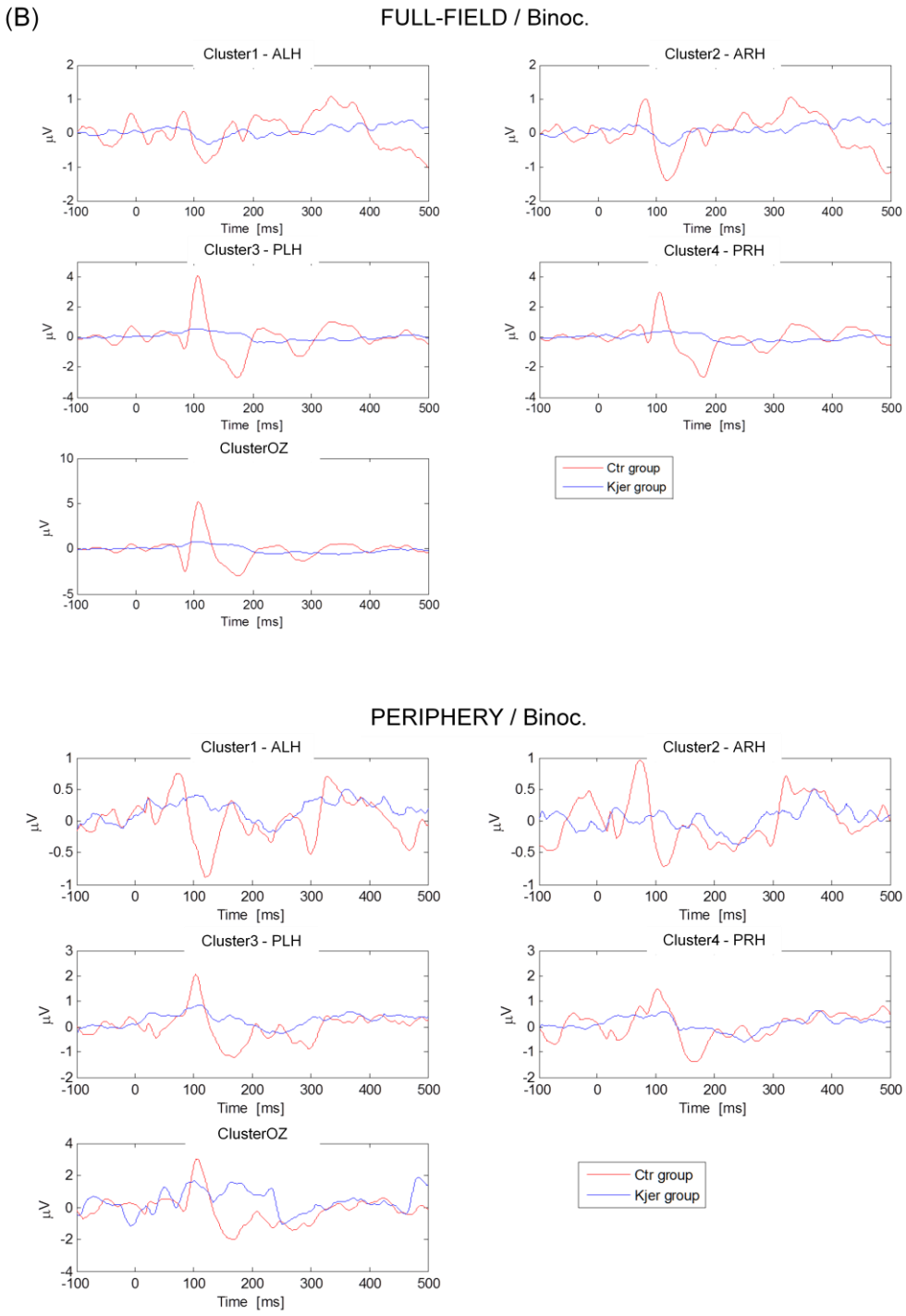

Fig. 42 – Average group responses obtained with HIGH SPATIAL FREQUENCY gratings presented in *full-field* or *peripheral* visual field, mono- (A) and binocularly (B) across cortical clusters. Controls present higher amplitude in the left hemisphere with full-field stimulation. Note the lack of responsiveness to these stimulus conditions, in the patient group.

Between group comparisons for different spatial and temporal stimulus configurations

General data distribution across cortical clusters

In controls, we can observe a progressive decrease in response amplitudes from the posterior to the anterior cortex, independently of parvo- and magnocellular biased stimulation or type of stimulus (checkers versus vertical bars) – Fig. 43A.

This pattern is not found in patients, where amplitudes remain undecayed across the posterior-anterior cortical pathway (with exception of some OZ responses), being of relatively preserved magnitude for the detectable responses in the anterior clusters as compared with controls – Fig. 43B.

(A) Monocular Responses

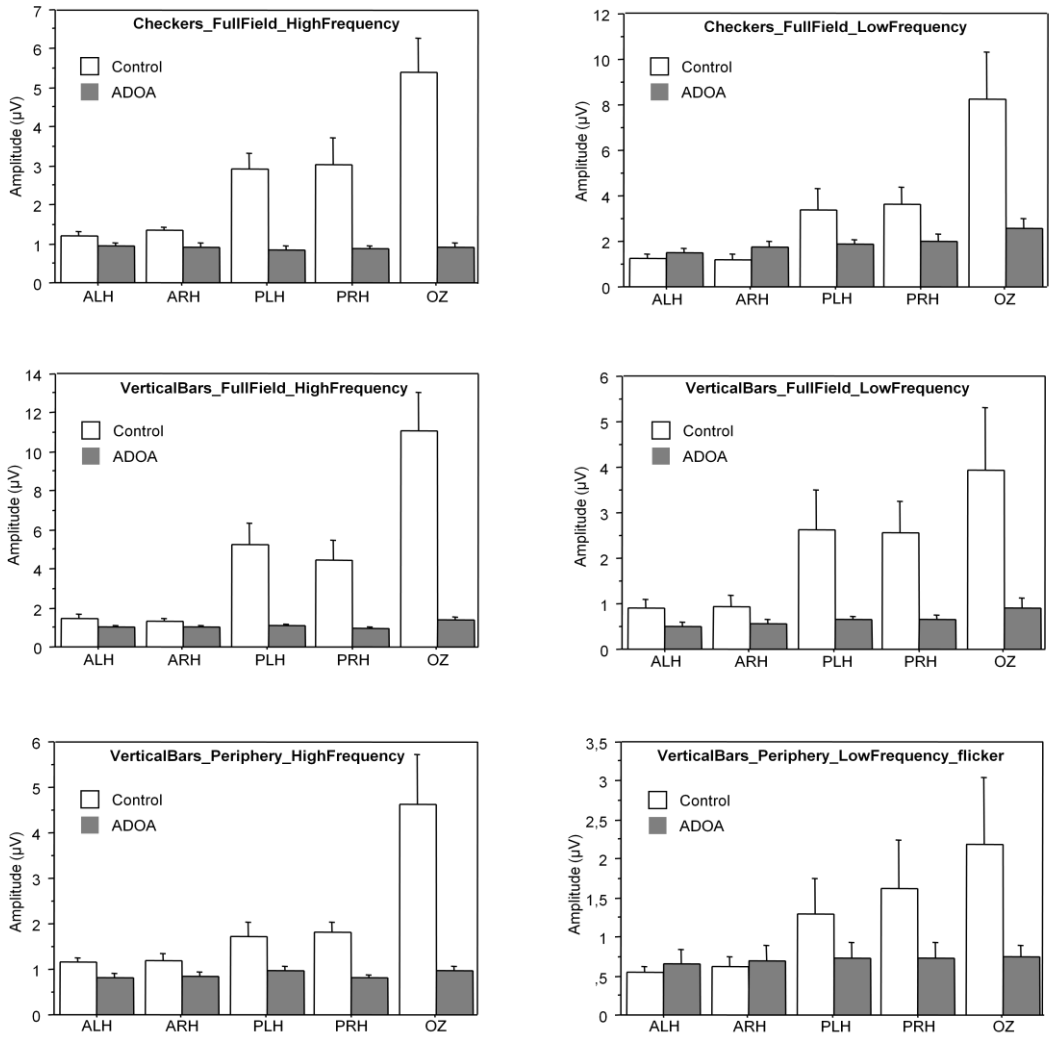

(B) Binocular Responses

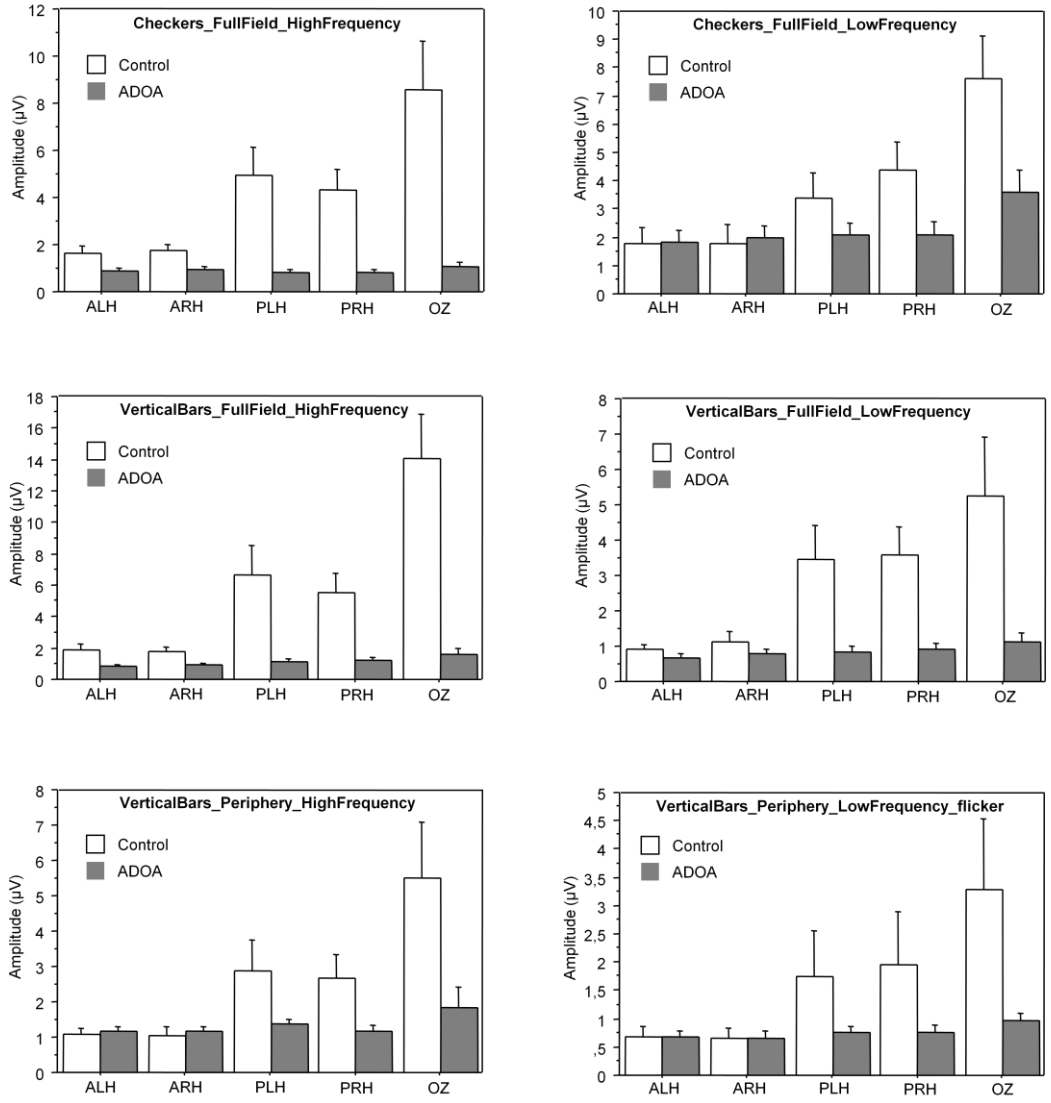

Fig. 43 – Comparison between controls and patients responses.
(A) Mono- and binocular (B) responses to different types of stimuli (mean ± SEM).
In addition to the significant between group differences, in controls,
a clear within group decrease in amplitude can be seen,
from posterior to anterior clusters, differently from ADOA patients.

Differences in responses biased for magno- and parvocellular stimulation

Table 19 presents statistical comparison between groups concerning the average amplitude responses for each cortical cluster, for monocular and binocular stimulation.

	Stimuli			ALH	ARH	PLH	PRH	OZ
Monocular Stimulation	P	FF	C_ HF	ns	p=0.01	p<0.0001	p<0.0001	p<0.0001
	M	FF	C_ LF	ns	ns	p=0.04	p=0.02	p=0.0003
	P	FF	VB_ HF	p=0.03	ns	p<0.0001	p<0.0001	p<0.0001
	M	FF	VB _LF_fl	p=0.03	ns	p=0.0005	p=0.0001	p=0.002
	P	Pf	VB_ HF	p=0.04	ns	p=0.002	p<0.0001	p<0.0001
	M	Pf	VB_ LF/fl	ns	ns	ns	ns	p=0.01
Binocular Stimulation	P	FF	C_ HF	p=0.003	p=0.0006	p<0.0001	p<0.0001	p<0.0001
	M	FF	C_ LF	ns	ns	ns	p=0.02	p=0.02
	P	FF	VB_ HF	p<0.0001	p=0.0008	p<0.0001	p<0.0001	p<0.0001
	M	FF	VB _LF_fl	ns	ns	p=0.0002	p<0.0001	p=0.0003
	P	Pf	VB_ HF	ns	ns	p=0.01	p=0.004	p=0.01
	M	Pf	VB_ LF_fl	ns	ns	p=0.05	p=0.04	p=0.003

Table 19 – Group comparison between amplitudes of neurophysiological responses evoked by different stimulus types presented mono- and binocularly.
P: parvocellular biased stimulus; M: magnocellular biased stimulus; FF: full-field; Pf: periphery; C: checkerboard; VB: vertical bars; HF: high spatial frequency; LF: low spatial frequency; fl: flicker; ALH: anterior left hemisphere; ARH: anterior right hemisphere; PLH: posterior left hemisphere; PRH: posterior right hemisphere; OZ: occipital midline.

The largest differences between patients and controls responses are present for parvocellular biased-stimulus (static, high spatial frequency – full field checkerboards or vertical bars).

Importantly, the lower differences between groups are found in responses evoked my magnocellular-biased stimuli (low spatial frequency checkers / low spatial gratins presented at 10Hz flicker, presented in full-field or just in the most peripheral locations). Note that the lowest difference is observed in the monocular responses evoked by the stimulus with increased sensitivity for magnocellular performance (low

frequency vertical gratings presented in the paracentral vision, in flicker), showing a p-value of 0.01 in OZ (monocular vision), with no significant differences in the other clusters. This is consistent with the undecayed anterior propagation of these responses in patients.

In spite of the amplitude differences between both study groups, no significant differences in latency values were detectable (possibly due to the nearly absent responses for parvo-biased conditions, and the distinct response waveforms for flickering conditions rendering direct comparisons difficult).

Within group comparisons of response asymmetries across different spatial and temporal stimulus configurations

Table 20 presents statistical comparison within groups concerning the average amplitude responses in mono- and binocular conditions, comparing the each type of stimuli (checkerboard, full-field gratings and peripheral gratings) at high spatial frequency (static stimuli) and low spatial frequency (with associated flicker), biased for parvo- (P) and magnocellular (M) systems, respectively (see also figure 44 for visualization of these results).

We can see very clearly that there is no statistic difference in amplitude values between the evoked responses to low and high frequency *checkerboard* stimuli, in controls. By opposition, responses are stronger (about 2-3 fold) when one presents the low frequency checkerboard stimulus to the patients, as compared with their responses obtained with high frequency (parvo-biased) stimulus.

A different pattern of response is observed with *vertical gratings full-field* stimulation: controls respond stronger with high frequencies than with low frequency stimulus (signal of about double magnitude), in monocular and binocular conditions. Patients present the same pattern, but only for monocular stimulation (in binocular conditions responses are almost of the same amplitude, due to the binocular summation of the obtained response with low frequency stimulus).

However, when high and low frequency gratings are applied only in the most *peripheral retina*, the responses remain within a similar range of values, in controls for both high and low spatial frequencies. In patients the same pattern is observed for monocular vision, but not for binocular responses, due to the summation phenomenon that was prominent in patients.

		Parvo vs Magno biased Stimulation	ALH	ARH	PLH	PRH	OZ
Controls	Monoc	Checkers	ns	ns	ns	ns	ns
		VB_FF	*(p=0.062)*	ns	p=0.034	ns	p=0.008
		VB_P	p=0.003	ns	ns	ns	*(p=0.063)*
	Binoc	Checkers	ns	ns	ns	ns	ns
		VB_FF	p=0.026	p=0.022	*(p=0.066)*	ns	p=0.004
		VB_P	ns	ns	ns	ns	p=0.046
Patients	Monoc	Checkers	p=0.006	p=0.002	p=0.0002	p=0.001	p=0.001
		VB_FF	p=0.0004	p=0.001	p=0.003	p=0.023	p=0.044
		VB_P	ns	ns	ns	ns	ns
	Binoc	Checkers	p=0.025	p=0.015	p=0.005	p=0.009	p=0.002
		VB_FF	ns	ns	ns	ns	ns
		VB_P	p=0.013	p=0.013	p=0.0003	p=0.027	ns

Table 20 – Within group comparison between responses obtained with high spatial frequency (and static – P biased) versus low spatial frequency (and flickering – M-biased) stimuli, in controls and patients, presented mono- and binocularly.
Interestingly, differences in patients tend to propagate across the cortical surface.
P: parvocellular biased stimulus; M: magnocellular biased stimulus; FF: full-field; Pf: periphery; VB: vertical bars; HF: high spatial frequency; LF: low spatial frequency.

Central versus Paracentral Responses

Table 21 presents within groups statistical comparison (in monocular and binocular conditions) concerning the average amplitude responses between full-field versus paracentral stimulation, using gratings biased for parvo- (static high frequency stimulus) and magnocelular activation (low frequency with flicker). Figure 44 shows bar graphs depicting these differences.

In controls, there are significant higher responses when high spatial frequency stimuli are presented in full-field configurations, mainly in binocular conditions, differently from when stimulating with flickering low spatial frequencies.

In ADOA patients, no significant differences were found between full-field and the most peripheral responses; the only exception is in the primary visual cortex (as

measured by OZ), where patients present higher responses when high spatial frequency stimuli are presented in full-field, monocularly. These findings are consistent with the relative preservation and anterior propagation of the most peripheral responses, in particular in which concerns M-biased stimuli.

		Full-Field vs Peripheral Stimulation		ALH	ARH	PLH	PRH	OZ
Controls	Monoc	P	VB_HF	ns	ns	p=0.012	p=0.017	p=0.005
		M	VB_LF_fl	p=0.039	ns	ns	p=0.026	*p=0.058*
	Binoc	P	VB_HF	*(p=0.066)*	p=0.027	p=0.013	p=0.009	p=0.002
		M	VB_LF_fl	ns	ns	ns	ns	*p=0.057*
Patients	Monoc	P	VB_HF	*(p=0.066)*	ns	ns	ns	p=0.019
		M	VB_LF_fl	ns	ns	ns	ns	ns
	Binoc	P	VB_HF	ns	ns	ns	ns	ns
		M	VB_LF_fl	ns	ns	ns	ns	ns

Table 21 – Comparison between full-field versus peripheral responses (P or M biased, see below) in controls and patients, evoked by different types of stimulation presented mono- and binocularly. In controls full-field responses are clearly higher than peripheral responses as compared with ADOA patients, where no significant differences are in general seen.
P: parvocellular biased stimulus; M: magnocellular biased stimulus; VB: vertical bars;
HF: high spatial frequency; LF: low spatial frequency; fl: flicker.

Mono versus Binocular Responses

Within-group comparisons between monocular versus binocular responses can be visualized in Fig. 44.

In posterior clusters, significant differences were found in patients (p=0.01) when applying high spatial frequency stimuli (peripheral gratings), showing specific binocular summation under these conditions.

(A) Controls

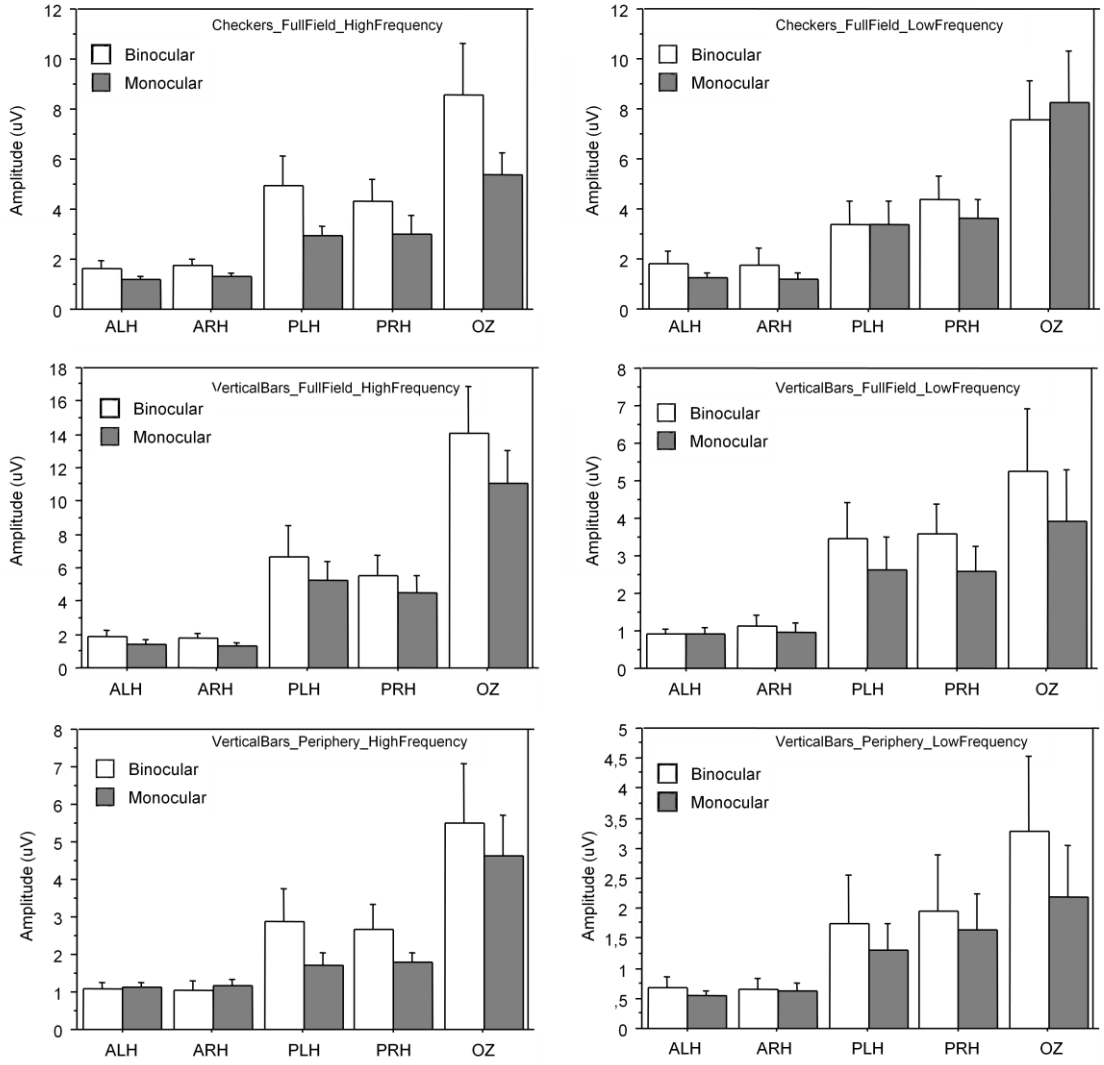
Checkers_FullField_HighFrequency
Checkers_FullField_LowFrequency
VerticalBars_FullField_HighFrequency
VerticalBars_FullField_LowFrequency
VerticalBars_Periphery_HighFrequency
VerticalBars_Periphery_LowFrequency
Binocular
Monocular
Amplitude (uV)
ALH
ARH
PLH
PRH
OZ

(B) Patients

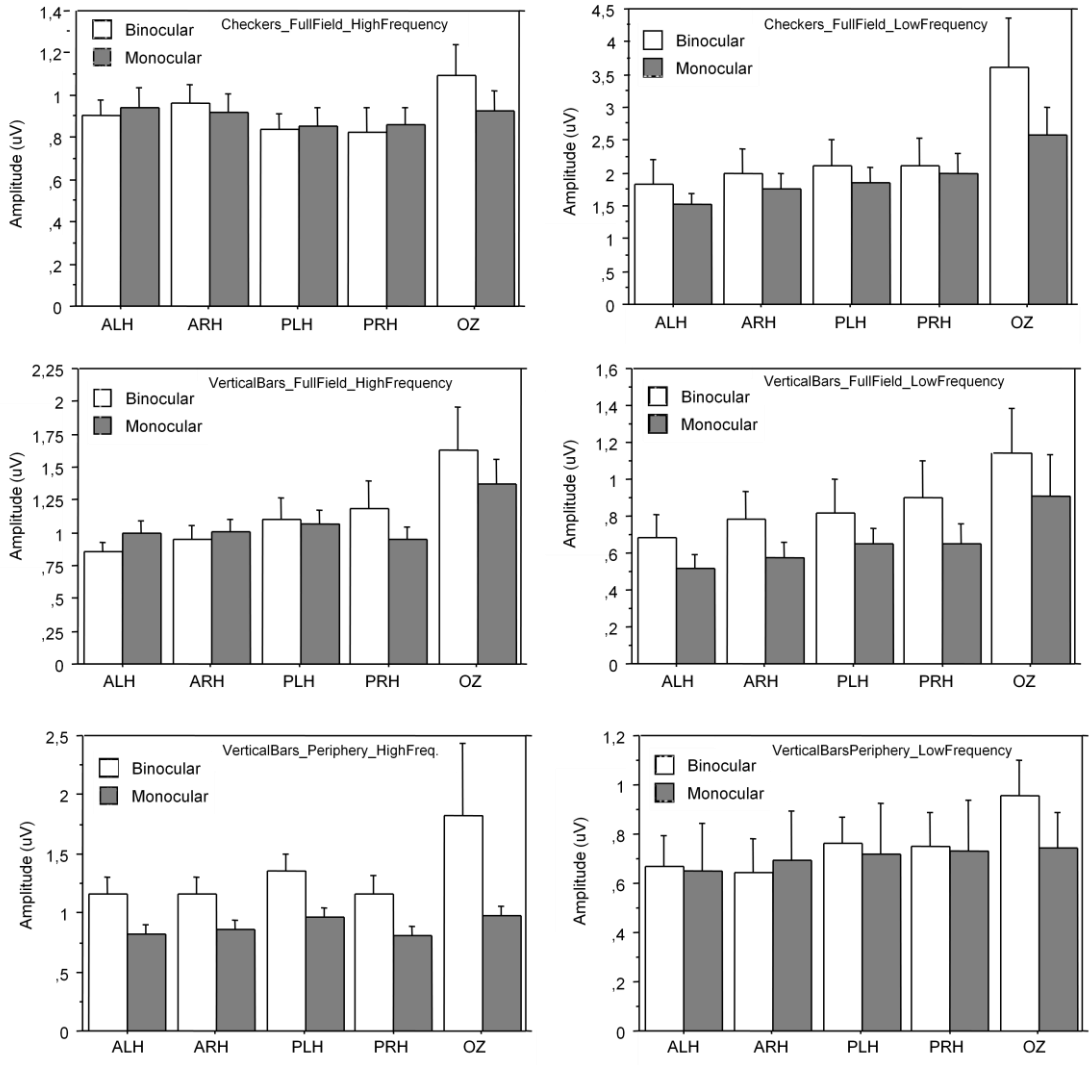

Fig. 44 – Within group comparison of mono- and binocular responses (mean ± SEM) to different types of stimuli, presented in full-field or in the paracentral visual field,
in controls (A) and patients (B).

Comparing occipital responses in a single occipital electrode – OZ as an index of striate cortex activation (between and within groups)

Within and between group comparisons were specifically examined at the OZ location which sits close to striate cortex locations (see last column of Table 19 and Figure 45).

(A) CHECKERBOARD (Full-Field) – High vs Low Spatial Frequency

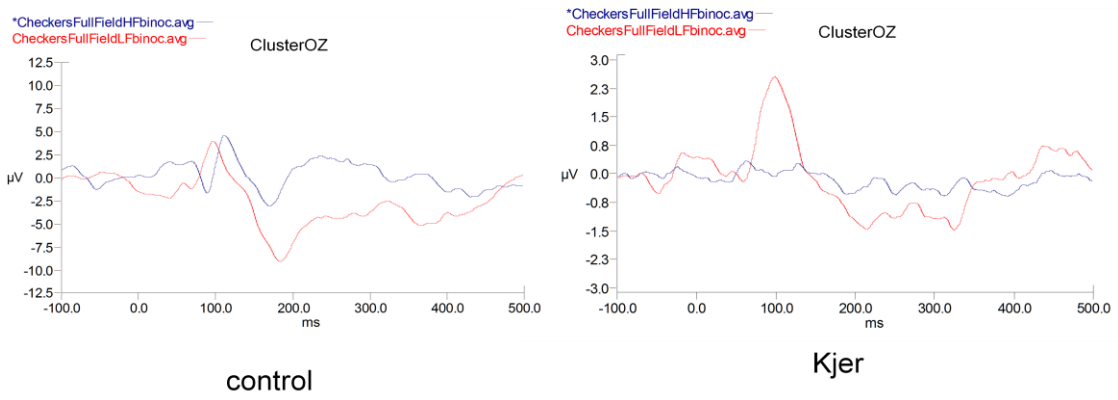

(B) VERTICAL GRATINGS (High Spatial Frequency) – Full-Field vs Periphery

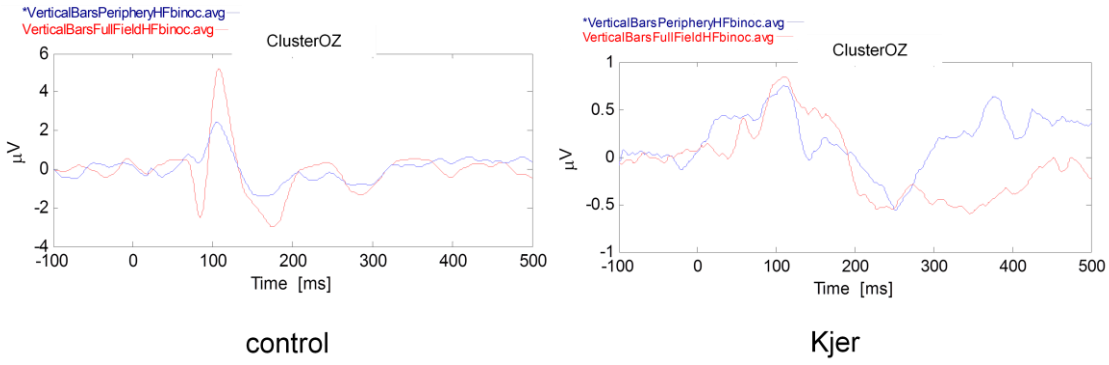

(C) FLICKERING VERTICAL GRATINGS (Low Spatial Frequency) – Full-Field vs Periphery

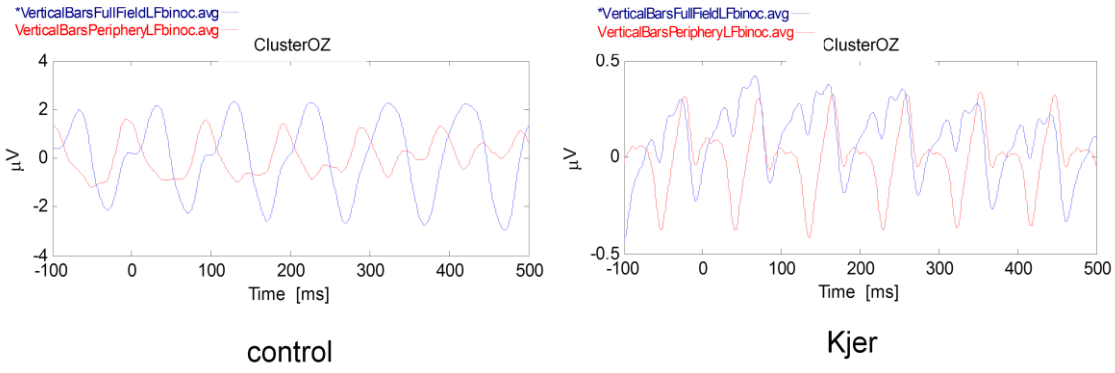

Fig. 45 – Summary of striate responses. Group comparison between average binocular OZ responses obtained with different type of stimulus: (A) High Frequency (static) versus Low Frequency (flicker) checkerboard presented in full-field; (B) Full-field versus Peripheral High Spatial Frequency Gratings / Static stimulation; (C) Full-field versus Peripheral Low Spatial Frequency Gratings / Flicker stimulation. Note the differences on scale and the relative preservation of peripheral responses in the patient group.

With checkerboards (presented in full-field), the magno- versus parvocellular biased responses (component at approximately 100 ms) are of similar amplitude in controls, while in patients magnocellular biased responses clearly dominates the parvocellular ones (which are absent).

High frequency vertical bars, presented statically (parvocellular-biased), induced higher amplitude response when presented in full-field configuration compared when presented most peripherally for both study groups, although the amplitudes are stronger in controls (see also Table 20).

Low frequency bars, presented with flicker (10 Hz), induces responses of larger amplitude, as expected, when presented in full-field versus most peripheral configurations in controls (suggesting that in this group the contribution is both from centre and periphery), when in patients the most peripheral responses similar amplitude of the full-field ones (suggesting a main peripheral contribution). However, responses in controls are still stronger than in patients (see also Table 21).

5. DISCUSSION

In this study, we have found evidence that the cortex is not a simple mirror of impaired retinocortical transmission, by showing differential reorganization of response patterns within physiological spatiotemporal channels in paracentral and central vision.

Our previous work (Reis et al., 2012), also discussed in this thesis (Part I of this Chapter), concerning exactly the same study population, reported a significant decrease of the P100-wave amplitude of PVEP in patients for both 60' and 15' stimuli, with implicit time concomitantly increased. In mfVEP (local multifocal visual cortical evoked potentials) significant amplitude differences were found mainly in central rings (1 and 2), with concomitant local increased implicit times only for the most central rings **(**1, 2 and 3). These results are consistent with those obtained by Pattern VEP, since it assesses central vision.

The current study has focused on spatiotemporal channels that are respectively more biased either to magno- or parvocellular activation, and found evidence for impaired parvo-biased responses both in central and more peripheral representations. Impaired magno-biased responses were still robust in the periphery and were absent in central vision representations. Indeed, the most peripheral responses were similar to and therefore accounted for the responses to full-field stimulation. Moreover, these magno-biased responses showed less decay in anterior cortical locations, suggesting distinct mechanisms of cortical propagation across different pathways in patients. In sum,

although the results confirm a central vision deficit stemming from the retina they also show specific deficits most peripherally. These patterns are clearly modulated by an independent cortical contribution.

High density recordings suggest an intriguing absence of decay of cortical responses in anterior locations in patients, raising the question whether this is a compensatory mechanism or it simply reflects abnormal pathophysiology. Accordingly, in the most anterior regions patients have relatively high responses to low frequency stimuli associated with temporal frequency (directly related with the magnocellular function).

Differences in full-field versus most peripheral responses in both groups could potentially be clinically used in the future. Higher amplitudes obtained with full-field stimuli (including thus central stimulation) were only found in controls, suggesting that the paracentral contribution conveyed most of the response in patients This may suggest the use, in the future, of a measure quantifying peripheral contributions for different spatiotemporal channels in patients.

Interestingly, patients showed evidence for binocular summation of peripheral high spatial frequency responses, suggesting a truly compensatory mechanism.

We conclude that cortical responses across different spatiotemporal channels in ADOA reflect both impaired visual responses (with larger preservation of magno-biased responses in the periphery), functional reorganization of propagation of visual information, and compensatory binocular summation for high frequency peripheral stimulation.

CHAPTER VI

VISUAL IMPAIRMENT IN
LEBER HEREDITARY OPTIC NEUROPATHY
CARRIERS OF THE SAME PEDIGREE

CHAPTER VI

EVIDENCE FOR EARLY CHANGES IN OUTER RETINAL CIRCUITS IN ASYMPTOMATIC CARRIERS OF LEBER'S HEREDITARY OPTIC NEUROPATHY OF THE SAME PEDIGREE

1. ABSTRACT

It is know that nonsymptomatic Leber's hereditary optic neuropathy (LHON) carriers can convert to affected status and that progressive changes lead to a crescendo of severe impairments that characterize this conversion. It is thus important to test the hypothesis that substantial functional and structural impact occurs at a preclinical stage. The goal of this work was to characterize the visual phenotype of asymptomatic LHON associated to mtDNA 11778G>A mutation in carriers from the same pedigree.

Psychophysical chromatic/achromatic contrast sensitivity (CS) methods (CCT: Cambridge Colour Test and CSF: Metropsis Contrast Sensitivity Function Test) were applied in a sample of 17 subjects of two generations of the same family (mean age ± SD = 27.94 ± 12.97 years; mean visual acuity ± SD = 1.25 ± 0.11) and an age-matched control group (n=18; mean age ± SD = 31.28 ± 13.48 years; mean visual acuity ± SD = 1.09 ± 0.17). Electrophysiological assessment included Pattern and Multifocal ERG, as well as Pattern, Multifocal and High Density VEP. Macular thickness / paripapillary and macular RNFL measurements were obtained using Stratus-OCT3. Statistical analysis was performed using ANOVA at a significance level of $p<0.05$.

We found evidence for early damage of all colour vision axes (Protan: p=0.0002; Deutan: p<0.0001; Tritan: p=0.01), implying concomitant damage of parvo- and koniocellular pathways already in the carrier state. No significant damage occurred in achromatic CS across all achromatic spatial frequency channels studied, suggesting a relatively preservation of achromatic pathways. PERG measures were normal, while mfERG showed a decrease in central ring amplitudes (P1-wave: p=0.006; N1-wave: p=0.02), suggesting pre-ganglion preclinical level damage. Retinal thickness was decreased in the inner rings (R1: p=0.012; R2: p=0.04), irrespective of changes in macular RNFL thickness. Cortical responses (pattern VEP) were delayed (60': p=0.002 / 15': p=0.02) with normal amplitudes. Topographic/local multifocal VEP showed no signs of functional damage.

Our results suggest that significant early loss of colour vision occurs in LHON, differently from achromatic contrast sensitivity, and that damage to outer retinal

circuits, in the presence of preserved ganglion cell (GC) and cortical response amplitudes, also contribute to preclinical impairment in LHON carriers. These pathophysiological findings are relevant to clinical practice because they may influence preclinical management.

2. INTRODUCTION

Leber Hereditary Optic Neuropathy (LHON) is a maternally inherited neuropathy associated with mitochondrial DNA (mtDNA) dysfunction underlying related mutation (Wallace et al, 1988).

Three point mutations, located at mtDNA positions 11778 (69%), 3460 (13%) and 14484 (14%), ("primary" LHON mutations) cause at least 90% of cases of LHON worldwide (Newman, 2005; Man et al., 2002).

Mutations at G11778A and G3460A appear to be associated with a similar visual acuity outcome (1/60 to 3/60), while mutation at nucleotide position (np) 11778 is particularly severe in one-third of female patients (Riordan-Eva and Harding, 1995) even with a later age of onset (Harding et al., 1995). Patients with the T14484C mutations are considerably better off than those with the other two types of primary mutations, having some recovery of vision in 50% of the cases, with a better visual outcome if the onset of visual loss is before the age of 20 years, reaching 6/24 or better in 71% of cases (Johns et al., 1993).

Besides these three mutations (found almost exclusively in multiple LHON families in regions corresponding to evolutionarily conserved amino acids) there are other rarer primary mutations, such as T14596A, C14498T, G13730A, G14459A, C14482G and A14495G (Votruba, 2004).

Mitochondrial respiratory chain deficits may lead to axoplasmic stasis and swelling, with intramitochondrial calcification (Kerrison et al., 1995), which can be reversible if apoptosis and ensuing GC loss is not yet activated. The first symptoms are unilateral painless acute central vision loss and colour vision desaturation. The second eye is usually sequentially affected weeks to months later (Newman, 2005), although it can be rarely affected simultaneously (Harding et al, 1995). This central visual loss, related with the preferential and earlier involvement of the vulnerable small diameter nerve fibres (Sadun et al., 2000), occurs most frequently between the ages of 15 and 35 years (although younger or older individuals have been reported) with a range of 2-80 years, stabilizing after months of visual function deterioration down to acuities worse than 20/200 (Newman, 2005). This is consistent with the observed visual field defect, initially characterized by a central scotoma that rapidly becomes centro-caecal. OCT

(RNFL thickness) usually confirms the early involvement of the papillomacular bundle (Barboni et al. 2010), as well as the predominant parvocellular (red-green) impairment in colour vision testing that is often observed even in asymptomatic carriers (Ventura et al., 2007).

Fundoscopic findings are characteristic during the acute stage, consisting of a triad of signs (Smith et al., 1973): circumpapillary telangiectatic microangiopathy, swelling of the nerve fibre layer around the optic disc (pseudoedema) with microvascular anomalies, and absence of leakage from the papillary region on fluorescein angiography (differently from truly edematous discs). Nevertheless, these signs can also be observed in presymptomatic eyes or in asymptomatic maternal relatives' eyes (Nikoskelainen et al., 1996). Although this triad is believed to be pathognomonic for LHON, its absence in the acute stage or in presymptomatic eyes does not exclude this diagnosis. In this case, pattern-reversal visual evoked responses can play an important role (Livingstone et al., 1980).

As the disease progresses, the telangiectatic vessels disappear and the pseudoedema of the disc resolves, and optic atrophy develops with loss of the nerve fibre layer (Newman, 2005; Votruba et al, 2003). In most patients with LHON visual dysfunction remains very poor and permanent, although some individuals can recover up to an excellent performance level, which is possibly related with the genetic background.

In most of the patients with LHON visual dysfunction is the only manifestation of the disease. However, some pedigrees have members with associated cardiac conduction or minor neurological deficits, although more severe neurological abnormalities can be found in multiple maternal members of some pedigrees (Newman, 2005). An intriguing association between LHON and Multiple Sclerosis has also been proposed. Accordingly, LHON mutations have been suggested to cause causing a worse prognosis of optic neuritis in patients with MS (Bhatti and Newman, 1999).

Asymptomatic LHON carriers may convert to the affected status at any point of time. Progressive changes usually lead to a crescendo of severe impairments that characterize this conversion (Sadun et al., 2006). It is thus relevant to test the hypothesis that a preclinical stage neural loss is alrealy occurring.

The goal of this work was to characterize the early visual phenotype of asymptomatic LHON carriers associated to the mtDNA 11778G>A mutation in the same pedigree, with physchophysical and electrophysiological methods (using parvo- and magnocellular biased-stimuli) testing retinal and cortical function.

3. METHODS

3.1. PATIENT SELECTION, DEMOGRAPHIC CHARACTERISTICS AND OPHTHALMOLOGICAL EXAMINATION

The study followed the tenets of the Declaration of Helsinki and was approved by our Ethics Committee. Prior to the inclusion in the study, informed consent was obtained from all subjects after a full given explanation.

We have tested a population of 17 asymptomatic Leber's hereditary optic neuropathy (LHON) associated to mtDNA 11778G>A mutation carriers from two generations of the same pedigree (mean age ± SD = 27.94 ± 12.97 years; mean visual acuity ± SD= 1.25 ± 0.11, decimal scale) which was compared with an age-matched control group (n=18; mean age ± SD = 31.28 ± 13.48 years; mean visual acuity ± SD = 1.09 ± 0.17).

In this cohort, only a girl with severe neurological deficits, that was previously reported (Grazina et al., 2007), was excluded because she is no longer a carrier (added to the inability to perform the tasks).

Participants were submitted to a complete ophthalmological examination, including the BCVA, slit lamp examination of anterior chamber, IOP measurement (Goldmann applanation tonometer), angle and fundus examination (non-contact lens) and the assessment of subjective visual complaints. Exclusion criteria included pseudophakic and aphakic eyes, media opacities, retinal and clinical neuro-ophtahlomological diseases, amblyopia and high ammetropies (sphere > ± 4D; cylinder > ± 2D).

3.2. MtDNA ANALYSIS

Family mtDNA studies were conducted in the blood of all members of the family, in order to confirm the presence of the 11778G4A mutation.

3.3. FUNCTIONAL ASSESSMENT

We have applied the following psychophysical and electrophysiological methods in all patients and controls (for details, see Chapter III- 2.2):

- Computerized chromatic contrast sensitivity – Cambridge Colour Test;

- Computerized achromatic contrast sensitivity – Metropsis (Cambridge Research Systems);
- Automated static perimetry (central 30º);
- Pattern ERG;
- Multifocal ERG;
- Pattern VEP;
- Multifocal VEP.

Besides these methods, High Density Visual Evoked Potentials were also performed (for details, see Part II of Chapter V – 3.2).

3.4. IMAGING

Structural characteristics of the macula and the optic disc and were assessed using an optical coherence tomography device (Stratus OCT3). This was also used to measure central global retinal thickness and the retinal nerve fibre layer (RNFL) thickness (centrally and peripapillary) which enabled the correlation with multifocal ERG and PERG responses (more related to preganglionic and ganglion/optic nerve neural substrates, respectively).

For details of OCT procedures, see Chapter III – 2.3.2.

3.5. STATISTICAL ANALYSIS

To prevent issues related to violations of independence, in our statistical analysis we have used the mean of both eyes values of each participant, since all variables were statistically correlated (Pearson correlation coefficients).

Given the normal distribution of the data, ANOVA parametric analyses were performed, at a significance level of $p \leq 0.05$, using StatView (SAS, Cary, NC).

4. RESULTS

Patient Demographic Characteristics and Ophthalmological Examination

The carriers group presents mean age ± SD = 27.94 ± 12.97 years and mean visual acuity ± SD = 1.25 ± 0.11 (decimal scale).

Ophthalmoscopy revealed no fundus changes in all members of the pedigree.

MtDNA Analysis

MtDNA studies conducted in the blood of all members of this pedigree confirmed the presence of the 11778G4A mutation.

Psychophysics

Evidence for damage of both Parvocellular and Koniocellular Pathways

Chromatic contrast sensitivity measures were significantly impaired in patients across the three chromatic axes (Protan: p=0.0002; Deutan: p<0.0001; Tritan: p= 0.0102 – Fisher's PLSD) – see Fig. 46.

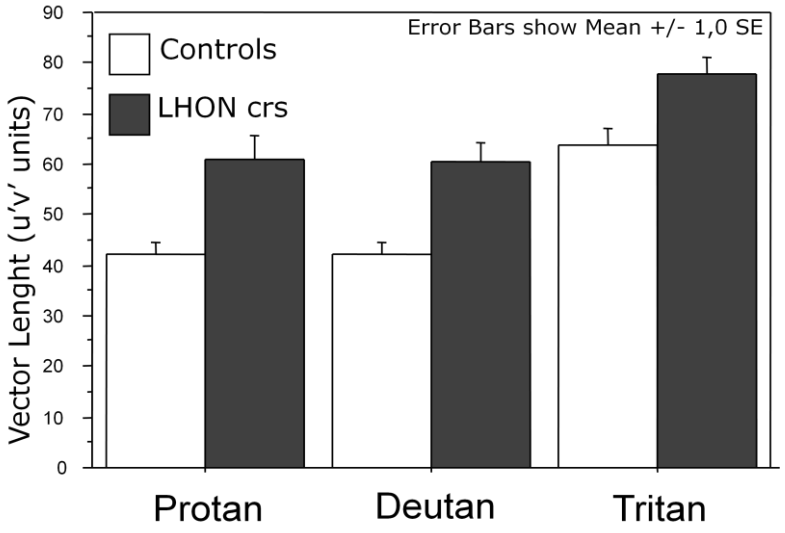

Fig. 46 – Chromatic Contrast Thresholds in patients and in controls.
Impairment is observed across the three chromatic axes.

Achromatic Contrast Sensitivity is preserved in all measured spatial frequency channels

No significant differences between LOHN carriers and controls were found, for all studied spatial frequencies.

Assessment of visual function across the visual field with Automated Static Perimetry

Although automated static perimetry (ASP) does not assess specific visual pathways it provides a valuable gold standard for visual function. According to our normative database, we found 82% of abnormal visual fields in at least one parameter, with a constant pattern of a paracentral defect.

Neurophysiology

Cortical Pattern Visual Evoked Potentials: normal response amplitudes but delayed retinocortical processing

While amplitude values of cortical responses were preserved, retinocortical processing in carriers was abnormal, as suggested by asignificant increase on implicit time of the P-100 wave for both 60' and 15' stimuli (60'stimuli: p=0.002; 15': p=0.02) – see Fig. 47 for details.

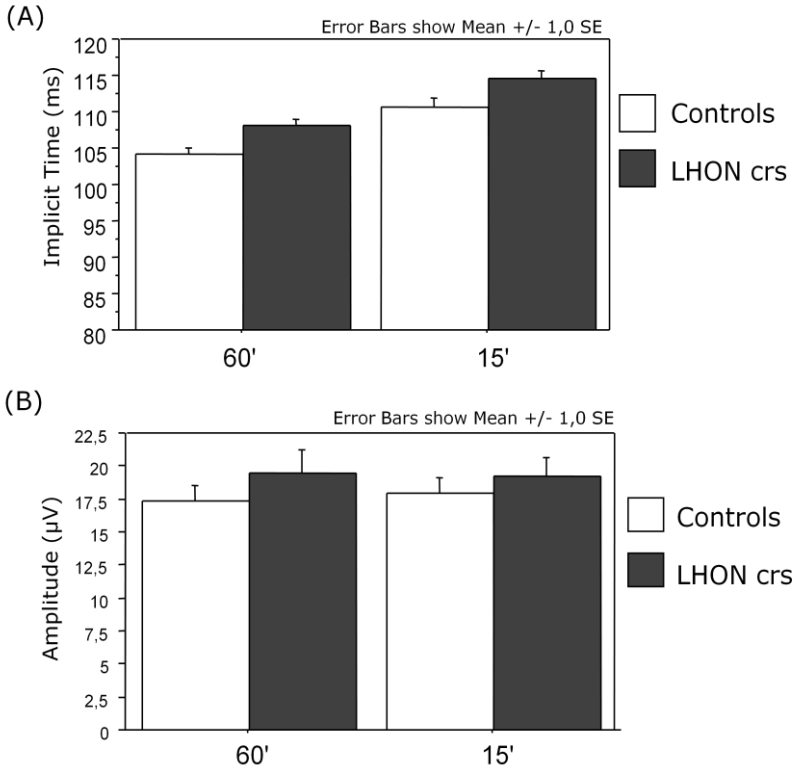

Fig. 47 – Cortical VEP results - comparison between groups. Patients present timing delayed (A) with normal amplitudes (B), for both spatial frequencies.

Multifocal Visual Evoked Potentials shows locally preserved and no delayed responses

Multifocal VEP recording allowed us to separate the contribution of central versus paracentral cortical responses.

Unexpectedly, we found a significant decrease on implicit time of central rings of carriers (ring 1: p=0.038; ring 2: p=0.019), as well as on the most peripheral one (ring 6: p=0.036). In the other rings, this tendency can also be observed, but did not reach significance (for details see Fig. 48-A). It is noteworthy to point out that amplitude of the central ring of mfVEP correlates significantly with the amplitude of PVEP, for both spatial stimuli (60´/15: r=0.58/p=0.013).

Amplitude values were normal or even higher in carriers when comparing with controls, reaching statistical significance in ring 2 – p=0.029 (Fig. 48-B).

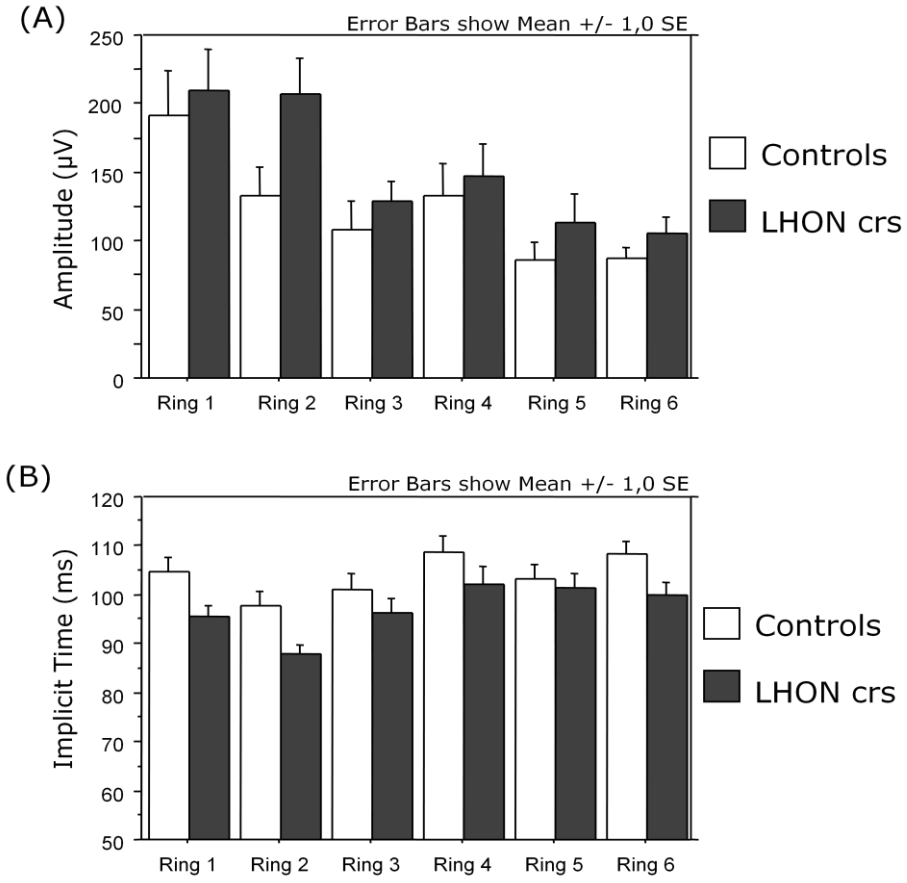

Fig. 48 – Amplitude (a) and Implicit Times (b) of P100-waves of cortical mfVEP, across eccentricity rings, in patients and in controls.

High Density Visual Evoked Potentials shows no clear pathological processing across posterior-anterior cortical pathways

Amplitude and implicit times of mono- and binocular responses to different type of stimuli are not statistically diferent from the controls, with two exceptions: increase of implicit times of the monocular OZ (located above striate cortex) response evoked by low frequency full-field gratings (p=0.026) and the binocular response of the posterior right electrode cluster, evoked by full-field high frequency checkerboards (p=0.009).

Pattern Electroretinogram shows robust preserved responses in the carrier stage

LHON carriers showed well preserved amplitudes of both P-50 and N-95 waves, with mean values normal or even higher than controls (and effect that was not statistically significant at the group level). N-95/P-50 ratio was also normal.

Multifocal Electroretinogram shows evidence for preganglion functional impairment in central vision

MfERG (testing preganglion pathways – outer retinal dominant sources) showed a significant decrease in amplitude of P1-wave (mainly bipolar cell component) of the central ring (p=0.006), an effect that was marginally lost in ring 2 (p=0.07). A reduced N1-wave (mainly cone component) in ring 2 (p=0.02), marginally lost in rings 3 and 4 (p=0.07 and 0.08, respectively), suggests a surprising pattern of pre-CG damage – see Fig. 49. No significant differences were found concerning implit times of both components.

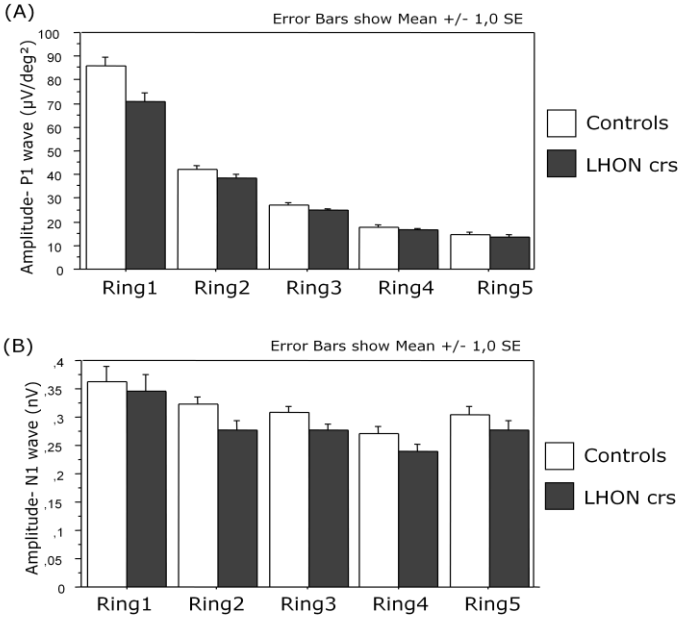

Fig. 49 – Amplitudes of P1 (A) and N1 (B) components of mfERG, across concentric rings. A central impairment is evident.

Optical Coherence Tomography provides evidence for central damage not dependent on the nerve fibre layer

Analysis by the rings centred to the fovea showed decreased values in central (1 mm) and pericentral (1-3 mm) rings (p=0.012 and p=0.043, respectively), with no significant difference in the peripheral (3-6 mm) ring – Fig. 50A.

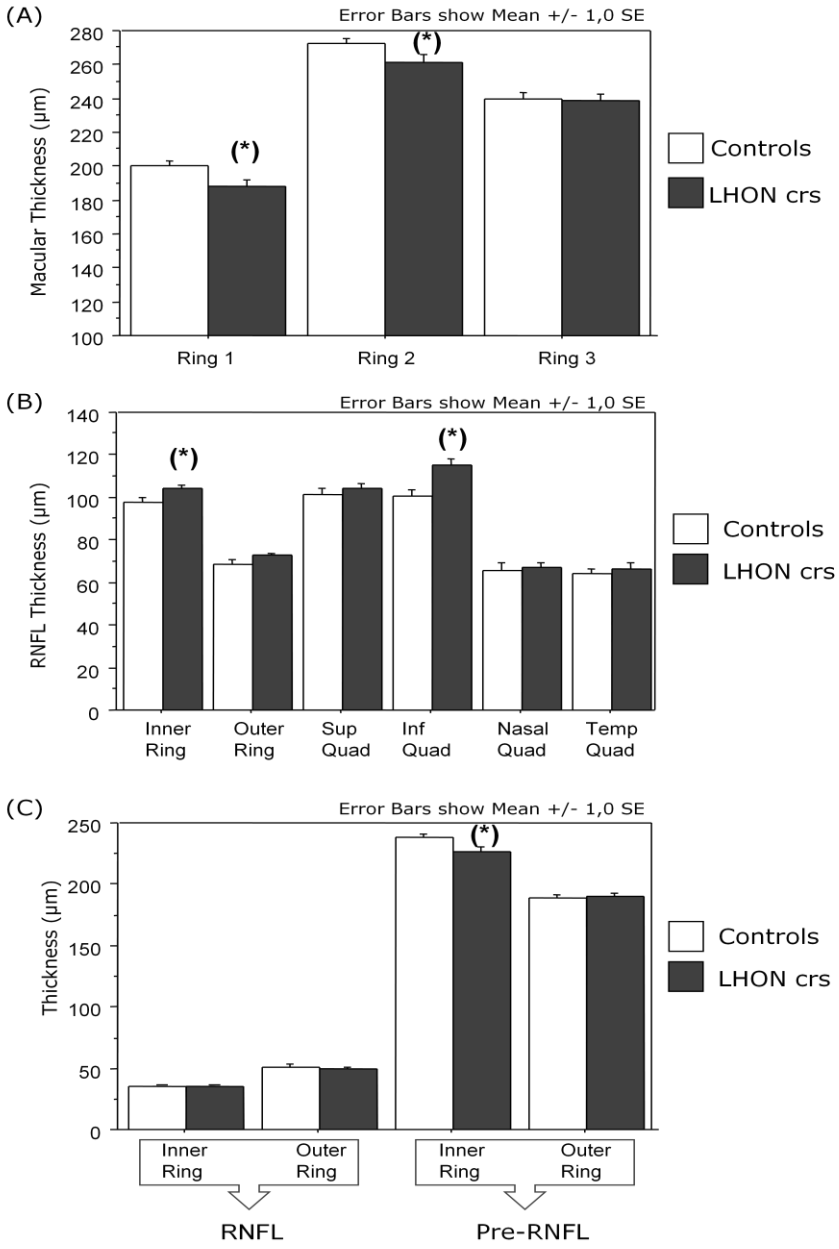

Fig. 50 – OCT measurements, obtained at different conditions:
(A) Retinal thickness across rings within the 6mm of central retina; (B) Peripapillary retinal nerve fibre layer thickness (RNFL) – by rings and by quadrants; (C) RNFL centred to the fovea and pre-ganglion macular thickness (global thickness subtracted from RNFL).
(*) – significant differences.

In contrast, RNFL measures showed a significant increase in the inner ring (ring 2) (p=0.04) and in the inferior peripapillary quadrant (p=0.0007) – Fig. 50B, which is not observed in the macular RNFL (Fig. 50C). Note that the most central measure (ring 1) cannot be used given the sparsity of ganglion cells fibres in the central part of the retina.

When subtracting macular RNFL from the total retinal thickness, we found a decrease in ring 2 thickness (p=0.028 – Fig. 50C), corroborating the deacreased total retinal tickness mentioned above (Fig. 50A), not dependent on the ganglion nerve fibre layer contributions.

Structure Function Correlations in LHON Carriers

Impairment along the Protan axis length showed a significant negative correlation with the amplitude of rings 2 and 3 of mfERG P1-wave (R2: r=-0.54; p=0.036 / R3: r=-0.55; p=0.033) and of ring 3 of N1-wave (r=-0.53; p=0.041). Deutan axis length correlates with the amplitude of P1-wave (R2: r=-0.54; p=0.035), being marginally lost in ring 3 (r=-0.47; p=0.07).

In general, chromatic contrast sensitivity values did not correlate with the different RNFL variables.

No significant patterns of correlation were also found between measures of chromatic contrast sensitivity and the amplitudes or implicit times of Pattern and mfVEP.

As expected from the normal visual acuity in the carrier group, no correlation was observed with any of the other parameters.

In general, amplitudes of mfERG responses were not correlated with mfVEP or PVEP. However, the implicit time of PVEP (when obtained with the higher spatial frequency stimulus) correlates strongly with the amplitude of P1-wave of mfERG, specially in pericentral rings (R2: r=-0.52; p=0.047; R3: r=-0.69; p=0.003; R4: r=-0.74; p=0.0009; R5: r=-0.71; p=0.002).

Concerning multifocal responses, in sum, no correlations were found between local retinal and local cortical signals.

The implicit time of PVEP (P-100 wave), as measured with the 15’ stimulus, significantly correlates with the implicit time of PERG (P-50 wave) – r=0.58; p=0.013. Implicit time of PVEP (when obtained with the lower fundamental spatial frequency

stimulus) correlates significantly with the macular RNFL thickness (ring 2) – r=0.53; p=0.026 (one should take into account that axonal swelling may be present in LHON).

Representative Examples

Figure 51 shows two representative examples of our phenotypic analysis of LHON carriers.

Some psychophysical deficits can be observed particularly in the field maps.

Responses with robust amplitudes can be observed in PERG and VEP measurements.

MfERG shows slight changes, while mfVEP are normal.

Retinal thickness is reduced in central ring.

#5 – Right Eye

A

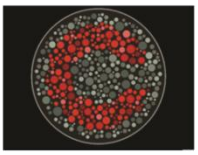

Protan: 36 Deutan: 43 Tritan: 83

B

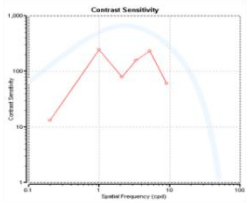

C

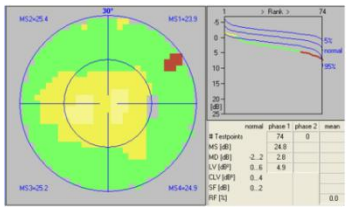

D

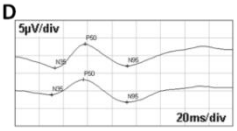

E

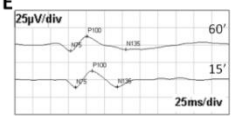

F

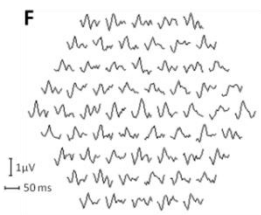

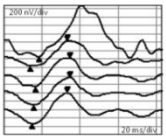

	Amp. P1 [nV/deg2]	Amp. P1 [µV]	Amp. N1 [µV]	PeT. P1 [ms]	PeT. N1 [ms]
1	81.4	1.240	0.235	40.4	18.7
2	28.8	0.624	0.184	33.5	13.8
3	22	0.692	0.250	34.5	16.8
4	15.6	0.681	0.290	34.5	15.8
5	12.9	0.751	0.278	33.5	14.8

G

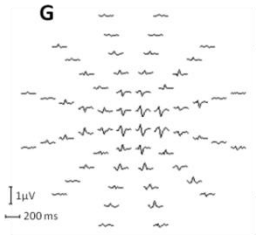

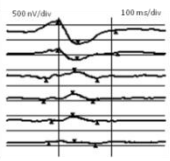

	Amp. P1 [µV]
1	0.79
2	0.37
3	0.21
4	0.17
5	0.12
6	0.01

H

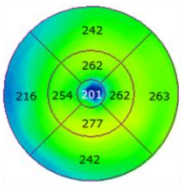

#5 – Left Eye

A

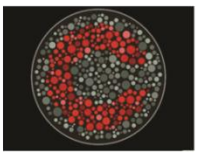

Protan: 45 Deutan: 61 Tritan: 67

B

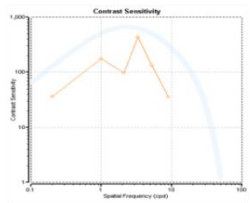

C

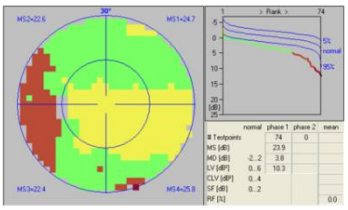

D

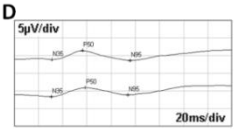

E

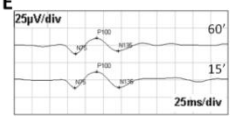

F

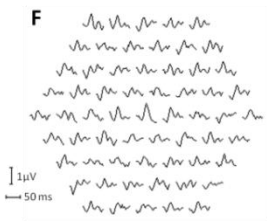

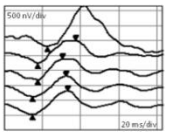

	Amp. P1 [nV/deg2]	Amp. P1 [µV]	Amp. N1 [µV]	PeT. P1 [ms]	PeT. N1 [ms]
1	91	1.39	0.32	41.4	22.7
2	35.8	0.77	0.31	37.5	17.7
3	22.9	0.72	0.28	30.6	17.7
4	16.2	0.71	0.29	32.5	14.8
5	14	0.82	0.26	33.5	14.8

G

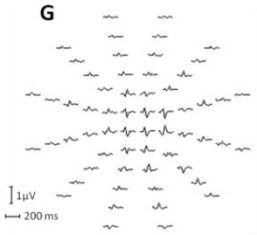

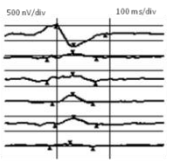

	Amp. P1 [µV]
1	0.723
2	0.128
3	0.165
4	0.201
5	0.160
6	0.036

H

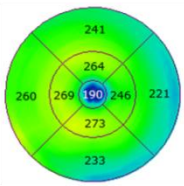

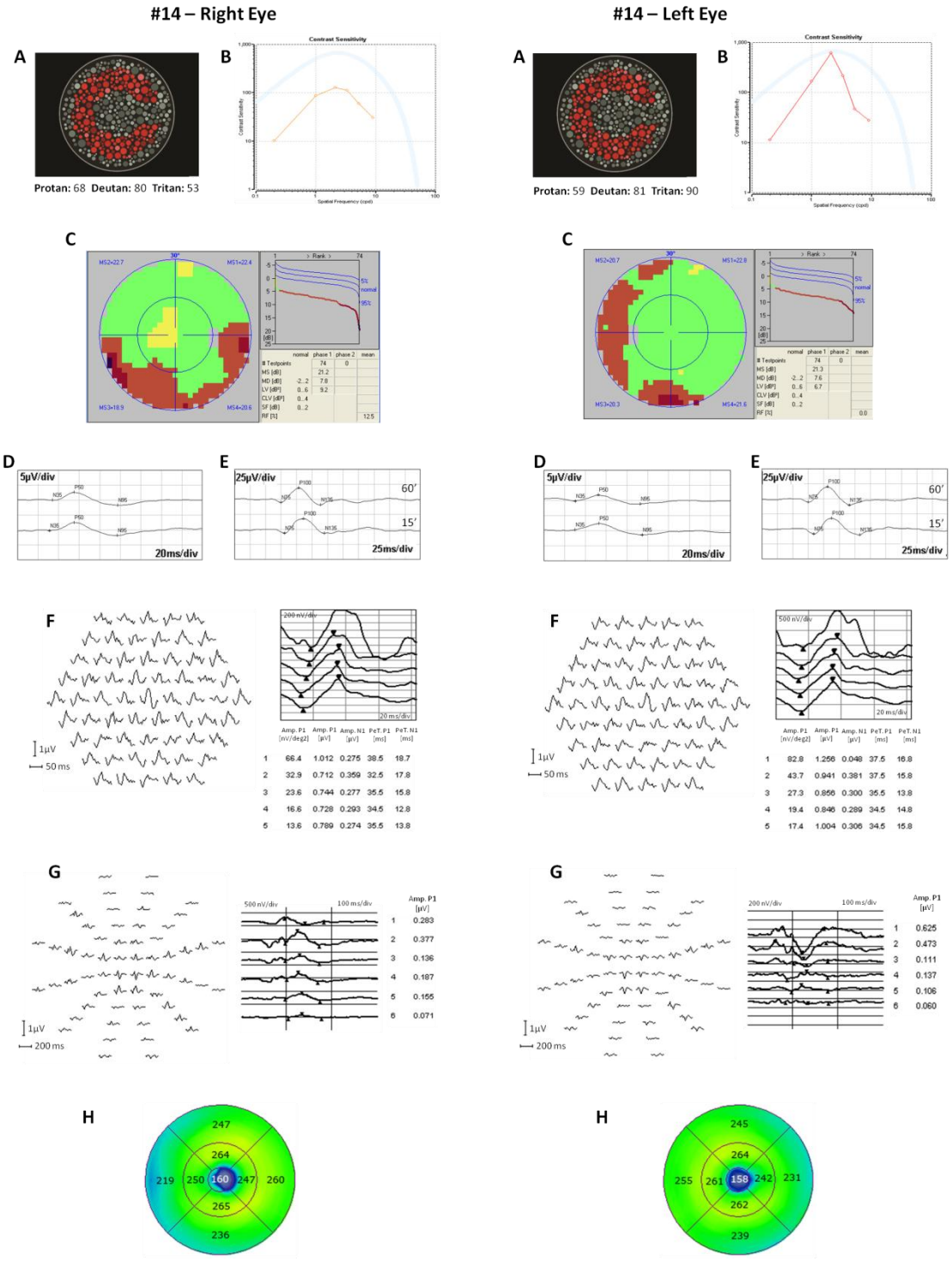

Fig. 51 – Representative examples of psychological performance and neurophysiological responses in LHON carriers – patients #5 and #14 (right and left eyes).
Strong responses obtained in PERG and VEP can be seen, while MfERG presents amplitude changes. MfVEP have normal amplitudes. Retinal thickness is reduced in central ring.
(A) Cambridge Colour Test; (B) Contrast Sensitivity Function; (C) Automated Static Perimetry; (D) PERG; (E) PVEP; (F) MfERG; (G) MfVEP; (H) OCT – Macular thickness.

5. DISCUSSION

In this study, we found that asymptomatic LHON carriers showed clear indication of preganglion cell damage, as probed by multifocal ERG recordings, which showed changes in its components that are known to be related to outer retinal function. In other words, damage to GC layer afferents of the retina seem to be present at an early stage. A decrease in pre-RNFL macular thickness is also present at this stage, as documented by OCT.

Evidence for damage of outer retinal circuits has also been described in our previous work in autosomal dominant optic atrophy (also described in this thesis) although in this case participants were already at a clinical stage (Reis et al., 2012). In the current report, participants were studied at an asymptomatic carrier stage, whereby measures of GC and retinocortical pathways were relatively preserved. These observations do therefore raise the possibility that preganglion damage occurs independently and may not be retrograde, as also suggested by correlation analysis (which did not show retinocortical amplitude correlations, but only an impact on cortical global implicit times).

Thus, besides the classical concept of ganglion cell dysfunction (Newman, 2005; Votruba, 2004) and evidence about inner retinal contributions in clinically established LHON (Kurtenbach et al., 2004), we identified evidence for preclinical impairment using measures where outer layer contributions dominate.

Damage within Parvo and Koniocellular Pathways

Damage of both parvo- and koniocellular pathways, as demonstrated by chromatic contrast sensitivity testing, was found to be consistent with previous studies (Ventura et al., 2007; Sadun et al., 2006).

Although characteristic small fibre damage in LHON patients have been observed histologically (Sadun et al., 2000), our results substantiate the notion that this condition is not restricted to parvocellular pathway, even at a preclinical stage. Indeed, the reported histological “small fibre” bias is likely related to central fibres being smaller and not to predominant damage of the parvocellular (“small neuron”) pathway.

Preservation of Achromatic Pathways

Achromatic contrast sensitivity across multiple spatial frequency channels is preserved in LHON carriers. As the magnocellular system is an achromatic pathway,

and probably contributes significantly to performance in this task, we predict that it should be preserved.

Accordingly, a previous study (Sadun et al., 2006) reports normal temporal contrast sensitivity in these subjects. A substantial parvocellular contribution is likely present for the higher tested spatial frequencies, which were also found to be yield normal contrast sensitivity.

Evidence for early Structural Damage

Damage at the pre-RNFL layers was proven by OCT with decreased thickness values in central rings independently of measures of the nerve fibre layer.

In fact, when subtracting macular RNFL from the total retinal thickness, we found a decrease in ring 2 thickness (fibres are not measured in the center of ring 1). The decreased global macular retinal thickness values of rings 1 and 2 obtained by OCT, as well as the ring 2 of the pre-RNFL layer thickness, showed a significant topographic correlation with the implicit time of P1-wave of mfERG.

Physiological evidence for Damage at the Pre-Ganglion Level

Physiological evidence of preganglion damage in LHON carriers extend those reported in previous studies conducted in clinically established LHON patients (Kurtenbach et al., Salomão et al., 2004). They provide a qualitative step because they occur in a preclinical stage without physiological changes at the ganglion cell level as shown by preserved PERG. The lack of impact of direct GC loss was also manifested by evidence for normal cortical responses, which showed preserved amplitudes and relatively small changes in latency.

In conclusion, we found evidence for abnormal outer retinal physiology in asymptomatic LOHN carriers even when measures of ganglion cell and cortical function were preserved. This suggests that independent changes may occur at the retinal outer layers in the absence of overt ganglion cell damage.

Functional impairment of colour vision (parvo- and koniocellular pathways) was also dominant in preclinical LHON, unlike achromatic contrast sensitivity.

CHAPTER VII

RETINAL NEURONAL DYSFUNCTION IN TYPE 1 DIABETIC PATIENTS WITHOUT BREAKDOWN OF THE BLOOD-RETINAL BARRIER AND ABSENT VASCULOPATHY

CHAPTER VII

RETINAL NEURONAL DYSFUNCTION IN TYPE 1 DIABETIC PATIENTS WITHOUT BREAKDOWN OF THE BLOOD-RETINAL BARRIER AND ABSENT VASCULOPATHY

1. ABSTRACT

The pre-retinopathy stage is the first one in the course of diabetic retinopathy (DR) which is characterized by no visible lesions in ocular fundoscopic examination but with some subclinical changes on blood-retinal barrier (BRB). However, it is possible that independent neural damage may also occur in this stage. The goal of this work was to characterize neurovisual function in type 1 diabetic patients, from the psychophysical and neurophysiological point of view, prior to breakdown of the BRB or onset of vasculopathy as compared with patients with early DR.

Visual function was assessed by Standard and HRA Multifocal Electroretinography (RetiScan – Roland Consult and Heidelberg Engineering), Colour Vision (parvocellular/koniocellular testing, CCT - Cambridge Research Systems) and Frequency-Doubling Perimetry (magnocellular testing, FDT - Zeiss) in a sample of 42 patients (age = 26.6 ± 5.3 years) with preserved visual acuity (VA), divided into 2 groups: with no DR (n=26; VA=1.088 ± 0.128) and with mild nonproliferative DR (n=16; VA=1.093 ± 0.137). These data were compared with those obtained in age-matched controls. Fundus photography and Fluorescein Angiography (TRC 50 IA - Topcon) were performed in order to determine the absence or presence of initial vascular lesions, and Vitreous Fluorometry (Fluorotron Master, Palo Alto, Ca) to quantify the BRB permeability. Investigation of changes in retinal thickness was done with Retinal Thickness Analyzer (RTA II, Talia, Israel). These parameters were correlated with the time duration of disease and metabolic control indicator (HbA1c). Non-parametric statistical analysis (Mann-Whitney testing) was performed at a significance cut-off level of $p<0.05$.

MfERG yielded a significant decrease in amplitude in all eccentricity rings in both patients groups, when compared with control subjects ($p<0.0001$). Interestingly, implicit time showed a paradoxical pattern between patient groups with a significant decrease in rings 2-4 ($0.002<p<0.02$) in the absence of clinical DR. Impaired contrast sensitivity along protan, deutan and tritan chromatic axes ($0.0001<p< 0.02$) was also observed in patients, except for the Deutan axis in the group without DR. FDT

quadrantic thresholds were also different between controls and both type of patients ($0.0009<p<0.002$), but the central location showed no difference between the controls and the patients with no DR. No correlation was found between the BRB permeability and the psychophysical and electrophysiological measurements, suggesting independent lesion mechanisms.

This work suggests that retinal neuronal changes can occur in Type 1 Diabetes, in magno-, konio- and parvocellular ganglion cell pathways even before breakdown of the blood-retinal barrier or onset of vasculopathy. Neurophysiological changes observed in electroretinography suggest that neuronal changes also occur at photoreceptor/bipolar layers.

2. INTRODUCTION

Diabetic Retinopathy (DR) is highly prevalent in the western world and is a major cause of vision loss. The prevalence of type 2 DR is much higher than type 1 DR (~9:1) due to the larger number of diabetic 2 patients in the human population (Eden and Klein, 2007). However, due to the earlier age of onset of type 1 diabetes (leading to longer time duration of disease in a lifetime), the prevalence of DR in type 1 diabetic patients is very high (~90% after 15 years of duration disease) as shown by long-term epidemiological studies (Klein et al., 2008).

There are several risk factors for the DR development, but the disease duration is probably the most consensual parameter (Cunha-Vaz, 2011; Williams et al., 2004; Henricsson et al., 2003; Likitmascul et al., 2006). Another important factor concerning likelihood of developing DR is the metabolic control. Correlation studies with these two variables show that patients with higher HbA1c percentages have higher risk for DR development when compared with patients with lower levels of HbA1c (Henricsson et al., 2033; Kullberg et al., 2002). Nevertheless, a fraction of patients presenting good metabolic control (about 10%) do develop DR and still another proportion of patients with poor metabolic control do not develop it (Zhang et al., 2001).

The role of vasculopathic mechanisms is important and cannot be underestimated. Accordingly, classification of changes in ocular fundus is relevant to the classification and determinant for the treatment of complications of this disease (Early Treatment Diabetic Retinopathy Study Research Group, 1987, 1991a, 1991b). The pre-retinopathy stage is the first one in the course of DR, which is characterized by no visible lesions in ocular fundoscopic examination but with some subclinical changes on blood-retinal barrier (BRB) (Cunha-Vaz, 2011; Lobo et al., 2000; Ludovico et al., 2003). However, it is possible that independent neural damage may also occur. This can

be studied by searching for evidence of changes on retinal neurons, even before the occurrence of retinal microvasculopathy. Biochemical, pharmacological and histological studies (Barber, 2003; Santiago et al., 2006a; Santiago et al., 2006b; Leal et al., 2005) do corroborate this concept. Some functional studies have further suggested visual impairment in diabetic patients without DR (Klein et al., 2008; Lopes de Faria et al., 2001; Di Leo et al., 1990). However, studies explicitly addressing neuronal dysfunction in pre-clinical stage tend to mix type 1 and type 2 patients (Lecleire-Collet et al., 2011; Fortune et al., 1999), or do not differentiate results obtained in patients without or minimal signs of DR (Krásný et al., 2006). The criterion for considering absence of DR lesions in type 1 diabetic patients also vary across studies – some of them are based on retinography analysis (van Dijk et al., 2011) and others based on angiography (Giusti, 2001).

In spite of these limitations, type 1 diabetic patients, namely without clinical evidence for DR, may show impaired objective responses to distinct spatial frequencies stimuli (Di Leo et al., 1990), sometimes concomitantly associated with different contrast levels (Lopes de Faria et al., 2001). A link with parvo- and magnocellular impairment is however missing. Besides the changes in contrast sensitivity (Lecleire-Collet et al., 2011; Krásný et al., 2006) there are also studies showing psychophysical and physiologic changes in these patients without DR, related to colour sensitivity (Giusti, 2001; Mulak et al., 2002) and multifocal ERG responses (Fortune et al., 1999). Structural studies changes and in particular retinal thickness are still quite controversial in type 1 diabetic patients in a pre-clinical stage (van Dijk et al., 2011; Ciresi et al., 2010).

Our study aimed to circumvent the above mentioned methodological limitations by combining different structural and functional methods (with information about central and paracentral vision), and most importantly in relation with the characterization, objective and quantitative, of the permeability of BRB. This aspect is absent in previous other work and the impact of relating BRB status with the found neuronal functional changes is of paramount importance.

The main goal of this study was to investigate retinal neural dysfunction in the preclinical stage DR in a population of type 1 diabetic patients, from the psychophysical and neurophysiological point of view, with concomitant characterization and quantification of the BRB permeability and the metabolic control level. We wanted to identify whether independent neural damage can occur aside from vascular damage, and prive additional potential early biomarkers of disease related to magno-, konio- and parvocellular function or the neurophysiology of the outer retina. These data were compared with those obtained in type 1 diabetic patients with early DR and also in age-matched healthy volunteers.

3. METHODS

3.1. PATIENT SELECTION, DEMOGRAPHIC CHARACTERISTICS AND OPHTHALMOLOGICAL EXAMINATION

The study followed the tenets of the Declaration of Helsinki and was approved by our Ethics Committee. Prior to the inclusion in the study, informed consent was obtained from all subjects after a full given explanation.

We have tested 42 patients (mean age ± SD = 26.6 ± 5.3 years) with preserved visual acuity (VA), divided into 2 groups: with no DR (n=26; VA=1.088 ± 0.128) and with mild nonproliferative DR (n=16; VA=1.093 ± 0.137). These data were compared with those obtained in age-matched controls (n=25; 27.4 ± 5.8 years).

Participants were submitted to a complete ophthalmological examination, including the best-corrected visual acuity (BCVA) slit lamp examination of anterior chamber, IOP measurement (Goldmann applanation tonometer), angle and fundus examination (non-contact lens) and the assessment of subjective visual complaints. Exclusion criteria included media opacities, amblyopia, neurophthalmological and retinal diseases (besides DR) and high ammetropies (sphere > ± 4D; cylinder > ± 2D).

3.2. LABORATORY ANALYSIS – Glycated Hemoglobin

In order to evaluate the patients' metabolic control level, blood samples were collected for routine analysis of glycated haemoglobin (HbA1c) and submitted to the same laboratory to ensure a standard method for all obtained results.

3.3. CHARACTERIZATION OF THE BLOOD-RETINAL BARRIER STATUS

3.3.1. COLOUR FUNDUS PHOTOGRAPHY

Colour fundus photographies (35º) of both eyes were taken in seven standard fields of the retina according ETDRS procedures (Early Treatment Diabetic Retinopathy Study Research Group, 1991a), with a Topcon TRC-50 IA Retinal Ophtalmic Camera, including a Sony DXC 950 P digital camera, with a resolution of 0.5 MPixels / 768x576.

These photos were always obtained after psychophysical and electrophysiological assessment to prevent artifactual changes in retinal adaptation.

3.3.2. FLUORESCEIN ANGIOGRAPHY

Besides colour fundus photography, fluorescein angiography (FA) was sequentially performed (TRC-50 IA Topcon, digital camera: B/W Megaplus 1.4i, resolution of 1 MPixel / 1340x1037) to increase sensitivity in detecting topographic changes on BRB permeability.

A red-free photography was taken before 10% fluorescein sodium solution administration, which was injected in the anticubical vein in a volume adjusted to the patients' weight, according to vitreous fluorometry procedures (for details see below).

A series of twenty early phase pictures during the arterial and capillary filling were taken in the eye with more lesions, when applicable. If no DR signs were visible, right eye was chosen if the year of the patient's birthday is a pair number and the left eye in case of birthday on an impair year. After this series, a macula-centred photography was taken from the contralateral eye, followed by acquisition of quadrantic field images of the selected and the contralateral eyes, respectively.

Bilateral late phase pictures (5 and 10 min.) were finally taken, in order to analyze the presence or absence of leakage, to consubstantiate the classification of DR level (Early Treatment Diabetic Retinopathy Study Research Group, 1991b).

3.3.3. VITREOUS FLUOROMETRY

Vitreous Fluorometry (VF) is a valuable tool for studying the intraocular fluid dynamics and the permeability of the blood-ocular barriers, namely the BRB. VF brought an important clinical contribution for quantifying BRB permeability in DR, being of particular interest in the pre-clinical stage, since diabetic eyes show increased values even in apparently normal ocular fundus (Cunha-Vaz et al., 1975; Waltman et al., 1978).

For this purpose, we used a commercial fluorophotometer, the FM-2 Fluorotron™ Master (Coherent, Palo Alto, CA) and we followed the standard protocol for BRB permeability measurement (Gray et al., 1985). A dose of 14 mg/kg of the patient weight was thus injected and measurements of fluorescein concentration in the posterior vitreous were obtained one hour after injection, after discounting the natural fluorescence of the ocular tissues (pre-injection scan). Blood samples were collected at

10, 15 and 50 minutes after injection, for posterior measurements of the plasmatic fluorescein concentration (a cuvette which was adapted to the optical head of the Fluorotron was used for measuring the concentration of fluorescein in plasmatic solutions). With all these parameters, it was possible to obtain the penetration ratio (PR) of the fluorescein across the BRB (Zeimer et al., 1983).

3.3.4. RETINAL THICKNESS ANALYZER

As a result of the BRB breakdown, abnormal fluid accumulation in retinal tissue can be found in early stages of DR (Smith et al., 1987), leading to an increase in macular thickness not always assessable by current clinical tools (Shahidi et al., 1991). Retinal thickness analyzer (RTA) is thus one of the methods for quantitative evaluation of retinal thickness (RT) and was proved to be more sensitive for detecting localized increases in RT in the initial stages of DR (Pires et al., 2002), at the time of the data collection for this study (before high-resolution optical coherence tomography equipments are available) and was chosen for this reason.

The RTA software version used was the 2.11 with analysis 6.35 (Talia Technology Ltd). The principle of this method analysis is based on projecting a thin laser slit (helium-neon, 543 nm) obliquely on the retina and viewing it at an angle, similarly to the slitlamp biomicroscopy visualization. The separation between the reflections (and scatter) from the vitreoretinal interface and the chorioretinal interface is a measure of the retinal thickness. The image of the intersections of the laser slit with the retina (optical cross-section of the retina) is recorded by a video camera and digitized. Nine scans are obtained, covering the central 20° (6 x 6 mm) area around the fovea in the posterior pole. Each acquisition yields 10 optical-cross sections of the retina (and also a fundus image), separated by 200 μm, measuring an area of 2000 x 2000 μm in 200 seconds. The total area scanned with this RTA version is 6000 x 6000 μm, with each unit representing an area of 200 x 200 μm, with a depth precision of 5-10 μm and a depth resolution of 50 μm. Finally, a detailed map of RT is generated (Zeimer et al., 1996).

3.4. FUNCTIONAL ASSESSMENT

We have applied different psychophysical and electrophysiological methods for characterize visual function and also to obtain neural based parameters for structure-function correlations.

Visual function was thus assessed by the following methods (for details, see Chapter III- 2.2):

- Computerized chromatic contrast sensitivity – Cambridge Colour Test;
- Computerized perimetric achromatic contrast sensitivity – FDT;
- Standard Multifocal ERG.

Besides these, HRA-MfERG was also performed (for details, see below).

3.4.1. HRA-MULTIFOCAL ELECTRORETINOGRAM

Besides standard multifocal electroretinogram, we have also recorded topographic retinal responses with another technique, with a mfERG device composed by a stimulation and a measurement unit (RETIscan System; Roland Consult, Germany) connected to a Confocal Scanning Laser Ophthalmoscope - SLO - with a blue laser of 488nm as the stimulus source (Heidelberg Retina Angiograph version 2: HRA2; Heidelberg Engineering, Germany).

The HRA2 system is a confocal scanning laser ophthalmoscope for digital angiography containing 3 different laser sources: a diode laser at 790 nm for indocyanine excitation (ICGA mode), a diode laser at 820 nm for fundus image acquisition (IR mode) and a solid state laser at 488 nm for excitation (FA mode).

The combination of these two equipments allowed for simultaneous stimulation, recording and visualization of the eye fundus. Simultaneous stimulation and imaging are useful because they allow for continuous assessment of fixation and to establish clear relations between mfERG responses and stimulus locations (Rudolph et al., 2002; Rudolph and Kalpadakis, 2003).

SLO stimuli consisted of 19 hexagon arrays covering a measured visual angle of 18º that were modulated by binary m-sequences (to achieve random independent patterns of stimulation of the 19 regions). Our SLO-based device allowed for monitoring fixation behavior and control of stimulus presentation on the retina.

Local responses (first kernels) were extracted by means of reverse correlation using software provided by Roland Consult, Germany. The first-order kernels from each location were used to obtain the functional topography as shown in the trace arrays (i.e., the compilation of the traces of all local responses). For each hexagon, the peak amplitude, defined as the difference between N1 and P1, was calculated and the implicit time of P1 determined.

3.5. STATISTICAL ANALYSIS

To prevent issues related to violations of independence, in our statistical analysis we have used the mean of both eyes values of each participant, since all variables (except latencies of multifocal electrophysiological measures of patients) were statistically correlated (Spearman correlation).

Given the observed violation of ANOVA assumptions non-parametric analyses (Mann-Whitney testing / Spearman correlation) at a significance level of $p \leq 0.05$ were performed, using StatView (SAS, Cary, NC).

4. RESULTS

Patient Demographic Characteristics, Ophthalmological Examination and DR Level

The study group included 42 type 1 diabetic patients (ages between 14 and 37 years) with preserved visual acuity (best-corrected decimal scale values ranging from 0.9 to 1.3), divided into two subgroups, according to ETDRS classification system (with the help of the colour fundus photography and fluorescein angiography results): one group with no DR (n=26; VA=1.088 ± 0.128) and another group, with mild nonproliferative DR (n=16; VA=1.093 ± 0.137), presenting eyes with ETDRS levels #20, #35C and #35D.

The mean time duration of disease was ranging from 7 to 29 years (group with no DR: mean ± SD = 15.92 ± 5.15 yrs; group with initial DR: mean ± SD = 20.13 ± 5.00 yrs).

Laboratory Analysis - HbA1C

These patients had thorough and systematic local surveillance of metabolic control level since childhood, at the time of their diagnosis of diabetes.

In the group with no DR, HbA1c varied from 6.2 % to 10.0 % (mean ± SD values = 7.99 % ± 1.16 %) and in the group of initial lesions of DR, HbA1c varied from 6.5 % to 13.0 % (mean ± SD values = 9.07 % ± 1.93 %). However, this difference was not statistically significant (p=0.09).

Characterization of Blood-Retinal Barrier status

Colour Fundus Photography and Fluorescein Angiography

These two methods were used in complementarity to classify DR level and the results were already mentioned in the first section of Results section (see above).

Vitreous Fluorometry

The penetration ration (PR) of fluorescein across the BRB was significant different between both patient groups (p=0.002). In the group with initial DR, PR values (10^{-6} x min^{-1}) are higher (mean ± SD = 5.06 ± 2.46, ranging from 1.56 to 9.29) than values obtained in the group without DR (mean ± SD = 2.83 ± 0.88, ranging from 1.64 to 4.71 which are similar to the normal values identified in the literature – Cunha-Vaz et al., 1985).

Retinal Thickness Analyzer

Analysis considering 9-ETDRS areas or concentric rings, or simply the average value, showed no significant structural differences between patient groups.

In Ring 1 (central ring), the retinal thickness (RT) in the group with no DR was 183.58 ± 16.28 µm (mean ± SD), ring 2 = 196.67 ± 13.87 µm and ring 3 = 190.54 ± 14.39 µm, while patients presenting initial DR showed the following values: ring 1 = 189.04 ± 28.60 µm, ring 2 = 204.06 ± 25.09 µm and ring 3 = 194.42 ± 26.88 µm.

However, RT was significantly higher in the central ring when comparing each patient group with controls (p=0.045 - group with no DR / p=0.042 - group with initial DR; control mean ± SD values: ring 1: 165.67 ± 17.69 µm, ring 2 = 203.71 ± 15.13 µm and ring 3 = 194.42 ± 26.88 µm).

Psychophysics

Chromatic Contrast Sensitivity - Evidence for damage of both Parvo- and Koniocellular Pathways even in Patients with No DR

As illustrated in Figure 52, chromatic contrast sensitivity measures were significantly different between controls and patients. Considering the group with initial

DR, the comparison with controls showed higher thresholds for all chromatic axes (Protan: p=0.02; Deutan: p=0.0001; Tritan: p=0.0009), while also significant higher thresholds are significant for Protan and Tritan axes in the group with no DR (p=0.007 and 0.0008, respectively). When comparing both patient groups, significant differences are only found for the Deutan axis (p=0.005).

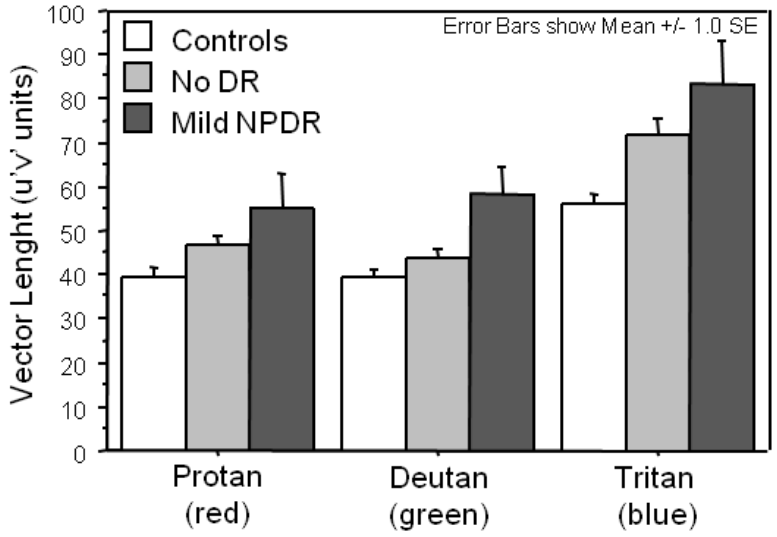

Fig. 52 – Chromatic Contrast Thresholds in patients and in controls, where impairment can be already observed in the group with no DR.

Achromatic Contrast Sensitivity showed Early Magnocellular Impairment

MD (mean deviation), the global parameter of magnocellular performance (FDT testing) yielded significant differences between controls and each group of patients (with no DR: p = 0.001; with initial DR: p=0.0004), with no significant effect detected between patient groups. Concerning PSD (field heterogeneity measure) no differences were found between groups. For details see Fig. 53-A.

To probe whether regional differences were underlying these effects, we then analyzed magnocellular achromatic contrast sensitivity in distinct regions. Significant differences were found in all five locations, between controls and both patient groups (with initial DR – ST: p=0.004, SN: p=0.004, IN: p=0.0002, IT: p=0.0009, C: p=0.002; without DR – ST: p=0.002, SN: p=0.002, IN: p=0.003, IT: p=0.006, C marginally lost: p=0.07). Comparisons between both patient groups were non significant – see Fig. 53-B for details.

(A)

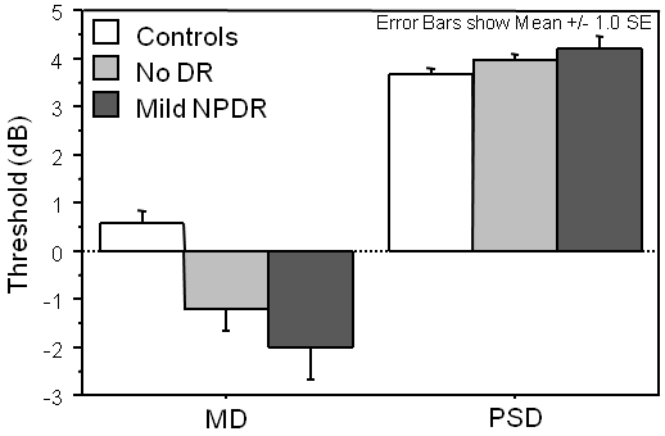

(B)

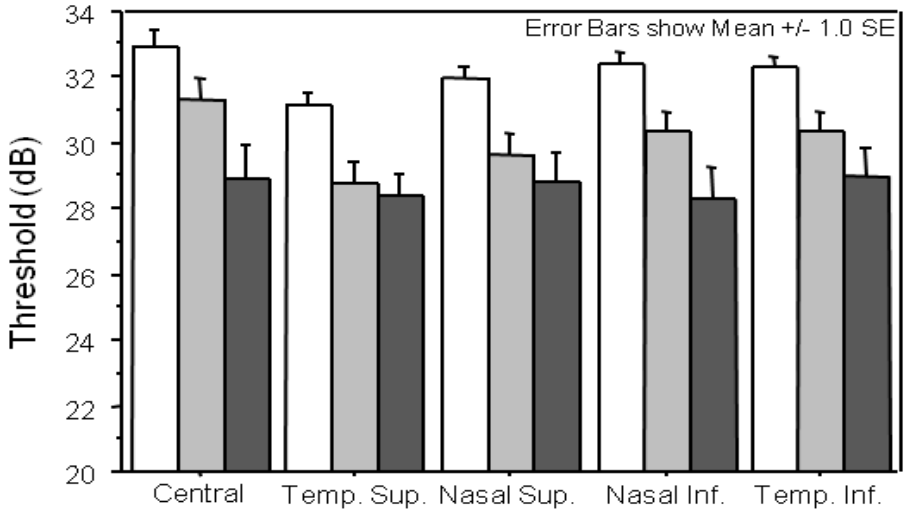

Fig. 53 – Magnocellular contrast sensitivity expressed in whole field deviation (MD - mean deviation) and in regional homogeneity (PSD – pattern standard deviation) measures in patients and in controls (A), as well as in central and quadrantic thresholds (B).

Neurophysiology

Standard Multifocal Electroretinogram – Direct Evidence for Neural Dysfunction

The MfERG showed a significant decrease in amplitude in all concentric rings in both patient groups when comparing with control subjects (P1-wave, all eccentricity rings: $p<0.0001$ – see also Fig. 54-A), suggesting a neural basis for damage at the bipolar cell circuit level.

Interestingly, analysis of P1-wave implicit times showed a significant decrease between controls and patients with no DR, for all concentric rings. This difference is only evident in ring 2 in the group with initial lesions of DR, with these timing parameters showing a clear tendency to reach normal values in this group type – see Fig. 54-B for details.

(A)

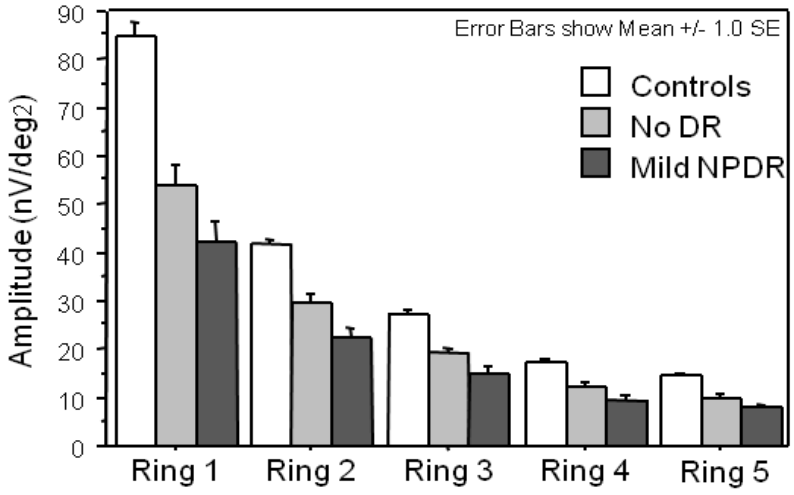

(B)

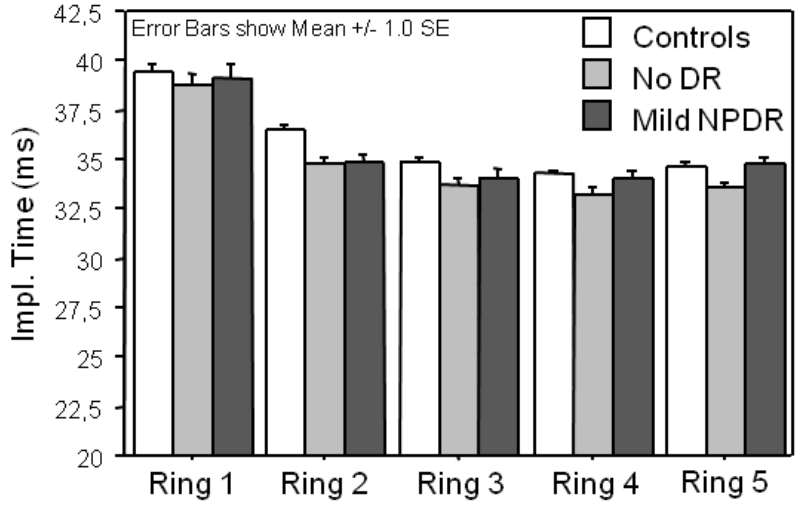

Fig. 54 – P1-wave amplitude (A) and implicit time (B) of mfERG, across concentric rings. Decreased amplitudes values are found in both patient groups, showing a different pattern in implicit time (decreased values in the group with no DR).

Similar results on amplitude and implicit time were found concerning the N1 component – see Fig. 55.

(A)

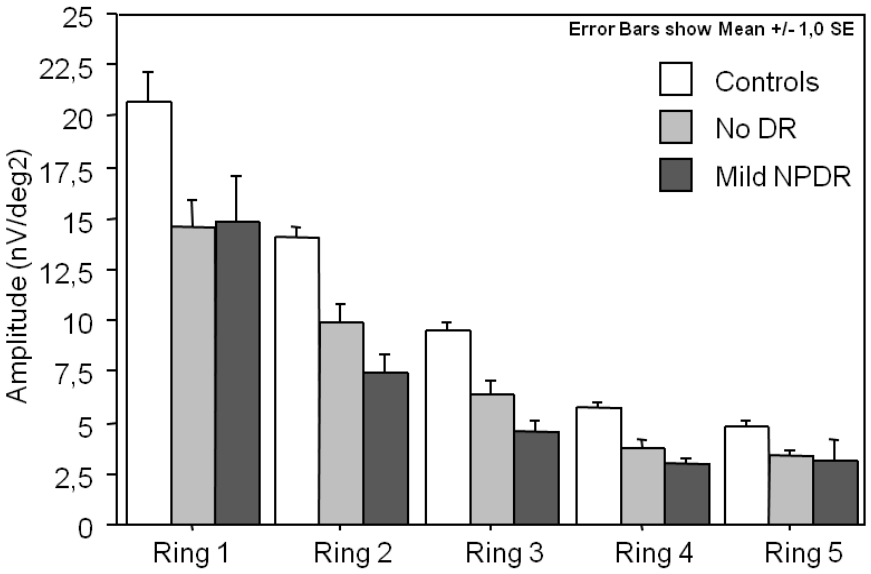

(B)

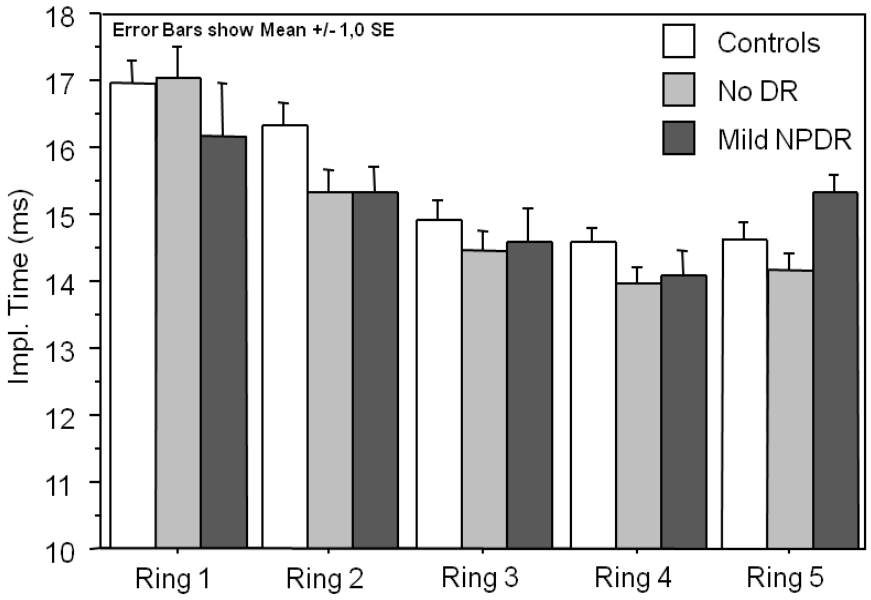

Fig. 55 – N1-wave amplitude (A) and implicit time (B) of mfERG, across concentric rings.

HRA-Multifocal Electroretinogram

According to the standard mERG results, analysis of HRA-mfERG by concentric rings also showed a decrease in amplitude values when compared with controls, more evident in ring 1 (group without DR – R1: p=0.0009, R2: p=0.016, R3: p=0.037 / group with initial DR – R1: p=0.001, R2: p=0.033, R3: significance marginally lost – p=0.06).

No significant differences in implicit times were found, which may be due to the much higher stimulus intensities used in this experiment.

Structure Function Correlations

Interestingly, no correlation was found between the BRB permeability (PR) and the psychophysical and electrophysiological parameters in both patients groups.

Significant correlation was also found between PR and HbA1c in the group with initial DR (r=0.42; p=0.023). No other correlations were found between HbA1c and the other studied parameters, except for the average value of RTA measures, in the group with no DR.

Again, no correlation was found between duration of diabetes and structural or functional parameters, with the exception of standard MfERG (average of amplitude of P1-wave: p=0.018 and average of timing: p=0.017), in the group with initial DR.

As expected from the good VA of the patients, no correlation was found between this parameter and the structural or functional parameters.

New Results after Refining Analysis

Given the evidence of isolated neuronal impairment in the group with no DR, we made a subsequent analysis in a sbugroup with no DR lesions, with normal PR values (Cunha-Vaz et al., 1985), to exclude the influence of outliers in the previous described results and thus to have a sample of diabetic patients with strictly normal BRB permeability values, using stringent criteria.

Table 22 shows the characterization of the group without DR and the cases selected for the new sample. All patients with abnormal PR values (> 3.1 x 10^{-6} x min^{-1}) were excluded for the new statistical analysis. Differences between these subgroups are shown in Table 23.

Note that these cases with increased BRB permeability corresponded of 30.8% of the patients with no DR – consistent with the literature) (Castillo et al., 1996). On the other hand, all the excluded cases have, at least, 12 years of duration disease.

The subgroup with normal PR was used for subsequent comparison with the control group.

Patient	Gender	VA	Disease duration (yrs)	PR (BRB)
1	M	1.3	12	1.88
3	M	1.3	15	1.72
5	M	1.0	12	1.53
6	F	1.0	7	2.81
7	M	1.0	13	4.69 *
8	M	1.0	17	3.41 *
9	M	1.3	24	1.82
11	M	1.3	15	2.20
14	M	1.3	14	1.08
15	M	1.0	18	1.60
17	M	1.0	12	2.22
18	M	1.0	12	2.64
21	F	1.0	24	1.91
23	M	1.0	10	2.63
25	M	1.0	19	1.70
27	F	1.0	13	2.55
28	M	1.0	14	3.42 *
29	F	1.0	15	3.30 *
30	F	1.0	12	3.28 *
32	M	1.0	13	3.68 *
33	F	1.0	25	3.40 *
34	M	1.0	19	2.45
38	F	1.3	29	2.12
39	M	0.9	17	2.58
40	F	1.0	13	2.46
42	M	1.0	20	3.21 *

(*) abnormal PR

Table 22 – Characterization of the diabetic group with no DR.

	No DR / Normal PR	No DR / Abnormal PR
Patients (n)	18	8
Duration of disease (yrs)	16.25 ± 5.77	16.13 ± 4.42
PR (10^{-6}x min^{-1})	2.47 ± 0.56	3.84 ± 0.60

Table 23 – Summary characterization of the subgroups with no DR, with normal and abnormal PR.

Chromatic Contrast Sensitivity

In the group of no DR with normal PR, changes in chromatic contrast sensitivity were only found in Tritan axis (p=0.02) with mean ± SD = 66.67 ± 14.18 x 10^{-4} u'v' units.

Achromatic Contrast Sensitivity

FDT results showed exactly the same pattern than previously: MD was significantly affected as compared to the normal group (p<0.005), with decreased thresholds in each peripheral quadrant: – ST: p=0.006, SN: p=0.011, IN: p=0.008, IT: p=0.019) with preserved threshold in central region.

Multifocal ERG

Standard mfERG also showed a significant decrease in amplitude in all concentric rings when comparing with control subjects (P1 wave, all eccentricity rings: p<0.0001; N1wave: ring 1 – p=0.008; ring 2 – p=0.0008; ring 3 – p=0.0002; rings 4 and 5 – p<0.0001).

Analysis of implicit times showed the same pattern verified previously, with P1-wave showing a significant decrease in timing for all concentric rings (0.002<p<0.02), except for the central and the most peripheral rings (significance marginally lost – p=0.06).

Implicit times of N1-wave showed the same tendency, with significant differences in rings 2, 4 and 5 (p=0.04 for all).

HRA-mfERG presented the same pattern obtained for the larger sample: significant decreases in amplitude values (ring 1: p=0.001; ring 2: p=0.006; ring 3: p=0.02) and, again, no significant differences in implicit times, when comparing with control group.

Clinical Examples

Figure 56 shows different examples of psychophysical and neurophysiological data in three patients with different patterns of damage. Patient #5 and #29 presents no DR (this one with increased impairment on visual function) and patient #4 presents initial DR.

5. DISCUSSION

In this study, we have found evidence of retinal neuronal changes occurring in type 1 diabetic patients before breakdown of the BRB or onset of vasculopathy, as probed by physchopysical (achromatic / chromatic contrast sensitivity) tests of magno-, parvo- and koniocellular pathways and electrophysiological recordings (mfERG) that correlate with neural substrates of the outer retina. Central retinal thickness corroborated this finding.

In the group of patients with initial DR the neuronal impairment did not correlate with increased BRB permeability, suggesting independent patterns of damage.

We identified damage of both parvocellular and koniocellular pathways (as demonstrated by chromatic contrast sensitivity testing). Some previous studies also report significant colour vision defects in diabetes type 1 using conventional non staircase based methods, not showing a well-defined axis of impairment (Giusti, 2001) or not differentiation across visual pathways (Mulak et al., 2002) (because only anomaloscopy using the Moreland equation was tested, for blue green impairments).

Impairment of magnocellular function was also observed (as evidenced by decreased thresholds in FDT, in central and peripheral regions), even in the group without clinical signs of DR. Previous studies reported a decrease in contrast sensitivity but without manipulating spatiotemporal frequency in a way that would be more selective to defined visual pathways (Lopes de Faria, 2001; Di Leo, 1990; Krásný et al.,

2006; Georgakopoulos et al., 2011). Our study used a specific test biased to the activation of the magnocellular performance, with the advantage to be perimetric, probing central and peripheral vision.

MfERG findings showed generalized decrease amplitudes which are consistent with changes at photoreceptor/bipolar cell circuits. Our study uniquely combines, unlike previous ones, objective measures of the BRB permeability, in addition to the functional information gathered from psychophysical and neurophysiological techniques.

Interestingly, a novel and surprising finding, occurred in our mfERG recordings, was a distinct reduction of implicit time in patients with no DR. This suggests a different neurophysiological pattern when neural changes dominate in relation to vascular abnormalities. Since our DR group was also at an early stages this might explain why we do not find the delay in mfERG responses observed for later stages of DR (Fortune et al., 1999). This finding suggests a distinct physiopathological mechanism in the pre-clinical stage of DR in type 1 patients, that may possibly be related with initial amplitude reduction, with concomitant change in wave shape that implies an associated decrease in implicit time (note that a similar neurophysiological mechanism was previously described in autosomal dominant optic neuropathies – Holder, 1987) possibly with timing increases in the subsequent stages of the retinal disease.

Evidence for neuropysiological of early impairment, independently of vascular lesions, raises the question why a discrete structural impact on retinal thickness could also already be observed, with increase in foveal area, even in the absence of initial vascular lesions. We also found topographic psychophysical and electrophysiological impairment beyond the central area, as mentioned above, raising the question that these independent mechanisms of damage do nevertheless covary in space.

Metabolic control levels, here evaluated by HbA1c, revealed no contribution for psychophysical and electrophysiological impairment, suggesting that such type of control is irrelevant as a contributing modulator of the neural phenotype. However, an impact of this metabolic parameter on the BRB permeability and retinal thickness can be observed, further corroborating the notion that different mechanisms are affecting these measures.

In general, time duration of diabetes did not influence the neuronal impairment except the mfERG measures in the group with initial DR.

In sum, our results suggest that retinal neuronal changes can occur in diabetes type 1 patients before breakdown of the BRB or onset of vasculopathy. In case of increased BRB permeability, neurophysiological impairment showed to be independent.

Magno-, konio- and parvocellular neural markers of visual function can be affected in Type 1 Diabetic Patients even in the absence of clinical evidence for DR, and absent vascular / BRB mechanisms and their respective temporal trajectories of damage.

Future studies should elucidate the time course of pure diabetes related neural impairment, and its causal mechanisms, as opposed to pure vascular mechanisms.

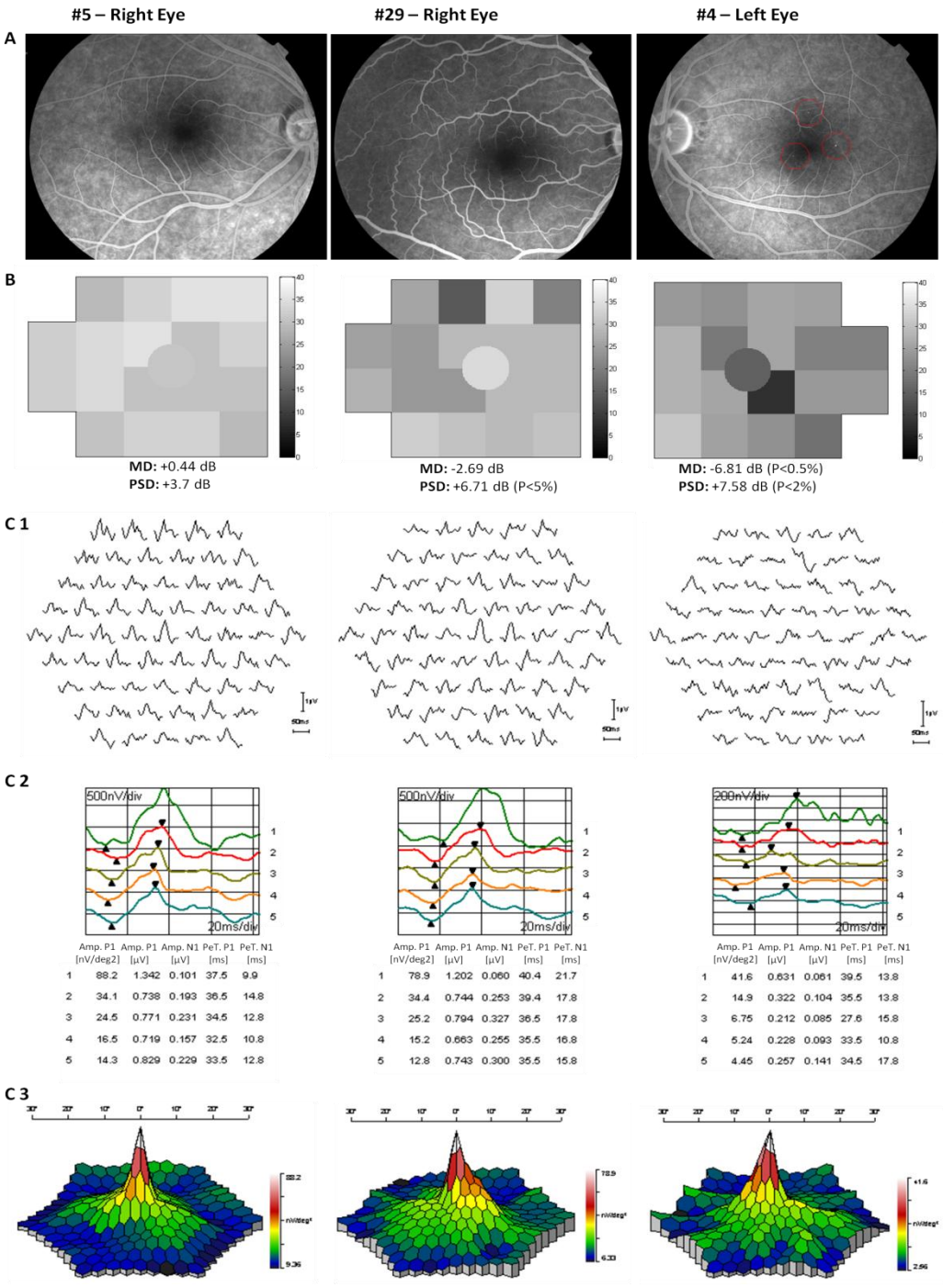

Fig 56 – Clinical examples of some results of two patients without DR (#5 without DR and minimal changes on functional testing; #29 without DR with more changes than #5) and a patient with initial DR (#4), with 3 microaneurisms identified. (A) Fluorescein angiography (B): Achromatic contrast sensitivity (FDT); (C) Standard mfERG (C1: plots; C2: analysis by concentric rings; C3: 3D-representation).

CHAPTER VIII

GENERAL DISCUSSION

CHAPTER VIII

GENERAL DISCUSSION

In this work we studied the impact of distinct disease models in the physiology of GC related pathways and the role of psychophysical and electrophysiological methods in the assessment of visual function loss.

For this purpose, we selected different types of optic neuropathies (with dominant GC or axonal damage): acquired (MS associated or not with overt optic neuritis) and inherited (ADOA and LHON). Complementarily, we also studied the pathophysiology of direct neural loss (including GC pathways) damage in type 1 diabetic patients with minimal or no DR.

Since it is known that there are different structural types of GC (with different intrinsic functions) and that this anatomophysiological specificity starts in retina and continues up to the visual cortex across parallel retinocortical pathways, we used different psychophysical and electrophysiological methods that allowed us to investigate the impact of GC dysfunction at pre- and post-CG levels.

In MS, and since the GCs receptive field structure is suited for contrast detection, we measured chromatic (parvo- and koniocellular impairment) and achromatic contrast sensitivity (magnocellular impairment). We also probed directly the impact of axonal damage on retinocortical function (with or without a previous ON episode) by measuring cortical VEPs. These methods evidenced thus the presence of subclinical deficits (even when visual acuity was largely preserved), since retinocortical deficits were found in patients without a previous episode of ON. Furthermore, a significant correlation between these deficits with disease stage was found only in this study group, suggesting a pathophysiological dichotomic pattern on disease mechanisms before and after the occurrence of the ON episode. This finding renders detection of subtle initial damage an important issue, given that conventional clinical colour vision and contrast sensitivity testing could not do it (in fact, these showed less sensitivity in damage detection even in the group with previous ON).

Concerning inherited optic neuropathies, a common finding was present: evidence for functional damage in afferent layers of the retina to the ganglion cell layer,

as probed by multifocal ERG. MfERG recordings were abnormal and correlated with functional psychophysical loss (suggesting that dysfunction is not confined to the GC/optic nerve, which was corroborated by structural changes as indexed by retinal thickness measures).

In spite of this common finding, functional differences could be observed, given the genetic differences between ADOA and LHON and distinct natural history (in our study LHON patients were just carriers of this disease).

In ADOA, retinocortical dysfunction (as assessed by PERG) had also a cortical impact, with an interesting pattern of deficit: multifocal responses revealed a decrease in central responses (which were not possible to measure directly with conventional electrophysiological methods, recording global responses). This central deficit was only moderately explained by changes in retinal measures. The distinct pattern obtained in central versus peripheral cortical multifocal responses also allowed us to conclude that the more peripheral retinal deficit is at least compensated at the cortical level, in contrast to the central pattern of deficit.

Furthermore, by means of high density visual evoked potentials, using visual stimuli with characteristics matched to the functional tuning properties of the neurons of the parvo- and magnocellular systems, we probed the impact of GC damage in the visual cortex, across these parallel pathways. These responses were compared in central versus peripheral location and for mono- versus binocular inputs. This method allowed to infer a surprisingly different propagation pattern of cortical responses in ADOA. Moreover, the dominant impairment of parvocellular deficit was partially compensated by binocular summation peripheral representations, thereby demonstrating a plasticity mechanism at the cortical level.

Concerning LHON carriers, no deficit in GC activity was found by conventional electrophysiological recordings (PERG), although a swelling of the retinal nervous fibres could be observed in structural imaging by OCT. In spite of this finding, we could observe psychophysical dysfunction within parvo- and koniocellular pathways, with a relative preservation of magnocellular function. Changes in the multifocal ERG showed that in the asymptomatic/pre-symptomatic phase, there are functional changes at a pre-ganglion cell level that may be subserve loss in visual function and structural changes that precede the clinically established affected status of LHON. Concerning cortical responses, although an increase of implicit time was found in pattern striate cortical evoked responses, both magno- and parvocellular biased responses showed similar characteristics as compared to control subjects in all extra-striated cortical clusters. These findings suggest relative cortical and GC preservation and raise the possibility that damage in afferent layers of GC may occur independently

In type 1 diabetic patients, psychophysical (achromatic / chromatic contrast sensitivity) tests of GC magno-, parvo- and koniocellular pathways and electrophysiological recordings evidenced relatively neuronal changes occurring even before breakdown of the BRB or onset of vasculopathy. MfERG findings showed generalized decrease amplitudes which are consistent with changes at pre-GC circuits. In patients with initial DR the neuronal impairment did not correlate with increased BRB permeability. These findings suggest the presence of a neuropathy that may occur prior to any endothelial and BRB based vascular damage.

Additional evidence for pure independent neural damage was the novel finding of a distinct reduction of implicit time of mfERG in patients with no DR.

These combined findings provided new insights for the physiopathology of DR, namely in the pre-clinical stage, by adding the notion of independent neural damage.

All these new findings focused on distinct disease mechanisms subjacent to the different studied optic neuropathies not only at GC level, but also at pre- and post-GC levels. Combined psychophysical and electrophysiological approaches allowed to infer that even in disease models believed to directly impact on GC structure and function, independent neural sources of impairment and compensatory mechanisms can be identified.

CHAPTER IX

FINAL CONCLUSIONS

CHAPTER IX

FINAL CONCLUSIONS

1. Ganglion cell-driven parallel pathways (parvo-, konio- and magnocellular) show preclinical impairment in multiple sclerosis, even in the absence of a previous episode of optic neuritis.

2. The observed retinocortical damage is independent (uncorrelated) across functional pathways only before an episode of optic neuritis, suggesting that the etiology of functional loss is distinct.

3. Axonal damage is already present in preclinical stages of optic neuritis.

4. Visual functional impairment is dependent on the MS stage (EDSS) only before the occurrence of optic neuritis, suggesting that is dependent on non-local disease factors.

5. In the ADOA (*OPA1* mutation) model of ganglion cell damage, all parvo-, konio- and magnocellular pathways are affected.

6. Physiological impairment and structural changes also occur at a pre-ganglionic level suggesting a retrograde damage mechanism in ADOA patients.

7. The impact of GC dysfunction is also observed at a post-GC (cortical) level in that condition.

8. Cortical impairment appears to be only moderately explained by the retinal phenotype, suggesting additional damage mechanisms at the central nervous system level.

9. Abnormal propagation of cortical responses, and dominance of parvocellular impairment, can be observed in ADOA patients.

10. In LHON carriers (11778G>A mutation) of the same pedigree, relatively normal electrophysiological responses can be found at the GC level.

11. Although no evidence of functional or structural GC lesion was observed, pre-GC responses are affected in LHON carriers.

12. At the pre-GC level local electrophysiological responses are abnormal, and correlated with changes on retinal thickness, independent of macular nerve fibre layer.

13. This pre-GC impairment may provide an explanation of the psychophysically identified parvo- and koniocellular impairment.

14. A slight delay is found in primary visual cortical responses with no differences in magno- and parvocellular biased responses beyond striate cortex in this pedigree.

15. Psyhcophysical changes can occur in type 1 diabetic patients, in magno-, konio- and parvocellular GC pathways even before breakdown of the blood-retinal barrier or onset of vasculopathy.

16. Neurophysiological changes can also occur at a pre-GC level.

17. In cases of increased blood-retinal barrier permeability, neurophysiological impairment occurs independently across distinct visual channels.

18. Metabolic control level (HbA1c) shows no correlation with measures of neuronal impairment.

19. Metabolic control level (HbA1c) has a direct impact on BRB function and retinal thickness.

20. Time duration of disease is not necessarily predictive of neuronal impairment (except for the mfERG changes in cases of minimal DR) or the BRB status in early DR.

21. Concerning the four studied pathologies in this work, a common finding is observed: colour vision impairment, obtained by psychophysical approach, which can provide a valuable preclinical biomarker (namely in cases of MS without optic neuritis, LHON carriers and type 1 diabetic patients in pre-clinical stage of DR).

22. Pre-GC impairment was mainly evidenced by local electrophysiological assessment.

23. Post-GC / cortical impairment can be characterized across different functional channels, even beyond primary visual cortex, by research electrophysiological methods.

24. Novel physiological and electrophysiological methods can provide neural biomarkers for detecting sub-clinical changes in optic neuropathies and in type 1 diabetic patients with no DR, with relevant implications for pre-clinical monitoring.

BIBLIOGRAPHY

Adler FH: Physiology of the eye. Clinical application. 3rd Edition. Mosby, St. Louis, Philadelphia 1959. Cap. 15; pp. 562-573.

Aijaz S, Erskine L, Jeffery G, Bhattacharya SS, Votruba M: Developmental expression profile of the optic atrophy gene product: OPA1 is not localized exclusively in the mammalian retinal ganglion cell layer. Invest Ophthalmol Vis Sci 2004; 45: 1667–1673.

Alexander C, Votruba M, Pesch UE, et al.: OPA1, encoding a dynamin-related GTPase, is mutated in autosomal dominant optic atrophy linked to chromosome 3q28. Nat Genet 2000; 26(2): 211-215.

Alper G, Wang L: Demyelinating optic neuritis in children. J Child Neurol 2009; 24: 45-48.

Arden GB, Hamiltom AM, Wilson-Holt J, et al: Pattern electroretinograms become abnormal when background diabetic retinopathy deteriorates to a pre-proliferative stage: Possible use as a screening test. Br J Ophthalmol 1986; 70: 330-335.

Barber AJ: A new view of diabetic retinopathy: a neurodegenerative disease of the eye. Elsevier, Progress In Neuro-Psychopharmacology & Biological Psychiatry 2003; 27: 283-290.

Barboni P, Carbonelli M, Savini G, et al.: Natural history of Leber's hereditary optic neuropathy: longitudinal analysis of the retinal nerve fiber layer by optical coherence tomography. Ophthalmology 2010; 117: 623-627.

Barboni P, Savini G, Parisi V, et al.: Retinal nerve fiber layer thickness in dominant optic atrophy measurements by optical coherence tomography and correlation with age. Ophthalmology 2011; 118(10): 2076–2080.

Barcellos LF, Sawcer S, Ramsay PP, et al.: Heterogeneity at the HLA-DRB1 locus and risk for multiple sclerosis. Hum Mol Genet 2006; 15(18): 2813-2824.

Baseler HA, Sutter EE, Klein SA, Carney T: The topography of visual evoked response properties across the visual field. Electroencephalogr Clin Neurophysiol 1994; 90: 65-81.

Batten B: A family suffering from hereditary optic atrophy. Trans Ophthalmol Soc UK 1896; 16: 125.

Benson WE, Brown GC, Tasman W: Treatment of macular edema. In: Benson, Brown, Tasman (eds). Diabetes and its ocular complications. WR Saubders Co, Philadelphia 1988, pp 154-162.

Bhatti MT, Newman NJ: A multiple sclerosis-like illness in a man harbouring the mtDNA 14484 mutation. J Neuro-ophthalmol 1999; 19: 28-33.

Biousse V: The optic neuropathies. Rev Neurol (Paris) 2005; 161: 519-530.

Bonneau D, Souied E, Gerber S, et al.: No evidence of genetic heterogeneity in dominant optic atrophy. J Med Genet 1995; 32: 951-953.

Booij JC, Bakker A, Kulumbetova J, et al.: Simultaneous mutation detection in 90 retinal disease genes in multiple patients using a custom-designed 300-kb retinal resequencing chip. Ophthalmology 2011; 118(1):160–167

Bradley WG, Whitty CW: Acute optic neuritis: prognosis for development of multiple sclerosis. J Neurol Neurosurg Pshychiatry 1968; 31: 10-18.

Brusa A, Jones SJ, Kappor R, Miller DH, Plant GT: Long term recovery and fellow eye deterioration after optic neuritis, determined by serial visual evoked potential. J Neurol 1999; 246: 776−782.

Brusa A, Jones SJ, Plant GT: Long-term remyelination after optic neuritis: a 2-year visual evoked potential and psychophysical serial study. Brain 2001; 124: 468−479.

Carelli V, Ross-Cisneros FN, Sadun AA: Optic nerve degeneration and mitochondrial dysfunction: genetic and acquired optic neuropathies. Neurochem Int 2002; 40(6): 573-584.

Carelli V, Ross-Cisneros FN, Sadun AA: Mitochondrial dysfunction as a cause of optic neuropathies. Prog Retin Eye Res 2004; 23(1): 53-89.

Caruana PA, Davies MB, Weatherby SJ, et al.: Correlation of MRI lesions with visual psychopysical deficit in secondary progressive multiple sclerosis. Brain 2000; 123: 1471−1480.

Castelo-Branco M, Faria P, Forjaz V, Kozak LR, Azevedo H: Simultaneous comparison of relative damage to chromatic pathways in ocular hypertension and glaucoma: correlation with clinical measures. Invest Ophthalmol Vis Sci 2004; 45: 499-505.

Castelo-Branco M, Mendes M, Silva MF, et al.: Specific retinotopically based magnocellular impairment in a patient with medial visual dorsal stream damage. Neuropsychologia 2006; 44: 238−253.

Castelo-Branco M: Retinal neural impairment. In: Diabetic Retinopathy. Cunha-Vaz JG Ed. Singapore: World Scientific Publishing 2011, pp. 83-95.

Castillo A, Benitez del Castillo JM, Diaz D, Sayagues O, Ruibal JL, Garcia-Sanchez J: Analysis of the blood-retinal barrier: its relation to clinical and metabolic factors and progression to retinopathy in juvenile diabetics: a 4-year follow-up study. Graefe's Arch Clin Exp Ophthalmol 1996; 234: 246-250.

Celesia GG, Kaufman DI, Brigell M, Toleikis S, et al.: Optic neuritis: a prospective study. Neurology 1990; 40: 919-923.

Chakrabarti S, Cukiernik M, Hileeto D, et al.: Role of vasoactive factors in the pathogenesis of early changes in diabetic retinopathy. Diabetes Metab Res Ver 2000; 16: 393-407.

Ciresi A, Amato MC, Morreale D, et al.: OCT is not useful for detection of minimal diabetic retinopathy in type 1 diabetes. Acta Diabetol 2010; 47(3): 259-263.

Ciulla TA, Amador AG, Zinman B: Diabetic retinopathy and diabetic macular edema. Pathophysiology, screening and novel therapies. Diabetes Care 2003; 26: 2653-2664.

Compston A: The 150th anniversary of the first depection of the lesions of multiple sclerosis. J Neurol Neurosurg Psychiatry 1988; 51(10): 1249-1252.

Cunha-Vaz JG, Faria de Abreu JR, Campos AJ: Early breakdown of the blood-retinal barrier in diabetes. Br J Ophthalmol 1975; 59: 649-656.

Cunha-Vaz JG, Gray JR, Zeimer RC, Mota MC, Ishimoto BM, Leite E: Characterization of the early stages of diabetic retinopathy by vitreous fluorophotometry. Diabetes 1985; 34(1): 53-59.

Cunha-Vaz JG: Clinical presentation of retinopathy. In: Diabetic Retinopathy. Cunha-Vaz JG Ed. Singapore: World Scientific Publishing 2011, pp. 37-50.

Curcio CA, Sloan KR Jr, Packer O, Hendrickson AE, Kalina RE: Distribution of cones in human and monkey retina: individual variability and radial asymmetry. Science 1987; 236: 579-582.

Dacey DM: Parallel pathways for spectral coding in primate retina. Annu Rev Neurosci 2000; 23: 743-775.

Delettre C, Lenaers G, Griffoin J-M, et al.: Nuclear gene OPA1, encoding a mitochondrial dynamin-related protein, is mutated in dominant optic atrophy. Nat Genet 2000; 26: 207-210.

Delettre C, Griffoin J-M, Kaplan J, et al.: Mutation spectrum and splicing variants in the OPA1 gene. Hum Genet 2001; 109: 584-591.

Di Leo MA, Falsini B, Caputo S, Ghirlanda G, Porciatti V, Greco AV: Spatial frequency-selective losses with pattern electroretinogram in type 1 (insulin-dependent) diabetic patients without retinopathy. Diabetologia. 1990; 33(12): 726-730.

Early Treatment Diabetic Retinopathy Study Research Group. Report nr 2: Treatment techniques and clinical guidelines for photocoagulation of diabetic macular edema. Ophthalmology 1987; 94: 761-774.

Early Treatment Diabetic Retinopathy Study Research Group. Report nr 10: Grading diabetic retinopathy from stereoscopic color fundus photographs. An extension of the modified Airlie house classification. Ophthalmology 1991a; 98: 786-806.

Early Treatment Diabetic Retinopathy Study Research Group. Report nr 11: Classification of diabetic retinopathy from fluorescein angiograms. Ophthalmology 1991b; 98: 807-822.

Ebers GC: Multiple sclerosis and other demyelinating diseases. In Asbury AH, McKhann GM, McDonald WI (eds): Diseases of the Nervous System, vol. 2. Philadelphia, WB Saunders, 1986, p. 1268.

Eden B, Klein K: Overview of epidemiologic studies of diabetic retinopathy. Ophthalm Epidemiol 2007; 14: 179-183.

Eiberg H, Kjer P, Rosenberg T: Dominant optic atrophy (OPA1) mapped to chromosome 3q region, I: linkage analysis. Hum Mol Genet 1994; 3: 977-980.

Elliot MD, Traboulsi EI, Maumenee IH: Visual prognosis in autosomal dominant optic atrophy (Kjer type). Am J Ophthalmol 1993; 115: 360-367.

Engell T, Trojaborg W, Raun NE: Subclinical optic neuropathy in multiple sclerosis: a neuro-ophthalmological investigation by means of visually evoked response, Farnsworth-Munsell 100 Hue test and Ishihara test and their diagnostic value. Acta Ophthalmol 1987; 65: 735-740.

Evangelou N, Konz D, Esiri MM, Smith S, Palace J, Matthews PM: Size-selective neuronal changes in the anterior optic pathways suggest a differential susceptibility to injury in multiple sclerosis. Brain 2001; 124: 1813-1820.

Ferré M, Amati-Bonneau P, Tourmen Y, Malthiery Y, Reynier P: eOPA1: an online database for OPA1 mutations. Hum Mutat 2005; 25: 423-428.

Fisher JB, Jacobs DA, Markowitz CE, et al.: Relation of visual function to retinal fiber layer thickness in multiple sclerosis. Ophthalmology 2006; 113: 324−332.

Fleishman JA, Beck RW, Linares OA, Klein JW: Deficits in visual function after resolution of optic neuritis. Ophthalmology 1987; 94: 1029-1035.

Fortune B, Schneck ME, Adams AJ: Multifocal electroretinogram delays reveal local retinal dysfunction in early diabetic retinopathy. Invest Ophthalmol Vis Sci 1999; 40(11): 2638-2651.

Fraser CL, Klistorner A, Graham SL, Garrick R, Billson FA, Grigg JR: Multifocal visual evoked potential analysis of inflammatory or demyelinating optic neuritis. Ophthalmology 2006; 113(2): 315-323.

Frederiksen JL, Petrera J: Serial visual evoked potential in 90 untreated patients with acute optic neuritis. Surv Ophthalmol 1999; 44: 54−62.

Georgakopoulos CD, Eliopoulou MI, Exarchou AM, Tzimis V, Pharmakakis NM, Spiliotis BE: Decreased contrast sensitivity in children and adolescents with type 1 diabetes mellitus. J Pediatr Ophthalmol Strabismus 2011; 48(2): 92-97.

Ghezzi A, Martinelli V, Rodegher M, et al.: The prognosis of idiopathic optic neuritis. Neurol Sci 2000; 21: 865-869.

Gilden DH: A search for virus in multiple sclerosis. Hybrid Hybridomics 2002; 21(2): 93-97.

Gilden DH: Infectious causes of multiple sclerosis. Lancet Neurol 2005; 4: 195-202.

Giusti C: Lanthony 15-Hue Desaturated Test for screening of early color vision defects in uncomplicated juvenile diabetes. Jpn J Ophthalmol 2001; 45(6): 607-611.

Gout O, Lebrun-Frenay C, Labauge P, Le Page GE, Clavelou P, Allouche S: PEDIAS Group. Prior suggestive symptoms in one-third of patients consulting for a "first" demyelinating event. J Neurol Neurosurg Psychiatry 2011; 82(3): 323-325.

Gray JR, Mosier MA, Ishimoto BM: Optimized protocol for Fluorotron Master. Graefe's Arch Clin Exp Ophthalmol 1985; 222: 225-229.

Grazina MM, Diogo, LM, Garcia, PC, et al.: Atypical presentation of Leber's hereditary optic neuropathy associated to mtDNA 11778G4A point mutation - A case report. Eur J Paed Neurol 2007; 11: 115-118.

Harding A, Sweeney MG, Govan GG, et al.: Pedigree analysis in Leber hereditary optic neuropathy families with a pathogenic mtDNA mutation. Am J Hum Genet 1995; 57: 77-86.

Harrison AC, Becker WJ, Stell WK: Colour vision abnormalities in multiple sclerosis. Can J Neurol Sci 1987; 14: 279−285.

Hauser SL, Oksenberg JR: The neurobiology of multiple sclerosis: genes, inflammation, and neurodegeneration. Neuron 2006; 52(1): 61-76.

Hee MR, Izatt JA, Swanson EA et al.: Optical coherence tomography of the human retina. Arch Ophthalmol 1995; 113: 325–332.

Hellige JB: Hemispheric asymmetry for visual information processing. Acta Neurobiol Exp (Wars) 1996; 56(1): 485–497.

Henderson AP, Trip SA, Schlottmann PG, et al.: An investigation of the retinal nerve fibre layer in progressive multiple sclerosis using optical coherence tomography. Brain 2008; 131: 277−287.

Henricsson M, Nystrom L, Blohmé G, et al.: The incidence of retinopathy 10 years after diagnosis in young adult people with diabetes. Results from the nationwide population-based Diabetes Incidence Study in Sweden (DISS). Diabetes Care 2003; 26: 349-354.

Holder GE: Abnormalities of the pattern ERG in optic nerve lesions: changes specific for proximal retinal dysfunction. In Barber C and Blum T, eds. Evoked Potentials III, Butterworths, London 1987; pp. 221-224.

Holder GE: The incidence of abnormal pattern electroretinography in optic nerve demyelination . Electroencephalogr Clin Neurophysiol 1991; 78: 18-26.

Holder GE, Votruba M, Carter AC, et al.: Electrophysiological findings in dominant optic atrophy (DOA) linking to the OPA1 locus on chromosome 3q 28-qter. Doc Ophthalmol 1999; 95(3-4): 217-228.

Holder GE: Pattern electroretinography (PERG) and an integrated approach to visual pathway diagnosis. Prog Retin Eye Res 2001; 20(4): 531–561.

Holder GE: Electrophysiological assessment of optic nerve disease. Eye (Lond) 2004; 18(11): 1133–1143.

Holder GE, Brigell MG, Hawlina M, et al.: ISCEV standard for clinical pattern electroretinography - 2007 update. Doc Ophthalmol 2007; 114: 111-116.

Holder GE, Gale RP, Acheson JF, Robson AG: Electrodiagnostic assessment in optic nerve disease. Curr Opin Neurol 2009; 22(1): 3–10.

Hood DC, Zhang X, Hong JE, Chen CS: Quantifying the benefits of additional channels of multifocal VEP recording. Doc Ophthalmol 2002; 104: 303-320.

Hood DC, Bach M, Brigell M, et al.: ISCEV Standard for clinical multifocal electroretinography (mfERG) (2011 edition). Doc Ophthalmol 2012; 124(1): 1-13.

Hoyt CS: Autosomal dominant optic atrophy: a spectrum of disability. Ophthalmology 1980; 87: 245-251.

Ito Y, Nakamura M, Yamakoshi T, Lin J, Yatsuya H, Terasaki H: Reduction of inner retinal thickness in patients with autosomal dominant optic atrophy associated with OPA1 mutations. Invest Ophthalmol Vis Sci 2007; 48(9): 4079–4086.

Jenkins TC, Cartwright JP: The electroretinogram in minimal diabetic retinopathy. Br J Ophthalmol 1990; 74(11): 681-684.

Johns DR, Heher KL, Miller NR., et al.: Leber's hereditary optic neuropathy. Clinical manifestations of the 14484 mutation. Arch Ophthalmol 1993; 111: 495-498.

Johnston PB, Gaster RN, Smith VC, Tripathi RC: A clinicopathological study of autosomal dominant optic atrophy. Am J Ophthalmol 1979; 88: 868-875.

Kalloniatis M, Luu C: Principles of Vision. In: Kolb H, Fernandez E, Nelson R editors: Webvision: The Organization of the Retina and Visual System. Salt Lake City (UT) 2007.

Kaplan E, Benardete E: The dynamics of primate retinal ganglion cells. Prog Brain Res 2001; 134: 17-34.

Ke T, Nie SW, Yang OB, et al.: The G401D mutation of OPA1 causes autosomal dominant optic atrophy and hearing loss in a Chinese family. Zhonghua Yi Xue Yi Chuan Xue Za Zhi 2006; 23(5): 481-485.

Kelly DH: Frequency doubling in visual responses. J Opt Soc Am 1966; 56: 1628−1633.

Kerrison JB, Howell N, Miller NR, et al.: Leber hereditary optic neuropathy. Electron microscopy and molecular genetic analysis of a case. Ophthalmology 1995; 102: 1509-1516.

Kerrison JB, Arnould VJ, Ferraz Sallum JM, et al.: Genetic heterogeneity of dominant optic atrophy, Kjer type: Identification of a second locus on chromosome 18q12.2-12.3. Arch Ophthalmol 1999; 117(6): 805-810.

Kiernan DF, Mieler WF, Hariprasad SM: Spectral-domain optical coherence tomography: a comparison of modern high-resolution retinal imaging systems. Am J Ophthalmol 2010; 149: 18–31.

Kjer B, Eiberg H, Kjer P, Rosenberg T: Dominant optic atrophy (OPA1) mapped to chromosome 3q region, II: Clinical and epidemiological aspects. Acta Ophthalmol Scand 1996; 74: 3-7.

Kjer P: Infantile optic atrophy with dominant mode of inheritance: a clinical and genetic study of 19 Danish families. Acta Opthalmol 1959; 37(54): 1-146.

Kjer P: Histopathology of eye, optic nerve and brain in a case of dominant optic atrophy. Acta Opthalmol 1982; 61: 300-312.

Kjer P, Jensen OA, Klinken L: Histopathology of eye, optic nerve and brain in a case of dominant optic atrophy. Acta Opthalmol 1983; 61: 300–312.

Klein BEK, Klein R: Diabetic Retinopathy. In: Johnson GJ, Minassian DC, Weale RA, West SK. (eds.), The Epidemiology of Eye Disease, 2nd ed. Oxford University Press 2003, Chap. 20; pp. 341-355.

Klein R, Knudston M, Lee K, Gangnon R, Klein B: The Winsconsin epidemiologic study of diabetic retinopathy XXII. The twenty-five-year progression of retinopathy in persons with type 1 diabetes. Ophthalmology 2008; 115: 1859-1868.

Kline LB, Glaser JS: Dominant optic atrophy. The clinical profile. Arch Ophthalmol 1979; 97(9): 1680-1686.

Kline VB, Eng EH, Siatkowski: Developmental and hereditary optic nerve disorders. In Kline and Foroozan (eds): Optic nerve disorders, 2nd ed. Oxford University Press 2007; pp. 151-175.

Klistorner AI, Graham SL: Objective perimetry in glaucoma. Ophthalmology 2000; 107: 2283-2299.

Kok-van-Alphen CC: Four families with the dominant infantile from of optic nerve atrophy. Acta Ophthalmol 1970; 48: 905-916.

Kolb H, Linberg KA, Fisher SK: The neurons of the human retina: A Golgi study. J Comp Neurol 1992; 318: 147-187.

Kolb H: The architecture of functional neural circuits in the vertebrate retina. Invest Ophtahlmol Vis Sci 1994; 35: 2385-2404.

Koprowski H: Search for viruses in multiple sclerosis. Neurology 1976; 26: 80-82.

Korsholm K, Madsen KH, Frederiksen JL, Skimminge A, Lund TE: Recovery from optic neuritis: an ROI-based analysis of LGN and visual cortical areas. Brain 2007; 130: 1244−1253.

Krásný J, Brunnerová R, Průhová S, et al.: The contrast sensitivity test in early detection of ocular changes in children, teenagers, and young adults with diabetes mellitus type 1. Cesk Slov Oftalmol 2006; 62(6): 381-394.

Kullberg C, Abrahamsson M, Arnqvist H, Finnstrom K, Ludvigssont J: VISS Study Group. Prevalence of retinopathy differs with age at onset of diabetes in a population of patients with type 1 diabetes. Diab Med 2002; 19: 924-931.

Kurtenbach A, Leo-Kottler B, Zrenner E: Inner retinal contributions to the multifocal electroretinogram: patients with Leber's hereditary optic neuropathy (LHON). Multifocal ERG in patients with LHON. Doc Ophthalmol 2004; 108(3): 231-240.

Kurtzke JF: Rating neurologic impairment in multiple sclerosis: an expanded disability status scale (EDSS). Neurology 1983; 33: 1444−1452.

Kurtzke JF, Hyllested K: Multiple sclerosis in the Faroe Islands. III. An alternative assessment of the three epidemics. Acta Neurol Scand 1987; 76: 317-339.

Lagrèze W: Treatment of optic neuropathies – State of the art. Klin Monbl Augenheilkd 2009; 226: 875-880.

Lang GK: Opthalmology. A text book atlas. Thieme, Stuttgard, New York 2000, Cap. 12; p. 301.

Leal EC, Santiago AR, Ambrósio AF: Old and new drug targets in diabetic retinopathy: from biochemical changes to inflammation and neurodegeneration. Curr Drug Targets CNS Neurol Disord 2005; 4: 421-434.

Lecleire-Collet A, Audo I, Aout M, et al.: Evaluation of retinal function and flicker light-induced retinal vascular response in normotensive patients with diabetes without retinopathy. Invest Ophthalmol Vis Sci 2011; 52(6): 2861-2867.

Li C, Kosmorsky G, Zhang K, et al.: Optic atrophy and sensorineural hearing loss in a family caused by an R445H OPA1 mutation. Am J Med Genet A 2005; 138A(3): 208-211.

Likitmascul S, Rawdaree P, Deerochanawong C, et al.: Thailand diabetes registry project; type of diabetes, glycemic control and prevalence of microvascular complications in children and adolescents with diabetes. J Med Assoc Thai 2006; 89(1): 10-16.

Livingstone IR, Mastaglia FL, Howe J, et al.: Leber's optic neuropathy: clinical and visual evoked response studies in asymptomatic and symptomatic members of a 4-generation family. Br J Ophthalmol 1980; 64: 751-757.

Lobo C, Bernardes R, Santos F, Cunha-Vaz J: Mapping retinal fluorescein leakage with confocal scanning laser fluorometry of the human vitreous. Arch Ophthalmol 1999; 117: 631-637.

Lobo C, Bernardes R, Cunha-Vaz J: Alterations of the blood-retinal barrier and retinal thickness in preclinical retinopathy in subjects with type 2 diabetes. Arch Ophthalmol 2000; 118: 1364-1369.

Lopes de Faria JM, Katsumi O, Caliero E, Nathan D, Hirose T: Neurovisual abnormalities preceding the retinopathy in patients with long-term type 1 diabetes mellitus. Graefes Arch Clin Exp Ophthalmol 2001; 239(9): 643-648.

Ludovico J, Bernardes R, Pires I, Figueira J, Lobo C, Cunha-Vaz J: Alterations of retinal capillary blood flow in preclinical retinopathy in subjects with type 2 diabetes. Graefes Arch Clin Exp Ophthalmol 2003; 41: 181-186.

Macarez R, Amati-Bonneau P, Burelle X, et al.: A novel mutation of the OPA1 gene responsible for isolated autosomal dominant optic atrophy in two brothers. J Fr Ophtalmol 2007; 30(2): 161-164.

Mackey DA: Epidemiology of Leber's hereditary optic neuropathy in Australia. Clin Neurosci 1994; 2: 162-164.

Man PYW, Turnbull DM, Chinnery PF: Leber hereditary optic neuropathy. J Med Genet 2002; 39: 162-169.

Man PYW, Griffiths PG, Brown DT: The epidemiology of Leber hereditary optic neuropathy in the northeast of England. Am J Hum Genet 2003; 72: 333-339.

Marmor MF, Hood DC, Keating D, et al.: Guidelines for basic multifocal electroretinography (mfERG). Doc Ophthalmol 2003;106: 105–115.

Marmor MF, Fulton AB, Holder GE, Miyake Y, Brigell M, Bach M: ISCEV Standard for full-field clinical electroretinography (2008 update). Doc Ophthalmol 2009;118: 69–77**.**

Marmor MF, Brigell MG, Westall CA, Bach M**.** ISCEV Standard for clinical electro-oculography (2010 update)**.** Doc Ophthalmol 2011; 122: 1–7.

Marrosu MG, Murru MR, Costa G, et al.: DRB1-DQA1-DQB1 loci and multiple sclerosis predisposition in the Sardinian population. Hum Mol Genet 1998; 7: 1235-1237.

Masland RH: The fundamental plan of the retina. Nat Neurosci 2001; 4: 877-886.

Milea D, Sander B, Wegener M, et al.: Axonal loss occurs early in dominant optic atrophy. Acta Ophthalmol 2010; 88(3): 342–346.

Miller NR: The hereditary optic neuropathies. In: Walsh and Hoyt's Clinical Neuro-Ophthalmology. 4th ed. Baltimore: Williams & Wilkins 1982, pp 311-317.

Morales J, Weitzmann ML, González de la Rosa M: Comparison between tendency-oriented perimetry (TOP) and Octopus threshold perimetry. Ophthalmology 2000; 107: 134-142.

Moreland JD, Kerr J: Optimization of stimuli for tritanomaloscopy. Mod Prob Ophthalmol 1978; 19: 162−166.

Morrison J: Anatomy and physiology of the optic nerve. In: Kline and Foroozan (eds): Optic nerve disorders, 2nd ed. Oxford University Press 2007; pp 3-23.

Moura AL, Teixeira RA, Oiwa NN, et al.: Chromatic discrimination losses in multiple sclerosis patients with and without optic neuritis using the Cambridge Colour Test. Vis Neurosci 2008; 25: 463−468.

Mulak M, Reniewska B, Kostuś E, Balcewicz A, Misiuk-Hojło M: The role of color vision disturbances in diagnostics of early diabetic retinopathy. Klin Oczna 2002; 104(3-4): 249-251.

Mullen KT, Plant GT: Colour and luminance vision in human optic neuritis. Brain 1986; 109: 1-13.

Newman NJ: Optic neuropathy. Neurology 1996; 46: 315-322.

Newman NJ, Biousee V: Hereditary optic neuropathies. Eye 2004; 18: 1144-1160.

Newman NJ: Hereditary optic neuropathies: from the mitochondria to the optic nerve. Am J Ophthalmology 2005; 140: 517-523.

Nikoskelainen EK, Huoponen K, Juvonen V, et al.: Ophthalmologic findings in Leber hereditary optic neuropathy, with special reference to mtDNA mutations. Ophthalmology 1996; 103: 504-514.

Noble J, Forooghian F, Sproule M, Westall C, O'Connor P: Utility of the National Eye Institute VFQ-25 questionnaire in a heterogeneous group of multiple sclerosis patients. Am J Ophthalmol 2006; 142(3): 464-468.

Noval S, Contreras I, Rebolleda G, Munoz-Negrete FJ: Optical coherence tomography versus automated perimetry for follow-up of optic neuritis. Acta Opthalmol Scand 2006; 84: 790−794.

Odom JV, Bach M, Brigell M, et al.**:** ISCEV standard for clinical visual evoked potentials (2009 update). Doc Ophthalmol 2010; 120: 111-119.

Olichon A., Emorine LJ, Descoins E, et al.: The human dynamin-related protein OPA1 is anchored to the mitochondrial inner membrane facing the inter-membrane space. FEBS Lett 2002; 523(1-3): 171-176.

Optic Neuritis Study Group: The 5-year risk of MS after optic neuritis. Experience of the optic neuritis treatment trial. Optic Neuritis Study Group. Neurology 1997; 49(5): 1404-1413.

Optic Neuritis Study Group: Multiple sclerosis risk after optic neuritis: final optic neuritis treatment trial follow-up. Optic Neuritis Study Group. Arch Neurol 2008; 65(6): 723-732.

Osterberg GA: Topography of the layer of the rods and cones in the human retina. Acta Ophthalmol 1935; 6: 1-102.

Parisi V, Manni G, Spadaro M, et al.: Correlation between morphological and functional retinal impairment in multiple sclerosis patients. Invest Ophthalmol Vis Sci 1999; 40: 2520−2527.

Pearce JM: Historical descriptions of multiple sclerosis. Eur Neurol 2005; 54: 49-53.

Pesch UE, Fries JE, Bette S, et al.: OPA1, the disease gene for autosomal dominant optic atrophy, is specifically expressed in ganglion cells and intrinsic neurons of the retina. Invest Ophthalmol Vis Sci 2004; 45(11): 4217-4225.

Pirenne M: Vision and the Eye, London 1945, The Pilot Press.

Pires I, Bernardes R, Lobo C, Soares M, Cunha-Vaz J: Retinal thickness in eyes with mild nonproliferative retinopathy in patients with type 2 diabetes mellitus: comparison of measurements obtained by retinal thickness analysis and optical coherence tomography. Arch Ophthalmol 2002; 120: 1301-1306.

Plant GT: Optic neuritis and multiple sclerosis: Curr Opin Neurol 2008; 21: 16-21.

Polman CH, Reingold SC, Edan G, et al.: Diagnostic criteria for multiple sclerosis: 2005 revisions to the "McDonald Criteria". Ann Neurol 2005; 58: 840−846.

Polyak SL: The retina. Chicago: University of Chicago Press 1941.

Polyak S: The vertebrate visual system. Chicago: University of Chicago Press 1957.

Porciatti V, Sartucci F: Retinal and cortical evoked responses to chromatic contrast stimuli. Specific losses in both eyes of patients with multiple sclerosis and unilateral optic neuritis. Brain 1996; 119: 723−740.

Poser CM, Patty DW, Scheinberg L, et al.: New diagnostic criteria for multiple sclerosis: guidelines for research protocols. Ann Neurol 1983; 13: 227-231.

Rayleigh, L : Experiments on colour. Nature 1881; 25: 64−66.

Regan BC, Reffin JP, Mollon JD: Luminance noise and the rapid determination of discrimination ellipses in colour deficiency. Vision Res 1994; 34: 1279-1299.

Reis A, Mateus C, Macário MC, de Abreu JR, Castelo-Branco M: Independent patterns of damage to retinocortical pathways in multiple sclerosis without a previous episode of optic neuritis. J Neurol 2011; 258: 1695-1704.

Reis A, Mateus C, Viegas T, et al.: Physiological evidence for impairment in autosomal dominant optic atrophy at the pre ganglion level. Graefes Arch Clin Exp Ophthalmol 2012 [Epub ahead of print].

Riordan-Eva P, Harding AE: Leber's hereditary optic neuropathy: the clinical relevance of different mitochondrial DNA mutations. J Med Genet 1995; 32: 81-87.

Rizzo JF III, Lessel S: Risk of developing multiple sclerosis after uncomplicated optic neuritis: a long-term prospective study. Neurology 1998; 38: 185-90.

Rodriguez M, Silva A, Cross SA, et al.: Optic neuritis: a population-based study in Olmsted County, Minnesota. Neurology 1995; 45: 244-250.

Roth A, Lanthony P. Vision des Couleurs. In: Risse ed. Exploration de la fonction visuelle. Applications au domaine sensorial de l'óeil normal et en pathologie. Paris: Société Française d'Opthtalmologie et Masson 1999a. p. 129−51.

Roth A, Lanthony P. Fonctions de sensibilité au contraste de luminance. In: Risse ed. Exploration de la fonction visuelle. Applications au domaine sensorial de l'óeil normal et en pathologie. Paris: Société Française d'Opthtalmologie et Masson 1999b. p. 81-98.

Rudolph G, Kalpadakis P. Bechmann M, La Rocca G, Hörmann C, Berninger T: Scanning laser ophthalmoscope-evoked multifocal-ERG (SLO-m-ERG) by using short msequences. Eur J Ophthalmol 2002; 12(2): 109-116.

Rudolph G, Kalpadakis P: Topographic mapping of retinal function with the SLO-mfERG under simultaneous control of fixation in Best's disease. Ophthalmologica 2003; 217(2): 154-159.

Sadovnick AD, Armstrong H, Rice GP et al.: A population base-study of multiple sclerosis in twins: update. Ann Neurol 1993; 33: 281-285.

Sadun AA, Win PH, Ross-Cisneros FN, et al.: Leber's hereditary optic neuropathy differentially affects smaller axons in the optic nerve. Trans Am Ophthalmol Soc 2000; 98: 223-232.

Sadun AA, Salomao SR, Berezovsky A, et al.: Subclinical carriers and conversions in Leber hereditary optic neuropathy: a prospective psychophysical study. Trans Am Ophthalmol Soc. 2006; 104: 51-61.

Sakai T, Matsushima M, Shikishima K, Kitahara K: Comparison of standard automated perimetry with matrix frequency-doubling technology in patients with resolved optic neuritis. Ophthalmology 2007; 114: 949-956.

Salomão SR, Berezovsky A, Andrade RE, Belfort R Jr, Carelli V, Sadun AA: Visual electrophysiologic findings in patients from an extensive Brazilian family with Leber's hereditary optic neuropathy. Doc Ophthalmol 2004; 108(2): 147-155.

Santiago AR, Pereira TS, Garrido MJ, Cristóvão AJ, Santos PF, Ambrósio AF: High glucose and diabetes increase the release of [3H]-D-aspartate in retinal cell cultures and rat retinas. Neurochem Int 2006a; 48: 453-458.

Santiago AR, Rosa SC, Santos PF, Cristóvão AJ, Barber AJ, Ambrósio AF: Elevated glucose changes the expression of ionotropic glutamate receptor subunits and impairs calcium homeostasis in retinal neural cell. Invest Ophtalmol Vis Sci 2006b; 47: 4130-4137.

Sater RA, Rostami AM, Galetta S, Farber RE, Bird SJ: Serial evoked potential studies and MRI imaging in chronic progressive multiple sclerosis. J Neurol Sci 1999; 171: 79−83.

Sawcer S, Jones HB, Feakes R, et al.: A genoma screen in multiple sclerosis reveals susceptibility loci on chromosome 6p21 and 17q22. Nat Genet 1996; 13: 464-468.

Shahidi M, Ogura Y, Blair NP, Rusin MM, Zeimer R: Retinal thickness analysis for quantitative assessment of diabetic macular edema. Arch Ophthalmol 1991; 109(8): 1115-1119.

Shapley RM, Hawken JM: Parallel retino-cortical channels and luminance. In: Gegenfurtner KR Sharpe LT (eds). Color vision: from genes to perception**.** Cambridge University Press Cambridge, UK 1999; pp. 221-234.

Silva MF, Faria P, Regateiro FS, et al.: Independent patterns of damage within magno-, parvo- and koniocellular pathways in Parkinson´s disease. Brain 2005; 128: 2260-2271.

Silva MF, Maia-Lopes S, Mateus C, et al.: Retinal and cortical patterns of spatial anisotropy in contrast sensitivity tasks. Vision Res 2008; 48: 127-135.

Smith JL, Hoyt WF, Susac JO: Ocular fundus in acute Leber optic neuropathy. Arch Ophthalmol 1973: 90: 349-354.

Smith R, Lee C, Charles H, Farber M, Cunha-Vaz J: Quantification of diabetic macular edema. Arch Ophthalmol 1987; 105: 218-222.

Souza GS, Gomes BD, Lacerda EM, Saito CA, da Silva Filho M, Silveira LC: Amplitude of the transient visual evoked potential (tVEP) as a function of achromatic and chromatic contrast: contribution of different visual pathways. Vis Neurosci 2008; 25(3): 317-325.

Stell WK: The structure and relationships of horizontal cells and photoreceptor-bipolar synaptic complexes in goldfish retina. Am J Anat 1967; 121: 401-424.

Sutter EE, Trans D: The field topography of ERG components in man – I.The photopic luminance response. Vision Res 1992; 32: 433-446.

Talley CL: The emergence of multiple sclerosis, 1870-1950: a puzzle of historical epidemiology. Perspect Biol Med 2005; 48(3): 383-395.

Tobimatsu S, Tomoda H, Kato M: Parvocellular and magnocellular contributions to visual evoked potentials in humans: stimulation with chromatic and achromatic gratings and apparent motion. J Neurol Sci 1995; 134(1-2): 73-82.

Tobimatsu S, Kato M: Multimodality visual evoked potentials in evaluating visual dysfunction in optic neuritis. Neurology 1998; 50: 715-718.

Travis D, Thompson P: Spatiotemporal contrast sensitivity and colour vision in multiple sclerosis. Brain 1989; 112: 283-303.

van Dijk HW, Verbraak FD, Stehouwer M, et al.: Association of visual function and ganglion cell layer thickness in patients with diabetes mellitus type 1 and no or minimal diabetic retinopathy. Vision Res 2011; 51(2): 224-228.

Ventura DF, Gualtieri M, Oliveira AG, et al.: Male prevalence of acquired color vision defects in asymptomatic carriers of Leber's hereditary optic neuropathy. Invest Ophthalmol Vis Sci 2007; 48: 2362-2370.

Votruba M, Fitzke FW, Holder GE, et al.: Clinical features in affected individuals from 21 pedigrees with dominant optic atrophy. Arch Ophthalmol 1998; 116: 351-358.

Votruba M, Aijaz S, Moore T: A review of primary hereditary optic neuropathies. J Inherit Metab Dis 2003; 26: 209-227.

Votruba M: Molecular genetic basis of primary inherited optic neuropathies. Eye 2004; 18: 1126-1132.

Wallace DC, Singh G, Lott MT, et al.: Mitochondrial DNA mutation associated with Leber's hereditary optic neuropathy. Science 1988; 242: 1427-1430.

Waltman SR, Oestrich C, Krupin T, et al.: Quantitative vitreous fluorometry: a sensitive technique for measuring early breakdown of the blood-retinal barrier in young diabetic patients. Diabetes 1978; 27: 85-87.

Wanger P, Persson HE: Early diagnosis of retinal changes in diabetes: a comparison between electroretinography and retinal biomicroscopy. Acta Ophthalmol 1985; 63(6): 716-720.

Weinshenker BG, Rodriguez M: Epidemiology of multiple sclerosis. In: Gorelick PB, Alter M, eds. Handbooks of neuroepidemiology. Vol 29 of Neurological disease and therapy. New York: Marcel Dekker 1994; pp. 533-567.

Wescott MC, Fitzke FW, Crabb DP, Hitchings RA: Characteristics of frequency-of-seeing curves for a motion stimulus in glaucoma eyes, glaucoma suspect eyes, and normal eyes. Vision Res 1999; 39: 631-639.

White AJ, Sun H, Swanson WH, Lee BB: An examination of physiological mechanisms underlying the frequency-doubling illusion. Invest Ophthalmol Vis Sci 2002; 43: 3590-3599.

Willer CJ, Dyment DA, Risch NJ et al.: Twin concordance and sibling recurrence rates in multiple slcerosis. Proc Natl Acad Sci USA 2003; 100: 12877-12882.

Williams R, Airey M, Baxter H, et al.: Epidemiology of diabetic retinopathy and macular oedema: a systematic review. Eye 2004; 18: 963-983.

Wray SH: Optic neuritis. In: Albert DM, Jakobiec FA eds. Principles and practise of ophthalmology. Philadelphia, Pa: WB Saunders 1994; pp. 2539-2550.

Yu-Wai-Man P, Griffiths PG, Hudson G, Chinnery PF: Inherited mitochondrial optic neuropathies. J Med Genet 2009; 46: 145-158.

Yu-Wai-Man P, Griffiths PG, Burke A, et al.: The prevalence and natural history of dominant optic atrophy due to OPA1 mutations. Ophthalmology 2010; 117: 1538-1546.

Yu-Wai-Man P, Shankar SP, Biousse V, et al.: Genetic screening for OPA1 and OPA3 mutations in patients with suspected inherited optic neuropathies. Ophthalmology 2011a; 118(3): 558-563.

Yu-Wai-Man P, Bailie M, Atawan A, Chinnery PF, Griffiths PG: Pattern of retinal ganglion cell loss in dominant optic atrophy due to OPA1 mutations. Eye 2011b; 25(5): 596-602.

Zeimer RC, Blair NP, Cunha-Vaz JG: Vitreous fluorophotometry for clinical research. II Methodology of data acquisition and processing. Arch Ophthalmol 1983; 11: 1757-1761.

Zeimer R, Shaidi M, Mori M, Zou S, Asrani S: A new method for rapid mapping of the retinal thickness at the posterior pole. Invest Ophthalmol Vis Sci 1996; 37: 1994-2001.

Zhang L, Krzentowsy G, Albert A, Lefebvre P: Risk of developing retinopathy in diabetes control and complications trial type 1 diabetic patients with good or poor metabolic control. Diabetes Care 2001; 24: 1275-1279.

Zhang X, Hood DC, Chen CS, Hong JE: A signal-to-noise analysis of multifocal VEP responses: an objective definition for poor records. Doc Ophthal 2002; 104: 287-302.

Other references (accessed: Oct 2011-Dec 2011):

colblindor.com

cs.cmu.edu

humaneresearch.org.uk

ipj.quintessenz.de

lbbma.univ-angers.fr/eOPA1/

lynnwei.com

ncbi.nlm.nih.gov

pathology.wustl.edu

philosophy.hku.hk

webvision.umh.es